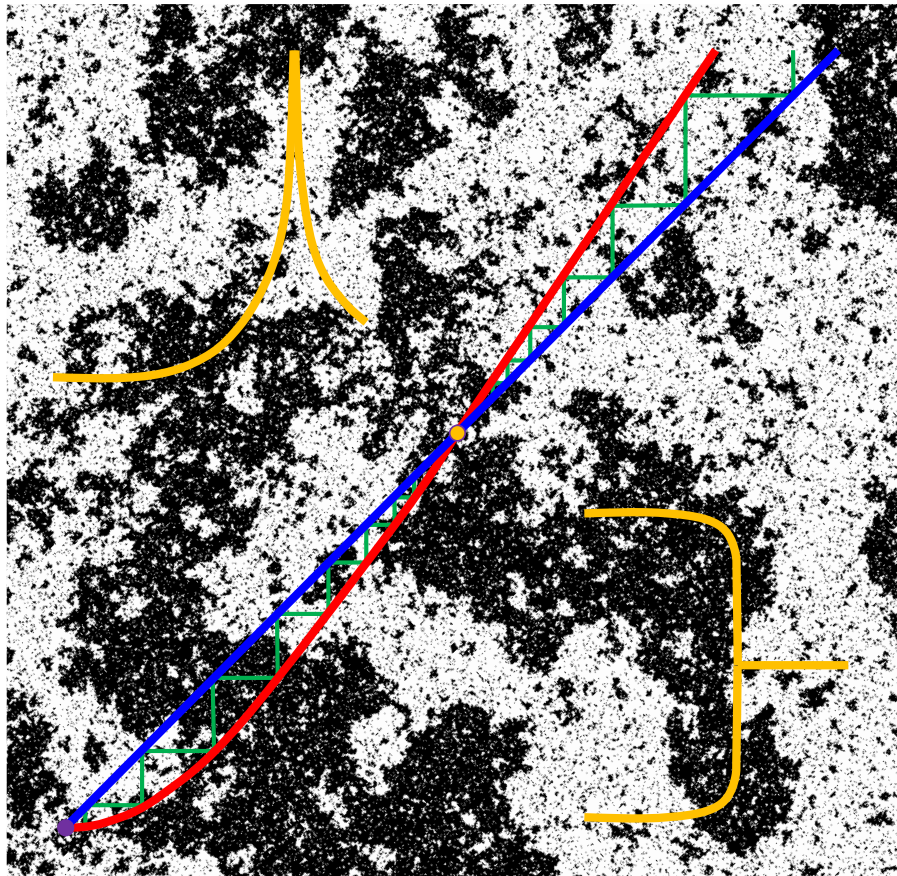


# Advanced Statistical Physics 2024

J. de Graaf

*October 29, 2024*



Written by R. van Roij, L. Filion, and J. de Graaf



## Introductory Remarks

The lecture notes for the course Advanced Statistical Physics (Voortgezette Statistische Fysica; NS-370B) were originally put together by R. van Roij and later extended and reworked by L. Filion. The version you have before you today, has been subsequently modified by J. de Graaf to account for changes in the content and structure of the course. This includes the repartitioning of material between academic years 2021-22 and 2022-23 to accommodate the topic of ideal quantum gases.

While care has been taken to avoid mistakes, some issues and typos may be present. The authors apologize in advance for any inconvenience this may cause. All feedback regarding mistakes, confusing text, typos, *etc.* is sincerely appreciated and will be used to improve future versions. Throughout the course, electronic versions of the updated notes will be made available on a weekly basis, which eliminate any remaining problems. Please direct feedback or other questions regarding the course to the course coordinator J. de Graaf *via* the e-mail address [j.degraaf@uu.nl](mailto:j.degraaf@uu.nl).

## Course Approach

At Utrecht University, Advanced Statistical Physics is the gateway to both the theoretical and experimental physics Master's programs. In addition, knowledge of statistical physics and thermodynamics will also prove extremely useful for climate physics. We therefore recommend that you try your best to grasp the concepts presented in this course, as you will encounter them throughout your career as a physicist. That is, the methodologies discussed here appear across all length and time scales that are considered in physical theories — from cosmic events to quantum systems — and beyond, *e.g.*, when considering the concept of entropy in biology, general complex systems, and even compute science.

Advanced Statistical Physics is probably the first third-year physics course that you encounter during your studies. As such, the approach taken during this course will be a bit different from what you are used to thus far. Lectures will focus more on conceptual aspects, less on working out problems or showcasing derivations from the notes. You are expected to work these out on your own, before the lecture. The problem classes will cover more material and the average student is *not* expected to be able to finish the exercises during the regular contact hours; more so than was the case for your second-year courses. In addition, you will also be asked to independently work through one of the chapters. This will help prepare you for the level of independence that you will need to show during any of the Master's programs, to which your Bachelor's grants access.

The intent is that any student who has worked through all the exercises independently, should not be able to fail the exam, barring exceptional circumstance. This is because 70% of the exam will comprise (parts of) example derivations and exercises that appear in the notes, which are for the most part covered by your homework. The reason for this approach is to incentivize you to complete all the problems before taking the exam. Have a look at some of the exams of the past years in the first few weeks of the course and you will see how this is implemented. This will also help prepare you (in terms of mindset) for the speed, at which you are expected to be able to move through the problem sets. The self-study chapter will be tested on during the exam, so studying it well is important. The material of the final exam covers all the homework, while the material of the midterm only tests the homework and sections covered up to that point.

No solutions to problems will be provided. This is done to force you to engage with the problems and get stuck. Being stuck on a problem is quite natural in and it is crucial to develop experience in becoming unstuck on your own. A physicist is expected to gain confidence in tackling problems, to which there are no set answers, be that in academia or industry. Thus, how you handle a no-answer course is telling

of your ability to engage with (physics) Master's programs, especially the tougher ones. As a class, you are, however, encouraged to cooperate to complete as many of the exercises as is possible, as physicists also work together. Lastly, it is strongly recommended that you prepare the exercises before the problem classes to ensure that you can make the most out of these. We appreciate your effort in this regard.

### Grading Scheme

The course will be graded as follows:

- Midterm 30%
- Final 70%

you will need to pass both parts with at least a 5 to pass the course. The date and time of the midterm will be announced on BlackBoard, where further course correspondence may also be found. MS-Teams will not be used for communication in general and no recordings of the lectures will be made available, unless there are exceptional circumstances, such as a public-transport strike or massive storm.

### Course Content

This course explores the principles and applications of thermodynamics and statistical physics, emphasizing the description of classical many-body systems and touching upon a few simple quantum gasses. We cover the following topics: phase transitions (gas-liquid condensation, magnetic ordering, crystallization, phase separation, and liquid-crystalline order), critical phenomena (exponents, divergent length scales, and fluctuations), and the structure and thermodynamic properties of non-ideal gasses, classical fluids, and liquid crystals. The theoretical framework comprises mean-field theory, a simple renormalization group of spin systems, Landau theory for first- and second-order phase transitions, nucleation theory, the virial expansion for non-ideal atomic gasses, and Onsager theory for anisotropic particles. In addition, the formal relationship of the various thermodynamic potentials (energy, free energy, enthalpy, Gibbs free energy, and grand potential) are related to each other via Legendre transformations; universal thermodynamic identities are also derived.

### Course Goals

By the end of this course, you will have learned and may be tested on the following aspects of (advanced) statistical physics:

- Associate (generalized) partition functions to thermodynamic potentials and derive corresponding thermodynamic identities. Connect potentials to each other via Legendre transforms.
- Formulate a (grand) canonical partition function for a simple model. Knows the classical and quantum mechanical distributions for ideal gasses. Can determine thermodynamic properties from these.
- Describe the phase transitions of (an)isotropic particles and study these using mean-field theory and renormalization-group calculations.
- Identify scalar order parameters and apply these to phase transitions. Use such parameters to describe first- and second-order phase transitions within the Landau theory.
- Compute thermodynamic quantities for classical non-ideal gasses and apply thermodynamic perturbation theory to a known reference system to chart the behavioral changes.

## Further Reading

The contents of these lecture notes heavily draw upon statistical physics textbooks and third-party lecture notes; too many to list here. However, the format of and approach taken in these lecture notes may not necessarily suit everyone. We therefore suggest the following extra reading material:

1. Introduction to Modern Statistical Mechanics (1987) by D. Chandler
2. Statistical Mechanics, Third Edition (2011) by P.K. Pathria & P.D. Beale
3. Statistical Mechanics, Second Edition (2016) by K. Huang
4. Theory of Simple Liquids (2006) by J.-P. Hansen & I.R. McDonald
5. Statistical Mechanics: Entropy, Order Parameters, and Complexity (2006) by J.P. Sethna

The books by Chandler and Pathria & Beale are more mathematically focussed. The former is more appropriate to a graduate level and might not be the easiest to get into without a solid understanding of statistical physics already. The book by Hansen & McDonald is also more appropriate for graduate students, while Sethna gives a quite different perspective on the material and provides a lot of interesting exercises. Lastly, Huang, might be a good source for additional information on ideal quantum gases.



# Contents

<b>1</b>	<b>Thermodynamics</b>	<b>13</b>
1.1	Intensive and Extensive Variables . . . . .	13
1.2	First Law . . . . .	14
1.2.1	Work . . . . .	14
1.2.2	Exact versus Inexact . . . . .	14
1.3	Second Law . . . . .	15
1.4	The $S, V, N$ Ensemble . . . . .	16
1.5	Legendre Transforms . . . . .	16
1.5.1	Geometric Interpretation of the Legendre Transformation . . . . .	17
1.5.2	The $N, V, T$ Ensemble . . . . .	18
1.5.3	The $N, P, T$ Ensemble . . . . .	18
1.5.4	The $\mu, V, T$ Ensemble . . . . .	18
1.5.5	The Gibbs-Duhem Relation . . . . .	19
1.6	Exercises . . . . .	20
<b>2</b>	<b>Statistical Mechanics</b>	<b>25</b>
2.1	The Microcanonical Ensemble: Fixed $U, V$ and $N$ . . . . .	25
2.2	Entropy and Temperature . . . . .	26
2.3	The Canonical Ensemble: Fixed $N, V$ , and $T$ . . . . .	26
2.4	The Grand-Canonical Ensemble: Fixed $\mu, V$ , and $T$ . . . . .	28

2.5	Constraints and Lagrange Multipliers . . . . .	29
2.6	Exercises . . . . .	31
<b>3</b>	<b>Classical Ensemble Theory</b>	<b>37</b>
3.1	Phase Space . . . . .	37
3.2	The Liouville Equation . . . . .	38
3.3	Time Averages and Ensemble Averages . . . . .	39
3.4	The Classical Ensembles . . . . .	40
3.4.1	The Microcanonical Ensemble . . . . .	40
3.4.2	The Canonical Ensemble . . . . .	41
3.4.3	The Grand-Canonical Ensemble . . . . .	42
3.5	The Equipartition Theorem . . . . .	44
3.6	Exercises . . . . .	49
<b>4</b>	<b>Classical and Quantum Ideal Gases</b>	<b>53</b>
4.1	The Classical Ideal Gas . . . . .	54
4.1.1	Entropy and Chemical Potential . . . . .	54
4.1.2	Maxwell-Boltzmann Distribution . . . . .	55
4.2	Dispersion Relation and Density of States . . . . .	55
4.2.1	State Density for a Particle in a Box . . . . .	56
4.2.2	Gapped Density of States for Relativistic Particles . . . . .	58
4.3	Bosons and Fermions . . . . .	59
4.4	Three Types of Statistics and Ideal Quantum Gases . . . . .	60
4.5	Maxwell-Boltzmann Statistics . . . . .	62
4.5.1	Deriving the Distribution . . . . .	64
4.5.2	Preparing for Quantum Systems . . . . .	65
4.6	Non-Interacting Bose Gas . . . . .	66
4.6.1	The High-Temperature Limit . . . . .	67

<i>CONTENTS</i>	9
4.6.2 Photons: A Relativistic Bose Gas . . . . .	69
4.7 Non-Interacting Fermi Gas . . . . .	71
4.7.1 The Low-Temperature Limit . . . . .	72
4.8 Exercises . . . . .	76
<b>5 Chemical Equilibria</b>	<b>81</b>
5.1 Chemical Reactions and the Gibbs Free Energy . . . . .	81
5.2 The Law of Mass Action . . . . .	82
5.3 Reaction Kinetics and Equilibrium Constants . . . . .	83
5.4 Doping of a Semi-Conductor . . . . .	84
5.5 Exercises . . . . .	86
<b>6 Phase Diagrams</b>	<b>89</b>
6.1 Criteria for Coexistence . . . . .	90
6.2 Closer Look at Coexistences . . . . .	91
6.3 Equilibrium and Metastability . . . . .	95
6.3.1 Isothermal Compressibility . . . . .	95
6.3.2 Convexity of the Free Energy . . . . .	96
6.4 Common Tangent in a Single-Component System . . . . .	97
6.5 Coexistence in a Binary Mixture . . . . .	98
6.6 Phase Transitions . . . . .	99
6.6.1 First-Order Phase Transitions . . . . .	100
6.6.2 Continuous Phase Transitions . . . . .	100
6.7 A Phase Transition involving Quantum Statistics . . . . .	102
6.8 Exercises . . . . .	107
<b>7 The Ising Model</b>	<b>113</b>
7.1 Introducing the Model . . . . .	113
7.2 Intuition for the Zero-Field Behavior . . . . .	114

7.3	Zero-Field Ising Model in One Dimension . . . . .	116
7.4	Zero-Field Ising Model in Two and Three Dimensions . . . . .	117
7.5	Transfer Matrix Method for 1D Ising Model with Field . . . . .	119
7.6	Exercises . . . . .	122
<b>8</b>	<b>Mean-Field Theory</b>	<b>125</b>
8.1	Mean-Field Ising Model . . . . .	125
8.2	Cell Theory for a Hard-Sphere Crystal . . . . .	128
8.3	Exercises . . . . .	131
<b>9</b>	<b>Landau Theory</b>	<b>139</b>
9.1	Introduction . . . . .	139
9.2	Case 1: A Continuous Phase Transition . . . . .	141
9.3	Case 2: A First-Order Phase Transition . . . . .	142
9.4	Example: Zero-Field Ising Model . . . . .	144
9.5	Example: Isotropic to Nematic Phase Transition . . . . .	144
9.6	Exercises . . . . .	148
<b>10</b>	<b>Real-Space Renormalization Group</b>	<b>153</b>
10.1	Site Percolation . . . . .	153
10.2	RG for the Zero-Field 1D Ising Model . . . . .	158
10.3	Exercises . . . . .	162
<b>11</b>	<b>Correlation Length and Functions</b>	<b>165</b>
11.1	Statistical Association and Causation . . . . .	165
11.2	Correlations and Ordering . . . . .	166
11.3	First-Order and Continuous Phase Transitions . . . . .	168
11.4	Correlation Function for the 1D Ising Model . . . . .	168
11.5	Correlations and Mean-Field Theory for the Ising Model . . . . .	170

<i>CONTENTS</i>	11
11.6 Exercises . . . . .	172
<b>12 Critical Exponents and Universality</b>	<b>175</b>
12.1 The Ising Model and the Gas-Liquid System . . . . .	175
12.2 Landau Theory Critical Exponents . . . . .	177
12.3 Exercises . . . . .	179
<b>13 Classical Non-Ideal Gases and Dilute Fluids</b>	<b>181</b>
13.1 Features of Atomic Gases . . . . .	181
13.2 Simple Interaction Models . . . . .	182
13.3 Van der Waals Theory . . . . .	183
13.4 Virial Expansion . . . . .	185
13.4.1 The Mayer Expansion . . . . .	186
13.4.2 The Second Virial Coefficient $B_2(T)$ . . . . .	187
13.4.3 The Third Virial Coefficient $B_3(T)$ . . . . .	188
13.4.4 Higher-Order Virial Coefficients and Diagrams . . . . .	188
13.5 Exercises . . . . .	191
<b>14 Classical Dense Fluids</b>	<b>195</b>
14.1 Structure Factor . . . . .	195
14.2 The Pair-Correlation Function . . . . .	197
14.3 Ornstein-Zernike Theory . . . . .	199
14.4 Thermodynamic Perturbation Theory . . . . .	202
14.5 Exercises . . . . .	205
<b>15 Gas-Liquid Interfaces and Classical Nucleation Theory</b>	<b>211</b>
15.1 Free Energy of the Interface . . . . .	211
15.2 Classical Nucleation Theory . . . . .	214
15.2.1 Homogeneous Nucleation . . . . .	215

15.2.2 Heterogeneous Nucleation . . . . .	216
15.3 Exercises . . . . .	218
<b>16 Multi-Component Fluids and Colloidal Suspensions</b>	<b>221</b>
16.1 Generalization of 1-Component Description to Mixtures . . . . .	221
16.2 Effective Interactions and the Osmotic Ensemble . . . . .	222
16.3 Effective Interaction induced by Ideal Component . . . . .	225
16.4 Colloid-Polymer Mixtures . . . . .	226
16.5 Exercises . . . . .	231
<b>17 Anisotropic Particles</b>	<b>233</b>
17.1 Partition Functions . . . . .	234
17.2 Onsager Theory . . . . .	236
17.3 The Hard-Rod Fluid . . . . .	238
17.4 Exercises . . . . .	241
<b>18 Moving away from Equilibrium</b>	<b>243</b>
18.1 Background to the Theory . . . . .	244
18.2 Static Fluctuation-Dissipation Theorem . . . . .	245
18.3 The Langevin Equation . . . . .	247
18.4 Dynamic Fluctuation-Dissipation Theorem . . . . .	249
18.4.1 Applying Fluctuation-Dissipation to Brownian Motion . . . . .	251
18.5 The Continuity Equation and Fickian Diffusion . . . . .	252
18.6 Active Brownian Particles . . . . .	253
18.7 Exercises . . . . .	256

# Chapter 1

## Thermodynamics

Before proceeding, it is important to once and for all make very clear the distinction between *thermodynamics*, *statistical physics*, and *statistical mechanics*. Thermodynamics describes the behavior of many-body systems using bulk quantities, such as pressure, temperature, *etc.* These quantities describe the *macroscopic* behavior of the system. In contrast, statistical mechanics starts with a *microscopic* picture of the system and uses this to determine macroscopic properties. Thus, thermodynamics follows from statistical mechanics in the limit of an infinite number of particles, which effectively holds for everyday situations. Statistical physics is a branch of physics that employs methods of probability theory and statistics, but does not focus exclusively on the derivation of thermodynamics from microscopic considerations. Statistical mechanics is therefore a subset of statistical physics, though the two terms are often loosely used, which has muddled the distinction.

In this chapter, we review the thermodynamics that we will need for this course. The topics herein are covered very briefly, as we assume familiarity with basic thermodynamics. Any reader that struggles with these concepts or requires a more in-depth refresher, is recommended to refer to a basic textbook on the subject (*e.g.*, Blundell & Blundell, the book used our Statistical Physics course [NS-204B]).

### 1.1 Intensive and Extensive Variables

The properties of any macroscopic system are characterized by measurable quantities, think temperature, mass, number of particles, pressure, volume, *etc.* We will frequently refer to such quantities as variables in a thermodynamic description of the system. The thermodynamic variables can be naturally divided into two types: *intensive* and *extensive*. The former do not depend on the size of the system; examples of such intensive variables are: temperature, pressure, and chemical potential. The latter, scale with the size of the system; examples of extensive variables are: volume, number of particles, entropy, and mass. The scaling is linear, *e.g.*, when bringing two (otherwise equivalent) systems with individual entropies  $S_1$  and  $S_2$  together the total entropy of the new system is  $S_t = S_1 + S_2$ . The same holds for the volume, number of particles. This leads to  $\lambda U(S, V, N) = S(\lambda S, \lambda V, \lambda N)$  with  $\lambda$  some scalar. You may recall that there is a natural pairing of extensive and intensive variables in formulating thermodynamic potentials, the elements of such a pair are referred to as *conjugate* variables. For instance, in writing down the change  $dU$  of the internal energy  $U$ , which we will turn to next, the pressure  $p$  is paired with volume  $V$  and the temperature  $T$  is paired with entropy  $S$ , where only one element of the pair is varied.

## 1.2 First Law

The first law of thermodynamics describes the empirical observation that the energy in a closed system is conserved. As a result, the internal energy  $U$  of a system can only be changed by: (i) performing work on the system or (ii) transferring energy to the system in the form of heat. Mathematically, we can write the first law as

$$dU = \delta Q + \delta W, \quad (1.1)$$

where  $dU$  is the change in internal energy,  $\delta Q$  is the heat added to the system and  $\delta W$  is the work done on the system. The underlined words are used here to indicate the direction which is associated with a positive sign. Note that  $dU$  is an *exact* differential, *i.e.*, a differential that does not depend on the path between two thermodynamic states. The differentials  $\delta Q$  and  $\delta W$  are *inexact*, which means that they do depend on the path between the two states.

### 1.2.1 Work

Given a generalized applied ‘force’  $\mathbf{f}$  and an associated (conjugate) extensive mechanical variable  $\mathbf{X}$ , the work done on a system is defined to be

$$\delta W = \mathbf{f} \cdot d\mathbf{X}. \quad (1.2)$$

We can exert many different types of  $\mathbf{f}$  on a system: pressure, an external field, a chemical potential, *etc.* In the case of an externally applied pressure, the conjugate variable would be the volume, leading to the expression for mechanical work:  $\delta W = -pdV$ . Here, the minus sign comes from the external application of the force on the system: for positive applied work the system’s volume shrinks as a consequence and its pressure goes up, hence the sign convention. Similarly, we can exert a mechanical force with magnitude  $f$  on a block resting on a floor, which moves as a consequence thereof. When the force is directed parallel to the floor, the distance  $x$  which the block moves is the conjugate variable; this gives us:  $\delta W = f dx$ . For chemical work, the force is the chemical potential  $\mu$  of the system, and the associated ‘distance’ is the change in the number of particles  $N$ . That is,  $N$  is the conjugate variable to  $\mu$  and this results in the work:  $\delta W = \mu dN$ . Positive chemical work on the system increases the number of particles in it. Lastly, we should note that electric and magnetic work can be performed, but that the latter is not without controversy [Macdonald, *Am. J. Phys.* **67**, 613 (1999)].

### 1.2.2 Exact versus Inexact

Before moving onto the second law of thermodynamics, let us briefly touch upon the concepts of (*in*)*exact* differentials again. In mathematics the concept of exact and inexact differentials is made precise using the language of calculus, where by exclusion *inexact* differentials are those differential forms that are not *exact*. An exact differential form (degree  $k + 1$ )  $g$ , is the exterior derivative of a (degree  $k$ ) differential form  $f$ . Thus, an exact form is in the image of  $d$  *via*  $g = df$ . This implies that  $g$  is closed ( $dg = 0$ ), because  $d^2f = 0$  for any differential form  $f$ . However, whether a closed form is exact depends strongly on the topology of the underlying space. The concept of exactness of differential forms on general manifolds touches upon the *Poincaré lemma* and *de Rham cohomology*. We will not further define these concepts here and refer to standard textbooks on differential calculus for more information. N.B. It is useful to consult a textbook written by physicists to gain a conceptual understanding.

Here, we will consider the paths shown in Fig. 1.1 to provide a minimal intuition into path dependence and hence the nature of exact and inexact differentials. In path I on the left, the volume  $V$  first increases

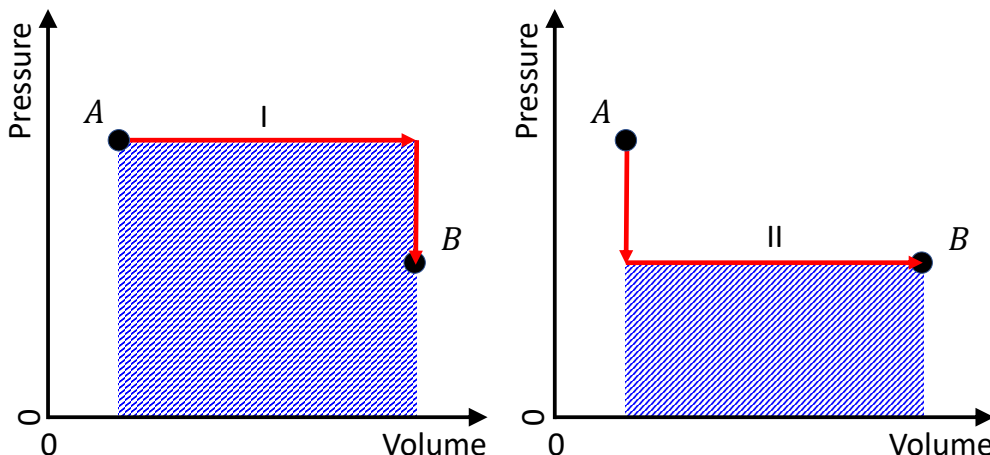


Figure 1.1: Comparison of two paths in a  $pV$ -diagram. The paths connect the points  $A$  and  $B$  that have identical coordinates on both diagrams. These respectively indicate the initial and final states of a closed system, for which work must be exerted to change the volume  $V$ . The hashing indicates the work performed during this process.

at constant pressure  $p$  ( $\Delta V > 0$ , external work done), then the pressure decreases at constant volume ( $\Delta V = 0$ , no work done). In path II on the right, these operations are performed in reverse order. In the  $pV$ -diagram, the area under the curve represents the work done during the transition from initial state to final state. This is represented by the hashed area. Clearly, the work done in passing from  $A$  to  $B$  is greater for path I than it is for path II. We conclude that unless the path is specified, the work done in the process  $A \rightarrow B$  cannot be determined. The associated differential  $\delta W$  must therefore be inexact. Referencing Eq. (1.1) and noting  $U_B - U_A$  is equal between the paths for a closed system, we know that  $\delta Q$  must also be different in such a way that the whole is an exact differential.

### 1.3 Second Law

There are many different (and equivalent) definitions for the second law given in literature; you may recall the Kelvin and Clausius statements from a basic statistical physics course and the proof of their equivalence. Common descriptions include: “heat can never flow spontaneously from a cold reservoir to a warmer one”, “it is impossible to convert heat to work with 100% efficiency”, and “the *entropy* in a closed system cannot decrease spontaneously”. For our purposes, we will write the second law in a mathematical formulation

$$dS \geq \frac{\delta Q}{T}, \quad (1.3)$$

where  $S$  is the entropy. This is an *extensive* thermodynamic variable that (historically) emerged in analyzing heat engines, such as the Carnot cycle. We will revisit this concept in Chapter 2, where we will consider the statistical mechanics definition in terms of microstates. A consequence of entropy is that certain processes are impossible, irrespective of conservation of energy, which is the requirement imposed by the first law of thermodynamics.

We note that the equality in Eq. (1.3) holds only when the heat  $\delta Q$  is taken up *reversibly* by the system. In this case, the entropy is a state function! A process is reversible, when taking the forward path

between two states  $A$  and  $B$  can be taken in reverse to arrive back at  $A$ . An example of a *reversible* process in thermodynamics is a slow compression of a gas (at fixed pressure and fixed number of particles) without going through a phase transition. Examples of *irreversible* processes are: plastic mechanical deformation under an applied force, heat flow from hot to cold with a finite temperature difference, and mixing of gasses. In general, reversible processes are idealizations of physical reality, where friction and dissipation are present. It is prudent to revisit your basic thermodynamic lecture notes and materials, if you struggle with the concepts of path dependence and entropy, and how these relate to heat engines and the laws of thermodynamics.

## 1.4 The $S, V, N$ Ensemble

Combining the first and second laws, we find the following expression for the change in internal energy of a system

$$dU = TdS - pdV + \mu dN. \quad (1.4)$$

From Eq. (1.4) it is clear that  $S$ ,  $V$ , and  $N$  are the natural variables for  $U$ . The internal energy is special among the thermodynamic potentials that we will introduce shortly, as it is the only one that exclusively depends on extensive variables. Note that  $dU$ ,  $dS$ ,  $dV$  and  $dN$  are all exact differentials and describe state functions, *i.e.*, functions that only depend on the current state of the system and not the path by which the system arrived at this state. As a result, Eq. (1.4) holds even in the case of irreversible processes, under the *strong* assumption that a (at least one) reversible process exists between the initial and final states. From this we can easily show that

$$T = \left( \frac{\partial U(S, V, N)}{\partial S} \right)_{V, N}, \quad p = - \left( \frac{\partial U(S, V, N)}{\partial V} \right)_{S, N}, \quad \mu = \left( \frac{\partial U(S, V, N)}{\partial N} \right)_{S, V}. \quad (1.5)$$

Thus, the conjugate — in this case intensive — variables may be obtained from the natural variables of the thermodynamic potential through partial differentiation. This implies that thermodynamic potentials are determined up to a constant, effectively irrelevant offset. That is, this offset drops out of any physical quantity that results from imposing the value of the natural variables.

## 1.5 Legendre Transforms

It is not always convenient to work at constant  $S$ ,  $V$ , and  $N$ . Experimentally, for instance, it is not feasible to control the entropy directly! Hence, we require a way to construct thermodynamic potentials that depend on other variables, *e.g.*,  $N$ ,  $V$ , and  $T$ . This can be done using Legendre transforms. You may recall this transformation from an advanced mechanics course or basic statistical physics. Unfortunately, Legendre transforms are often relegated to a footnote in a textbook, or worse presented as a complicated mathematical procedure. Before we proceed, we shall briefly rectify this situation here, showing that it is nothing more than an application of the product rule to differentials.

Assume we have a real-valued function  $f$  which is a natural function of a set of  $n$  variables  $\{x_i\}$ . Then the differential may be written as

$$df = \sum_{i=1}^n u_i dx_i, \quad \text{with} \quad u_i = \left( \frac{\partial f}{\partial x_i} \right)_{\{x_j \neq i\}}. \quad (1.6)$$

Here, the  $u_i$  serve as the conjugate variables to the  $x_i$ . Now, let us define a new function  $g$  such that

$$g = f - u_k x_k, \quad (1.7)$$

for some chosen  $k$  between 1 and  $n$ . If we now calculate  $dg$ , we see

$$dg = df - (u_k dx_k + x_k du_k) = \sum_{\substack{i=1 \\ i \neq k}}^n u_i dx_i + (-x_k) du_k, \quad (1.8)$$

meaning that  $g$  is a natural function of variables  $x_1, x_2, \dots, x_{k-1}, u_k, x_{k+1}, \dots$ , and  $x_n$ . Now  $g$  is the Legendre transform of  $f$ .

Note that we have swept two rather important aspects of  $f$  under the rug in our above derivation. In order to be able to Legendre transform  $f$ : (i) The function must be strictly convex. For a single-variable function, this implies that its second derivative is strictly positive. This, in turn, implies strict monotonic increase of the first derivative, *i.e.*, it may be inverted. (ii) The function must be sufficiently smooth. The latter is casually assumed to be true for most physical systems.

### 1.5.1 Geometric Interpretation of the Legendre Transformation

A representation of the Legendre-transform is provided in Fig. 1.2 that motivates the above mathematical statements. It is included here to provide graphical insight into choice for Eq. (1.7) as originally made by Legendre. The left panel shows the difference between a convex (solid blue) and non-convex function (dotted red). We will encounter the shape of the latter again in Chapter 6, where we will discuss the implications of being non-convex on phase transitions.

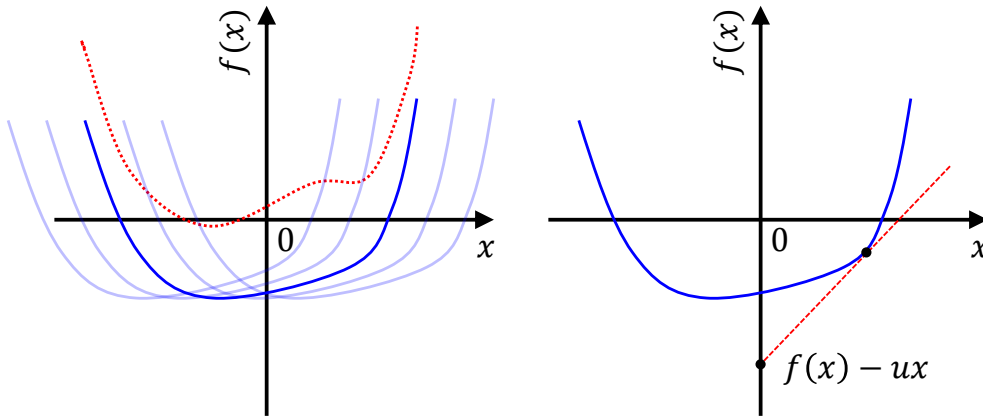


Figure 1.2: Graphical representation of the Legendre transformation. (left) A convex function  $f(x)$  (solid blue curve) and a non-convex function (dotted red curve). We also indicate a family of functions  $\tilde{f}$  (solid light-blue curves) that follow from  $f$ . If we assign  $u = \partial f / \partial x$  for the slope, then each member of the family gives rise to the same value of  $f(u)$ , where we have used inversion to write  $x(u)$ . (right) The tangent line (dashed red) construction for the Legendre transform.

Let us consider a single-variable, single-valued function  $f(x)$ . We want to somehow express  $f$  as a function of its slope  $u(x) = \partial f / \partial x$ . Simply writing  $f(u)$  is insufficient, as the left-hand side of Fig. 1.2 shows. There is a family of functions  $\tilde{f}$  that gives the same value of  $f$  as a function of their respective derivative  $\tilde{u}$ . This implies that in transitioning from  $f(x)$  to  $f(u)$  information is lost, *i.e.*, there is no unique back transformation from  $f(u)$  to  $f(x)$ , even if  $u$  is invertible.

Taking the tangent line to a specific point of  $f$ , we can construct the intercept with the vertical axis, see the right-hand panel to Fig. 1.2. Note that this intercept is  $g(x)$  as defined in Eq. (1.7). However, this is still not sufficient, because we require  $g(u)$ , which is where we rely on the convexity condition on  $f$  to invert  $u(x)$  to  $x(u)$ . Why is this an acceptable definition of a Legendre transform? The intercept seems an arbitrary choice. However, note that this is a number for which a line with slope  $u(x)$  is tangent to  $f(x)$ . That is, given  $g(u)$ ,  $u$ , and  $x$ , you will uniquely define  $f(x)$ , rather than a family of curves as on the left-hand side of Fig. 1.2. We refer the interested (or confused) reader to the pedagogical discussion of the Legendre transform by Zia *et al.* [Am. J. Phys. **77**, 614 (2009)] for further information.

### 1.5.2 The $N, V, T$ Ensemble

We can now use the Legendre transformation to switch between different thermodynamic potentials, *i.e.*, ones that depend on natural variables. Specifically, at constant  $N$ ,  $V$ , and  $T$ , the relevant free energy is called the *Helmholtz free energy* and it is constructed by

$$dF = dU - TdS - SdT = -SdT - pdV + \mu dN. \quad (1.9)$$

Hence,  $F = U - TS$  and

$$S = - \left( \frac{\partial F(N, V, T)}{\partial T} \right)_{N, V}, \quad p = - \left( \frac{\partial F(N, V, T)}{\partial V} \right)_{N, T}, \quad \mu = \left( \frac{\partial F(N, V, T)}{\partial N} \right)_{V, T}. \quad (1.10)$$

Lastly, we remark that in literature, the Helmholtz free energy is often simply referred to as the free energy and can be denoted by  $A$  rather than  $F$ .

### 1.5.3 The $N, P, T$ Ensemble

Similarly, we can construct a free energy at constant  $N$ ,  $p$ , and  $T$  in the following manner

$$dG = dU - TdS - SdT + pdV + Vdp = -SdT + Vdp + \mu dN \quad (1.11)$$

such that  $G = U - TS + pV$ . This is called the *Gibbs free energy* and has the following derivatives

$$S = - \left( \frac{\partial G(N, p, T)}{\partial T} \right)_{N, p}, \quad V = \left( \frac{\partial G(N, p, T)}{\partial p} \right)_{N, T}, \quad \mu = \left( \frac{\partial G(N, p, T)}{\partial N} \right)_{p, T}. \quad (1.12)$$

### 1.5.4 The $\mu, V, T$ Ensemble

The case with independent variables  $(T, V, \mu)$  corresponds to the *grand potential*  $\Omega$  and is given by

$$d\Omega = -SdT - pdV - Nd\mu \quad (1.13)$$

with

$$S = - \left( \frac{\partial \Omega(T, V, \mu)}{\partial T} \right)_{V, \mu}, \quad p = - \left( \frac{\partial \Omega(T, V, \mu)}{\partial V} \right)_{T, \mu}, \quad N = - \left( \frac{\partial \Omega(T, V, \mu)}{\partial \mu} \right)_{T, V}. \quad (1.14)$$

### 1.5.5 The Gibbs-Duhem Relation

It follows from Eq. (1.14) that at fixed  $T$  and  $\mu$ :  $d\Omega = -pdV$ . Hence, the corresponding changes of  $\Omega$  are identical to the mechanical work on the system. The requirement of extensiveness of  $\Omega$  and  $V$  leads directly to

$$\Omega(T, V, \mu) = -p(\mu, T)V. \quad (1.15)$$

which implies that  $p$  is a function of  $T$  and  $\mu$ . From  $\Omega = -pV$  we also deduce that  $d\Omega = -pdV - Vdp$ , which upon combination with  $d\Omega = -SdT - pdV - Nd\mu$  yields the Gibbs-Duhem relation  $dp = \rho d\mu + \sigma dT$  with  $\rho = N/V$  the particle density and  $\sigma = S/V$  the entropy density. Alternatively, one writes the Gibbs-Duhem relation as  $d\mu = vdp - sdT$  with  $v = V/N$  the volume per particle and  $s = S/N$  the entropy per particle, *i.e.*,  $\mu$  is a function of  $p$  and  $T$ . In other words, there is a relation between the intensive variables describing the system. This implies that in a one component system there are 2 rather than 3 degrees of freedom. The generalization of this statement is referred to as the *phase rule*.

## 1.6 Exercises

### Q1. Intensive Variables

Consider constructing a thermodynamic potential for an ensemble where all the intensive variables ( $T$ ,  $p$ , and  $\mu$ ) are fixed. Would this be possible? Explain.

### Q2. Legendre Transforms *from David Chandler (Introduction to Modern Physics)*

As we discussed in class, Legendre transforms are a very useful way to convert between different ensembles. Determine the Legendre transform of the entropy which is a natural function of:

- (a)  $1/T$ ,  $V$ ,  $N$
- (b)  $1/T$ ,  $V$ ,  $\mu/T$

### Q3. Maxwell Relations

Maxwell's relations allow us to examine the way many different types of measurements can be related. For instance, we can look at how the entropy changes as we change the volume if we hold  $N$  and  $T$  constant:

$$\left(\frac{\partial S}{\partial V}\right)_{T,N}. \quad (1.16)$$

Note that  $df = adx + bdy$  implies  $(\partial a/\partial y)_x = (\partial b/\partial x)_y$ . Hence, from the Helmholtz free energy  $dF = -SdT - pdV + \mu dN$ , we can directly obtain the Maxwell relation

$$\left(\frac{\partial S}{\partial V}\right)_{T,N} = \left(\frac{\partial p}{\partial T}\right)_{V,N}. \quad (1.17)$$

- (a) If we define

$$C_V = T \left(\frac{\partial S}{\partial T}\right)_{V,N}, \quad (1.18)$$

then show that

$$\left(\frac{\partial C_V}{\partial V}\right)_{T,N} = T \left(\frac{\partial^2 p}{\partial T^2}\right)_{V,N}. \quad (1.19)$$

- (b) Derive an analogous formula for

$$\left(\frac{\partial C_p}{\partial p}\right)_{T,N}, \quad (1.20)$$

assuming

$$C_p = T \left(\frac{\partial S}{\partial T}\right)_{p,N}. \quad (1.21)$$

### Q4. The Triple-Product Relation

By now you are familiar with the formula

$$dE = TdS - PdV + \mu dN. \quad (1.22)$$

Using this formula, one can derive the definition for, *e.g.*, the pressure

$$P = - \left(\frac{\partial E}{\partial V}\right)_{S,N}. \quad (1.23)$$

- (a) Rewrite the above equation to the form
- $dS = \dots$
- , and find expressions for

$$\left(\frac{\partial S}{\partial V}\right)_{N,E} \quad \text{and} \quad \left(\frac{\partial S}{\partial N}\right)_{V,E}. \quad (1.24)$$

- (b) Now, consider the more general formula of this type
- $Adx + Bdy + Cdz = 0$
- . By finding expressions for

$$\left(\frac{\partial z}{\partial x}\right)_y, \quad \left(\frac{\partial z}{\partial y}\right)_x, \quad \text{and} \quad \left(\frac{\partial y}{\partial x}\right)_z, \quad (1.25)$$

derive the triple product relation

$$\left(\frac{\partial x}{\partial y}\right)_z \left(\frac{\partial y}{\partial z}\right)_x \left(\frac{\partial z}{\partial x}\right)_y = -1. \quad (1.26)$$

- (c) You can also derive the triple product relation in a more intuitive way using geometry, see Fig. 1.3. Imagine a surface given by
- $z(x, y)$
- with a triangle drawn on it, see the figure below.

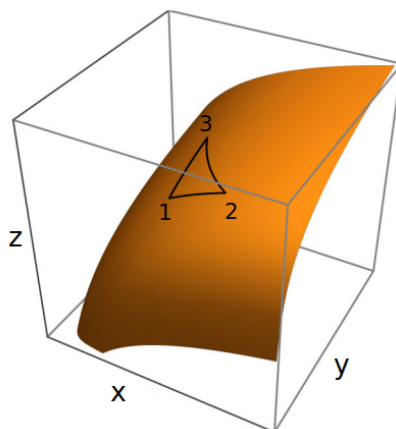


Figure 1.3: Geometric representation of the triple-product rule.

This particular triangle is special: when you go from point 1 to point 2,  $y$  is kept constant. Similarly,  $z$  is kept constant going from 2 to 3, and  $x$  is kept constant going from 3 to 1. Starting at point 1, which has the position  $(x_0, y_0, z_0)$ , we follow the line from 1 to 2 to find an expression for the position of point 2

$$(x_0 + \Delta x, y_0, z_0 + \left(\frac{dz}{dx}\right)_y \Delta x), \quad (1.27)$$

where  $\Delta x$  is the distance traveled in the  $x$ -direction going from point 1 to 2. In a similar fashion, continue following the line to point 3, and find an expression for the position of point 3. Then, follow the line from point 3 to point 1, and find an expression for the position of point 1. Compare this expression to  $(x_0, y_0, z_0)$  to derive the triple product relation.

- (d) Use the triple-product rule to show that entropy maximization implies internal energy minimization for an isolated system. Start by writing down the conditions for having a maximum in
- $S$
- in terms of
- $U$
- and the other thermodynamic variables.

## Q5. The Second Law

Theorem: “It is impossible to build a machine that converts a certain amount of heat deducted from a heat bath into work without any other change in the machine or the environment.” In this exercise, we show that this theorem implies that there has to be a function of state  $S$  (that we call entropy), without making use of any microscopic information, *e.g.*, that matter consists of many atoms and hence can be in many microstates.

- (a) Figure 1.4 represents a heat bath at temperature  $T$ . A (according to the theorem impossible) machine takes up an amount of heat  $Q$  from that heat bath in order to conduct an amount of work  $W$ , after which the machine and the environment return to their initial state, such that the process can repeat itself. Argue that the entropy of the machine and its environment

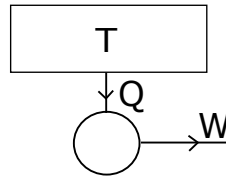


Figure 1.4: Schematic of a machine capable of taking up an amount of heat  $Q$  from a heat bath at temperature  $T$  and converting this into work  $W$ .

does not change during the process, and that the entropy of the heat bath decreases. By how much? Is the theorem a version of the second law of thermodynamics?

- (b) Although it is not possible to convert all heat from a heat bath to work, it is certainly possible to convert a part of the heat to work. Figure 1.5 shows the machine  $M$  that takes up an

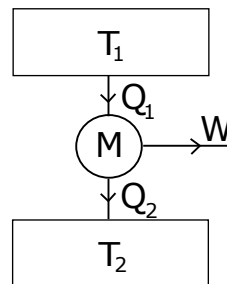


Figure 1.5: A more involved machine that not only takes up heat  $Q_1$  from a bath at temperature  $T_1$ , but also puts some of it  $Q_2$  back into another bath at temperature  $T_2$ , while converting some of the heat taken up into work  $W$ .

amount of heat  $Q_1$  from a heat bath (“boiler”) at temperature  $T_1$ , conducts work  $W$  and deposits heat  $Q_2$  in a cold heat bath (“condenser”) at temperature  $T_2$ . What is the relation between  $Q_1$ ,  $Q_2$  and  $W$  according to the first law of thermodynamics?

We next assume that  $M$  is reversible, *i.e.*, the machine can go backwards through reversing the inputs and outputs (the machine hence takes up work  $W$  from the environment, takes up heat  $Q_2$  from the cold heat bath and deposits heat  $Q_1$  in the warm heat bath) [think about a fridge]. We consider now another machine  $M'$ , not necessarily reversible, that also operates between the

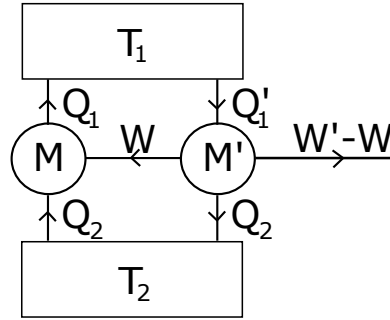


Figure 1.6: Representation of coupled heat engines, of which  $M$  is reversible and  $M'$  is not necessarily reversible, also see the description in the question.

temperatures  $T_1$  and  $T_2$ . This machine takes up an amount of heat  $Q'_1$  from the warm bath, conducts work  $W'$ , and is constructed such that precisely  $Q_2$  is dumped into the cold bath (not  $Q'_2$ ). As indicated in the sketch below, work  $W'$  is partly used to turn back machine  $M$ , and the rest  $W' - W$  can be used for other purposes, this situation is represented in Fig. 1.6.

- Show that the theorem applied to the combined machine  $M+M'$  forbids that  $W' - W > 0$ . It follows that  $W' \leq W$ . Check that this implies that no machine can be more efficient than a reversible machine! You should define efficiency as delivered work per amount of heat taken up from the boiler.
- Assume now that  $M'$  is also a reversible machine. Show that then  $W = W'$ . The brilliant conclusion drawn by Carnot is that every reversible machine regardless of the design delivers the same amount of work per unit heat for fixed  $T_1$  and  $T_2$ . The function  $W(Q_1, T_1, T_2)$  is therefore a property of nature, not of the machine!
- Since every reversible machine delivers the same amount of work  $W(Q_1, T_1, T_2)$ , it can be calculated by considering a very simple machine, *e.g.*, the Carnot cycle of a classic monoatomic ideal gas. Use that  $Q_1/T_1 = Q_2/T_2$  for a Carnot engine (this can be shown, but you do not need to do that). Combine this with your answer to part (b) and calculate the universal maximum amount of work  $W(Q_1, T_1, T_2)$ .
- Now consider an infinitesimal reversible change in the state of a certain quantity of matter by means of an amount of work  $dW$  done by the system and/or a receiving an amount of heat  $dQ$ . We know already that  $dE = dQ - dW$  does not depend on the path chosen from the initial to the final state, but  $dQ$  and  $dW$  do. Why was this again? Consider the quantity

$$\int_b^e \frac{dQ}{T}$$

over a reversible path from an initial state  $b$  to another final state  $e$ . The question is now if this integral depends on the chosen path. The answer is no. Argue that based on the fact that each reversible cycle can be built up by a large number of small Carnot cycles, such that it follows for each reversible loop process  $\oint dQ/T = 0$ . It follows then that  $dS = \frac{dQ}{T}$  is a total differential, and thus  $S$  is a function of state (that is hence independent of how the system arrived at a certain state). To understand the meaning of  $S$  requires a microscopic theory (such as statistical mechanics), but the existence of a state function  $S$  follows purely macroscopic (thermodynamic) considerations as you have in this exercise.



## Chapter 2

# Statistical Mechanics

In thermodynamics, we describe the behavior of many-body systems using bulk quantities, such as pressure, temperature, *etc.* These quantities describe the *macroscopic* behavior of the system. In contrast, in statistical mechanics, also often referred to as statistical thermodynamics for this purpose, we start with a *microscopic* picture of the system and use it to derive the macroscopic properties. To this end, we often distinguish between microstates and macrostates. In a microstate, we specify the value of every degree of freedom available to our system. For instance, the position and momentum of all particles in a gas, or the direction of all spins in a magnet. A macrostate, however, contains many microstates, and classifies systems based on macroscopically measurable quantities. The information that is lost by translating between a microstate and macrostate description of a system gives insight into the concept of entropy, as we shall see.

Formulating the link between microscopic realizations of the system and macroscopic observables is one of the major success stories in modern physics. It is particularly appealing that the theory hinges on a single fundamental assumption, which leads to thermodynamics, after some (times laborious) mathematical derivations. Throughout this chapter, we will assume discrete (countable) microstates and we refer to Chapter 3 for a discussion of classical continuous ensemble theory.

### 2.1 The Microcanonical Ensemble: Fixed $U$ , $V$ and $N$

The microcanonical ensemble consists of all microstates that correspond to a fixed choice of number of particles  $N$ , volume  $V$ , and total energy  $U$ . The microcanonical ensemble corresponds to a closed system, *i.e.*, it cannot exchange energy, volume, or particles with the rest of the world, see Fig. 2.1(left).

The *fundamental assumption of statistical mechanics* states that: When a system is in equilibrium, all microstates of a closed system are equally likely. In other words, if we have some way of counting the number of possible states  $\Omega(N, V, U)$ , then the probability to find a closed system in a microstate  $m$  is given by

$$P(m) = \begin{cases} \frac{1}{\Omega(N, V, U)} & \text{if } U(m) = U \\ 0 & \text{if } U(m) \neq U \end{cases} . \quad (2.1)$$

Here,  $U(m)$  is the total energy of microstate  $m$ . Note that the above expression conditions microstates  $m$  to satisfy the internal energy criterion, *i.e.*, only states with internal energy  $U$  are permitted. This

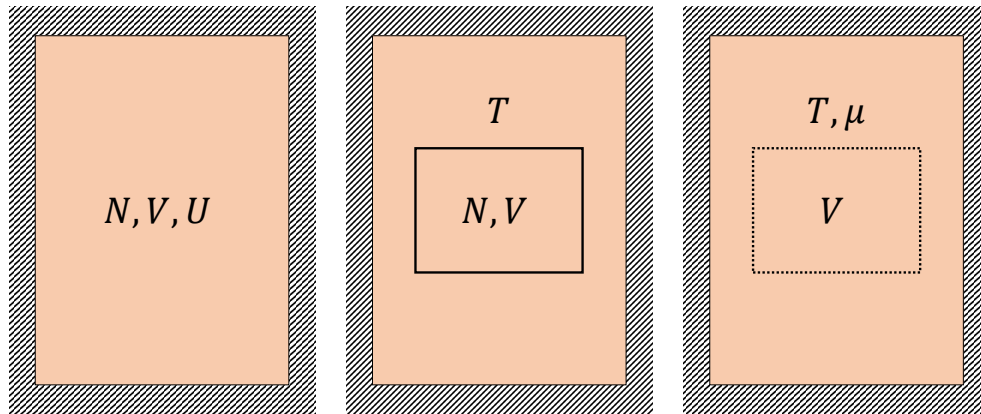


Figure 2.1: Visual representation of the ensemble construction that is discussed in this chapter. (left) The microcanonical ensemble. This ensemble is characterized by an isolated system with fixed volume  $V$ , number of particles  $N$ , and energy  $U$ . (middle) The canonical ensemble. We consider a region of interest with fixed particle number  $N$  and volume  $V$  (black rectangle) that is embedded in a much larger microcanonical volume. This volume serves as a reservoir with effective temperature  $T$ , which can exchange energy with the canonical region of interest. This canonical region is thus maintained at temperature  $T$ , but has fluctuations in  $U$ . (right) The grand canonical ensemble. We now consider a region with fixed volume  $V$  (dashed black rectangle) that can exchange energy and particles with its embedding microcanonical reservoir with associated temperature  $T$  and chemical potential  $\mu$ .

type of, admittedly slightly convoluted, notation will be useful in discussing the microcanonical ensemble in continuum phase space in Chapter 3.

## 2.2 Entropy and Temperature

We define the entropy of the system as

$$S(N, V, U) = k_{\text{B}} \log \Omega(N, V, U), \quad (2.2)$$

where  $k_{\text{B}} = 1.38 \cdot 10^{-23} \text{ J/K}$  is Boltzmann's constant. The temperature is then obtained through the relation

$$\frac{1}{T} = \left( \frac{\partial S}{\partial U} \right)_{N, V}. \quad (2.3)$$

Note that in the following we will often use the inverse thermal energy, which we define as  $\beta = 1/(k_{\text{B}}T)$ , and which is sometimes referred to as an inverse temperature. Note that this also makes sense from our combined expression of the first and second law in Chapter 1, as  $V$  and  $N$  are fixed.

## 2.3 The Canonical Ensemble: Fixed $N$ , $V$ , and $T$

Thus far, we have explored the microcanonical ensemble. Here, we see how we can use the microcanonical ensemble to derive the canonical ensemble. Assume we have a subsystem with a fixed number of particles

$N$  and fixed volume  $V$  that is sitting in a large reservoir, see Fig. 2.1(middle). Assume further that the total system (subsystem plus reservoir) is closed, and that the subsystem can exchange energy with the reservoir. Let  $\Omega_r(U_r)$  be the number of microstates of the reservoir with energy  $U_r$ , and let  $\epsilon_m$  be the energy of the subsystem in microstate  $m$ . The total energy of the closed system is given by  $U_{\text{tot}} = U_r + \epsilon_m$ . The total number of microstates of the closed system can be expressed as

$$\Omega_{\text{tot}} = \sum_m \Omega_r(U_{\text{tot}} - \epsilon_m), \quad (2.4)$$

where  $\sum_m$  indicates a sum over all microstates of the subsystem. From the fundamental assumption of statistical physics, every microstate of the closed (total) system is equally likely. Then, if  $P_m$  is the probability of finding the subsystem in state  $m$ , we have

$$P(m) = \frac{\Omega_r(U_{\text{tot}} - \epsilon_m)}{\Omega_{\text{tot}}}. \quad (2.5)$$

That is,  $P(m)$  is the fraction of the total number of microstates, for which the subsystem is in state  $m$ .

We will now rewrite the probability using the mathematical identity (“log” denotes the natural logarithm throughout):

$$\Omega_r(U_{\text{tot}} - \epsilon_m) = \exp[\log[\Omega_r(U_{\text{tot}} - \epsilon_m)]]. \quad (2.6)$$

If we assume the reservoir is very large, then  $U_{\text{tot}} \gg \epsilon_m$ . Next, we Taylor expand Eq. (2.6) around  $U_{\text{tot}}$  to obtain

$$\Omega_r(U_{\text{tot}} - \epsilon_m) \approx \exp[\log[\Omega_r(U_{\text{tot}})] - \beta\epsilon_m], \quad (2.7)$$

where we have used

$$\beta \equiv \frac{\partial \log \Omega_r(U_{\text{tot}})}{\partial U_{\text{tot}}}, \quad (2.8)$$

which follows from the definition of temperature given in Eq. (2.3). Plugging this into the probability  $P(m)$  we obtain

$$P(m) = \frac{\Omega_r(U_{\text{tot}})e^{-\beta\epsilon_m}}{\Omega_r(U_{\text{tot}})\sum_m e^{-\beta\epsilon_m}} \equiv \frac{e^{-\beta\epsilon_m}}{Z(T, V, N)}, \quad (2.9)$$

where  $Z(T, V, N)$  is the *partition function*, which is given by

$$Z(N, V, T) = \sum_m e^{-\beta\epsilon_m}. \quad (2.10)$$

The distribution function  $e^{-\beta\epsilon_m}$  is called the Boltzmann distribution and indicates the probability of encountering a state with energy  $\epsilon_m$  given a fixed temperature  $T$ . The associated Helmholtz free energy, *i.e.*, the free energy in the  $N$ ,  $V$ , and  $T$  ensemble, is given by  $\beta F(N, V, T) = -\log(Z(N, V, T))$ .

Now that we have access to the probability distribution, we can determine averages, such as the average energy

$$E \equiv \langle \epsilon_m \rangle = \sum_m \epsilon_m P(m) = \frac{1}{Z} \sum_m \epsilon_m e^{-\beta\epsilon_m}. \quad (2.11)$$

This itself can be cast into a derivative of the partition function

$$E = \frac{1}{Z} \sum_m \left[ -\frac{\partial}{\partial \beta} e^{-\beta\epsilon_m} \right] = -\frac{\partial}{\partial \beta} \log Z, \quad (2.12)$$

where in the second step we used the chain rule. In statistical mechanics, the partition functions contain the properties of the system within them. Thus, once we know the partition function — which may in

practise be very hard to compute — we can derive from it the macroscopic physical quantities of interest. Here, one must be careful in recognizing that the thermodynamic relations between averaged quantities, such as  $U$ ,  $S$ , and  $F$ , hold only in the thermodynamic limit, but they can be extended to effectively hold for systems containing  $N \gg 1$  particles. Thus, it is commonplace to make the identification  $U = E$ , but that technically requires our small subsystem to be sufficiently large that the energy fluctuations on  $E$  are negligible. You will encounter several examples of this in the exercises associated with this chapter.

## 2.4 The Grand-Canonical Ensemble: Fixed $\mu$ , $V$ , and $T$

Assume we have a closed system with a total energy  $U_{\text{tot}}$  and a total number of particles  $N_{\text{tot}}$ . Consider a relatively small subvolume  $V$  in thermal and diffusive contact with the rest of the closed system, see Fig. 2.1(right). That is, the rest of the system plays the role of a heat and particle reservoir. The subsystem can be in many microstates, which we label by  $(m, N)$ , where  $N$  denotes the number of particles in the subvolume  $V$  and  $m = m(N, V)$  denotes the number of microstates with  $N$  particles in a volume  $V$  that have energy  $\epsilon_m$ . If the subsystem is in microstate  $(m, N)$ , then the reservoir must have an energy  $U_r \equiv U_{\text{tot}} - \epsilon_m$  and a number of particles  $N_r \equiv N_{\text{tot}} - N$ . The number of microstates in the reservoir is  $\Omega_r(U_r, N_r)$ .

The total number of states of the closed system as a whole is thus

$$\Omega_{\text{tot}} = \sum_{N=0}^{N_{\text{tot}}} \sum_m \Omega_r(U_{\text{tot}} - \epsilon_m, N_{\text{tot}} - N), \quad (2.13)$$

and the probability for each of these states is  $1/\Omega_{\text{tot}}$  as they are all equally probable according to the fundamental assumption. Equation (2.13) leads to the grand-canonical probability for a microstate  $(m, N)$  that reads

$$\begin{aligned} P_{m,N}^{(\text{gc})} &= \frac{\Omega_r(U_{\text{tot}} - \epsilon_m, N_{\text{tot}} - N)}{\Omega_{\text{tot}}}; \\ &= \frac{\Omega_r(U_{\text{tot}}, N_{\text{tot}}) \exp(-\beta\epsilon_m + \beta\mu N)}{\Omega_r(U_{\text{tot}}, N_{\text{tot}}) \sum_{N=0}^{N_{\text{tot}}} \sum_m \exp(-\beta\epsilon_m + \beta\mu N)} \equiv \frac{\exp(-\beta\epsilon_m + \beta\mu N)}{\Xi(\mu, V, T)}, \end{aligned} \quad (2.14)$$

where we have used

$$\beta\mu \equiv -\frac{\partial \log \Omega_r(U_{\text{tot}}, N_{\text{tot}})}{\partial N_{\text{tot}}} \quad (2.15)$$

and

$$\beta \equiv \frac{\partial \log \Omega_r(U_{\text{tot}}, N_{\text{tot}})}{\partial U_{\text{tot}}}. \quad (2.16)$$

Note that  $\mu$  and  $\beta = 1/k_{\text{B}}T$  are the chemical potential and inverse thermal energy of the reservoir, respectively. We also used the fact that  $N_{\text{tot}} \gg N$  and  $U_{\text{tot}} \gg U$ , *i.e.*, that the reservoir is sufficiently large that the relation

$$\Omega_r(U_{\text{tot}} - \epsilon_m, N_{\text{tot}} - N) = \Omega_r(U_{\text{tot}}, N_{\text{tot}}) \exp(\beta\mu N - \beta\epsilon_m) \quad (2.17)$$

is exact. Note that the existence of the reservoir only appears through the parameters  $\beta$  and  $\mu$ . Lastly, above we have defined

$$\Xi(\mu, V, T) \equiv \sum_{N=0}^{N_{\text{tot}}} \sum_m \exp[\beta\mu N - \beta\epsilon_m] = \sum_{N=0}^{N_{\text{tot}}} \exp(\beta\mu N) Z(N, V, T), \quad (2.18)$$

which is called the grand-canonical partition function. Note that often the number of particles in the reservoir may be assumed to be infinite, so that the above sum runs to infinity. However, this need not always be the case in practical examples, as we will encounter in the exercises.

All microstates of the subsystem with volume  $V$  are allowed: high-energy states, low-energy states, and states with small and large numbers of particles. Clearly, these states are not all equally probable as their statistical weight depends on  $\epsilon_m$  and  $N$  through Eqs. (2.14) and (2.18) for given  $T$  and  $\mu$ . One can show, however, that the average energy  $U = \langle \epsilon_m \rangle$  and the average number of particles  $\langle N \rangle$  are at the maximum of strongly peaked Gaussian distributions for macroscopically large systems, allowing for fluctuations that scale with  $\langle N \rangle^{1/2}$ . These fluctuations can thus be ignored in the thermodynamic limit, where we can speak of the number of particles  $N$  and the energy  $U$  of the system. The grand potential, *i.e.*, the free energy in the  $\mu, V$ , and  $T$  ensemble is given by

$$\beta\Omega(\mu, T, V) = -\log \Xi(\mu, V, T). \quad (2.19)$$

## 2.5 Constraints and Lagrange Multipliers

In this chapter, we will see the first instance of constraint minimization (or maximization) in one of the exercises. We will encounter this type of calculation several times throughout the course and therefore dedicate some time to it presently. Constraint minimization is most easily handled by the introduction of Lagrange multipliers. The Lagrangian and Lagrange multipliers are typically covered in advanced mechanics lectures, which you may not have followed yet. The gist of how they work is therefore laid out in this subsection.

For a two-dimensional function  $f(x, y)$  subjected to a constraint  $g(x, y) = c$ , a new function  $L(x, y, \lambda) = f(x, y) - \lambda(g(x, y) - c)$  may be introduced, where,  $\lambda$  is called the *Lagrange multiplier*. The idea is to minimize  $L$  so that the minimum of  $f$  is found under the constraint  $g = c$ . Geometrically the picture is as follows. The constraint  $g = c$  maps out a surface in  $(x, y)$  space. For a value in the range of the function  $f$ , say  $q$ , the equation  $f = q$  maps out another surface. If  $q$  is chosen much smaller than the value for which  $f$  also satisfies the constraint, then the surface of  $f = q$  is disjoint from that generated by  $g = c$ . By slowly increasing  $q$ , the point at which the surfaces first touch is found. This is the desired value of  $q$  (say  $q^*$ ) with associated contact point  $(x^*, y^*)$ .

When two surfaces just touch, their tangent spaces coincide, so the gradient of  $f$  with respect to the space coordinates (this maps out the tangent space) is some multiple of that of  $g$  ( $\lambda$  of course). In algebraic form this condition is obtained by  $\nabla L(x, y, \lambda) = 0$ , which gives the extremal points  $(x^*, y^*)$  for which  $\nabla f = \lambda \nabla g$ , *i.e.*, exactly the necessary condition for the tangent requirement. Note that  $(x^*, y^*)$  are dependent on  $\lambda$  and by plugging these solutions into  $g = c$ , an equation for  $\lambda$  is obtained, which may be solved for to eliminate  $\lambda$  from the problem. Note that this condition is readily recovered from the Lagrangian by minimization

$$\frac{\partial L(x, y, \lambda)}{\partial \lambda} = 0. \quad (2.20)$$

We can also provide a proof of the formalism. Let  $\mathbf{p}(t)$  be a path, which lies on the  $n$ -dimensional constraint surface imposed by  $g(\mathbf{r}) = c$ , where  $\mathbf{r}$  denotes the spatial coordinates. Suppose that the function  $f(\mathbf{r})$  has an extremum at the point  $\mathbf{P}$  on the constraint surface and that  $\mathbf{p}(0) = \mathbf{P}$ . Let  $h(t) = f(\mathbf{p}(t))$ . Then our setup guarantees that  $h(t)$  has a maximum at  $t = 0$ . Taking the derivative of  $h(t)$  and using the chain rule, we find

$$\frac{dh}{dt}(t) = \nabla_{\mathbf{r}} f(\mathbf{r})|_{\mathbf{r}=\mathbf{p}(t)} \cdot \frac{d\mathbf{p}}{dt}(t), \quad (2.21)$$

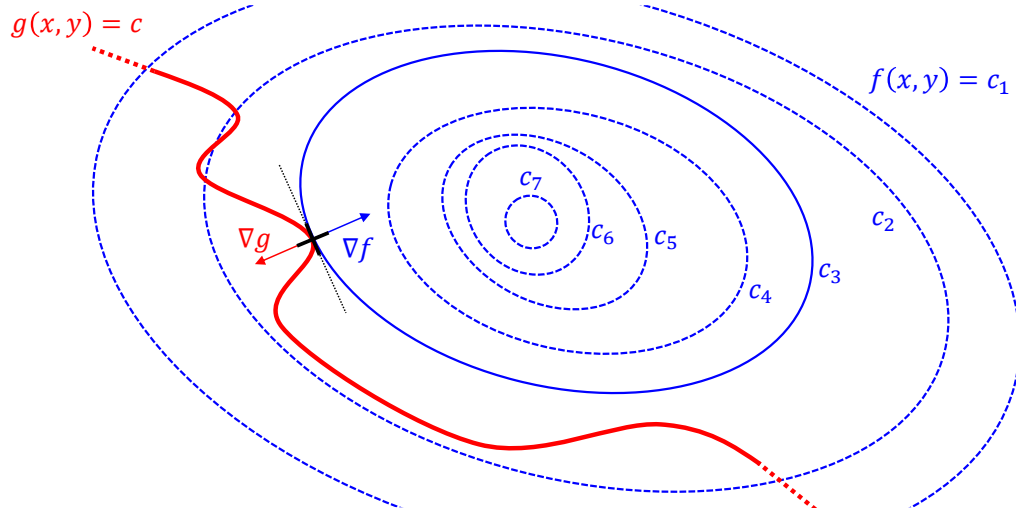


Figure 2.2: Illustration of constraint minimization *via* the Lagrange-multiplier formalism. We have function  $f$  that takes two-dimensional coordinates  $(x, y)$  to a real number. In this case  $f$  can be thought of as creating a landscape, to which the blue (dashed) curves are iso-height contours. The function  $g$  — also taking coordinates  $(x, y)$  — defines a constraint that our minimization must satisfy, through the contour  $g(x, y) = c$ , which is illustrated by the thick red curve. The  $f$  contour marked with  $c_3$  (solid blue) just touches the  $g$  contour, in the point marked with a black cross. At this point, the tangent space (black, dotted line) is shared by both curves and their gradients point in the same direction (up to a sign), as illustrated by the use of the arrows and labels  $\nabla f$  and  $\nabla g$ , respectively.

where  $\nabla_{\mathbf{r}}$  denotes the gradient with respect to the variable  $\mathbf{r}$ . We have that  $t = 0$  is a local maximum, therefore

$$0 = \frac{dh}{dt}(0) = \nabla_{\mathbf{r}} f(\mathbf{r})|_{\mathbf{r}=\mathbf{P}} \cdot \frac{d\mathbf{p}}{dt}(0). \quad (2.22)$$

Thus,  $\nabla_{\mathbf{r}} f(\mathbf{r})$  is perpendicular to any curve on the constraint surface through  $\mathbf{P}$ . This implies that  $\nabla_{\mathbf{r}} f(\mathbf{r})$  is perpendicular to the surface. Since  $\nabla_{\mathbf{r}} g(\mathbf{r})$  is also perpendicular to the surface defined by  $g(\mathbf{r}) = c$ , we have that  $\nabla_{\mathbf{r}} f(\mathbf{r})$  is parallel to  $\nabla_{\mathbf{r}} g(\mathbf{r})$  in the extremum. This implies that there exists a real-valued  $\lambda \neq 0$ , such that  $\nabla_{\mathbf{r}} f(\mathbf{r}) = \lambda \nabla_{\mathbf{r}} g(\mathbf{r})$ . We may therefore introduce the function  $L(\mathbf{r}, \lambda) = f(\mathbf{r}) - \lambda(g(\mathbf{r}) - c)$ , which equals the original function  $f(\mathbf{r})$  at each point of the level set and which is extremized at the point  $\mathbf{P}$ .

Lastly, we should note that multiple (say  $N$ ) constraints may be introduced *via* a set of Lagrange multipliers

$$L(\mathbf{r}, \boldsymbol{\lambda}^N) = f(\mathbf{r}) - \sum_{i=1}^N \lambda_i (g_i(\mathbf{r}) - c_i), \quad (2.23)$$

where  $\boldsymbol{\lambda}^N = \{\lambda_1, \dots, \lambda_N\}$  and the constraints are specified by level sets  $g_i(\mathbf{r}) = c_i$ . Checking whether an extremal point found by using Lagrange multipliers is a maximum, minimum, or saddle point along the subspace defined by the constraints is not trivial. This involves properties of the *bordered* Hessian, with the Hessian referring to the double-derivative matrix. We refer to a course on multivariate calculus or classical mechanics if you wish to learn more about the use of Lagrange multipliers. In this chapter, we will give a few exercises, by which you can familiarize yourself with the concept, so that you can work with it throughout these lecture notes.

## 2.6 Exercises

### Q6. A Refresher on Notation

In the following exercises, we will be working with exponents, logarithms, multivariate integrals and products thereof. Here, we have a brief look at some of the more common notations and we will highlight some of the convention differences between physics and mathematics.

- (a) We write  $e^{a+b} = \exp(a+b) = \exp(a)\exp(b) = e^a e^b$ . The  $N$ -variable generalization of this expression is written

$$\exp\left(\sum_{i=1}^N a_i\right) = \prod_{i=1}^N \exp(a_i), \quad (2.24)$$

where we have introduced the product notation and the  $a_i$  are some (real or complex) numbers. Use this relation to write down the analogous form for the natural logarithm — commonly denoted by “log” in statistical physics — of a product of  $N$  variables  $a_i$ .

- (b) In statistical physics, it is commonplace to write integrals in the left-acting operator form

$$\int_{-1}^1 dx x^2 = \frac{1}{3} x^3 \Big|_{x=-1}^{x=1} = \frac{2}{3}. \quad (2.25)$$

This is convenient, as we will see in Chapter 3, because it allows us to write a multivariate integral over  $N$  three-dimensional (3D) positions  $\mathbf{r}_i$  (with  $i \in \{1, \dots, N\}$ ) as follows

$$\int d\mathbf{r}^N \Phi(\mathbf{r}^N) = \int d\mathbf{r}_1 \int d\mathbf{r}_2 \cdots \int d\mathbf{r}_{N-1} \int d\mathbf{r}_N \Phi(\mathbf{r}^N) = \left( \prod_{i=1}^N \int d\mathbf{r}_i \right) \Phi(\mathbf{r}^N), \quad (2.26)$$

where  $\mathbf{r}^N$  is the set of all  $\mathbf{r}_i$ , *i.e.*,  $\mathbf{r}^N = \{\mathbf{r}_1, \dots, \mathbf{r}_N\}$ , and  $\Phi$  is some function that depends on all of these variables. Now assume that

$$\Phi(\mathbf{r}^N) = \exp\left(-\sum_{i=1}^N a_i |\mathbf{r}_i|^2\right), \quad (2.27)$$

where all  $a_i > 0$  are real valued, and that the integrals in Eq. (2.26) are all over  $\mathbb{R}^3$ . Make optimal use of the sum and product notation to evaluate the integral, providing the requisite intermediate steps.

### Q7. Using Lagrange Multipliers

Using the methods of Lagrange multipliers, find  $x$  and  $y$  that extremize the following function,

$$f(x, y) = 3x^2 - 4xy + y^2, \quad (2.28)$$

subject to the constraint  $3x + y = 0$ . Next, optimize  $f(x, y, z) = yz + xy$  subject to the constraints  $xy = 1$  and  $y^2 + z^2 = 1$ . Note that “optimize” requires you to find all extrema, please do not try to prove which type of extremum these are.

### Q8. Definition of the Helmholtz Free Energy

In Section 2.3, we defined the free energy as  $\beta F(N, V, T) = -\log(Z(N, V, T))$ . Show that this definition is commensurate with the thermodynamic expression for  $F(N, V, T)$  that you recovered from the Legendre transform in the thermodynamic limit in Chapter 1.

**Q9. Gibbs and Boltzmann Entropy**

Recall that there is another definition of entropy in statistical mechanics, namely that by Gibbs:

$$S = -k_B \sum_s p_s \log p_s, \quad (2.29)$$

where the sum is over all states and  $p_s$  is the probability of being that state.

- Show that the Gibbs definition reduces to that of Boltzmann in the microcanonical ensemble.
- Show that in the canonical ensemble, the Gibbs definition of entropy gives rise to a well-known thermodynamic identity.
- Argue in a *few* words why the Gibbs definition is more general.
- Show that the Gibbs definition leads to an extensive entropy.

For an enlightening and surprisingly recent discussion of the difference between the two definitions we refer the interested reader to [Frenkel and Warren, *Am. J. Phys.* **83**, 163 (2015)]. Next, we will consider unifying the various definitions of probability in the ensembles using the Gibbs entropy *via* a variational principle.

- Use the fact that  $\sum_s p_s = 1$  as a constraint to maximize Eq. (2.29). Why should you maximize rather than minimize the equation? You should find  $p_s = \exp(\lambda/k_B - 1)$ , with  $\lambda$  the Lagrange multiplier. Why is this reasonable? Explain in a *few* words.
- Assume that there are  $\Omega$  states in total and use this to solve for the Lagrange multiplier. Is the answer you obtain the one you expect?
- Introduce a second condition that sets the average energy to a constant  $E = \langle \epsilon_s \rangle$ . Call the Lagrange multiplier  $\beta$  and maximize Eq. (2.29) with respect to these two constraints. What do you find for the probability now? Show that one of the constraints naturally leads to the canonical partition function  $Z$ .

This approach can also be extended to include other quantities that are conserved on average and we will see this in Chapter 4 in the context of the grand-canonical probability.

**Q10. Three-State System**

Consider a system of  $N$  identical, non-interacting particles, each of which has three possible energy levels:  $E_1 = -2\delta/3$ ,  $E_2 = E_3 = \delta/3$ . Assume that the particles can exchange places, but are not moving freely throughout space.

- What do the microstates in this system look like?
- Write down the canonical partition function for this system.

Hint: Think carefully on what statements effect indistinguishability and how.

**Q11. Canonical Partition Function for a Polymer**

Consider a simple, lattice model for a polymer. In this model, the polymer sits on a square lattice. At every lattice point, the polymer can do one of three things: go straight or choose between the two directions that are at right ( $90^\circ$ ) angles to its current direction. Each time the polymer bends [follows a right angle ( $90^\circ$ )], it pays a bending energy penalty of  $\epsilon$ . There is no energy cost to continuing straight. Additionally, assume that the starting segment of the polymer is fixed somewhere on the lattice. Further assume the polymer consists of  $N + 1$  segments and assume that it is free to overlap itself.

- (a) What do the microstates in this system look like? Sketch at least two.
- (b) Calculate the canonical partition function  $Z$  for this system.
- (c) What would happen to  $Z$  if the end was no longer pinned to the origin, but instead in its center? Explain in a *few* words.

**Q12. The Partition Function of Draughts**

Consider a draughts board (draughts is UK for checkers), i.e., a pattern with alternating black and white squares. In total there are  $L^2$  squares, with  $L$  the edge length. You can place  $N_b$  black and  $N_w$  white pieces on the board. The rules are:

- Only one piece (black or white) can occupy a square, be that a black or white square.
- Black pieces have  $-\epsilon$  energy on a white square.
- White pieces do not interact with either type of square.

We will now determine the canonical partition function  $Z(N_w, N_b, L, T)$  for this system, with  $T$  the temperature.

- (a) Assume that there is no preference for black pieces to be on white squares (set  $\epsilon = 0$  for now) and that  $N_w + N_b \leq L^2$ .

We now assume an equimolar mixture (50:50) of black and white pieces occupying all squares. Next, we switch the interaction between the black pieces and the white squares back on (*i.e.*,  $\epsilon > 0$ ).

- (b) Will there be a phase transition in this system when switching on  $\epsilon$ ? Explain why.
- (c) Provide the canonical partition function for the new situation.

**Q13. Non-Interacting Spins** *from David Chandler (Introduction to Modern Physics)*

Consider a system of  $N$  distinguishable, non-interacting spins, in an external magnetic field denoted  $H > 0$ . Assume that each spin carries a magnetic moment  $\mu$ , which points either parallel or anti-parallel to the applied field. The energy of a specific state can then be expressed as

$$-\sum_{i=1}^N n_i \mu H; \quad n_i = \pm 1, \quad (2.30)$$

where  $n_i \mu$  is the magnetic moment in field direction.

- (a) What do the microstates of this system look like? Draw a few.
- (b) What is the internal energy of this system as a function of  $\beta = 1/k_B T$ ,  $H$ , and  $N$  (use the ensemble characterized by these variables).
- (c) Determine the entropy of this system as a function of  $\beta$ ,  $H$ , and  $N$ .
- (d) Determine the behavior of the energy and entropy for this system as  $T \rightarrow 0$ .

**Q14. Energy Fluctuations and Heat Capacity**

Show that at fixed  $V$  and  $N$  within the canonical ensemble

$$-\frac{\partial \langle \epsilon_s \rangle}{\partial \beta} = \langle \epsilon_s^2 \rangle - \langle \epsilon_s \rangle^2. \quad (2.31)$$

Combine this result with extensiveness arguments to show that the standard deviation of the energy is much smaller than the average energy in thermodynamically large systems. Use this to show that the constant-volume heat capacity

$$\frac{\partial \langle \epsilon_s \rangle}{\partial T} \bigg|_V \quad (2.32)$$

can be written as

$$C_V = \frac{\langle \epsilon_s^2 \rangle - \langle \epsilon_s \rangle^2}{k_B T^2}. \quad (2.33)$$

**Q15. Model for the Adsorption of a Gas at a Crystal Surface from Daan Frenkel (Lecture Notes)**

Consider a simple model for a surface which consists of  $M$  adsorption sites which are arranged on a square lattice. Assume that the molecules of a gas are indistinguishable and can be adsorbed onto one of the lattice sites, but that each lattice site can only adsorb a single molecule. Further assume that an occupied site has binding energy  $\epsilon$  and that the adsorbed gas is in thermal equilibrium at temperature  $T$ . Note that for a two-dimensional system (such as an adsorbed layer) the area  $A$  and surface pressure  $\Pi$  play the same role as the volume  $V$  and pressure  $P$  in a 3D system.

- If there are  $N$  molecules adsorbed onto the surface, what do the microstates for this system look like? Calculate the canonical partition function.
- Compute the grand partition function. Express  $\Pi$  as a function of  $z$ ,  $A$ , and  $T$ , where  $z = e^{\beta\mu}$  is the fugacity, with  $\beta = 1/k_B T$ .
- Calculate  $\langle N \rangle$ .
- Calculate the occupied fraction of sites  $f = \langle N \rangle / M$ .
- Use the quantities you just derived to calculate the equation of state  $\Pi(f, T)$ . What is the surface pressure in the limit of low coverage. Is this what you would expect? Explain.

**Q16. Defects in a Crystal**

Generally when we consider a crystal, we ignore the possibility of defects like vacancies and interstitials. A vacancy corresponds to an empty lattice site, while an interstitial corresponds to an “extra” particle without its own lattice site. In reality, however, all crystals have a finite concentration of such defects, even in equilibrium. In this exercise, we explore the equilibrium vacancy concentration of the hard-sphere crystal.

Assume that we know the Helmholtz free energy of a perfect crystal  $F^{\text{perfect}}(N = M, V, T)$ , where  $N$  is the number of particles,  $M$  is the number of lattice sites,  $V$  is the volume, and  $T$  is the temperature. Note that in a perfect crystal, the number of lattice sites  $M$  equals the number of particles  $N$ . Additionally, assume that the Helmholtz free energy associated with changing a specific particle into a vacancy, *i.e.*, removing that specific particle, is given by  $f^{\text{vac}}(\rho_M, T)$ , where  $\rho_M = M/V$ , with  $M$  the number of lattice sites. Define  $N^{\text{vac}}$  as the number of vacancies, such that  $M = N + N^{\text{vac}}$ . Finally, we assume that the vacancies do not interact with each other.

- What is the Helmholtz free energy of a crystal with  $M$  lattice sites,  $N$  particles, and temperature  $T$ ? Hint: Note that since the vacancies do not interact, they are randomly distributed through the crystal; you will have to incorporate this into the free energy.
- Assume that the equation of state (the pressure as a function of density) is not affected by the presence of vacancies. In other words, the pressure  $P(M, N, V, T)$  is not dependent on the number of particles. Show that the Gibbs free energy is given by

$$\begin{aligned} \beta G(M, N, P, T) &= \beta N \mu^{\text{perfect}}(P, T) + \beta (M - N) \mu^{\text{vac}}(P, T) \\ &\quad + N \log \frac{N}{M} + (M - N) \log \frac{M - N}{M}, \end{aligned} \quad (2.34)$$

where  $\mu^{\text{perfect}}(P, T)$  is the chemical potential of the perfect crystal,  $\mu^{\text{vac}} = \mu^{\text{perfect}}(P, T) + \tilde{f}^{\text{vac}}(P, T)$ , with  $\tilde{f}^{\text{vac}}(P, T)$  equal to  $f^{\text{vac}}(\rho_M, T)$ , evaluated at the density corresponding to pressure  $P$  in a perfect crystal. Hint: Use that  $G = \mu N$  for a single-component system.

- (c) Simulations have found that (close to the melting point of the crystal) the chemical potential of a vacancy  $\mu^{\text{vac}}$  is approximately  $8.7k_B T$ . Assuming that the concentration is very small, show that the equilibrium vacancy concentration at this point is approximately  $\frac{M-N}{M} = 1 \cdot 10^{-4}$ . Hint: This will require minimizing the free energy in Eq. (2.34) with respect to one of its variables, which one can be determined by thinking about what is fixed in the ensemble.



## Chapter 3

# Classical Ensemble Theory

In this chapter, we make the transition from partition functions and thermodynamic potentials for countable states to continuous distributions. State-counting arguments follow by adopting an atomic or even quantum view of the world. However, we have yet to touch upon situations where there is a natural and continuous microscopic dynamics to the system. For example, in a gas, the trajectories of the molecules are described by Newton's equations of motion. Through collisions, the gas molecule may (eventually) explore all possible positions and momenta in the system. This complicates our state-counting procedure, at the very least in terms of normalization. The macroscopic properties of a system may be derived from the microscopic dynamics by means of *kinetic theory*, as was for instance considered by Maxwell and Boltzmann. However, it is possible to recover a 'state-counting' formalism as well, which substantially cuts down on the mathematical manipulation required to obtain equilibrium quantities. We will examine aspects of both formalisms in this chapter.

### 3.1 Phase Space

Consider an isolated system of  $N$  identical classical particles in a three-dimensional volume  $V$ . If we assume that each particle has three translational degrees of freedom, then the microscopic state of this system is fully characterized by the  $3N$  coordinates  $\mathbf{r}^N \equiv \{\mathbf{r}_1, \dots, \mathbf{r}_N\}$  and the  $3N$  conjugate momenta  $\mathbf{p}^N \equiv \{\mathbf{p}_1, \dots, \mathbf{p}_N\}$  of the particles. The values of these variables define a *phase point*  $\Gamma \equiv (\mathbf{r}^N, \mathbf{p}^N)$  in a  $6N$ -dimensional *phase space*<sup>1</sup>. The concept of phase space is illustrated in Fig. 3.1 for a simple pendulum, which admits a one-dimensional description.

The time evolution of the system can be seen as a motion of the phase point along its *phase trajectory*. This motion follows from the Hamiltonian  $\mathcal{H}(\mathbf{r}^N, \mathbf{p}^N)$  of the system, which is written here as

$$\mathcal{H}(\mathbf{r}^N, \mathbf{p}^N) = \sum_{i=1}^N \frac{\mathbf{p}_i^2}{2m} + \Phi(\mathbf{r}^N), \quad (3.1)$$

where  $m$  is the mass of the particles and  $\Phi(\mathbf{r}^N)$  the potential energy, which includes the external potential that defines the volume  $V$ . The Hamiltonian thus depends parametrically on the number of particles

---

<sup>1</sup>In general, the dimension of phase space can be determined by counting degrees of freedom. For example, if each particle has  $n$  other internal degrees of freedom (*e.g.*, vibrations), then the dimension becomes  $(6 + 2n)N$ .

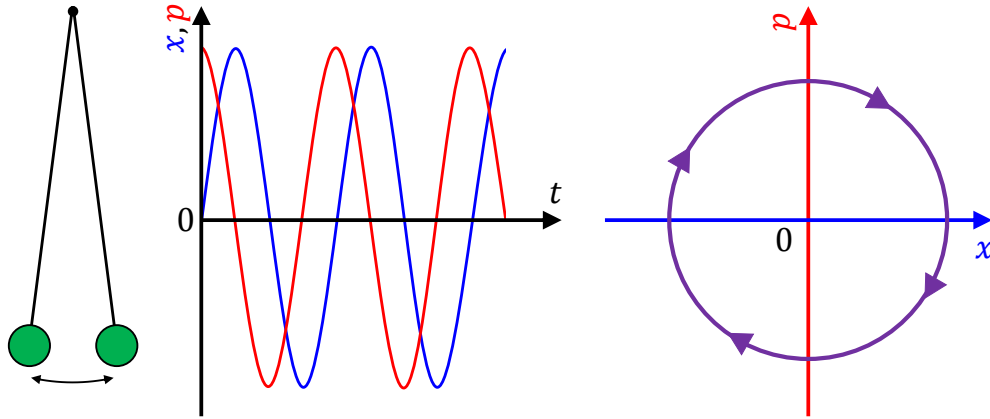


Figure 3.1: The phase portrait of a simple pendulum. (left) A sketch of the system. (middle) The  $x$  component of the position (blue) and the associated momentum  $p$  (red). Note that these are out of phase by a quarter period, *i.e.*, the momentum is zero at the maximal extension and maximal at zero extension. (right) The phase-space representation of this simple oscillatory motion.

$N$  and the volume  $V$  (or parameters that describe the volume  $V$ ). This form of the Hamiltonian is not suitable for electromagnetic systems with velocity-dependent forces, but the formalism can be extended to include these as well. The Hamilton equations

$$\dot{\mathbf{r}}_i = \frac{\partial \mathcal{H}}{\partial \mathbf{p}_i} \quad \text{and} \quad \dot{\mathbf{p}}_i = -\frac{\partial \mathcal{H}}{\partial \mathbf{r}_i}, \quad (3.2)$$

together with  $6N$  initial conditions determine the trajectory uniquely and completely. It follows that trajectories in phase space do *not* intersect. This is a consequence of the dynamics being conservative. For example, in Fig. 3.1(right), oscillations with greater amplitude would correspond an origin-centered circle with a larger radius; the various concentric circles clearly do not intersect.

## 3.2 The Liouville Equation

It will turn out to be useful to consider an arbitrary large collection of macroscopically identical systems that only differ by their position in phase space. Such a collection is called an *ensemble*. At a given time  $t$  an ensemble is characterized by a phase-space probability density  $f(\mathbf{\Gamma}, t)$ , with  $f(\mathbf{\Gamma}, t)d\mathbf{\Gamma}$  the probability that the system is in a microscopic state lying in the infinitesimal  $6N$ -dimensional volume element  $d\mathbf{\Gamma} = d\mathbf{r}^N d\mathbf{p}^N$  around  $\mathbf{\Gamma}$ . Note that the physical dimension of this infinitesimal volume is  $\text{kg}^{3N} \text{m}^{6N} \text{s}^{-3N} = (\text{kgm}^2 \text{s}^{-1})^{3N}$ . The Planck constant  $h$  has the same units as the single-particle phase-space volume and we will see it appear later as a unit of measure.

The time evolution of  $f(\mathbf{\Gamma}, t)$  is governed by the Liouville equation

$$\frac{\partial f(\mathbf{\Gamma}, t)}{\partial t} + \frac{\partial}{\partial \mathbf{\Gamma}} \cdot (\dot{\mathbf{\Gamma}} f(\mathbf{\Gamma}, t)) = 0, \quad (3.3)$$

where  $\partial/\partial \mathbf{\Gamma}$  denotes the phase space gradient operator, and  $\dot{\mathbf{\Gamma}}$  the  $6N$ -dimensional vector  $(\dot{\mathbf{r}}^N, \dot{\mathbf{p}}^N)$ . Here, it is important to note the use of *partial* derivatives. We can interpret  $\dot{\mathbf{\Gamma}}$  as a generalized velocity

that advects the phase-space probability  $f$  (in much the same way as a fluid velocity  $\mathbf{u}$  moves suspended particles  $\mathbf{j} = \mathbf{u}c$  with  $c$  the particle concentration). The associated flux in this picture is  $\mathbf{j} = \dot{\mathbf{\Gamma}}f(\mathbf{\Gamma}, t)$ . The change of  $f$  with time this produces is then  $\dot{f} = -(\partial/\partial\mathbf{\Gamma}) \cdot \mathbf{j}$ , where we imply conservation of the phase space probability (the particle analogy is  $\dot{c} = -\nabla \cdot \mathbf{j}$ ). Imposing the continuity equation makes sense, as the total integral over  $f$  should always be equal to 1 and thus the dynamics of  $f$  should conserve probability. Or in other words, phase-space points can neither be created nor destroyed as time evolves.

From the Hamilton equations (3.2) it follows directly that  $(\partial/\partial\mathbf{\Gamma}) \cdot \dot{\mathbf{\Gamma}} = 0$ , which allows us to write Eq. (3.3) as

$$\begin{aligned} \frac{\partial f(\mathbf{\Gamma}, t)}{\partial t} &= -\dot{\mathbf{\Gamma}} \cdot \frac{\partial f}{\partial \mathbf{\Gamma}} \\ &= \sum_{i=1}^N \left[ \frac{\partial \mathcal{H}}{\partial \mathbf{r}_i} \frac{\partial f}{\partial \mathbf{p}_i} - \frac{\partial \mathcal{H}}{\partial \mathbf{p}_i} \frac{\partial f}{\partial \mathbf{r}_i} \right] \equiv \{\mathcal{H}, f\}, \end{aligned} \quad (3.4)$$

where  $\{, \}$  denotes the Poisson bracket. If you have not seen this notation yet, you may think of it as a classical analogue to the commutator that you know from quantum mechanics (the Poisson bracket was obviously introduced first historically speaking). The Liouville equation is the starting point of most theories of non-equilibrium statistical mechanics, *e.g.*, kinetic theory.

### 3.3 Time Averages and Ensemble Averages

Before continuing with the definition of classical ensembles, we need to address time dependence one last time. The aim of equilibrium statistical mechanics is to calculate observables that result from a macroscopic measurement. Such a measurement typically constitutes a time average  $\bar{\mathcal{A}}$  of a corresponding function  $\mathcal{A}(\mathbf{\Gamma})$  — this function associates microscopic realizations with macroscopic observables — over a phase-space trajectory for a time interval  $t_0 \leq t \leq t_0 + \tau$ :

$$\bar{\mathcal{A}} \equiv \frac{1}{\tau} \int_{t_0}^{t_0+\tau} dt \mathcal{A}(\mathbf{\Gamma}(t)). \quad (3.5)$$

Even if  $\tau$  is very large compared (say  $\tau = 1$  s) to that of atomic and molecular collisions (in air these occur roughly every  $10^{-10}$  s per molecule), this average depends, strictly speaking, on the initial time  $t_0$  and on the particular trajectory of the measured system.

It is common experience, however, that repeating the measurement on the same equilibrium system at later times  $t_0$  yields an indistinguishable answer. Apparently, most values of a phase function (with a macroscopic meaning) are close to their average value along a particular trajectory. Moreover, repeating the measurement on a replica of the original system, *i.e.*, following a different trajectory through phase space, often also yields the same answer for  $\bar{\mathcal{A}}$ . This suggests an alternative microscopic description of a macroscopic equilibrium state: instead of time averaging over a single phase trajectory, as proposed in Eq. (3.5), we can average over a suitably constructed equilibrium *ensemble* with a corresponding equilibrium probability density  $f(\mathbf{\Gamma})$  that does not depend on time explicitly. The ensemble average is now defined as

$$\langle \mathcal{A} \rangle = \int d\mathbf{\Gamma} f(\mathbf{\Gamma}) \mathcal{A}(\mathbf{\Gamma}), \quad (3.6)$$

where the normalization  $\int d\mathbf{\Gamma} f(\mathbf{\Gamma}) = 1$  is understood.

Systems for which  $\bar{\mathcal{A}} = \langle \mathcal{A} \rangle$  for all continuous phase functions  $\mathcal{A}(\mathbf{\Gamma})$  are called *ergodic*. Although ergodicity can almost never be proven, it is often assumed to hold. There are, however, manifestly

nonergodic systems. Nonergodicity results if trajectories are restricted, for macroscopically long times to a subspace. This can be caused the presence of other conserved quantities besides energy (*e.g.*, angular momentum), or due to spontaneous symmetry breaking (*e.g.*, in antiferromagnets). Also systems with an extremely slow dynamics compared to the observation time, *e.g.*, glasses, are nonergodic.

It should now be obvious that our common experience is based around fully ergodic systems in equilibrium. For such systems,  $f(\mathbf{\Gamma}, t)$  is stationary, *i.e.*,  $(\partial f / \partial t) = 0$  in Eq. (3.4). Equilibrium ensembles are therefore characterized by phase-space distributions  $f(\mathbf{\Gamma})$  that satisfy  $\{\mathcal{H}, f\} = 0$ . That is, the distribution Poisson-commutes with the Hamiltonian. This implies that the  $\mathbf{\Gamma}$ -dependence of  $f$  can only involve conserved quantities: typically the mass, momentum, and energy. In most cases of interest here, the energy is the only conserved quantity<sup>2</sup>, so that then  $f(\mathbf{\Gamma}) = \tilde{f}(\mathcal{H}(\mathbf{\Gamma}))$  for some function  $\tilde{f}$ . We will see how this translates to the functional form of the ensembles shortly.

Before we continue on, we should remark that the two types of average discussed here are also manifest in present-day computer simulations of model systems for condensed matter. In Molecular Dynamics simulations the equations of motion, Eqs. (3.2), are integrated numerically for typically  $N = 100 - 10,000$  particles, starting from some initial configuration. This generates a phase trajectory over which time averages are taken. Conversely, in Monte Carlo simulations, configurations are randomly generated, and then accepted or rejected in such a way that configurations (and hence observables) are sampled with the correct statistical weight  $f(\mathbf{\Gamma})$ .

## 3.4 The Classical Ensembles

### 3.4.1 The Microcanonical Ensemble

The microcanonical ensemble describes the equilibrium properties of a closed ergodic system with fixed energy  $E$ , volume  $V$ , and number of particles  $N$ . It is characterized by the phase-space distribution

$$f_m(\mathbf{\Gamma}) = \frac{\delta(E - \mathcal{H}(\mathbf{\Gamma}))}{\omega(E, V, N)}, \quad (3.7)$$

where the Dirac- $\delta$  ensures that only those phase-space points are selected for which the total energy is  $E$ . In other words, the distribution is such that it is zero anywhere except on the  $(6N - 1)$ -dimensional hypersurface  $\mathcal{H}(\mathbf{\Gamma}) = E$ . The normalization is given by

$$\omega(E, V, N) = \int d\mathbf{\Gamma} \delta(E - \mathcal{H}(\mathbf{\Gamma})), \quad (3.8)$$

which can be interpreted as the hypersurface area.

It is tempting to identify  $\omega$  as a measure for the number of states available to the system by making the analogy to the way microcanonical probability was normalized in Chapter 2. That, is Eq. (3.7) has the appearance of a continuous-space extension of the  $1/\Omega$ , where  $\Omega$  is the total number of states in a finite, discrete system. Thus, surely,  $\omega$  should relate to the total number of states. This way of thinking is, however, not entirely without risk, as it is difficult to assign a number to the amount of states that  $\omega$  represents, *i.e.*, we require a form of normalization to recover our analysis from Chapter 2.

We will shortly demonstrate that a natural unit of measure for phase-space volume is given by the Planck constant  $h$ , but for now we will assume this is the case. Thus, one could write  $\omega/h^{3N}$  for the number

---

<sup>2</sup>Linear and angular momentum are not conserved due to collisions with the wall of the container that specifies the volume (unless the wall itself is considered part of the system).

of states. However, this is where the issues come to the fore. A hyper surface has dimension  $6N - 1$  and is a set of measure zero<sup>3</sup> in the embedding  $6N$ -dimensional phase-space volume, *e.g.*, a sphere has a 2D area but no volume in 3D. This means that the effective number of states on the sphere should be counted using a phase-space volume element that has the appropriate dimension. In our example of a sphere, the elements should have dimension of area, rather than of volume. For measuring a  $6N - 1$  dimensional hyperspace, one would need to introduce some fraction or residual of  $h$ .

One can bypass this dimensionality issue by defining a thin shell with energies between  $E - \Delta E$  and  $E$  for some small, yet finite  $\Delta E > 0$ . In this case, the probability of being in a small volume  $d\mathbf{\Gamma}$  around a specific phase space point  $\mathbf{\Gamma}$  can be normalized correctly, *i.e.*, using  $h^{3N}$ . Nonetheless, the introduction of an arbitrary  $\Delta E$  is not entirely satisfactory. This issue has led to controversy in the statistical physics community even up to the 2000s. Presently, the preferred resolution to the issue is the introduction of a  $\Delta E$  that can be made arbitrarily small.

### 3.4.2 The Canonical Ensemble

A system of  $N$  particles in a volume  $V$  in contact with a heat bath at temperature  $T$  can change its energy by exchanging heat with the reservoir. For this reason, the system is no longer restricted to the constant-energy hyper surface. Instead, one can prove that a phase point  $\mathbf{\Gamma}$  with energy  $\mathcal{H}(\mathbf{\Gamma})$  has a probability distribution  $f_c(\mathbf{\Gamma}) \propto \exp(-\mathcal{H}(\mathbf{\Gamma})/k_B T)$ . It turns out to be convenient to write the canonical distribution function as

$$f_c(\mathbf{\Gamma}) = \frac{\exp[-\beta\mathcal{H}(\mathbf{\Gamma})]}{N!h^{3N}Z(N, V, T)}, \quad (3.9)$$

with associated canonical partition ‘sum’ or rather partition function

$$Z(N, V, T) = \frac{1}{N!h^{3N}} \int d\mathbf{\Gamma} \exp[-\beta\mathcal{H}(\mathbf{\Gamma})]. \quad (3.10)$$

The factor  $h^{3N}$  is included to make  $Z$  dimensionless (Exercise Q19 will clarify the choice), and the factor  $N!$  to make  $\log Z$  extensive. We (re-)introduced the short-hand notation  $\beta = 1/(k_B T)$ .

The relation with thermodynamics follows from

$$-k_B T \log Z(N, V, T) \equiv F(N, V, T) = \langle E \rangle - T \langle S \rangle, \quad (3.11)$$

where  $F$  is the Helmholtz free energy, as you have derived in the exercises to Chapter 2. We know from thermodynamics that  $F(N, V, T)$  generates the full thermodynamics of systems with fixed  $(N, V, T)$ , just as  $S(E, V, N)$  does for systems with fixed  $(E, V, N)$ ; this can be readily shown using Legendre transforms. We already saw that the energy of the system at temperature  $T$  fluctuates. In the thermodynamic limit, however, the relative fluctuations become vanishingly small as they are of order  $N^{-1/2}$ , and the average energy  $\langle E \rangle$  therefore plays the role of the internal energy  $U$  in thermodynamics, also see Chapter 2. This also implies that the microcanonical and the canonical ensemble are equivalent, for most purposes, in the thermodynamic limit.

---

<sup>3</sup>It has measure zero this and most physical situations. However, one can construct pathological mathematical counter examples of space filling submanifolds.

Note that the Maxwell-Boltzmann velocity distribution is easily obtained in the canonical ensemble, *viz.*

$$\begin{aligned}
 f_{\text{MB}}(\mathbf{p}) &\equiv \langle \delta(\mathbf{p}_1 - \mathbf{p}) \rangle_c; \\
 &= \frac{1}{N!h^{3N}Z} \int d\Gamma \delta(\mathbf{p}_1 - \mathbf{p}) \exp[-\beta H(\Gamma)]; \\
 &= \frac{\exp[-\mathbf{p}^2/(2mkT)]}{(2\pi mk_{\text{B}}T)^{3/2}}.
 \end{aligned} \tag{3.12}$$

is the probability density that a given particle of mass  $m$  has momentum  $\mathbf{p}$  at temperature  $T$ .

The canonical average of momentum independent observables, *i.e.*, observables described by phase functions  $\mathcal{A}(\Gamma) = \mathcal{A}(\mathbf{r}^N)$ , can be written as

$$\begin{aligned}
 \langle \mathcal{A} \rangle &= \frac{1}{N!h^{3N}Z(N, V, T)} \int d\Gamma \exp[-\beta \mathcal{H}(\Gamma)] \mathcal{A}(\mathbf{r}^N); \\
 &= \frac{1}{Q(N, V, T)} \int d\mathbf{r}^N \exp[-\beta \Phi(\mathbf{r}^N)] \mathcal{A}(\mathbf{r}^N),
 \end{aligned} \tag{3.13}$$

where the *configurational integral* is defined as

$$Q(N, V, T) = \int d\mathbf{r}^N \exp[-\beta \Phi(\mathbf{r}^N)]. \tag{3.14}$$

This integral will turn out to play a much more important role in systems that have interactions between the particles, see Chapter 13. Note that

$$Z(N, V, T) = \frac{Q(N, V, T)}{N! \Lambda^{3N}}, \tag{3.15}$$

where the thermal (De Broglie) wavelength is defined by

$$\Lambda = \frac{h}{\sqrt{2\pi m k_{\text{B}} T}}. \tag{3.16}$$

### 3.4.3 The Grand-Canonical Ensemble

Although many physical systems can be characterized by fixed  $(N, V, T)$  and therefore by the canonical ensemble, there are also many cases where the number of particles  $N$  can fluctuate. This can be caused, *e.g.*, by the presence of the permeable walls or reactive surface in the system. Examples of the former include membrane equilibria, where some chemical species can and others cannot cross a semi-permeable membrane, and gas-liquid coexistences, where particles can move from the liquid to the gas and *vice versa* through the meniscus. One can also consider a system that is part of a bigger ‘reservoir’, *e.g.*, a subvolume that contains a fluctuating number of particles. The ensemble of systems that can exchange energy and particles with their environment is called the *grand-canonical ensemble*.

The probability distribution to find the system in a state with  $N$  particles at a phase space point  $\Gamma$  is given by the grand-canonical distribution function

$$f_g(\Gamma, N) = \frac{1}{N!h^{3N}\Xi(\mu, V, T)} \exp[-\beta \mathcal{H}(\Gamma) + \beta \mu N], \tag{3.17}$$

with the associated grand-canonical partition function reading

$$\begin{aligned}\Xi(\mu, V, T) &= \sum_{N=0}^{\infty} \frac{\exp[\beta\mu N]}{N!h^{3N}} \int d\mathbf{\Gamma} \exp[-\beta\mathcal{H}(\mathbf{\Gamma})]; \\ &\stackrel{(3.10)}{=} \sum_{N=0}^{\infty} \exp[\beta\mu N] Z(N, V, T).\end{aligned}\tag{3.18}$$

The grand-canonical ensemble can be regarded as a linear combination of canonical ensembles with different numbers of particles. Similarly, one can regard the canonical ensemble as a linear combination of microcanonical ensembles with different energies.

The relation between the grand-canonical ensemble and thermodynamics is given by

$$\beta\Omega(\mu, V, T) = -\log \Xi(\mu, V, T),\tag{3.19}$$

where  $\Omega$  is the grand potential. Indeed, the thermodynamic potential of a system with  $\mu$ ,  $V$ , and  $T$  as independent variables. For a homogeneous system we have  $\Omega = -p(\mu, T)V$  with  $p$  the pressure. The number of particles fluctuates in the grand-canonical ensemble, therefore the probability  $W(N)$  to find exactly  $N$  particles in the system (regardless the state point  $\mathbf{\Gamma}$  of these  $N$  particles) is obtained by integrating out the phase-space coordinates,

$$\begin{aligned}W(N) &= \int d\mathbf{\Gamma} f_g(\mathbf{\Gamma}, N); \\ &\stackrel{(3.17)}{=} \frac{\exp[\beta\mu N]}{N!h^{3N}\Xi(\mu, V, T)} \int d\mathbf{\Gamma} \exp[-\beta\mathcal{H}(\mathbf{\Gamma})]; \\ &\stackrel{(3.18)}{=} \frac{\exp[\beta\mu N]Z(N, V, T)}{\Xi(\mu, V, T)}.\end{aligned}\tag{3.20}$$

One now calculates straightforwardly that

$$\langle N \rangle = \sum_{N=0}^{\infty} NW(N) = \frac{1}{\Xi} \frac{\partial}{\partial \beta\mu} \sum_{N=0}^{\infty} \exp[\beta\mu N] Z(N, V, T) = \frac{1}{\Xi} \frac{\partial \Xi}{\partial (\beta\mu)}\tag{3.21}$$

$$\langle N^2 \rangle = \sum_{N=0}^{\infty} N^2 W(N) = \frac{1}{\Xi} \frac{\partial^2 \Xi}{\partial (\beta\mu)^2}.\tag{3.22}$$

It follows that the width of the distribution  $W(N)$  is strongly peaked about the average value  $\langle N \rangle$ , with typical relative fluctuations of order  $1/\sqrt{N}$ , *i.e.*, these are extremely small in the thermodynamic limit. This implies that  $\langle N \rangle$  can be identified with the number of particles  $N$  in a thermodynamic description. One can now readily show, using that  $pV = k_B T \log \Xi$  for a homogeneous system, that the relative variance in the number of particles is related to the compressibility through

$$\frac{\langle N^2 \rangle - \langle N \rangle^2}{\langle N \rangle} = k_B T \left( \frac{\partial \rho}{\partial p} \right)_T.\tag{3.23}$$

Lastly, for later reference, we define the *fugacity* as

$$z = \exp[\beta\mu],\tag{3.24}$$

which is, for any temperature  $T$ , one-to-one related to  $\mu$ .

### 3.5 The Equipartition Theorem

Imagine that we can write the Hamiltonian for a system in a fully quadratic form, *i.e.*, a form that may be written as

$$\mathcal{H} = \sum_i^M a_i s_i^2 \quad (3.25)$$

where  $s_i$  a generalized coordinate of the system, *e.g.*, a position coordinate or a momentum coordinate, while  $a_i$  are positive parameters, and  $M$  is the number of degrees of freedom. Examples of degrees of freedom are provided in Fig. 3.2. The left-hand panel shows several kinetic and one possible vibrational degree of freedom for a dumbbell-shaped molecule. The right-hand panel shows that many-body interaction potentials  $\Phi$  may admit to a quadratic expansion about some thermodynamically favored minimum. This fact makes the result we outline below much more generally applicable than is perhaps suggested by the shape of Eq. (3.25).

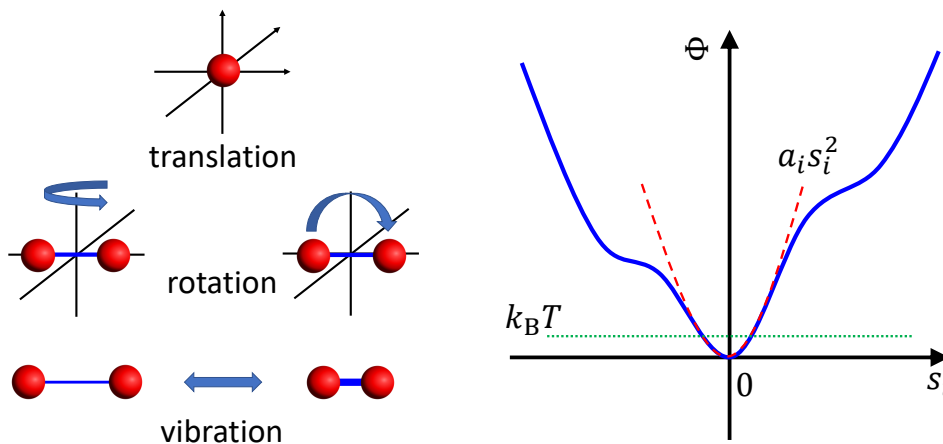


Figure 3.2: Interpretation of the degrees of freedom used in an equipartition argument. (left) A *rigid* dumbbell-shaped molecule has: 3 translational degrees of freedom; 2 rotational ones (assume point masses). If there is a *harmonic* bond between the two spheres, then it will gain one potential-energy degree from vibrations and 1 degree of freedom from the kinetic energy term associated with the two parts of the dumbbell moving closer and further away from each other. (right) A general interaction potential  $\Phi$  (blue curve) may admit a quadratic expansion about a minimum in some generalized coordinate  $s_i$  (dashed red curve), we will see an example of this in exercise Q25. N.B., here we plot the multi-dimensional potential landscape only along one coordinate. When this local quadratic nature is pronounced compared to the thermal energy  $k_B T$  (green dotted line), this degree of freedom contributes  $\frac{1}{2}k_B T$  to the total energy of the system.

Due to the quadratic nature of the variables in the Hamiltonian in Eq. (3.25), the expectation value of the Hamiltonian can be written

$$\langle \mathcal{H} \rangle = \frac{1}{2} \sum_i \left\langle s_i \frac{\partial \mathcal{H}}{\partial s_i} \right\rangle. \quad (3.26)$$

Now, if we assume we are in the canonical ensemble, then the expectation value on the right-hand side

of Eq. (3.26) can be recast into the form

$$\left\langle s_j \frac{\partial \mathcal{H}}{\partial s_j} \right\rangle = \frac{\int d\mathbf{\Gamma} \left( s_j \frac{\partial \mathcal{H}}{\partial s_j} \right) e^{-\beta \mathcal{H}}}{\int d\mathbf{\Gamma} e^{-\beta \mathcal{H}}} = \frac{\int d\mathbf{\Gamma}_{(s_j)} \left[ -\frac{1}{\beta} s_j e^{-\beta \mathcal{H}} \Big|_{(s_j)_1}^{(s_j)_2} + \frac{1}{\beta} \int ds_j e^{-\beta \mathcal{H}} \right]}{\int d\mathbf{\Gamma} e^{-\beta \mathcal{H}}}, \quad (3.27)$$

where  $d\mathbf{\Gamma}_{(s_j)}$  indicates an integral over  $d\mathbf{\Gamma}$  excluding  $ds_j$  and  $(s_j)_1$  and  $(s_j)_2$  are the extreme values of the variable  $s_j$ . At the extreme values, the Hamiltonian of the system becomes infinite. Specifically, if  $s$  represented a position coordinate, then the extreme values of the coordinate correspond to the boundary, and hence the potential energy at these points becomes infinite as the system must be bounded. Similarly, if  $s$  corresponded to the momentum, then the extreme values are  $\pm\infty$ , and the kinetic energy becomes infinite. In either case, the Hamiltonian becomes infinite, and the contribution from the first term on the right-hand side of Eq. (3.27) goes to zero. This leaves

$$\left\langle s_j \frac{\partial \mathcal{H}}{\partial s_j} \right\rangle = \frac{\int d\mathbf{\Gamma}_{(s_j)} \left[ \frac{1}{\beta} \int ds_j e^{-\beta \mathcal{H}} \right]}{\int d\mathbf{\Gamma} e^{-\beta \mathcal{H}}} = \frac{1}{\beta}. \quad (3.28)$$

Plugging this result into Eq. (3.26) results in

$$\langle \mathcal{H} \rangle = \frac{1}{2\beta} M. \quad (3.29)$$

This result is typically referred to as the *equipartition theorem* and implies that each quadratic degree of freedom contributes  $(1/2)k_B T$  to the internal energy of the system.

It should be clear that the above argument holds in a classical system. However, our modern understanding tells us that matter is quantum mechanical in nature with discretized energy levels. In Exercise Q19, you will demonstrate that a quantum harmonic oscillator will behave classically when the temperature  $T \gg \hbar\omega/k_B$ , where  $\omega$  is the frequency and  $h = 2\pi\hbar$ . This transition between a quantum description and an effective classical one has consequences for the behavior of molecules. The interpretation one can give to the transition is that at sufficiently low temperatures (compared to  $\hbar\omega/k_B$ ) a bond is in its ground state or some of the lower excited states. However, there is nothing quadratic about this degree of freedom, it is discrete and not excited, which means it will not contribute  $k_B T/2$  to the internal energy of the system. Raising the temperature (sufficiently) above  $\hbar\omega/k_B$  will make the bond behave classically and harmonic, meaning that it now contributes  $k_B T/2$  to the system. Be careful, we only speak of the bond here, but when a bond becomes classical, the system will typically also gain an additional (quadratic) momentum degree of freedom, which needs to be taken into account. Let us go into this point a bit further next.

You will have encountered a change in degrees of freedom in studying a classical system, namely, when you considered the ratio of the constant-pressure  $C_p$  and constant-volume heat capacity  $C_V$  of diatomic gases. One can readily show that  $C_V = (n/2)k_B N$ , where the number of degrees of freedom per particle is given by  $n$ . Similarly,  $C_p = (n/2 + 1)k_B N$ , which means that  $\gamma \equiv C_p/C_V = (n+2)/n$ . For a diatomic gas like nitrogen, we have  $n = 5$  if the bond between the two atoms is close to the ground state: three translational degrees and two rotational (because of symmetry); we will come back to this shortly. If, however, the bond is vibrating, *i.e.*, temperatures are sufficiently high for it to behave like an effective harmonic spring, then  $n = 7$ . These seven degrees come from the 5 original degrees of freedom of the ground-state molecule, plus 1 for the classically-behaving (harmonic) bond, and 1 additional one for the

associated kinetic degree of freedom. That is, we have that the two atoms moving with respect to each other along the bond and the relative motion of these masses gives rise to a kinetic energy. This means that upon increasing the temperature  $\gamma$  is expected to reduce from  $7/5$  to  $9/7$ .

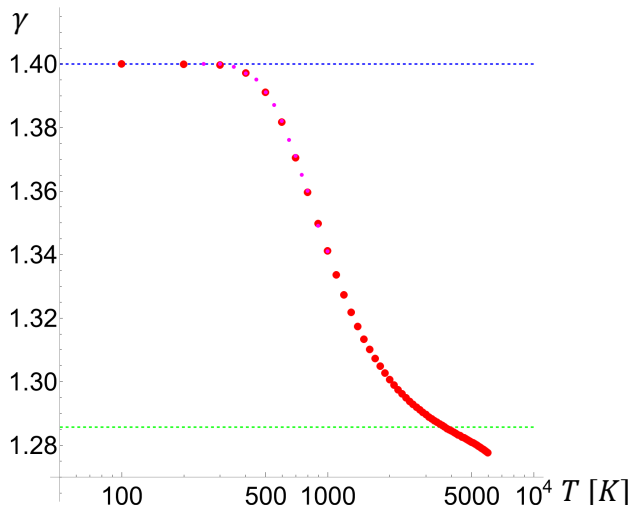


Figure 3.3: Effect of temperature on the degrees of freedom in pure nitrogen gas. The ratio  $\gamma$  of the constant-pressure  $C_p$  and constant-volume heat capacity  $C_V$  as a function of the temperature  $T$  in Kelvin. The experimental data (red points) was converted from the  $C_p$  values listed in the table prepared by M.W. Chase [NIST-JANAF Thermochemical Tables, Fourth Edition, J. Phys. Chem. Ref. Data, Monograph 9, 1-1951 (1998)]. The magenta data is from table A-4M in [K. Wark, Thermodynamics, 4th ed., p. 783 (New York: McGraw-Hill, 1983)], but only goes up to 1000 K. The dashed blue line shows the value  $\gamma = 7/5$ , while the dashed green line shows the ratio  $\gamma = 9/7 \approx 1.29$ .

Figure 3.3 illustrates the change in heat-capacity ratio for pure nitrogen as a function of temperature. Here, we can clearly see that there is indeed a well-defined plateau value of  $\gamma = 7/5$  at low temperatures, when the vibrational degrees of freedom are effectively frozen out. Between 400 and 500 Kelvin, we start seeing departures from  $\gamma = 7/5$  and the value of the ratio decreases. However, there is no plateau at  $\gamma = 9/7$ . This is due to the fact that the molecules begin to ionize at sufficiently high temperatures. Intriguingly, lowering the temperature sufficiently, it can be shown that there is an additional plateau at  $\gamma = 5/3$ , which corresponds to the angular momentum degrees of freedom becoming quantum-mechanically discretized. This plateau is not shown in Fig. 3.3.

In the above example we commented on there being 5 degrees of freedom for the low-temperature state, while there are 7 degrees of freedom in the high-temperature state. This might not be entirely obvious, nor is it simple to intuit how many states a molecule has, when it comprised many atoms and bonds that become harmonic at different temperatures. We will explore this matter further in Exercise Q22. Let us briefly illustrate a degree-counting principle in preparation for this. Assume we have a monoatomic gas, like argon. Then in 3D, an atom can move in the  $x$ ,  $y$ , and  $z$  direction of some chosen coordinate frame. Each of these directions has associated with it a kinetic term  $p_i^2/(2m)$  in the Hamiltonian ( $i \in \{x, y, z\}$ ), which contributes  $k_B T/2$ . Thus, for an ideal gas in three dimensions, the internal energy is  $U = 3Nk_B T/2$ , as you are familiar with.

Implicitly, we have assumed that rotations of the atom do not contribute to the Hamiltonian. Each valid axis of rotation would contribute its own kinetic energy term  $\propto I\omega^2$ , where  $I$  is the relevant moment of inertia and  $\omega$  the angular velocity about that axis. Why then do we not get  $U = 3Nk_B T$  for argon gas? You could think that we should treat the argon atom essentially like a point particle,<sup>4</sup> for which the rotation is irrelevant. However, this is not the right way of looking at the problem. Classically, argon has a covalent radius of 106 pm ( $\sim 10^{-10}$  m), so it could be seen as a spinning billiard ball, which would have rotational-energy contributions. This is really not how you should think of argon, though. Firstly, the mass of this atom is mostly concentrated in the nucleus, which has a very small moment of inertia (if we were to view argon as a classical object)<sup>5</sup>, so it is really not a ball. Secondly, this line of argument is not entirely satisfactory in itself, because nowhere in our derivation of Eq. (3.28), did we consider the relative magnitude of the prefactors in front of the harmonic terms in the Hamiltonian. Therefore, these should not matter! The fact that there is a term quadratic in the generalized degrees of freedom is sufficient to obtain factors of  $k_B T/2$ , irrespective of the spring strength (magnitude of the prefactor). We conclude that our thinking in terms of spinning balls (and rigid dumbbells for  $N_2$ ) fails us in predicting the right number of quadratic degrees of freedom, at least if we had naively written down all possible quadratic contributions to the Hamiltonian.

Clearly, some degrees of freedom matter, while others do not! The decision of which ones matter and which ones do not, must be made at the point of writing down the (classical) Hamiltonian describing the system. But it is not clear how to do that yet. The resolution should be sought in the fact that the physics of the system does not change with rotations of the argon molecules about their centers, nor does it with rotations about the connecting axis of the  $N_2$  molecules. This makes sense, because classically, any spinning of the nucleus is not going to be a detectable quantity to begin with, meaning that argon only has classical translational degrees of freedom that lead to quadratic expressions in the momenta. However, spinning about axes orthogonal to the connecting one in a  $N_2$  molecule, can be observed. Thus, we need to write down two angular-momentum terms with the associated with this in our Hamiltonian. Let us make this more explicit next, also see Chapter 17..

The rotation of any general shape in 3D can be prescribed using three angles, referred to as Euler angles. Water molecules do not possess a convenient rotational symmetry, meaning that their motion must be described using three momenta and three angular momenta that each contribute a harmonic kinetic term to the Hamiltonian. So for  $H_2O$  we expect 6 degrees of freedom, provided the bonds between the oxygen and hydrogen remain in or close to their ground state. An  $N_2$  molecule has one rotational axis about which it is rotationally symmetric, hence this only has 5 total degrees of freedom (when the bond are not vibrating). Note that this would also hold for a CO molecule, which is not mirror symmetric, but is rotationally symmetric. In colloidal particles, *e.g.*, micron-sized objects suspended in a fluid, the friction with the surrounding fluid removes the inertia from the dynamics of the colloids. Still, an *effective* description in terms of a Hamiltonian with quadratic degrees of freedom of *only* the colloids can be put forward. The way in which to arrive at that description will be covered in Chapter 16. In such a case, symmetry arguments may be similarly invoked to establish which *effective* quadratic degrees of freedom should appear in the Hamiltonian. Rotations about objects with symmetry axes that leave the system invariant should not contribute to measurable thermodynamic properties in this case. At least, this should be the intuition that we have on the basis of our understanding of statistical mechanics. It

---

<sup>4</sup>Or the nitrogen molecule as an infinitely thin rod. Note that is what is being ‘suggested’ by the data, as we get a  $\gamma$  factor of 1.4 in Fig. 3.3 at low temperature. Had rotations about the axis connecting the two atoms mattered, we would have expected a ratio of  $8/6 \approx 1.33$ , which we clearly do not find!

<sup>5</sup>Similarly for the nitrogen molecule, we know that the (classical) covalent radius of a single nitrogen is 71 pm ( $0.71 \cdot 10^{-10}$  m), while the (triple bonded) bond length is 1.09 Å ( $1.09 \cdot 10^{-10}$  m). However, here too we must realize that this extent is representative for the electron cloud, while most of the molecule’s mass is in the nuclei. Thinking classically, we could argue that the moment of inertia about the axis connecting the two nuclei will be very small compared to the one about the orthogonal axes.

turns out that it is indeed correct.

Vibrational degrees of freedom are more tricky still. If we consider our example of  $N_2$  again, then the implicit assumption behind a count of  $n = 5$  is that the entire motion can be described by referencing the center of mass two angles. When the bond becomes effectively harmonic at high temperatures, we have that the potential connecting the two N atoms gives a quadratic contribution to the Hamiltonian. However, this contribution is only meaningful if we account for the relative motion of the two bonded atoms. There is a kinetic energy associated with this relative motion as well, which provides another  $k_B T/2$  contribution. Hence, there are  $n = 7$ , rather than  $n = 6$  relevant quadratic degrees of freedom.

Note that in general, equipartition is powerful, but it should be used sensibly. We can count degrees of freedom that are quadratic. However, it can be that the Hamiltonian contains non-quadratic contributions. In such cases, the internal energy cannot be computed using equipartition arguments alone. For example, in non-dilute gases, we have contributions coming from the interactions between the molecules.

## 3.6 Exercises

### Q17. The Stirling Formula

The approximative expression for the factorial

$$\log N! = N \log N - N + \log \sqrt{2\pi N} \quad (N \rightarrow \infty), \quad (3.30)$$

is used frequently in statistical physics. Here we derive it.

- (a) Show by induction that  $\Gamma(N + 1) = N!$  for integer  $N \geq 0$ , with the Euler  $\Gamma$ -function

$$\Gamma(x) = \int_0^\infty dt \exp[-t] t^{x-1}. \quad (3.31)$$

- (b) The function  $g_N(x)$  is defined by

$$N! = \int_0^\infty dx \exp[Ng_N(x)]. \quad (3.32)$$

Provide the expression for  $g_N(x)$ . Note: You should not get hung up on the pedagogically motivated reuse of variables.

- (c) Calculate  $x_0$  and give a Taylor expansion of  $g_N(x)$  about  $x_0$  up to  $\mathcal{O}((x - x_0)^2)$ . Argue that  $\exp[Ng_N(x)]$  is extremely peaked about  $x = x_0$  if  $N \gg 1$  and  $g_N(x_0)$  is a maximum.
- (d) Now derive the Stirling formula, and calculate or estimate the (relative) contribution from the third term for  $N = 2, 69$ , and  $10^{20}$ . Conclude that the third term is utterly irrelevant for many applications in statistical physics.

### Q18. Phase-Space Trajectories

Consider a classical point particle on a (1D) line. We denote its position by  $x$  and the momentum by  $p_x$ ; the total energy of the particle is  $E$  and is assumed fixed — the system is assumed closed. The mass of the particle is  $m$ .

Sketch the phase-space trajectory of this particle in the case that it is confined to a “box” with two hard walls, one at  $x = 0$  and the other at  $x = L$ , with  $L$  the size of the 1D box. Collisions with the walls are assumed purely elastic.

### Q19. Quantum and Classical Harmonic Oscillators

The eigenstates of a 1D harmonic oscillator, denoted by the quantum number  $n = 0, 1, 2, \dots$ , have energies  $\epsilon_n = \hbar\omega(n + 1/2)$ . Here  $\omega$  is the frequency. At temperature  $T$ , the quantum mechanical canonical partition function is defined by  $Z_q(T) = \sum_{n=0}^\infty \exp[-\beta\epsilon_n]$ , with  $\beta = 1/(k_B T)$ .

- (a) Calculate  $Z_q(T)$ .
- (b) Calculate  $Z_q(T)$  in the high-temperature limit  $T \gg \hbar\omega/k_B$ .

The same oscillator is classically described by a Hamiltonian of the form  $H(x, p_x) = p_x^2/2m + m\omega^2 x^2/2$ , with  $m$  the mass,  $p_x$  the momentum in the  $x$ -direction, and  $x$  the amplitude of the oscillator. The classical partition function is given by

$$Z_c(T) = \frac{1}{Y} \int_{-\infty}^\infty dp_x \int_{-\infty}^\infty dx \exp[-\beta H(x, p)], \quad (3.33)$$

with  $1/Y$  a prefactor that we will determine by imposing  $Z_c(T)$  to be equal to the high-temperature limit of  $Z_q(T)$ , *i.e.*, where we expect the classical behavior should be recovered.

- (c) Use your knowledge of gaussian integrals to calculate  $Z_c(T)$  in terms of  $Y\omega/(k_B T)$ . Does  $Z_c(T)$  depend on  $m$ ?
- (d) Compare (c) with (b) and conclude that  $Y = h$ , with  $h = 2\pi\hbar$  Planck's constant.

### Q20. Particles and the Chemical Potential

- (a) Show that within the grand-canonical ensemble at fixed  $T$  and  $V$  the following relation holds

$$k_B T \left( \frac{\partial \langle N \rangle}{\partial \mu} \right)_{V,T} = \langle N^2 \rangle - \langle N \rangle^2. \quad (3.34)$$

- (b) Use the Gibbs-Duhem equation to prove the thermodynamic identity

$$\left( \frac{\partial N}{\partial \mu} \right)_{V,T} = N \left( \frac{\partial \rho}{\partial p} \right)_T, \quad (3.35)$$

and then derive that

$$k_B T \left( \frac{\partial \rho}{\partial p} \right)_T = \frac{\langle N^2 \rangle - \langle N \rangle^2}{\langle N \rangle}. \quad (3.36)$$

### Q21. Particles in Wells

Assume we have a system of  $N$  non-interacting particles in a volume  $V$ . The particles are attracted to a well and experience a potential given by

$$\beta U(r) = \begin{cases} \lambda \left( \left| \frac{r}{r_c} \right| - 1 \right) & \text{if } r < r_c \\ 0 & \text{if } r \geq r_c \end{cases} \quad (3.37)$$

where  $r_c$  is the range of the interaction between the particles and the well, and  $V_0 = (4/3)\pi r_c^3$ . Show that the free energy can be written

$$\beta F/N = \log(\rho \Lambda^3) - 1 - \log \left( 1 - \frac{V_0}{V} + 3 \frac{V_0}{V} \int dx x^2 e^{-\lambda(x-1)} \right), \quad (3.38)$$

where  $\Lambda$  is the de Broglie wavelength. Hint: Use a transformation to spherical coordinates, assuming that the total volume  $V$  is roughly spherical to obtain the result. A 'cleaner' transformation that does not make this assumption will be treated in a later exercise.

### Q22. Equipartition

What is the correct value of the internal energy *per particle* for the following situations? Provide a physical argument to support your calculation for each, referencing properties of the Hamiltonian, using only a *few* words.

- (a) An ideal gas in seven dimensions (7D).
- (b) Two ideal gas particles in a harmonic trap in 1D.
- (c) A dilute monoatomic gas (like argon) in 3D.
- (d) Dilute oxygen gas in a 1 L container at room temperature. Hint: what is the shape of the molecule? Does the size or shape of the container matter?
- (e) A dilute gas of carbondioxide in a similar container at a range of temperatures from very cold to just a bit below ionization. Hint: What is the shape of this molecule?

- (f) A gas of rigid (infinitely thin) rods in 2D, assume that they are sufficiently small that you can use symmetry arguments.
- (g) A gas of rigid, thin triangular prisms in 3D; make the same assumptions as in (f).

For each of these, identify what the degrees of freedom are that contribute to the Hamiltonian and provide the proper symmetry arguments, if applicable. For (e) it may be convenient to graph the  $\gamma$  value as in Fig. 3.3.

### Q23. Refresher on Matrix Properties

In this exercise, we refamiliarize ourselves with some basic matrix properties.

- (a) Let  $\underline{\mathbf{A}}$  be a square, real-valued matrix. Is  $\underline{\mathbf{A}}$  diagonalizable? And what if  $\mathbf{A}$  is also positive definite? Show this for a  $2 \times 2$  variant. Does this give you any insight into the eigenvalues?
- (b) Let  $\underline{\mathbf{B}}$  be a matrix. Show that the determinant is preserved under orthogonal transformations. What is the physical interpretation of this? If  $\underline{\mathbf{B}}$  is additionally invertible, then what is the determinant of the inverse?
- (c) Let  $\underline{\mathbf{C}}$  be a square matrix. Show that the trace is preserved under orthogonal transformations. Unlike the determinant, the trace of a product of equal-sized matrices is not always the product of the traces. What is the physical interpretation of the trace?

### Q24. Equipartition in a Solid

Assume we have an  $N$ -particle system with Hamiltonian

$$\mathcal{H}(\mathbf{r}^N, \mathbf{p}^N) = \sum_{i=1}^N \frac{\mathbf{p}_i^2}{2m} + \Phi(\mathbf{r}^N), \quad (3.39)$$

where  $\mathbf{p}_i$  is the translational momentum of particle  $i$ ,  $m$  is its mass, and  $\mathbf{r}_i$  indicates the position coordinates. Here, we assume that the potential energy  $\Phi$  depends on all particle coordinates, but may be complicated. For example, the potential may not be decomposable in pair interactions and some external field may be encompassed within it. Additionally, we assume that the temperature is sufficiently high that the particles interact classically. The system is, however, still in a solid phase. Let  $\mathbf{R}_i$  denote the equilibrium positions of the  $i$ -th atom in this phase and  $\mathbf{u}_i \equiv \mathbf{r}_i - \mathbf{R}_i$  the (instantaneous) deviation away from this. Provided the temperature is sufficiently low — meaning far away from the melting temperature in this context — we expect  $|\mathbf{u}_i| \ll \sigma_i$ , where  $\sigma_i$  is a measure for the  $i$ -th particle's extent.

- (a) Argue in a *few* words that in this case the Hamiltonian may be written as a truncated Taylor expansion

$$\mathcal{H}(\mathbf{r}^N, \mathbf{p}^N) \approx \sum_{i=1}^N \frac{\mathbf{p}_i^2}{2m} + \Phi(\mathbf{R}^N) + \mathbf{U}^T \underline{\mathbf{M}} \mathbf{U}, \quad (3.40)$$

where  $\mathbf{U} = (\mathbf{u}_1, \dots, \mathbf{u}_N)$  is the  $3N$ -dimensional vector that contains all deviations, the superscript  $T$  indicates transposition, and  $\underline{\mathbf{M}}$  is a complicated  $3N \times 3N$  matrix.

- (b) Explain in a *few* words why there are no linear terms in  $\mathbf{U}$  or even any of the  $\mathbf{u}_i$ .
- (c) Similarly explain why the matrix  $\underline{\mathbf{M}}$  must be both real-valued and symmetric. What does this imply for the eigenvalues of the matrix?
- (d) Show that the average energy  $U = \Phi(\mathbf{R}^N) + 3Nk_B T$  irrespective of the exact shape of original potential. Hint: You are making a physical assumption here, on top of the mathematical requirements imposed by (c). These are not sufficient to complete the argument, as per Q23.

- (e) Give a physical interpretation of the eigenvectors to  $\underline{M}$ . In a course on solid-state physics you will learn that these “modes” of  $\underline{M}$  represent phonons.
- (f) What does this exercise teach you about the nature of degrees of freedom in statistical physics? Explain in a *few* words, referencing the eigenvectors of  $\underline{M}$  and how they relate to  $\underline{U}$ .

**Q25. Hydrostatic Equilibrium in the Earth’s Gravity Field**

The hydrostatic equilibrium in the Earth’s gravity field is governed by the force balance

$$\frac{dp(z)}{dz} = -g\rho_m(z), \quad (3.41)$$

where  $p(z)$  and  $\rho_m(z)$  denote the height-dependent pressure and mass density, respectively, and  $g$  denotes the gravitational acceleration. Note that  $z$  denotes the height in the vertical direction, it has *nothing* to do with the fugacity.

- (a) Derive the hydrostatic equilibrium condition by considering an infinitesimally thin slab between height  $z$  and  $z + dz$ . Consider the balance of the gravitational downward force on the mass in the slab and the upward force due to a different pressure at different heights.
- (b) Solve the force balance for a dilute (ideal) gas of particles of mass  $m$ , density  $\rho(z)$ , and constant temperature  $T$  such that  $p(z) = k_B T \rho(z)$ .
- (c) Solve the force balance for an incompressible molecular solvent of mass density  $\delta_s$ , and denote the resulting pressure profile by  $p_s(z)$ .
- (d) Calculate the upward force, exerted by an incompressible fluid with the pressure profile  $p_s(z)$  calculated in (c), on a sphere of radius  $a$  with center-of-mass at height  $z$ . Hint: the force on a surface element  $dS$  with outward normal  $\hat{n}$  is  $-p_s(z + a\hat{n} \cdot \hat{z})dS\hat{n}$ , and the result is named after an ancient Greek natural philosopher who experimented in his bath tub.

We consider a suspension of colloidal spheres of diameter  $\sigma$  and mass density  $\delta_c$  suspended in an incompressible molecular solvent of mass density  $\delta_s$  at temperature  $T$ , in sedimentation-diffusion equilibrium in the Earth’s  $g$ -field. The total pressure is written as  $p(z) = p_s(z) + \Pi(z)$ , with  $p_s(z)$  the (hydrostatic) background contribution due to the solvent, as calculated in (c), and with  $\Pi(z)$  the additional (osmotic) contribution due to the colloidal particles.

- (e) If the number density profile of the colloids is denoted by  $\rho(z)$ , argue that the mass density of the system can be written as  $\rho_m(z) = \delta_s + (\delta_c - \delta_s)\eta(z)$ , with  $\eta(z) = (\pi/6)\sigma^3\rho(z)$  the colloidal packing fraction at height  $z$ .
- (f) Show that hydrostatic equilibrium reduces to  $d\Pi(z)/dz = -mg\rho(z)$  with  $m = (\pi/6)\sigma^3(\delta_c - \delta_s)$  the so-called buoyant mass of a colloidal particle. Note (i) that  $m$  can be negative (this leads to so-called *creaming*, the opposite of *settling*), and (ii) that so-called *density-matching* allows for  $m = 0$  to study gravity-free systems on Earth (which is much cheaper than space experiments). Is the definition of  $m$  consistent with your finding in (d).
- (g) If the suspension is extremely dilute, its osmotic pressure satisfies Van ’t Hoff’s law  $\Pi = \rho k_B T$ . Calculate the resulting profile  $\rho(z)$  for the case that  $\rho(z = 0) = \rho_0$ .
- (h) It turns out that the profile  $\rho(z)$  can be measured in dense as well as dilute suspensions at fixed temperature  $T$ , e.g. by confocal microscopy or by light scattering. Explain how the complete equation of state  $\Pi(\rho)$  can be obtained from this *single* measurement of  $\rho(z)$ . This method is very efficient to obtain information about effective colloidal interactions.

## Chapter 4

# Classical and Quantum Ideal Gases

In this chapter, we describe ideal gases, *i.e.*, gases which (classically) have no intrinsic interaction to their Hamiltonian and are instantaneous thermalized. Ideal gases admit to straightforward analysis using the techniques introduced in Chapter 3 and allow us to build additional intuition for some of the more abstract quantities that we have covered thus far. In the context of real systems — atomic or molecular gases — the ideal description should be a limiting case of a model accounting for interactions. That is, infinitely dilute gases tend to behave in a (close-to) ideal manner, provided that the particle interactions decay sufficiently fast, also see Chapter 13. Before we turn to interacting systems, we should understand the dilute, non-interacting limit first.

There is another way in which the ideal-gas description can break down. In a quantum-mechanical picture, particles can have a wave-like character with an associated ‘extent’ that is captured by the De Broglie wavelength  $\Lambda$  (3.16). Such quantum particles are only dilute (and weakly interacting) whenever, the particle separation  $d$  is significantly larger than  $\Lambda$ . This can be expressed as follows

$$\Lambda = \frac{h}{\sqrt{2\pi m k_B T}} \ll d \propto \left(\frac{V}{N}\right)^{1/3} = \rho^{-1/3}. \quad (4.1)$$

Clearly, this approximation fails at low temperatures (and obviously at high density  $\rho = N/V$ , where we do not expect ideality). In this limit, we will need to take into account quantum-mechanical effects, such as quantization. This quantization is a positive aspect from the perspective of a statistical description of matter. It allows us to justify the (somewhat arbitrary) cutoff  $h^3$  for the continuum phase-space volume of a single state, which we used in Chapter 3 to obtain a countable number of classical states. Here, we will delve slightly deeper into the justification of this result than we did in Exercise Q19.

Another important difference between classical and quantum-mechanical systems is how to deal with identical particles. In quantum mechanics, identical particles of half-integer spin (*fermions*), like the electron, can never occupy the same state by the Pauli exclusion principle. The associated wave-function is antisymmetric under particle exchange and we will show that this naturally leads to *Fermi-Dirac* statistics. Identical particles of integer spin, like the photon, have symmetric exchange properties and can therefore occupy the same state. This will lead *bosons* to obey *Bose-Einstein* statistics. These two are distinct from *Maxwell-Boltzmann* statistics, which describes the distribution of classical particles over various energy states in thermal equilibrium. We will cover how these statistics impact the behavior of ideal (quantum) gases. Specifically, what this implies for photons emitted from a black-body radiator and electrons that move in solid-state materials like semiconductors, among others.

## 4.1 The Classical Ideal Gas

Continuing our analysis in Chapter 3, the canonical partition function for  $N$  classical noninteracting particles in a volume  $V$  at temperature  $T$  is given by

$$\begin{aligned} Z_{\text{id}}(N, V, T) &= \frac{1}{N! h^{3N}} \int d\mathbf{\Gamma} \exp[-\beta H(\mathbf{\Gamma})]; \\ &= \frac{V^N}{N!} \frac{1}{h^{3N}} \int d\mathbf{p}^N \exp\left[-\beta \sum_{i=1}^N \frac{\mathbf{p}_i^2}{2m}\right]; \\ &= \frac{V^N}{N! \Lambda^{3N}}. \end{aligned} \tag{4.2}$$

Here, we have used that the configurational integral of a non-interacting system is simply  $Q(N, V, T) = V^N$  and we have accounted for indistinguishability through the  $N!$  term. We will return to the implications of this term later, when we contrast the classical and quantum statistics. The ideal-gas Helmholtz free energy follows from Eq. (4.2) and reads

$$\beta F_{\text{id}}(N, V, T) = N \left[ \log\left(\frac{N\Lambda^3}{V}\right) - 1 \right], \tag{4.3}$$

using the Stirling approximation in the thermodynamic (large- $N$ ) limit. One should expect systems with finite-range interactions to behave ideal-gas-like at sufficiently low densities. That is, the above expression is a limiting form<sup>1</sup> for  $\rho = N/V \rightarrow 0$ .

### 4.1.1 Entropy and Chemical Potential

The entropy can be readily obtained from the free-energy, which is given by

$$S_{\text{id}} = - \left( \frac{\partial F_{\text{id}}}{\partial T} \right)_{N, V} = N k_{\text{B}} \left[ \log\left(\frac{N\Lambda^3}{V}\right) - \frac{5}{2} \right]. \tag{4.4}$$

This result is known as the *Sackur-Tetrode* equation and it is extensive by virtue of introducing indistinguishability of the particles. That is to say, the factor  $N!$  is crucial to obtain the scaling  $S \propto N$  at constant density for particles that are free to move. Note that appearance of a (quantum-mechanical) factor  $\Lambda$  in the expression for the entropy is not problematic, because in practice, we are only able to compute entropy differences. The  $\Lambda$  factor will drop out of any entropy difference, meaning that any classically measurable or derivable values is independent of  $\Lambda$ . Such a difference can be equivalently computed by integrating over the heat capacity weighted by the inverse temperature (convince yourself that this is accurate by referencing exercise Q3).

You will compute the grand-canonical partition function  $\Xi$  in Exercise Q26. In the  $\mu VT$  ensemble described by  $\Xi$ , the chemical potential  $\mu$  imposes the average value of the number of particles in the system. Let us use the ideal-gas system to gain additional intuition for this quantity. In the  $NVT$

<sup>1</sup>Often, the limit  $\rho \rightarrow 0$  leads to confusion among more mathematically inclined students. It simply means that there is a small value of  $\rho$  greater than zero, below which the difference between Eq. (4.3) and the free-energy of the interacting system is small and vanishing in a relative sense as  $\rho$  approaches 0. The limit is not explicitly taken, as the logarithm evidently diverges. Expansions around the ideal-gas limit involving the free energy or chemical potential expressions are therefore always about some finite, but small density  $\rho_0$  that can be made arbitrarily small.

ensemble,  $\mu$  can also be computed from the free energy  $F$  and the corresponding relation between  $\mu$  and  $N$  (thermodynamically identical to the  $\mu VT$  result) reads

$$\mu_{\text{id}} = \left( \frac{\partial F_{\text{id}}}{\partial N} \right)_{T,V} = k_{\text{B}} T \log \left( \frac{N \Lambda^3}{V} \right). \quad (4.5)$$

Note that  $\mu$  is negative whenever  $\Lambda^3 N/V < 1$ , which is what we demanded earlier for the system to behave like an ideal gas. This might be considered peculiar, as we had understood  $\mu$  to be the energy cost associated with adding a particle to a subsystem (at least in the picture that we had of the  $\mu VT$  ensemble). Why should  $\mu$  be negative? Especially in a regime where the classical description (4.1) should hold. Examining the relation in the  $SVN$  ensemble, we have the identity

$$\mu = \left( \frac{\partial U}{\partial N} \right)_{S,V}. \quad (4.6)$$

Thus, the interpretation we could give  $\mu$  is that of an energy cost associated with adding an extra particle at fixed entropy and volume. However, adding a particle provides the system with an increased number of ways in which to share the energy amongst the particles, thereby increasing the entropy. For a fixed entropy, the energy must therefore be reduced to add an additional particle, hence  $\mu < 0$ .

### 4.1.2 Maxwell-Boltzmann Distribution

The ideal gas further has a *Maxwell-Boltzmann distribution* (3.12) for the particle momentum. This can be cast into the following form for the (kinetic) energy distribution using the relation between momentum  $p$  and energy  $E = p^2/(2m)$ :

$$f(E) = \frac{2}{\sqrt{\pi}} \beta^{3/2} \sqrt{E} \exp(-\beta E). \quad (4.7)$$

Note that this relation holds for any interacting particle system in equilibrium, as we saw previously. This is, however, not the same as Maxwell-Boltzmann statistics, which provides average number of molecules present in the given single-molecule microstate, corrected for the degeneracy. We will derive this statistics in Section 4.5, where we also consider distinguishability further.

## 4.2 Dispersion Relation and Density of States

We begin moving toward the quantum gases by (re)introducing the concept of a density of states (DoS). Here, this introduction will seem somewhat artificial, but it will become more clear how a DoS should be used as we make progress in this chapter. In quantum mechanics, each particle is described by a wavefunction  $\psi(\mathbf{r}, t)$  that depends on a position vector  $\mathbf{r} = (x, y, z)$  and time  $t$ . The evolution of  $\psi$  can be obtained by solving the Schrödinger equation

$$i\hbar \frac{\partial}{\partial t} \psi(\mathbf{r}, t) = -\frac{\hbar^2}{2m} \nabla^2 \psi(\mathbf{r}, t) + V(\mathbf{r}) \psi(\mathbf{r}, t), \quad (4.8)$$

with  $\hbar = h/(2\pi)$  the reduced Planck constant,  $m$  the particle mass,  $i$  the imaginary unit, and  $V$  the external potential (accounting for walls and barriers). Whenever  $V(\mathbf{r}) = 0$  throughout space, it may be tempting to look for plane-wave solutions, *i.e.*, (combinations of) sines and cosines. Though, one has to be careful, as unbound waves are not normalizable, and therefore do not correspond to physically realizable states. It is, however, true that sines and cosines are a natural starting point for analyzing the Schrödinger equation.

### 4.2.1 State Density for a Particle in a Box

Now let us consider an ideal gas of  $N$  quantum particles trapped in a cubic box with edge length  $L$  (infinite potential outside). The vertices coincide with the positive axes and one of the corners of the cube is located at the origin. The energy eigen states of the system are found by solving the time-independent variant of the Schrödinger equation

$$E\psi(\mathbf{r}) = -\frac{\hbar^2}{2m}\nabla^2\psi(\mathbf{r}) + V(\mathbf{r})\psi(\mathbf{r}), \quad (4.9)$$

with  $E$  the energy. For our choice of  $V$  this gives rise to standing-wave solutions

$$\psi(\mathbf{r}) = \sqrt{\frac{8}{L^3}} \sin\left(\frac{\pi n_x}{L}x\right) \sin\left(\frac{\pi n_y}{L}y\right) \sin\left(\frac{\pi n_z}{L}z\right), \quad (4.10)$$

where the prefactor ensures normalization and the quantum numbers  $n_i$  with  $i \in \{x, y, z\}$  are elements of  $\mathbb{N}$  (the positive integers). Clearly, the system is quantized through the introduction of the boundary condition, see Fig. 4.1, which shows the examples of the wave solutions for a 1D system that is slightly easier to visualize.

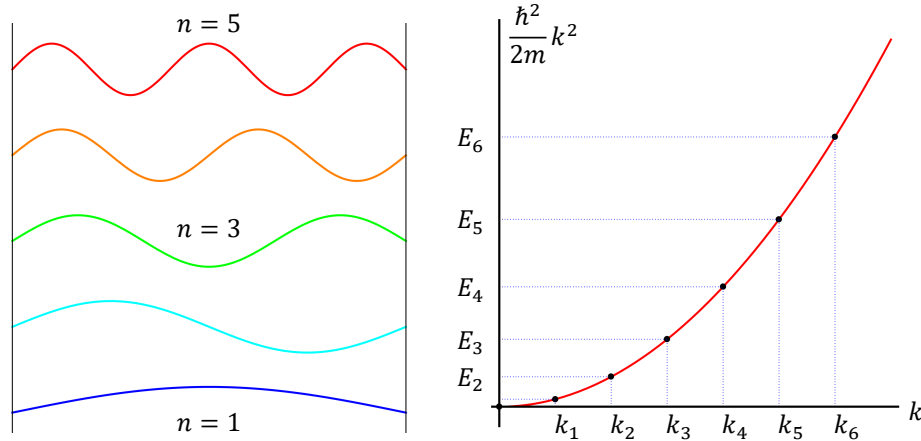


Figure 4.1: (left) The first few one-dimensional (1D) standing waves in a box. The three-dimensional (3D) system considered in this section is a multiplicative composition of these 1D systems. (right) The quadratic relation between energy  $E$  and wave number  $k$  is provided on the right. The red curve is drawn to guide the eye along a quadratic, but note that the energy levels are discrete!

Negative  $n_i$  are not considered, as changing  $n_i$  to  $-n_i$  merely changes the phase of the wavefunction by a factor of  $\pi$ , which is expressed by its sign changing from  $+$  to  $-$ . That is, sign inversion does not produce a function describing a new state of the particle. It also does not affect the probability density for the position of the particle, as this is given by  $|\psi|^2$ . The wave vectors associated with the quantum numbers are given by

$$k_i = \frac{\pi}{L}n_i. \quad (4.11)$$

and we recall that the particle momentum is given by  $p = \hbar k$ . This implies that changing the sign is equivalent to having the particle travel in the opposite direction. However, the waves we obtain for

the particle in the box are standing waves, *i.e.*, they are a superposition of waves traveling in opposite directions. That can be appreciated by recognizing that  $2 \sin(k_i x) = \exp(k_i x) - \exp(-k_i x)$ .

The permissible energy levels for the particle in our 3D box are

$$E_{\mathbf{n}} = \frac{\hbar^2}{2m} k^2 = \frac{\pi^2 \hbar^2}{2mL^2} (n_x^2 + n_y^2 + n_z^2), \quad (4.12)$$

where  $k = |\mathbf{k}|$  and  $\mathbf{n} = (n_x, n_y, n_z)$ . The above expression is also referred to as a *dispersion relation* as it connects momentum to frequency (recall  $E = \hbar\omega$  according to the De Broglie relations). The dispersion relation takes a quadratic form. In general, such a nonlinear relation implies that propagation speed of any ‘particle pulse’ will not be equal to its phase velocity. Additionally, a nonlinear dispersion relation typically leads to the spreading of the pulse with time, which is what is referred to as dispersion. This will prove relevant later.

The quantum-mechanical partition function for a single particle can now be written as

$$Z_1 = \sum_{\mathbf{n}} \exp(-\beta E_{\mathbf{n}}). \quad (4.13)$$

This sum can be evaluated by making use of an integral, see Exercise Q19 for the 1D variant of this argument; Exercise Q28 covers the general case. This is a reasonable approximation at high temperature, where quantum effects are limited. The approximative integral is given by

$$\sum_{\mathbf{n}} \approx \int d\mathbf{n} = \frac{L^3}{\pi^3} \int d\mathbf{k} = \frac{1}{8} \frac{4\pi L^3}{\pi^3} \int dk k^2, \quad (4.14)$$

where in the last step we have transitioned to spherical coordinates (hence the factor  $4\pi k^2$ ) and the factor  $1/8$  accounts for the octant to which  $\mathbf{n}$  is bounded. It will be useful to further convert the integral to one over energy  $E$  instead

$$E = \frac{\hbar^2}{2m} k^2 \quad \rightarrow \quad dE = \frac{\hbar^2}{m} k dk. \quad (4.15)$$

This results in

$$\frac{L^3}{2\pi^2} \int dk k^2 = \sqrt{2m} \frac{mL^3}{2\pi^2 \hbar^3} \int dE \sqrt{E} = \int dE \frac{L^3}{4\pi^2} \left( \frac{2m}{\hbar^2} \right)^{3/2} \sqrt{E} \equiv \int dE g(E), \quad (4.16)$$

where  $g(E)$  is the *density of states* (DoS). That is,  $g(E)dE$  counts the number of states with an energy between  $E$  and  $E + dE$ . This is simply a measure for integration, which we can apply to any function, including  $\exp(-\beta E)$  to arrive at the partition function.

Note that while we used approximations to arrive at the DoS, in practice, it is possible to replace any sum over states by an integration over a suitable density of states without significant loss of precision. Direct application the above integral form to a bosonic quantum system would lead to an oversight. This will not turn out to be of relevance to the calculations that we perform in this chapter. However, it will be relevant for the formation of a low-temperature Bose-Einstein condensate, which we will cover in Chapter 6. For the sake of completeness, we also provide more mathematical route toward defining a density of states. This starts from the partition function and makes the formal rewrite

$$Z_1 = \sum_{\mathbf{n}} \exp(-\beta E_{\mathbf{n}}) = \sum_{\mathbf{n}} \int d\mathbf{k} \exp(-\beta E) \delta(E - E_{\mathbf{n}}(\mathbf{k})), \quad (4.17)$$

where the Dirac  $\delta$  was introduced. This allows us to identify the density of states as

$$g(E) = \sum_{\mathbf{n}} \int d\mathbf{k} \delta(E - E_{\mathbf{n}}(\mathbf{k})) \approx \frac{L^3}{4\pi^2} \left( \frac{2m}{\hbar^2} \right)^{3/2} \sqrt{E}. \quad (4.18)$$

### 4.2.2 Gapped Density of States for Relativistic Particles

The DoS will prove useful to describe the behavior of a wide range of systems. That is, when we consider a occupation per energy level in describing the classical and quantum statistics, we can switch between particles with various degeneracy per energy level relatively easily. To contextualize the differences between DoS, let us consider relativistic particles. For such particles freely moving in a space-time with three space dimensions and one time dimension (*i.e.*, D3+1), the kinetic energy  $E$  is given by

$$E = \sqrt{\hbar^2 k^2 c^2 + m^2 c^4}, \quad (4.19)$$

with  $c$  the speed of light. Note that we have used the De Broglie relation to express the momentum of the particle in terms of  $\hbar \mathbf{k}$  and  $m$  should be interpreted as the rest mass.

For particles with a finite rest mass, the system is said to be ‘gapped’. Repeating the basic manipulation above, we obtain

$$g(E) = \frac{VE}{2\pi^2 \hbar^3 c^3} \sqrt{E^2 - m^2 c^4}, \quad (4.20)$$

for the DoS with  $V$  the volume of the system. It is clear that there is a band of energies  $0 \leq E < mc^2$  for which  $g(E)$  is imaginary. This is an important result, as we will discuss shortly. For massless particles the DoS reduces to

$$g(E) = \frac{VE^2}{2\pi^2 \hbar^3 c^3}, \quad (4.21)$$

which is real for all  $E \geq 0$ . The DoS in dimensions lower than 3 are different and will be considered in Exercise Q27. This difference will turn out to have strong implications for the phase behavior of bosons.

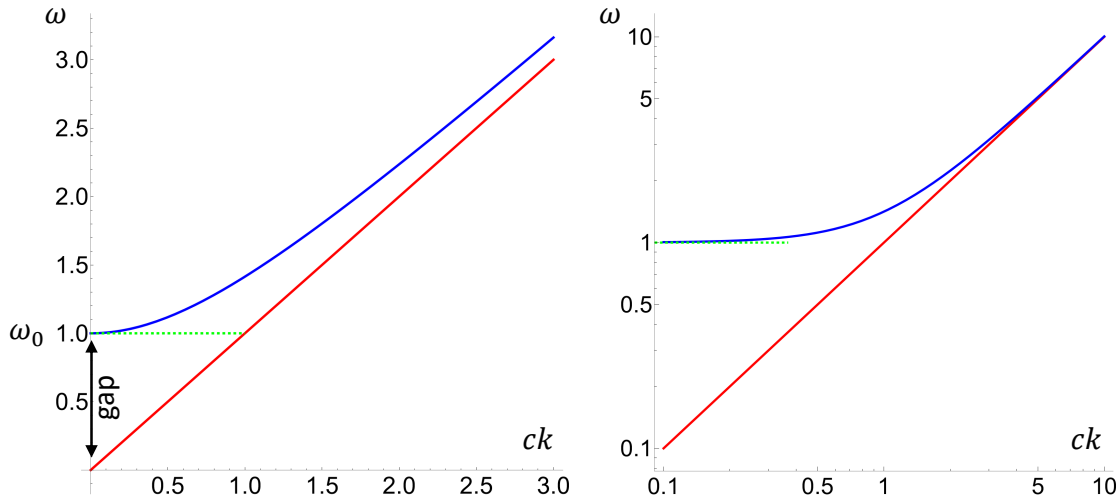


Figure 4.2: Representation of the relativistic dispersion relation for a particle with rest mass  $m$  (blue) and without (red). (left) The particle wave frequency  $\omega$  is given as a function of the wave number  $k$ . For the particle with a rest mass, the low- $k$  limit approaches a constant  $\omega_0$ . The presence of a constant  $\omega_0$  at  $k = 0$  makes the system gapped. (right) The curves approach each other in the high- $k$  limit, *i.e.*, a particle with rest mass  $m_0$  will tend toward the massless dispersion  $\omega = ck$ .

Turning Eq. (4.19) into a dispersion relation, we find  $\omega^2 = c^2k^2 + \omega_0^2$ , with  $E = \hbar\omega$  via the Planck relation and  $\omega_0 = mc^2/\hbar$ . Figure 4.2 shows this result. Here, we see that for large wavelengths, or small  $k$ ,  $\omega \propto \omega_0$ , while for short wavelengths, or large  $k$ ,  $\omega \propto ck$ . Waves in the former regime possess a vanishing group velocity and diverging phase velocity<sup>2</sup>. In other words, for frequencies below the cutoff  $\omega_0$ , the wave number is imaginary. In practical terms, this implies that such matter waves do not propagate; propagation implies a finite real value of  $k$ . Any wave that does form with a lower energy is evanescent and the amplitude characterized by decaying exponentials. The interpretation of the above result is that there are no ‘free’ states between zero energy and the gap.

Turning to solid-state electronic systems (*e.g.*, metals, semiconductors, and superconductors<sup>3</sup>), a gapped dispersion relation implies there is an energy range where no electronic states (free electrons) can exist. An intuitive example is found in a semiconductor, the ‘band gap’ in such a material generally refers to the energy difference between the top of the valence band and the bottom of the conduction band. The energy difference is what is required to promote a valence electron bound to an atom to a conduction electron, which is free to move and serves as a charge carrier. You already considered this scenario in an approximative manner in Chapter 5. The interpretation of evanescence in this context is, *e.g.*, that a thermal fluctuation kicks an electron into the conduction band briefly. However, because there is insufficient energy available for it to propagate over the lattice, eventually it falls back into the ground state, in which it is again bound to its original lattice site.

### 4.3 Bosons and Fermions

Before we continue with our evaluation of the partition function of Eq. (4.13), let us refresh our knowledge of *bosons* and *fermions*. Consider a quantum system for which the wavefunction  $\psi$  describes two particles with spin. Then  $\psi$  depends on two space coordinates  $\mathbf{r}_1$  and  $\mathbf{r}_2$  and two spin quantum numbers  $s_1$  and  $s_2$ . The amplitude  $|\psi(\mathbf{r}_1, s_1; \mathbf{r}_2, s_2)|^2$  gives the probability of finding the particles at their respective positions. Assume that the particles are identical, then exchanging the particles leads to

$$|\psi(\mathbf{r}_1, s_1; \mathbf{r}_2, s_2)|^2 = |\psi(\mathbf{r}_2, s_2; \mathbf{r}_1, s_1)|^2. \quad (4.22)$$

Given two complex numbers with identical modulus, these must differ only by a phase  $e^{i\theta}$  with  $\theta$  some real phase-angle value. Thus we have that

$$\psi(\mathbf{r}_1, s_1; \mathbf{r}_2, s_2) = e^{i\theta} \psi(\mathbf{r}_2, s_2; \mathbf{r}_1, s_1). \quad (4.23)$$

Swapping the particles back leads to the following identity

$$\psi(\mathbf{r}_1, s_1; \mathbf{r}_2, s_2) = e^{2i\theta} \psi(\mathbf{r}_1, s_1; \mathbf{r}_2, s_2), \quad (4.24)$$

which implies  $e^{2i\theta} = 1$  and<sup>4</sup>  $e^{i\theta} = \pm 1$ . The positive value is associated with bosons ( $\psi$  is symmetric under particle exchange) and the negative one with fermions ( $\psi$  behaves antisymmetrically). Quantum

<sup>2</sup>A divergent phase velocity that can easily exceed  $c$  might be somewhat concerning. However, this is a completely artificial limit that has no bearing on information transport and does not induce causality violations.

<sup>3</sup>In a superconductor, emergence of the gap at the critical temperature marks the superconducting transition, but discussing this transition in detail goes beyond the scope of these notes.

<sup>4</sup>N.B. There is a subtlety that we have swept under the rug here, this result holds for systems with three or more spatial dimensions. In 2D, there is a manner in which to construct phase factors with values  $e^{i\theta} \neq \pm 1$  that lead to identities upon double exchange. This is because in 2D clockwise and counter-clockwise rotations are well-defined concepts. The particles that are associated with this more general interchange rule are called *anyons* and these possess a statistics that continuously ‘interpolates’ between that of bosons and fermions. They play an important role in the fractional quantum Hall effect. A detailed discussion of anyons goes beyond the scope of these lecture notes and we refer the interested reader to a textbook on solid-state quantum statistics for further information.

field theory will tell you that bosons are those particles with integer spin values  $s = 0, 1, 2, \dots$  and fermions are the ones with half-integer spins  $s = 1/2, 3/2, 5/2, \dots$ .

The main implication of the (anti)symmetry under exchange is the *Pauli exclusion principle*. It can be readily shown from the above that

$$\psi(\mathbf{r}_1, s_1; \mathbf{r}_2, s_2) = \frac{1}{\sqrt{2}} (\psi(\mathbf{r}_1, s_1)\psi(\mathbf{r}_2, s_2) \pm \psi(\mathbf{r}_2, s_1)\psi(\mathbf{r}_1, s_2)), \quad (4.25)$$

where the plus symbol represents two bosons, the minus symbol two fermions, and the two-entry  $\psi$  are *normalized* single-particle wave functions<sup>5</sup> Assume now that we have fermions and that both particles are in the same state, as represented here by the identical quantum number  $s_k$ , then  $\psi(\mathbf{r}_1, s_k; \mathbf{r}_2, s_k) = 2^{-1/2} (\psi(\mathbf{r}_1, s_k)\psi(\mathbf{r}_2, s_k) - \psi(\mathbf{r}_2, s_k)\psi(\mathbf{r}_1, s_k)) = 0$ . This shows that two fermions cannot occupy the same single-particle state, *i.e.*, have all identical quantum numbers. In other words, identical fermions *must* occupy different states. When multiple are added to a system, they start filling energy levels from the bottom up, as we will see later. Note that it is crucial to realize that an energy level may be multiply degenerate, so that there may still be many fermions with the same energy. Having multiple bosons in the same single-particle state, is, however, completely acceptable. This allows bosons to undergo Bose-Einstein condensation, which we will cover in Chapter 6.

## 4.4 Three Types of Statistics and Ideal Quantum Gases

We now turn to the main difference between a classical, fermionic, and bosonic system. Let us consider systems with  $N$  identical particles and a countable number of states  $k$  labeled according to the associated energy  $\epsilon_s$ . The energies  $\epsilon_s$  may be degenerate, but it is understood that the underlying  $k$  states can always be distinguished. N.B. We should not confuse this statement about distinguishable states with the concept of (in)distinguishability for particles. It is good to keep in mind that classical particles are localized objects, *i.e.*, they have a well-defined center of mass, whereas the quantum mechanical system is described by a wave function  $\psi$ . The amplitude  $|\psi|^2$  tells us the probability of finding the system in some configuration. However, it does not allow us to localize the particles exactly, unless we give up other information such as knowledge about the momentum. This concept is captured by Heisenberg's uncertainty principle. In view of this, we can 'distinguish' classical particles, whereas in a quantum system we must always consider the states and the particles themselves are 'indistinguishable'.

Whether classical particles must be treated as distinguishable or as indistinguishable for the purpose of statistics, depends on the specifics of the system. If, for example, such identical particles are bound to lattice sites and we can see this bond, we may distinguish them by labeling them according to the associated site, which does not change. If they are, however, free to move, then it will be impossible to tell which particle is which, when contrasting two snapshots of the system. The particles are identical, after all. In this case, we must treat the particles as indistinguishable and correct for configurational overcounting. This is, for example, the case for a classical ideal gas, as you have seen.

Generally speaking, classical particles that must be considered indistinguishable, have a canonical partition sum given by  $Z = (1/N!) \sum_s \exp(-\beta\epsilon_s)$  with  $\epsilon_s$  the energy associated with state  $s$ . For convenience, we ignore any possible freedom to move, as would be the case for an ideal gas. Perhaps somewhat confusingly, we first compute the partition function  $\sum_s \exp(-\beta\epsilon_s)$  as though the particles can be distinguished (at least the states associated with each individual), only to correct for their actual indistinguishability

---

<sup>5</sup>You may not recognize the expression in its waveform representation, if you are more familiar with bra-ket notation, but the principle is the same.

afterward<sup>6</sup> by introducing the dividing factor  $N!$ .

For the fermionic system,  $Z = \sum_s \exp(-\beta\epsilon_s)$ , where  $s$  counts the number of states in the system. There is no double counting here (so no factor  $N!$ ), as quantum-mechanical  $N$ -particle states can be distinguished, *e.g.*, by their representation with respect to an orthonormal set of basis functions. These composite or many-body states are, however, subject to the condition that no two particles can occupy the same single-particle state, imposing restrictions on the sum over  $s$ , as we will see. For the bosonic system, the same argument of state distinguishability holds, thus  $Z = \sum_s \exp(-\beta\epsilon_s)$ , but now several particles can be in the same single-particle state, reducing the limitations.

fermion (indistinguishable)	boson (indistinguishable)	classical (‘distinguishable’)
$\epsilon_1$	$\epsilon_1$	$\epsilon_1$
$\epsilon_2$	$\epsilon_2$	$\epsilon_2$
$\epsilon_3$	$\epsilon_3$	$\epsilon_3$
A	AA	AB
A	A	A
	AA	B
	A	A
	A	B
	A	AB
	AA	B
	A	A
	AA	A
	AA	AB

Figure 4.3: Visualization of the permissible state occupation for, from left to right, two (identical) fermionic, bosonic, and classical particles, respectively, having three possible internal states each, labelled according to their (in this case unique) energy levels  $\epsilon_0$ ,  $\epsilon_1$ , and  $\epsilon_2$ . Two quantum-mechanical particles cannot be distinguished and we therefore duplicate the label ‘A’ for these, whilst two classical particles can be ‘distinguished’, hence we label them ‘A’ and ‘B’. (left) The two fermions cannot be in the same single-particle state, hence we have exactly three possible combinations. (middle) Two bosons can occupy the same single particle state, leading to 6 possible combinations. Here, the indistinguishable character of quantum particles is expressed:  $AA = AB = BA$  is one state! (right) We treat classical particles as distinguishable, *i.e.*,  $AB \leftrightarrow BA \neq AA$ , and these can occupy the same single-particle state, leading to a total of  $3^2 = 9$  occupation combinations. However, in writing down a partition function must introduce a factor  $1/2!$  to account for the fact that exchange of A and B leaves the system invariant.

The above discussion is perhaps a bit abstract, even potentially confusing. Let us therefore illustrate the consequences of the classical, bosonic, and fermionic conditions on state occupation. Figure 4.3 shows state-occupation tables for two identical particles, labeled A (and B), which can each (separately) be in states with energy  $\epsilon_0$ ,  $\epsilon_1$ , and  $\epsilon_2$ . These energy levels are associated with some single-particle quantum number that distinguishes the states; in practice the energies can be the same. Consulting Fig. 4.3, we

<sup>6</sup>Including the factor  $N!$  ensures the extensiveness of (certain) physical quantities, as we have argued previously. However, this does not imply that there is an issue with extensiveness of classical distinguishable particles.

see that we obtain the respective partition functions:

$$Z_{\text{clas.}} = \frac{1}{2!} \left( e^{-2\beta\epsilon_1} + e^{-2\beta\epsilon_2} + e^{-2\beta\epsilon_3} + 2e^{-\beta(\epsilon_1+\epsilon_2)} + 2e^{-\beta(\epsilon_1+\epsilon_3)} + 2e^{-\beta(\epsilon_2+\epsilon_3)} \right); \quad (4.26)$$

$$Z_{\text{bos.}} = e^{-2\beta\epsilon_1} + e^{-2\beta\epsilon_2} + e^{-2\beta\epsilon_3} + e^{-\beta(\epsilon_1+\epsilon_2)} + e^{-\beta(\epsilon_1+\epsilon_3)} + e^{-\beta(\epsilon_2+\epsilon_3)}; \quad (4.27)$$

$$Z_{\text{ferm.}} = e^{-\beta(\epsilon_1+\epsilon_2)} + e^{-\beta(\epsilon_1+\epsilon_3)} + e^{-\beta(\epsilon_2+\epsilon_3)}. \quad (4.28)$$

We reiterate that here we have treated the  $\epsilon_i$  as distinct, even though it should be emphasized that these are simply proxies for distinct states and may represent equal energy. We will capture this later using the DoS. In the table, we already see the significant differences between bosonic, fermionic, and classical systems. Examining the first energy level, we see that for fermions, 2/3 of the possible states have occupation of this state, for bosons the fraction is 1/2, and for classical particles the ratio goes up to 5/9. More importantly, for fermions there is no double occupation, for bosons 1/3 of the states is doubly occupied, and for classical particles the double-occupation fraction is 1/5. We might, therefore, expect the quantum departures from the classical ideal gas at low temperature be in opposite directions. A more involved calculation will show that this is indeed the case.

Extending this to  $k$  possible energy levels per particle for  $N$  particles, there are

$$\Omega_{\text{clas.}} = k^N; \quad (4.29)$$

$$\Omega_{\text{bos.}} = \frac{(N+k-1)!}{N!(k-1)!}; \quad (4.30)$$

$$\Omega_{\text{ferm.}} = \binom{k}{N}, \quad (4.31)$$

states, respectively. Note that for fermions, this implies  $k \geq N$  to accommodate all particles. For bosons, the combinatorics is that of placing  $N$  balls in  $k$  baskets; Exercise Q30 works this out.

Next, we turn to question of computing the mean occupation number  $\langle n_i \rangle$  for a state  $\epsilon_i$  (accounting for degeneracy). This will give the classical Maxwell-Boltzmann statistics and the two quantum statistics: Fermi-Dirac for fermions and Bose-Einstein for bosons. The latter two will prove instrumental for computing quantities in quantum systems. However, we shall first deal with a classical system to gain intuition for these statistics and how the DoS comes into play.

## 4.5 Maxwell-Boltzmann Statistics

Assume that we have a container with  $N$  identical ‘classical’ particles — we assume these distinguishable for now, see Fig. 4.4. Each particle can assume one of a total of  $k$  discrete energies  $\epsilon_j$ ,  $j \in \{1, \dots, k\}$ . Note, and we have to be very careful here, that we enumerate over discrete energies, rather than discrete levels. Multiple levels may have the same energy. This means that this energy level is degenerate in terms of states (enumerated using  $g_j$ ), see the illustration in Fig. 4.4. In mathematical notation, there can be  $m$  single-particle levels, where  $m \geq k$ . We assume the number of particles  $N$  and internal energy  $U$  of the system is fixed, so that we can write

$$N = \sum_{j=1}^k n_j \quad \& \quad U = \sum_{j=1}^k n_j \epsilon_j, \quad (4.32)$$

where  $n_j$  is the number of particles that have energy  $\epsilon_j$ .

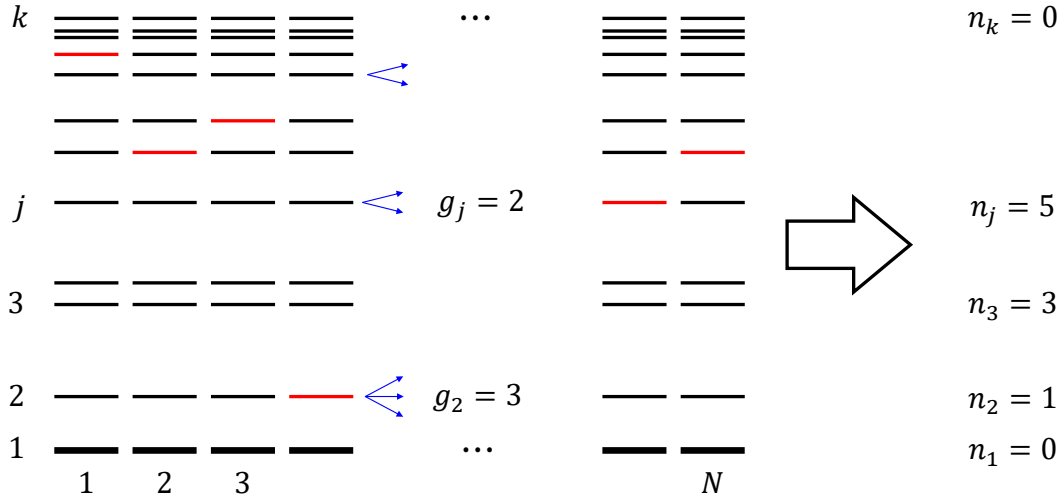


Figure 4.4: Representation of a system with  $N$  identical classical particles, which each have  $k$  discrete energy levels, as illustrated by the black lines. These levels are iterated over using index  $j$ . The red coloring indicates the current level at which a particle is. An energy level may be degenerate, as indicated by the small blue arrows and the value of  $g_j$ . The numbers  $n_j$  count the number of particles in the system that are in a specific (single-particle) energy level  $\epsilon_j$ . Note that we do not show all particles, so that  $n_3 = 3$  is not an error. The three particles that are at  $\epsilon_3$  are located in the  $\dots$  region.

We will now consider the total number of ways in which  $N$  particles may be distributed over the  $k$  possible levels. Let us assume that we know the value of the  $n_j$ . Then the various ways in which this subdivision can be picked out of the  $N$  particles available is given by the multinomial expression

$$w = \frac{N!}{n_1!n_2!\cdots n_k!} = N! \prod_{j=1}^k \frac{1}{n_j!}. \quad (4.33)$$

Let us now further assume that for each energy level  $\epsilon_j$ , there are  $g_j$  states that lead to this energy. Then the total number of combinations  $\tilde{w}$  may be written as

$$\tilde{w} = N! \prod_{j=1}^k \frac{g_j^{n_j}}{n_j!}. \quad (4.34)$$

The multiplication accounts for each particle in the  $j$ -th level to be in any of the  $g_j$  states, leading to  $g_j^{n_j}$  different possible state combinations. The total number of states  $w$  in equation (4.33) is thus a special case of  $\tilde{w}$  that describes a system, where each energy level corresponds to exactly one state. Finally, we can assume that the particles are indistinguishable and arrive at the total number of combinations  $\Omega$  for our  $k$ -energy-level gas

$$\Omega = \prod_{j=1}^k \frac{g_j^{n_j}}{n_j!}. \quad (4.35)$$

The idea that we should now have is that we should pick our  $n_j$  sensibly, such that the number of states  $\Omega$  is maximized. For example, if we chose  $n_1 = N$ , then the total number of states  $\Omega = g_1^N/N!$ .

However, by choosing a different distribution of  $n_j$ , we can increase the value of  $\Omega$  substantially. Your statistical mechanics intuition should inform you that the choice we want is the one that maximizes the entropy in the system. However, this maximization must be carried out under the constraints in Eq. (4.32), for which turn to the Lagrange-multiplier formalism of Chapter 2.

### 4.5.1 Deriving the Distribution

In practice, it will turn out to be more convenient to maximize  $\log \Omega$  than  $\Omega$  itself, but this is equivalent due to the monotonic nature of the logarithm. Using Stirling's approximation, we obtain

$$\log \Omega \approx \sum_{j=1}^k (n_j \log g_j - (n_j \log n_j - n_j)), \quad (4.36)$$

where we ignore higher-order terms. We now introduce the Lagrange multipliers to account for the constraints of Eq. (4.32) and find the extremum

$$\begin{aligned} L &= \log \Omega + \lambda_1 \left( N - \sum_{j=1}^k n_j \right) + \lambda_2 \left( U - \sum_{j=1}^k n_j \epsilon_j \right); \\ &= \lambda_1 N + \lambda_2 U + \sum_{j=1}^k [n_j \log g_j - n_j \log n_j + n_j - (\lambda_1 + \lambda_2 \epsilon_j) n_j]. \end{aligned} \quad (4.37)$$

This procedure leads to

$$0 = \frac{\partial L}{\partial n_j} = \log g_j - \log n_j - (\lambda_1 + \lambda_2 \epsilon_j), \quad (4.38)$$

and as a consequence

$$n_j = g_j \exp [-(\lambda_1 + \lambda_2 \epsilon_j)]. \quad (4.39)$$

Equation (4.39) provides basic form of the Maxwell-Boltzmann statistics, but we will need to clarify a few more points before we come to the final form.

Note that according to our constraint minimization, we still need to determine the values of  $\lambda_1$  and  $\lambda_2$ . If we have that  $N \gg 1$ , then we can extract the result by manipulating Eq. (4.38). Multiplying Eq. (4.38) by  $n_j$ , summing over  $j$ , and substituting the expression for  $\log \Omega$ , we obtain

$$\log \Omega = \lambda_1 N + \lambda_2 U, \quad (4.40)$$

and subsequently

$$dU = \frac{1}{\lambda_2} d \log \Omega - \frac{\lambda_1}{\lambda_2} dN. \quad (4.41)$$

But this may be identified with the relation  $dU = TdS - pdV + \mu dN$  that holds in thermodynamic limit. It should be clear that  $\log \Omega$  serves the role of  $S/k_B$  and thus we arrive at  $\lambda_2 = \beta$  and  $\lambda_1 = -\beta\mu$ . Substituting these relations back into our equation for  $n_j$ , we arrive at

$$n_j = \frac{g_j}{\exp [\beta(\epsilon_j - \mu)]}, \quad (4.42)$$

and the expression

$$N = \sum_{j=1}^k n_j = \sum_{j=1}^k \frac{g_j}{\exp [\beta(\epsilon_j - \mu)]}. \quad (4.43)$$

Here, we recognize that the  $g_j$  serve as a (discrete) density of states! That is, the number of states present for a given energy level  $\epsilon_j$ . Generally, as we have seen in this chapter, the density of states can vary depending on the nature of the particle (relativistic or not). It is therefore desirable to separate the DoS from occupation of a single-particle energy level.

The energy-level statistics corrected for the DoS, has the following form

$$f_{\text{MB}}(\epsilon) = \frac{1}{\exp[\beta(\epsilon - \mu)]}, \quad (4.44)$$

which is referred to as *Maxwell-Boltzmann statistics*. Quantities such as energy and particle number for general classical gases can be derived from this statistics and an appropriate DoS. For example the number of particles  $N$  and energy  $E$  in the system are given by

$$N = \int dE g(E) f_{\text{MB}}(E); \quad (4.45)$$

$$E = \int dE g(E) E f_{\text{MB}}(E), \quad (4.46)$$

respectively. Here, we have made the necessary transformation to go from a sum over energy levels to an integral representation.

### 4.5.2 Preparing for Quantum Systems

In practice, a closed system is not the most practical for comparing quantum and classical gases, because to do so, we wish to take a high-temperature limit, in which the quantum-mechanical nature of the system breaks down<sup>7</sup>. This would more naturally lend itself to the  $NVT$  ensemble. We could write down the expressions for the canonical partition sums describing an ideal<sup>8</sup> boson and fermion gas composed of identical particles. However, for practical intents and purposes, evaluating the state sums in  $Z$  taking into account occupancy rules is challenging. We could make an analogy to our derivation of the Maxwell-Boltzmann statistics for a classical gas, however, it will prove more convenient to take a different route.

Let us consider the grand-canonical ensemble, where we have — referencing Eq. (2.18) — the following equalities

$$\Xi(\mu, V, T) = \sum_{N=0}^{\infty} \sum_s \exp[\beta\mu N - \beta\mathcal{E}_s] = \sum_{N=0}^{\infty} \sum_E \exp[\beta\mu N - \beta E], \quad (4.47)$$

with  $s$  indexing individual states of the *entire* system with  $N$  particles in it. We assign an energy  $\mathcal{E}_s$  to such an  $N$ -particle state  $s$ ; the particle and thermal reservoir are assumed infinitely large. In the second equality, we have replaced the sum over states by a sum over the various energies  $E$  that are present in a system with  $N$  particles. It is important to understand that each  $E$  may be multiply degenerate; both in terms of ways in which to have single-particle levels come together to obtain  $E$  and internal degeneracy of a single-particle level (multiple quantum-number combinations give the same single-particle energy).

To make this mathematically clear, we introduce the single-particle energy levels  $\epsilon_i$ ; the  $\mathcal{E}_s$  are thus a sum over the relevant values  $\epsilon_i$  contributing to a given state  $s$ . However,  $E$  is also a sum over  $\epsilon_i$ ,

<sup>7</sup>It should be noted that the Maxwell-Boltzmann statistics can equally be derived by considering the quantum gases and taking the appropriate high-temperature limit, in which their statistics both reduce to the result derived above.

<sup>8</sup>We assume that the particles are non-interacting, which is an approximation that allows us to write the total energy as the sum of the individual particle energies. For dilute, free electrons in a (semi-)conductor, a fermionic particle, the system turns out to satisfy this condition, though this is far from obvious in view of the long-ranged nature of Coulomb interactions. Clearly, for photons, a bosonic particle, the approximation is excellent, because the electromagnetic field does not interact with itself, due to the linearity of Maxwell's equations.

but a simpler one, since there are  $n_i$  particles that have this energy level  $\epsilon_i$ ;  $N = \sum_i n_i$ . This means that the occupancy of this level (throughout the system) contributes  $\epsilon_i n_i$  and that the total energy is  $E = \sum_i \epsilon_i n_i$ . Note that (again) we must be careful, as the energy levels  $\epsilon_i$  may be degenerate in terms of quantum numbers, but this will not impact  $E = \sum_i \epsilon_i n_i$ .

Introducing the expressions for  $N$  and  $E$  into the equation for  $\Xi$ , allows us to break up the exponent of a sum into a product of the individual terms. We can then exchange the sums over  $N$  and  $E$  with the product to obtain

$$\Xi(\mu, V, T) = \prod_i \sum_{n_i} \exp[\beta n_i (\mu - \epsilon_i)] \equiv \prod_i Z_i, \quad (4.48)$$

where now we sum over the all the various occupancies of *single-particle* energy levels that can occur in the system. Here, we define the factor  $Z_i$  to be the effective single-level ‘grand’-canonical partition function. Sketching the situation out might help in your understanding as to how to arrive at this result. We have purposefully kept the indexing of the sum over  $n_i$  ambiguous, as this will be where we will impose the fermionic and bosonic character of our particles; we will come back to this shortly.

A key point in interpreting the exchange of the product and sum is that in Eq. (4.47) we sum over all possible number of particles. The infinity in the sum over potential particle allows us to consider instead all *possible* occupations of the single particle levels instead. This is because which particles carry a certain energy level does not matter, because they are *intrinsically* indistinguishable in quantum mechanics! For example, let us assume that we have fermions, then energy level  $j \in \{0, \dots, k\}$  may be assumed by one particle or none of the particles. Suppose we have one of the particles carry that energy level, we cannot know which one it is. So, unlike classical, distinguishable objects (which we may label, but for which the labelling may not be unique), there is only one state corresponding to that level being occupied. This means that we do not get unpleasant combinatorial factors from exchanging the sum and the product, as would be the case classically, since putting that level on, *e.g.*, particle 1 out of 10 is different from putting it on particle 3 out of 10, and so on. Likewise, for bosons, there might be 25 particles with the single-particle energy level  $\epsilon_j$ . Again, however, which particles those are, does not matter. This is also expressed in the fact that  $Z_i = \exp[\beta n_i (\mu - \epsilon_i)] = \exp[\beta (\mu - \epsilon_i)]^{n_i}$ , where we recognize that all the occupations (that are permissible) are independent of each other. This last observation is relevant for bosons, as they can be in the same single-particle state multiple times.

The result in Eq. (4.48) is quite powerful, because each energy level can be dealt with independently, meaning that finding  $n_i$  particles in state  $i$  is independent of what is happening in the other states. For example, it is now straightforward to compute  $\langle n_i \rangle$  using the grand-canonical partition function, from which we will extract *Bose-Einstein* and *Fermi-Dirac* statistics next. These computations will assume no degeneracy factor (a single state per energy level), but a DoS may be readily added after completing the calculation, in complete analogy to the Maxwell-Boltzmann scenario treated earlier.

## 4.6 Non-Interacting Bose Gas

For bosons there can be any number of particles in state  $i$  with energy  $\epsilon_i$  (again emphasizing that these states are not degenerate for now), which implies

$$Z_i = \sum_{n_i=0}^{\infty} \exp[\beta n_i (\mu - \epsilon_i)] = \frac{1}{1 - \exp[\beta (\mu - \epsilon_i)]}, \quad (4.49)$$

using the geometric series. We find for the grand-canonical partition function

$$\Xi(\mu, V, T) = \prod_i \frac{1}{1 - \exp[\beta(\mu - \epsilon_i)]}, \quad (4.50)$$

and for the associated grand potential

$$\beta\Omega = -\log \Xi = \sum_i \log(1 - \exp[\beta(\mu - \epsilon_i)]) = \sum_i \log(1 - z \exp[-\beta\epsilon_i]), \quad (4.51)$$

with  $z = \exp(\beta\mu)$  the fugacity in the last equality.

Taking a derivative of  $\Omega$  with respect to  $\mu$  (keep track of prefactors!), the energy-level occupancy is found to read

$$\langle n_i \rangle = \frac{1}{\exp[\beta(\epsilon_i - \mu)] - 1}, \quad (4.52)$$

where you should note the inversion of the elements in the exponent. When  $\epsilon_i < \mu$  the number of particles is negative, which means that  $\mu < \epsilon_i$  for all  $i$ . Because the ground state is often chosen<sup>9</sup> to have energy  $\epsilon_0 = 0$ , the chemical potential must be negative. This is consistent with our earlier observations on the classical ideal gas.

The expression for  $\langle n_i \rangle$  defines the *Bose-Einstein* distribution:

$$f_{\text{BE}}(\epsilon) = \frac{1}{\exp[\beta(\epsilon - \mu)] - 1}. \quad (4.53)$$

This result has similarities to the expression we found for the Maxwell-Boltzmann statistics. However, there is now the addition of a ‘ $-1$ ’ in the denominator. Since we have just argued that  $\mu < 0$ , this implies that as the chemical potential approaches the energy of the ground state from below, the number of particles in the ground state diverges at fixed temperature. Similarly, the ground-state occupation diverges when the temperature goes to zero at fixed  $\mu$ . In practice, we will need to be a lot more subtle, as we will see next.

### 4.6.1 The High-Temperature Limit

Before moving onto ideal gases of fermions in the next section, let us consider the high-temperature limit and how the ideal Bose gas approaches the classical ideal gas. The DoS for non-relativistic quantum particles (recall Eq. (4.16)) reads

$$g(E) = g_s \frac{V}{4\pi^2} \left( \frac{2m}{\hbar^2} \right)^{3/2} \sqrt{E}, \quad (4.54)$$

where  $V$  is the system’s volume. The factor  $g_s = 2s + 1$  accounts for the degeneracy of an energy level according to the number of spin states  $s$  that it represents. Using the above DoS, we can compute the total number of particles in the gas

$$N = \int dE g(E) f_{\text{BE}}(E) = \int dE \frac{g(E)}{z^{-1} \exp[\beta E] - 1}. \quad (4.55)$$

---

<sup>9</sup>The specific choice of the ground-state energy will impact the integration boundaries and expression for the DoS.

Note that because technically we are in the grand-canonical ensemble, we compute an average. By inverting this relation, we obtain  $\mu$  as a function of  $N$  for a given  $T$ , which we will come back to shortly. The average energy is given by

$$E = \int dE g(E) E f_{\text{BE}}(E) = \int dE \frac{E g(E)}{z^{-1} \exp[\beta E] - 1}. \quad (4.56)$$

Finally, in the grand-canonical ensemble we can compute the pressure from the grand potential, as you will do yourself in Exercise Q32. Identifying the energy *via* partial integration gives us  $pV = 2E/3$ . This is referred to as the caloric equation of state — we will see this quantity again in Chapter 14, when we cover structure factors and pair-correlation functions in dense fluids — and it holds in general for bosonic, fermionic, and classical ideal gases. Note that  $E$  is still a function of  $z$  and that this depends on temperature as well<sup>10</sup>.

At high temperatures, the fugacity  $z \ll 1$ . At first glance this result seems strange,  $z = \exp(\beta\mu)$ , so clearly,  $z \rightarrow 1$  as the temperature goes to infinity. What we are missing is that simultaneously we must guarantee that  $\rho\Lambda^3 \ll 1$ , such that we can employ the ideal-gas approximation. This implies that as the temperature goes up, the chemical potential must tend toward  $-\infty$  faster. In practice, we want to use a constant density, which implies that to leading order  $z/\Lambda^3$  should be constant. The underlying issue is that we derived our statistics in the grand canonical ensemble, but we are interested in quantities that conform to the canonical ensemble. This problem will crop up again when we study Bose-Einstein condensation in Chapter 6. Unfortunately, there is no straightforward manner in which to remedy this situation. Deriving the statistics in the  $NVT$  ensemble is not pleasant and we are better off compromising here by introducing a temperature dependence to  $\mu$ .

From the above discussion, we conclude that we must have that  $z \propto T^{-3/2} \ll 1$  as  $T \uparrow \infty$ . Using this information, we can now expand Eq. (4.55) to

$$\rho = \frac{N}{V} = g_s \frac{z}{\Lambda^3} \left( 1 + \frac{z}{2\sqrt{2}} + \dots \right), \quad (4.57)$$

and we can perform a similar expansion on Eq. (4.56) to obtain

$$\frac{E}{V} = g_s \frac{3z}{2\beta\Lambda^3} \left( 1 + \frac{z}{4\sqrt{2}} + \dots \right). \quad (4.58)$$

We can insert the inverted form of Eq. (4.57) into Eq. (4.58) to obtain an expression for  $E$  in terms of  $\rho$ . That is,  $z$  is obtained as a function of  $\rho$  by truncating the series and solving for  $\rho$ , picking the correct root of the quadratic equation and Taylor expanding this. The more elegant way of inverting Eq. (4.57) relies on the concept of *series reversion*, where  $z$  is expanded as a series in  $\rho$ , *i.e.*,  $z = \sum_{n=1}^{\infty} c_n \rho^n$  with the  $c_n$  unknown coefficients. Plugging this series into Eq. (4.57) and matching orders of  $\rho$ , allows one to identify the values of the  $c_n$  sequentially. If you use series reversion, you will need to go up to second order in  $\rho$  to find the final result. As an intermediate step you will obtain

$$z(\rho) = \frac{\Lambda^3}{g_s} \rho - \frac{\Lambda^6}{2^{3/2} g_s^2} \rho^2 + \frac{(9 - 4\sqrt{3})\Lambda^9}{36 g_s^3} \rho^3 - \dots \quad (4.59)$$

The expression  $E(\rho)$  can subsequently be substituted in the equation for the pressure  $pV = 2E/3$  to achieve the final result

$$\beta p = \rho - \frac{\Lambda^3}{4\sqrt{2} g_s} \rho^2, \quad (4.60)$$

<sup>10</sup>The relevant expressions are provided at the end of Chapter 6, should you want to verify your results.

which reproduces the equation of state for the classical ideal gas in the limit  $T \uparrow \infty$ . Note that the relation  $pV = 2E/3$  is called the caloric equation of state and in the classical ideal gas can be readily derived using equipartition and the ideal gas law. In quantum systems you can show that this holds for both fermions and bosons using properties of the grand canonical partition function.

Note the second (quadratic in  $\rho$ ) term in Eq. (4.60) is a low-density correction that accounts for quantum effects. We will encounter this type of expansion again, when we examine the classical virial coefficients in Chapter 13. In this case, however, the term emerges solely from quantum statistics, as we had explicitly removed any interactions from our description. At high temperature, the effect of this term is to reduce the pressure. This makes sense, because more bosons can occupy the same single-particle state quantum mechanically than classical particles can. Referencing Fig. 4.3, we indeed see this reflected in the difference in fraction of doubly occupied energy levels between the boson and classical system. What is perhaps potentially more disturbing is the appearance of the De Broglie wavelength, which always drops out of any classically measurable quantity. However, this expression charts how the quantum system approaches the classical limit and in any non-ideal gases other effects will dominate over this term in the classical limit. We will consider the low-temperature limit of the Bose gas in Chapter 6, where we discuss Bose-Einstein condensation.

### 4.6.2 Photons: A Relativistic Bose Gas

Photons are a spin 1 particle, for which the energy is given by  $E = \hbar\omega$ . They have (as we saw before) the relativistic dispersion relation  $\omega = kc$ . This allows us to write

$$\tilde{g}(\omega)d\omega = \frac{V\omega^2}{\pi^2 c^3}d\omega, \quad (4.61)$$

with  $\tilde{g}$  the photon-frequency DoS<sup>11</sup>. Following our Bose-gas analysis, the partition function is written

$$Z_\omega = \frac{1}{1 - \exp(-\beta\hbar\omega)}, \quad (4.62)$$

where we use photons have chemical potential  $\mu = 0$ . This is because the chemical potential is the (rest-mass) energy cost for inserting a photon into the system, but photons are massless particles. That is to say, for any vanishingly small energy, a photon can be created, albeit with a very long wavelength.

Evaluating the grand potential — referencing Eq. (4.51) and switching to an integral representation — we thus have

$$\beta\Omega = -\log \Xi = \frac{V}{\pi^2 c^3} \int d\omega \omega^2 \log(1 - \exp[-\beta\hbar\omega]). \quad (4.63)$$

We know the relation between the average energy and the grand potential, which leads to

$$E = -\frac{\partial}{\partial\beta} \log \Xi = \frac{V\hbar}{\pi^2 c^3} \int d\omega \frac{\omega^3}{\exp[\beta\hbar\omega] - 1}, \quad (4.64)$$

<sup>11</sup>N.B. We might expect a factor of 2 in the denominator of our density of states, referencing Eq. (4.21). We also need to multiply this result with a factor of  $g_s$  as in the case of Eq. (4.54), to account for ‘spin’ degeneracy, which we had not accounted for in obtaining Eq. (4.21). However, we do not find a degeneracy factor of  $g_s = 3$ , as one might expect for a spin 1 particle like the photon, based on our previous discussion. Instead, we have accounted for a factor of 2 degeneracy to account for the two classical states of polarization. Why is this permitted? Photons are a massless boson and their spin algebra works differently from that of bosons with mass, a photon turns out to have helicity rather than spin. A full discussion of this goes beyond the scope of the notes, but we refer the interested reader to Wigner’s original paper on unitary representations of the inhomogeneous Lorentz group. N.B. This is a rather advanced text, other treatments of helicity may be found.

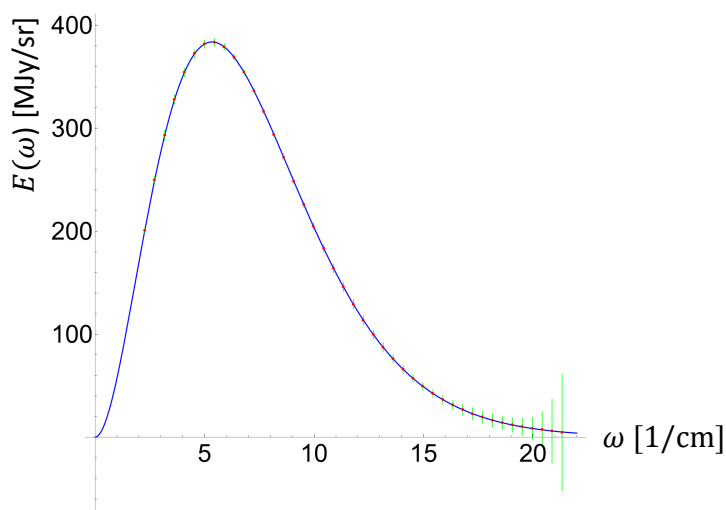


Figure 4.5: Visualization of the measured cosmic microwave background radiation spectrum (red dots, in MJy/sr, where “Jy” is Jansky and “sr” stands for steradian) fitted with a Planck distribution (blue) that leads to an effective temperature  $T \approx 2.725$  K. The error bars (green) are expanded by a factor of 200 to make them visible. Data was obtained from [D.J. Fixsen *et al.*, *Astrophys. J.* **473**, 576 (1996)], who processed the COBE satellite results.

from which the Planck distribution  $E(\omega)d\omega$  can instantly be recognized. Note that this is the spectrum that belongs to a *thermalized* photon gas!

This fact should strike a chord with any physicist: the (nearly perfectly uniform) cosmic microwave background (CMB) radiation has the Planck spectrum, see Fig. 4.5. The implication is that the CMB is thermalized across the entire observable universe! But this is strange. Suppose we observe light from the CMB coming from two opposite directions. Then by Einstein’s theory of relativity, the matter emitting this light cannot have interacted with each other, as it belongs to causally disconnected regions of the universe. How can it be that it is at the same temperature? Or in the language of statistical mechanics, how can it be that these regions have come into thermal equilibrium with each other? Discussion of the potential solution to this problem (inflation) belongs to the realm of cosmology and will not be covered in this course. However, you should take away from this small aside that statistical mechanics finds application throughout physics.

Next, we use the Planck spectrum to relate temperature to the color of an object, as you may recall from courses that discuss black-body radiation. First we can make a rough estimate for the relation between temperature and the wavelength of the emitted light. Assume that the dominant emission comes from the peak of the distribution, then we see that the associated angular frequency is given by

$$\omega_{\max} = \zeta \frac{k_{\text{B}}T}{\hbar}, \quad (4.65)$$

where  $\zeta \approx 2.822$  solves  $3 - \zeta = 3e^{-\zeta}$ . Rewriting this expression, the maximum wavelength is given by

$$\lambda_{\max} = \frac{hc}{\zeta k_{\text{B}}T} \approx \frac{5.1 \cdot 10^{-3} \text{ m K}}{T}, \quad (4.66)$$

where  $T$  is in Kelvin. For visible light, we have wavelengths of 380 nm to 700 nm, meaning that we require temperatures of around  $10^4$  K. Care has to be taken in using this result, as there is an entire spectrum of frequencies being emitted for a given temperature by a black-body radiator. Our approximation generally overestimates the temperature required to produce a given color. In addition, our eyes will interpret the spectrum, leading to unexpected results. For example, a black-body radiator of  $7 \cdot 10^3$  K will be perceived to emit white light, rather than the expected color green, if we were to use the maximum wavelength result.

The total energy  $E$  emitted at a given temperature  $T$  can also be straightforwardly determined from the Planck spectrum. We will outline the results here and leave the algebra to Exercise Q33. The full calculation involves a Gamma function and leads to the energy-density expression

$$\mathcal{E} \equiv \frac{E}{V} = \frac{\pi^2 k_B^4}{15 \hbar^3 c^3} T^4. \quad (4.67)$$

From this the Stefan-Boltzmann law for the energy emitted by an object at temperature  $T$  can be obtained, where  $j$  is the energy flux

$$j = \frac{\mathcal{E}c}{4} \equiv \sigma T^4. \quad (4.68)$$

Here,  $\sigma$  is the Stefan constant and the first identity follows from a geometric consideration, namely that for a finite object photons are only emitted in one direction.

Lastly, we consider the high-temperature limit for the photon system. In this case, we mean  $\hbar\omega \ll k_B T$ . Then Planck's distribution reduces to

$$E(\omega) \approx \frac{V}{2\pi^2 c^3} \omega^2 k_B T. \quad (4.69)$$

Note that all hints of the quantum-mechanical character of light, as described by  $\hbar$ , have disappeared from this expression. You may have encountered it before as the *Rayleigh-Jeans* law for the distribution of classical radiation. This law had a serious problem — arguing from a pre-quantum perspective — as the total energy diverges: an effect which is referred to as an ultraviolet catastrophe. The quantization of light eliminated this catastrophe, as for  $\hbar\omega \gg k_B T$  there is simply not enough energy to create a single photon. This implies that the high-frequency modes remain unpopulated<sup>12</sup>.

## 4.7 Non-Interacting Fermi Gas

Turning to fermions there can be at most one particle in state  $i$  with energy  $\epsilon_i$ , which implies

$$Z_i = \sum_{n_i=0}^1 \exp[\beta n_i (\mu - \epsilon_i)] = 1 + \exp[\beta (\mu - \epsilon_i)]. \quad (4.70)$$

This makes the grand-canonical partition function

$$\Xi(\mu, V, T) = \prod_i (1 + z \exp[-\beta \epsilon_i]), \quad (4.71)$$

<sup>12</sup>There is a similar issue with sound waves propagating through solids, called *phonons*. At first glance, the relevant expressions are roughly the same, except that the speed of light is replaced by the speed of sound  $c_s$  and that phonons can possess three polarizations, rather than two. However, a lengthy discussion of this topic goes beyond the scope of these notes and we refer you to a basic course on solid-state physics for a discussion of the Debye model for phonons and its shortcomings, which were rectified by Einstein.

and the associated grand potential

$$\beta\Omega = - \sum_i \log(1 + z \exp[-\beta\epsilon_i]). \quad (4.72)$$

Computing the energy-level occupancy leads to the *Fermi-Dirac* distribution:

$$f_{\text{FD}}(\epsilon) = \frac{1}{\exp[\beta(\epsilon - \mu)] + 1}. \quad (4.73)$$

At low  $T$ , states with energy greater than  $\mu$  are essentially unoccupied and states with energy less than  $\mu$  are completely filled, we will come back to this in the next section.

Following the steps from the section on bosons, it is straightforward to compute the particle number, average energy, and pressure, using the DoS. Here too, the factor  $g_s = 2s + 1$  needs to be accounted for. The equation of state in the high-temperature limit now becomes (following steps analogous to the ones taken for the Bose gas)

$$\beta p = \rho + \frac{\Lambda^3}{4\sqrt{2}g_s} \rho^2 + \dots. \quad (4.74)$$

Thus, the correction to the classical result is an increase in the ideal-gas pressure by the fermionic character of the quantum particles. That the pressure should increase also makes sense, as each state can only be occupied by a single fermion.

### 4.7.1 The Low-Temperature Limit

The low-temperature limit of fermions is rather interesting for applications, as it has a bearing on (semi-)conductor physics. We have already learned about phonons in Exercise Q24. These can also be described as free-traveling sound waves, as we observed in the last footnote to Section 4.6.2. Since their statistics satisfies that of bosons, they are expected to produce an energy density  $\propto T^4$  and thus a heat capacity that scales as  $T^3$ . Measurements of the heat capacity of metals indeed reveals this scaling, but for low temperatures there is a noticeable deviation. This may be explained by considering the heat capacity of electrons, which scales as  $T$ . In this section, we will provide the more mathematical route toward this result, while we explore the physical interpretation in Exercise Q34.

Let us start by considering the zero-temperature limit of an ideal fermion gas. This would seem like a terrible approximation to the physics of actual electrons in a metal, as these experience Coulomb interactions. However, trying this simplest of approximation will turn out to yield a surprisingly accurate result. We note that taking the limit  $T \downarrow 0$  leads to reduced Fermi-Dirac distribution

$$f_{\text{FD}}(\epsilon) \rightarrow \begin{cases} 1 & \text{if } \epsilon < \mu \\ 0 & \text{if } \epsilon > \mu \end{cases}. \quad (4.75)$$

The interpretation is that each fermion added to the system (value of  $\mu$ ) settles in the lowest energy state. As more particles are added, the states are successively filled. The *Fermi energy* is the energy level associated with this state<sup>13</sup>, *i.e.*,  $E_{\text{F}} = \mu(T = 0)$ . The value of  $E_{\text{F}}$  is computed by determining the relation between  $N$  and  $E$  from

$$N = \int dE g(E) f_{\text{FD}}(E) = g_s \frac{V}{4\pi^2} \left( \frac{2m}{\hbar^2} \right)^{3/2} \int_0^{E_{\text{F}}} dE \sqrt{E}. \quad (4.76)$$

<sup>13</sup>This definition works well for metals, but can lead to confusion for semi-conductors and insulators, for which the chemical potential can lie between two (conduction) bands.

and inverting the expression to obtain  $E$  as a function of  $\rho$ . Then the limit  $T \downarrow 0$  is taken to obtain

$$E_F = \frac{\hbar^2}{2m} \left( \frac{6\pi^2}{g_s} \rho \right)^{2/3}. \quad (4.77)$$

Using the Boltzmann constant an equivalent Fermi temperature  $T_F \equiv E_F/k_B$  may be defined. This temperature divides what is considered a high- $T$  and low- $T$  limit. Note, however, that it is not typically a low temperature in an absolute sense: the Fermi temperature for electrons in a metal is typically around  $10^4$  K. It also does not define a phase transition; we will find a transition for the ideal Bose gas in Chapter 6, though that too will be more subtle than the classical examples that follow later.

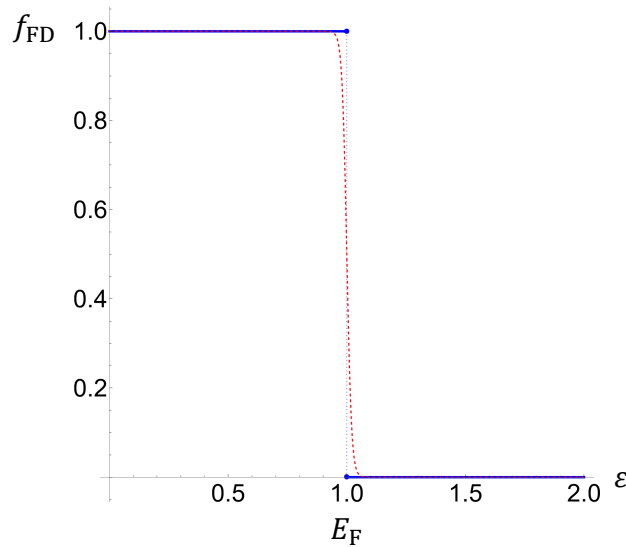


Figure 4.6: Perturbations of the Fermi-Dirac distribution  $f_{\text{FD}}(\epsilon)$  away from temperature  $T = 0$ . At absolute zero, the distribution is Heaviside-like (blue;  $T = 0$ ). For small departures (red),  $k_B T$  much smaller than the Fermi energy  $E_F$ , the profile is smoothed out.

When  $T = 0$ , it is easy to compute that the average energy is  $E = (3/5)NE_F$  and the pressure is given by  $\beta p = (2/5)NE_F$ , again using the caloric identity. This implies that there is a residual pressure at  $T = 0$  that comes from the exclusion principle, as both the classical and Bose ideal gas have vanishing pressure at this temperature. The story becomes more complicated, when we perturb away from  $T = 0$ . The usual approach is to intuit that only those states which are within  $k_B T$  of the Fermi surface are affected by temperature, see Fig. 4.6. This implies that the Heaviside-like form of Eq. (4.75) is only weakly affected. Insisting that the number of particles remains the same, when the temperature is changed, implies  $\partial N/\partial T = 0$ . This leads to an expression for the heat capacity of the system, see Exercise Q34.

Here, we will instead use the more mathematical Sommerfeld expansion, which provides the prefactors to the above argument. This analysis will also set the stage for our analysis of Bose-Einstein condensation in Chapter 6, wherein we will make extensive use of families of functions. Note that the particle and

energy densities are given by

$$\rho = \frac{g_s}{\Lambda^3} \frac{2}{\sqrt{\pi}} \int_0^\infty dx \frac{x^{1/2}}{z^{-1}e^x + 1} \equiv g_s \Lambda^{-3} f_{3/2}(z); \quad (4.78)$$

$$\frac{E}{V} = \frac{g_s}{\Lambda^3} k_B T \frac{2}{\sqrt{\pi}} \int_0^\infty dx \frac{x^{3/2}}{z^{-1}e^x + 1} \equiv \frac{3g_s}{2\Lambda^3} k_B T f_{5/2}(z), \quad (4.79)$$

respectively, where we have introduced  $x = \beta E$  and the family of functions

$$f_n(z) = \frac{1}{\Gamma(n)} \int_0^\infty dx \frac{x^{n-1}}{z^{-1}e^x + 1}. \quad (4.80)$$

The factor  $\Gamma(n)$  represents the gamma function and the following two values will be important  $\Gamma(3/2) = \sqrt{\pi}/2$  and  $\Gamma(5/2) = 3\sqrt{\pi}/4$ . To approach the small temperature limit, we now write

$$\begin{aligned} \Gamma(n)f_n(z) &= \int_0^{\beta\mu} dx \frac{x^{n-1}}{z^{-1}e^x + 1} + \int_{\beta\mu}^\infty dx \frac{x^{n-1}}{z^{-1}e^x + 1}; \\ &= \int_0^{\beta\mu} dx x^{n-1} \left(1 - \frac{1}{1 + ze^{-x}}\right) + \int_{\beta\mu}^\infty dx \frac{x^{n-1}}{z^{-1}e^x + 1}; \\ &= \frac{(\log z)^n}{n} - \int_0^{\beta\mu} dx \frac{x^{n-1}}{1 + ze^{-x}} + \int_{\beta\mu}^\infty dx \frac{x^{n-1}}{z^{-1}e^x + 1}. \end{aligned} \quad (4.81)$$

Making the substitutions  $y_1 = \beta\mu - x$  for the first integral and  $y_2 = x - \beta\mu$  for the second, we arrive at

$$\Gamma(n)f_n(z) = \frac{(\log z)^n}{n} - \int_0^{\beta\mu} dy_1 \frac{(\beta\mu - y_1)^{n-1}}{1 + e^{y_1}} + \int_0^\infty dy_2 \frac{(\beta\mu + y_2)^{n-1}}{1 + e^{y_2}}. \quad (4.82)$$

Approximating  $\beta\mu \gg 1$  as  $\infty$  in the integration boundary of the first expression, we are making a mistake order  $z^{-1} = \exp(-\beta\mu) \ll 1$ . This is vanishing in the limit of  $T \downarrow 0$  and is therefore acceptable. The approximation allows us to combine the two integrals

$$\Gamma(n)f_n(z) = \frac{(\log z)^n}{n} + \int_0^\infty dy \frac{(\beta\mu + y)^{n-1} - (\beta\mu - y)^{n-1}}{1 + e^y}. \quad (4.83)$$

Using Taylor expansion of the numerator to  $2(n-1)(\beta\mu)^{n-2}y + \dots$ , gives us

$$\Gamma(n)f_n(z) = \frac{(\log z)^n}{n} + 2(n-1)(\log z)^{n-2} \int_0^\infty dy \frac{y}{e^y + 1}, \quad (4.84)$$

where we used the relation between  $\beta\mu$  and  $z$ . The integral can be evaluated analytically by identifying a series or using an analytic integration software. The final result is written as

$$f_n(z) = \frac{(\log z)^n}{\Gamma(n+1)} \left(1 + \frac{\pi^2}{6} \frac{n(n-1)}{(\log z)^2} + \dots\right). \quad (4.85)$$

The above result can be plugged back into our original expressions for  $\rho$  and  $E/V$ . The former leads to a relation between  $\mu$  and  $\rho$ , which can be expressed in terms of the Fermi energy as

$$\mu = E_F \left(1 - \frac{\pi^2}{12} \left[\frac{k_B T}{E_F}\right]^2 + \dots\right). \quad (4.86)$$

The chemical potential is maximal at  $T = 0$  and decreases, when  $T$  is raised. This corresponds to our intuition for the classical ideal gas, where the chemical potential can be at most zero and is otherwise increasingly negative as particles are added to the system. Using the expression for  $E$  and a few lines of algebraic manipulation, we arrive at a heat capacity of

$$C_V = Nk_B \frac{\pi}{2} \frac{T}{T_F}. \quad (4.87)$$

The above heat capacity form finds use in the study of metals. The conduction electrons, *i.e.*, the ones that carry current and are free to move, can be approximated as an ideal gas. This is slightly surprising, because one might naively think that the long-ranged Coulomb potential would interfere with such a description. However, the approximation turns out to work remarkably well. This  $\propto T$  scaling is experimentally recovered at very low temperatures and for many metals this prefactor is reasonably close the one we have just computed; to within 20%!

We refer the curious reader to a standard textbook solid-state physics for more information on the quality of the ideal-gas approximation, the Drude model by which the linear scaling can also be computed, and why these approximations work to begin with. The concepts set out above and more formally handled in a course on solid-state physics, maybe also be applied to more esoteric scenarios. You will encounter the statistical mechanics of fermions in the study of white dwarves and the Chandrasekhar limit. Additionally, the theory in this chapter can also be used to treat para- and diamagnetism with some modifications; all of this, unfortunately, goes beyond the scope of these notes.

## 4.8 Exercises

### Q26. Classical Ideal Gas

Calculate the grand-canonical partition function  $\Xi(\mu, V, T)$  of an ideal gas, and show that it can be written as  $\Xi = \exp(zV)$  with  $z(\mu, T) = e^{\beta\mu}/\Lambda^3$ . Calculate the pressure  $p(z, T)$  and the density  $\rho(z, T)$  of the classical ideal gas from  $\Xi$ . (Assume 3D)

### Q27. Density of States in any Dimension

In this exercise, we will consider the density of states (DoS) for a particle with mass  $m$  in a  $d$ -dimensional system with size  $L$  that is free to move within its confining volume.

- (a) Show that the DoS is given by

$$g(E) = \frac{1}{2}\Omega_d \left(\frac{L}{2\pi}\right)^d \left(\frac{2m}{\hbar^2}\right)^{d/2} E^{\frac{d}{2}-1} \quad (4.88)$$

where  $\Omega_d$  represents the surface area of the  $d$ -dimensional unit sphere:  $\Omega_1 = 2$ ,  $\Omega_2 = 2\pi$ ,  $\Omega_3 = 4\pi$ , etc.

- (b) Sketch the behavior of the three cases.  
 (c) Comment on the implication of this result for the possibility of having a Bose-Einstein condensate in dimensions  $d = 1$  and  $2$ , respectively. Hint: Page through the final section of Chapter 6 to get an idea.

### Q28. Particle in a Box

A quantum particle in a one-dimensional box of size  $L$  along the  $x$ -axis, say with  $x \in [0, L]$ , has wavefunctions  $\psi_k(x) \propto \sin(kx/2)$  with a discrete set of allowed wavenumbers  $k = \pi n/L$  with quantum numbers  $n = 1, 2, 3, \dots$ , i.e., such that  $\psi(0) = \psi(L) = 0$ . The energy with quantum number  $n$  is given by  $\epsilon_n = \hbar^2 k^2 / (2m) = \hbar^2 n^2 / (8mL^2)$ , such that the partition function at temperature  $T$  equals  $Z_q(T) = \sum_{n=1}^{\infty} \exp(-\beta\epsilon_n)$ .

- (a) At sufficiently low  $T$ , the partition sum contains only a few terms that contribute substantially to its value. Define the temperature  $T^*$  as the temperature below which the system is essentially in the ground state. In the case that  $T \gg T^*$  there are many contributing terms to  $Z_q(T)$ , and hence  $Z_q(T) \simeq \int_0^{\infty} dn \exp(-\beta\epsilon_n)$  is an accurate approximation. Evaluate this high-temperature limit of  $Z_q(T)$ .

The classical Hamiltonian of this particle is  $H(x, p) = p_x^2/2m + V(x)$  with  $V(x) = 0$  for  $x \in (0, L)$  and  $V(x) = \infty$  otherwise. The classical partition function is therefore

$$Z_c = (1/Y) \int_{-\infty}^{\infty} dp_x \int_{-\infty}^{\infty} dx \exp(-\beta H(x, p_x)), \quad (4.89)$$

with  $1/Y$  a prefactor such that the classical and high-temperature quantum result agree.

- (b) Calculate  $Z_c(T)$  and choose  $Y$  such that it agrees with your answer in (a). Compare your result with the one you obtained for the harmonic oscillator in Chapter 3.

**Q29. More on a Particle in a Box**

It is well known that the Gaussian integral is given by  $\int_{-\infty}^{\infty} dx \exp[-ax^2] = \sqrt{\pi/a}$  for any  $a > 0$ .

- (a) Use this to calculate the canonical partition function  $Z_1$  of a single classical point particle in a 1D box of length  $L$  (see exercise Q19) at temperature  $T$ , where  $Z_1$  is defined as

$$Z_1(T, L) = \frac{1}{h} \int_{-\infty}^{\infty} dp_x \int_0^L dx \exp[-p_x^2/(2mk_B T)], \quad (4.90)$$

with  $h$  Planck's constant and  $m$  the mass of the particle.

- (b) Rewrite your answer of (a) as  $Z_1(T, L) = L/\Lambda$ , and give an expression for  $\Lambda$ .
- (c) The free energy of this single particle is given by  $F_1 = -k_B T \log Z_1$ , and its entropy by  $S_1 = -\partial F_1/\partial T$ . Calculate  $F_1$  and  $S_1$ , and also the average energy  $E_1$  using that  $F_1 = E_1 - TS_1$ .
- (d) Write down the canonical partition function  $Z_3$  for a single particle in a 3D cubic box of volume  $V = L \times L \times L$ , and show that it equals  $Z_3 = Z_1^3$ . Calculate the free energy, entropy, and average energy of this 3D case.

**Q30. Combinatorics**

Suppose you had  $n$  indistinguishable balls and  $k$  distinguishable baskets. Enumerate the ways of distributing the balls into boxes. Some boxes may be empty. To start, represent each distribution as  $n$  stars and  $k - 1$  vertical lines (the stars and bars representation). For example, for  $n = 7$  and  $k = 3$ , a valid distribution is:  $3 + 2 + 2 = ***|**|**$ . Convince yourself that in general this representation enumerates the various configurations for a bosonic system. Argue how this leads to the expression found in Eq. (4.30).

**Q31. Three Different Statistics**

In this exercise, we will consider the consequences of having bosonic, fermionic, and classical statistics. Sketch the Maxwell-Boltzmann, Fermi-Dirac, and Bose-Einstein distributions in one graph. Put the occupation  $\langle n \rangle$  on one axis and  $\beta(\epsilon - \mu)$  on the other, where  $\epsilon$  is the state energy,  $\beta$  the inverse thermal energy, and  $\mu$  the chemical potential. Assume you are working at relatively high temperature. Argue how the shape of the distributions conforms to the way the bosons and fermions depart from the classical ideal gas limit.

**Q32. Bose Gas at High Temperatures**

At high temperatures, a gas of conserved bosons behaves similar to a classical ideal gas. In this problem, the goal is to determine the leading-order corrections to the classical ideal gas law  $pV = Nk_B T$ . This can be done along the following lines.

- (a) Start with the particle number  $N$  in integral representation. For high temperatures  $T$  the chemical potential  $\mu$  becomes large but negative, such that  $z = e^{\beta\mu} \ll 1$ . Expand the particle number (or particle density  $\rho = N/V$ ) in orders of  $z$ . Hint: It is convenient to express your result in terms of the De Broglie wavelength  $\Lambda$  and you might want to look up the Gamma function  $\Gamma(x)$ .
- (b) Now, determine the energy  $E$  or the energy density  $\epsilon = E/V$  analogously to the particle number/density, *i.e.*, *via* expansion in terms of  $z$ .
- (c) Finally, determine an expression for the pressure  $p$  via  $pV = 2E/3$ , use the expression for the particle number/density to eliminate  $z$ , and write your result analogous to the classical ideal gas, such that the leading-order correction can be easily identified. Hint: an expansion up to second order in  $z$  is sufficient.

**Q33. Black-Body Radiation**

This exercise covers the historically very important problem of black-body radiation. Consider a cubic box with volume  $V$  in three dimensions. Note that photons are non-conserved spin-1 bosons with a linear dispersion relation  $\omega = ck$ ; but, other than one might expect for spin-1 particles, photons have only two (not three) spin states.

Assuming that the photon system is in thermal equilibrium (with the walls of the box) at temperature  $T$ , the goal of this problem is to determine the energy density and the energy flux out of the box (if it has a small hole). This can be done as follows.

- (a) Starting from the factorized grand-canonical partition function

$$\Xi(\mu, V, T) = \prod_i \sum_{n_i}^{\infty} \exp[-\beta n_i(\epsilon_i - \mu)] = \prod_i Z_i, \quad (4.91)$$

determine  $Z_i$  based on the above information about photons.

- (b) Using  $E = -\partial \log \Xi / \partial \beta$ , write the energy in form of a continuous frequency integral. For that purpose, you will need to determine the photon density of states (either in advance or along the way).
- (c) Find the temperature dependence of the energy density  $\epsilon = E/V$  by making the integral dimensionless; that is, by substituting  $x = \beta \hbar \omega$ . Note that, by making the integral dimensionless, you can find the temperature dependence of  $\epsilon$  without evaluating the integral; the dimensionless integral is just a number. However, in the present case, you can also evaluate the integral or look it up.
- (d) Finally, assume that the cubic box has a small hole through which light can escape. Using that photons travel with the speed of light  $c$ , determine the energy flux out of the cubic box from basic geometry considerations.

**Q34. Fermi Gas far below the Fermi Level**

In this exercise, we will take the non-Sommerfeld route toward computing the heat capacity of the ideal Fermi gas.

- (a) Begin by showing that the change in the number of particles when perturbing away from  $T = 0$  by  $k_B T \ll E_F$  can be approximated as:

$$\frac{\partial N}{\partial T} \approx g(E_F) \int_0^{\infty} dE \frac{\partial}{\partial T} \left( \frac{1}{e^{\beta(E-E_F)} + 1} \right), \quad (4.92)$$

where  $E_F$  is the Fermi energy and  $g$  denotes the density of states. Hint: start from the definition of  $N$  and Taylor expand the density of states (DoS).

- (b) Perform the differentiation and show that

$$\frac{\partial N}{\partial T} \approx g(E_F) \int_0^{\infty} dE \left( \frac{E - E_F}{k_B T^2} \right) \frac{1}{4 \cosh^2(\beta(E - E_F)/2)} \approx 0. \quad (4.93)$$

Why should the integral (approximately) vanish? Hint: Make use of the small range  $\sim k_B T$  over which the integrand is contributing to the integral in your argument.

- (c) Compute, using the same approximations as above the change of the energy with respect to the temperature and show

$$C_V = \left. \frac{\partial E}{\partial T} \right|_{N,V} \approx \int_0^{\infty} dE \left[ E_F g(E_F) + \frac{3}{2} g(E_F)(E - E_F) \right] \frac{\partial}{\partial T} \left( \frac{1}{e^{\beta(E-E_F)} + 1} \right). \quad (4.94)$$

This will require a Taylor expansion to capture the linear term in the DoS. Using the argument from (b) to eliminate the constant term, argue that the integral takes on the form

$$C_V \approx \frac{3}{2} g(E_F) k_B^2 T \int_{-\infty}^{\infty} dx \frac{x^2}{4 \cosh^2(x/2)}, \quad (4.95)$$

where  $x = \beta(E - E_F)$ .

- (d) Consider the following intuitive argument. At low temperatures, only fermions with energy within  $k_B T$  are participating in the physics. What is (roughly) the number of such fermions? Estimate the energy that these carry in total. Argue from the scaling of your result with  $T$  that this implies that  $C_V \propto T$ .



## Chapter 5

# Chemical Equilibria

In this chapter, we examine the equilibrium behavior of a system, where the elements can react with each other *via* a chemical reaction. In this situation, chemical species are continuously exchanged, but the macroscopic concentrations are unaffected. That is, the net reactive flux of species is zero. To emphasize that processes are taking place in this equilibrium, the term *dynamic equilibrium* is often used. We shall see that in chemical equilibrium, the fraction of each chemical species involved in the reaction is controlled by the chemical potential of that species. Using statistical mechanics to describe this situation leads to the equilibrium *law of mass action*: the ratio between the concentration of reactants and products is constant. This is an extension of Le Châtelier's principle: The equilibrium in a chemical system responds to a change in concentration, temperature, or pressure by shifting in the direction which partially counteracts the imposed perturbation. We will also briefly touch upon the relation between the constant ratio and the processes that underlie a return to equilibrium upon perturbing the system. We close this chapter by giving another example of the use of chemical equilibria in a doped semiconductor.

### 5.1 Chemical Reactions and the Gibbs Free Energy

Let us start by considering a chemical reaction between  $M$  chemical species  $X_i$ ,  $i \in \{1, \dots, M\}$ , and  $M'$  chemical species  $X'_j$ ,  $j \in \{1, \dots, M'\}$ . Then the reaction scheme becomes

$$\sum_{i=1}^M v_i X_i \rightleftharpoons \sum_{j=1}^{M'} v'_j X'_j, \quad (5.1)$$

where  $v_i$  is the stoichiometric coefficient for species  $X_i$  and  $v'_j$  is the stoichiometric coefficient for species  $X'_j$ . The expression essentially says that each individual reaction that takes place, changes the number of molecules of each species according to their respective stoichiometric coefficients. For example, the combustion of methane into carbon dioxide and water would be written as:



Of course, the equilibrium concentrations of these molecules may be shifted far to one side of the reaction or the other depending on the ambient pressure and temperature.

Assume that the reaction is taking place in a closed, isothermal system, for which the pressure is fixed, *i.e.*, at constant  $T$  and  $P$ . In this ensemble, the free energy that will govern the equilibrium behavior is the Gibbs free energy. We can gain insight into the reactions taking place by isolating a single species  $N_r$  and changing the system by  $dN_r$ . Then the change in the Gibbs free energy due to the  $dN_r$  chemical reactions is

$$v_r dG = \left( - \sum_{i=1}^M v_i \mu_i + \sum_{j=1}^{M'} v'_j \mu'_j \right) dN_r, \quad (5.3)$$

where  $\mu_i$  is the chemical potential of species  $X_i$ , and  $\mu'_j$  is the chemical potential of species  $X'_j$ . Here, it is important to note that the chemical reactions lead to interdependencies between the various species participating in the reactions: changing the amount of species  $N_r$  modifies all other reactant species  $X_i$  and product species  $X'_j$ . Thus, the expression in Eq. (5.3) is obtained by applying the chain rule to  $G$  and rearranging. Since our choice of species  $N_r$  was arbitrary, the result holds in general. As we will discuss further in Chapter 6, when a system is in equilibrium, the relevant free energy is at a minimum. Hence, at equilibrium we expect  $dG = 0$ , we have

$$\sum_{i=1}^M v_i \mu_i = \sum_{j=1}^{M'} v'_j \mu'_j. \quad (5.4)$$

Equation (5.4) is an expression of matter conservation, but its practical use is limited as, experimentally one can access the density or pressure, but not the chemical potential.

## 5.2 The Law of Mass Action

We can make progress towards a more familiar formalism by rewriting Eq. (5.4) in the dilute-limit approximation. That is, the only interactions between the particles are the chemical reactions themselves. The free energy of the total system is then well approximated by the sum of the free energies of the individual species. The Helmholtz free energy of a specific species can now be written as

$$\beta F_i = \beta N_i f_i + N_i \log(\rho_i \Lambda_i^3) - N_i, \quad (5.5)$$

where  $f_i$  is the free energy of a molecule of species  $X_i$  including its ground-state energy and any internal degrees of freedom. Note that the last two terms of Eq. (5.5) correspond to the ideal-gas free energy, and thus arise from the molecule's (translational) degrees of freedom. That is, we have made an expansion of the free energy around the ideal-gas free energy; this approach to dealing with free energies is quite natural and we will pursue it further in Chapter 13. Similarly, the chemical potential of species  $X_i$  is

$$\beta \mu_i = \beta \left( \frac{\partial F}{\partial N_i} \right)_{T,V} = \beta f_i + \log(\rho_i \Lambda_i^3). \quad (5.6)$$

Combining Eqs. (5.4) and (5.6), we obtain:

$$\frac{\prod_{i=1}^M \exp(\beta v_i f_i)}{\prod_{j=1}^{M'} \exp(\beta v'_j f'_j)} = \frac{\prod_{j=1}^{M'} (\rho'_j \Lambda_j^3)^{v'_j}}{\prod_{i=1}^M (\rho_i \Lambda_i^3)^{v_i}}, \quad (5.7)$$

where the right-hand side of the equation has the features of an equilibrium constant for the concentration, if you recall your high-school chemistry; but it is not quite the constant you encountered there.

Unfortunately, the density in Eq. (5.7) is measured in units of the individual De Broglie wavelengths ( $\Lambda_i$ ) of the molecules. In practice, it is more convenient to instead define the density in terms of a ‘standard’ reference density. Typically, for gases, this reference density is chosen to be that of an ideal gas at temperature  $T$  and a pressure of 1 atmosphere. For aqueous solutions, the reference is a concentration of one mole per liter at the same pressure of 1 atmosphere. Denoting this standard density by  $\rho_0$ , we can rewrite Eq. (5.7) as

$$\frac{\prod_{i=1}^M [X_i]^{v_i}}{\prod_{j=1}^{M'} [X'_j]^{v'_j}} = \exp\left(-\beta\Delta\mu^{(0)}\right), \quad (5.8)$$

where

$$[X_i] \equiv \frac{\rho_i}{\rho_0}; \quad (5.9)$$

$$\Delta\mu^{(0)} \equiv \sum_{i=1}^M v_i \mu_i^{(0)} - \sum_{j=1}^{M'} v'_j \mu'_j{}^{(0)}, \quad (5.10)$$

and

$$\beta\mu_i^{(0)} = \beta f_i + \log(\rho_0 \Lambda_i^3). \quad (5.11)$$

Note that  $\mu_i^{(0)}$  is the chemical potential of species  $i$  at the standard density  $\rho_0$ . Equation (5.8) is known as the *law of mass action*; technically speaking, it is the equilibrium consequence of the more generalized form of this law. The implication is that whenever you adjust the concentration of one of the species, the reactions drive the system to such a state that the ratio again satisfies Eq. (5.8). The law of mass action does not only apply to chemical reactions, but can be applied to a range of systems that form bonds. For instance, some nuclear reactions can be explained using this simple expression.

Returning to our methane-combustion example of Eq. (5.2), the expression takes the familiar form

$$\frac{[X_{\text{CH}_4}][X_{\text{O}_2}]^2}{[X_{\text{CO}_2}][X_{\text{H}_2\text{O}}]^2} = K_c^{-1}, \quad (5.12)$$

with  $K_c$  the equilibrium constant for the concentration. It is important to keep in mind that many equilibrium constants can be created by choosing the reference differently, *e.g.*, instead of a reference density  $\rho_0$ , a partial pressure could have been chosen. These equilibrium constants can be related to each other using the equation of state. Lastly, it is clear that predicting  $K_c$  from microscopic theory is complicated, as it requires knowledge of the relevant chemical potentials.

### 5.3 Reaction Kinetics and Equilibrium Constants

Thus far, we have commented on the situation wherein equilibrium is established and we have observed that when the system is brought out of equilibrium, it will tend toward a new equilibrium such that the concentration ratio remains fixed. This ratio may be identified as the equilibrium constant. However, we also know reactions in a dynamical sense, for which the equilibrium constant is the ratio of the individual reaction rates. Let us take the simplest example



where the forward reaction  $A \rightarrow B$  has reaction rate  $k_f$  and the backward reaction  $B \rightarrow A$  has rate  $k_b$ . Near equilibrium, most reactions are well described by linear proportionalities between the rates

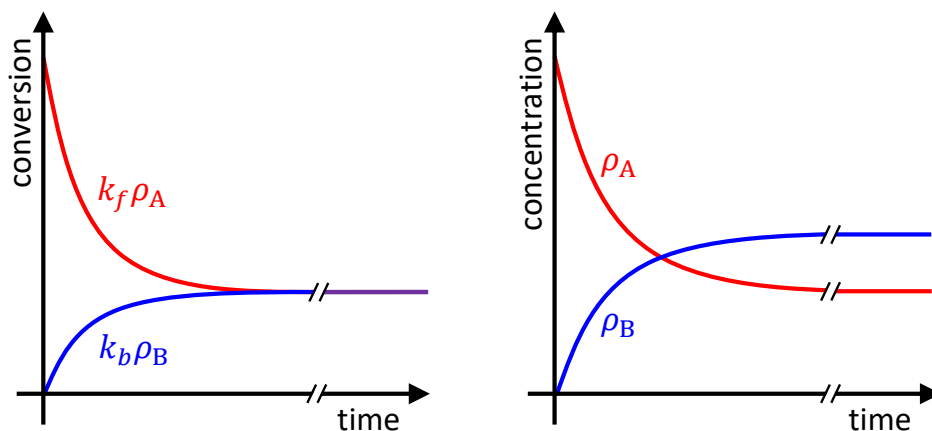


Figure 5.1: Sketch of the time evolution of a two species system tending toward the chemical equilibrium  $A \rightleftharpoons B$ . We start with a situation where there is only species  $A$ ; the respective densities are given by  $\rho_A$  (red) and  $\rho_B$  (blue). (left) The effective conversion rates:  $A \rightarrow B$  has reaction rate  $k_f$  and the backward reaction  $B \rightarrow A$  has rate  $k_b$ . The use of the cut marks indicates the behavior as  $t \rightarrow \infty$ , where the two rates are equal (purple horizontal line). (right) The evolution of the densities during the equilibration.

concentration of reactants:

$$\dot{\rho}_A(t) = -k_f \rho_A(t) + k_b \rho_B(t); \quad (5.14)$$

$$\dot{\rho}_B(t) = k_f \rho_A(t) - k_b \rho_B(t). \quad (5.15)$$

Here,  $\rho_A$  and  $\rho_B$  are the numbers of particles of each species,  $t$  is time, and the dot denotes the time derivative. The equilibration process from a state of pure  $A$  is illustrated in Fig. 5.1. Clearly,  $\rho_A(t) + \rho_B(t)$  is constant for all time and the equilibrium concentrations satisfy

$$K'_c \equiv \frac{\rho_B^{\text{eq}}}{\rho_A^{\text{eq}}} = \frac{k_f}{k_b}. \quad (5.16)$$

Here,  $K'_c$  is the equilibrium constant associated with the kinetic picture.

It is tempting to identify  $K'_c = K_c$  for a given reaction, however, one has to be very careful. This simplified approach does not take into account the conceptual differences between the true thermodynamic equilibrium constant and the ratio of rate constants that is the kinetic equilibrium constant. These constants are generally not equal, except at chemical equilibrium, for ideal systems, and elementary reactions; and even then with some caveats. In particular, the kinetic reaction rates cannot simply be obtained by exponentiating the  $\beta\mu_i^{(0)}$  and the law of mass action only delimits the *ratio* of these rates in general. Computing the rates requires the notion of out-of-equilibrium thermodynamics, which goes beyond the scope of these notes.

## 5.4 Doping of a Semi-Conductor

Let us consider a semiconductor, say silicon, of which the atoms in the crystal are covalently bound to four neighbors. Impurities are added to dope the silicon. For example, a small fraction of the Si sites is

instead occupied by a P, As, or Sb atom. These dopants have an additional electron and nuclear charge, which is ‘left over’ when the 4 covalent bonds have formed with neighboring Si atoms. The electron can be localized around the dopant nucleus, which has a binding energy of about  $I = 30$  to  $50$  meV, depending on the specific dopant. Chemical equilibria can be used to establish which fraction of the dopant electrons is bound and which is freed into the conduction band. When the electron is in the conduction band, it is able to traverse the Si lattice, thereby allowing for charge transport. Note that this is also a case of simple adsorption dynamics.

Let us consider a single dopant atom and treat that as a system in contact with the reservoir formed by the Si crystal. The dopant is assumed to be in thermal and chemical equilibrium with the Si crystal, exchanging electrons and energy. There are now three possible configurations: (i) The dopant is ionized and the electron is in the reservoir, (ii) the electron localized at the dopant with spin up, and (iii) the same as (ii) but with spin down. These three configurations can be written as  $(N = 0, \epsilon = 0)$  and  $(N = 1, \epsilon = -I)$ , respectively, where we use that there is no energy difference between the two bound states in the absence of a magnetic field. The Gibbs sum is given by  $\Xi = 1 + 2 \exp(\beta(I + \mu))$ , so that the probability of being ionized is given by  $P_{\text{ion}} = 1/\Xi$ . For small temperatures  $P_{\text{ion}} \approx \exp(-\beta(I + \mu)) \ll 1$ , such that the charge carriers from doping freeze out. This argument gives a simple relation for the scaling of conductivity with temperature. Unfortunately, the real temperature dependence measured in a semiconductor is more complicated. The model is thus in need of some refinement, as we will gain an impression of in Chapter 4.

## 5.5 Exercises

### Q35. Small Clusters

Consider a square-lattice model with  $A$  sites and  $n$  occupied sites (or particles). If two particles are adjacent, they bond with bonding energy  $-\epsilon$  (with  $\epsilon > 0$ ). However, a particle that is already bonded cannot bond with any other particles. Thus, the system consists of monomers and dimers. Here, we develop an approximate solution to the problem for low densities.

Assume that there is an average monomer density  $\rho_1 = n_1/A$  and dimer density  $\rho_2 = n_2/A$ , with  $n_{1,2}$  the number of monomers and dimers. Also assume that the monomers and dimers do not interact, so both behave like an ideal gas.

- What is the canonical partition sum  $Q_1(n_1, A, T)$  for the monomers? And for the dimers? Remember that the dimers can have two orientations, and assume periodic boundary conditions.
- Calculate the Helmholtz free energy  $F(n_1, n_2, A, T)$  of the system, using Stirling's approximation  $\log n! = n \log n - n$ .
- Show that in equilibrium the chemical potentials of monomers and dimers should obey:  $2\mu_1 = \mu_2$ . Then show that this requires:

$$\frac{\rho_2}{\rho_1^2} = 2 \exp(\beta\epsilon). \quad (5.17)$$

- What is the relationship between  $\rho_1, \rho_2$ , and  $\rho$ ? Calculate  $\rho_1$  and  $\rho_2$  in terms of  $\rho$  and  $\epsilon$ . What happens in the limit where  $\epsilon \rightarrow 0$  (assuming low density)? And  $\epsilon \rightarrow \infty$ ?

### Q36. Gas Adsorbing to an Interface

Consider a system of  $N$  ideal gas particles with mass  $m$  at a temperature  $T$ . The mean pressure is  $P$  and  $N_g$  gas particles move freely in a volume  $V = L^3$ . Another  $N_s$  (identical) particles are absorbed to a surface with area  $L^2$  (forming one of the faces of our cubic volume), where they also behave as two-dimensional ideal gas. The total number of particles in this system is  $N = N_g + N_s$ . The total energy of an absorbed particle is given by  $E = p^2/2m - \epsilon_0$ , where  $\mathbf{p}$  is a 2D momentum and  $\epsilon_0$  is the binding energy per particle.

- Calculate the partition functions of the free and absorbed gas, label these  $Z_g$  and  $Z_s$ , respectively. The particles are to be treated as indistinguishable.
- Determine the Gibbs free energies  $G_g$  and  $G_s$  using the partition functions.
- Use this to derive the respective chemical potentials  $\mu_g$  and  $\mu_s$ .
- The two systems are in chemical equilibrium at temperature  $T$ . Compute the mean number of gas particles absorbed per unit area in terms of the given variables.
- Keeping temperature  $T$  and total number of particles  $N$  the same, now the volume in which the free gas particles can move is increased. What consequences does this have for the equilibrium between the free gas particles and the gas particles absorbed on the surface, *i.e.*, are more or less particles absorbed compared to the case with smaller volume? Justify your answer using a *few* words only.

### Q37. Saha's Equation

In this exercise, we will use the law of mass action to examine the number of atoms that are ionized in a stellar atmosphere. This is captured by the Saha equation, which was used to explain the relatively rapid decay of Balmer-absorption-line intensity with increasing temperature. The

spectroscopy details are not relevant here<sup>1</sup>, we merely aim to illustrate how chemical equilibrium can be used to describe physical phenomena across a wide variety of systems.

- (a) Consider the reaction  $e^- + p^+ \rightleftharpoons H + \gamma$ , where  $e^-$  is a free electron,  $p^+$  a proton (ionized hydrogen),  $H$  is a neutral hydrogen atom, and  $\gamma$  a photon. Argue why chemical equilibrium for this reaction satisfies  $\mu_{e^-} + \mu_{p^+} = \mu_H$ .
- (b) Assume that all involved particles behave like an ideal gas and write their respective number densities as  $\rho_{e^-}$ ,  $\rho_{p^+}$ , and  $\rho_H$ . Argue using a few words under what conditions we may assume  $\rho_{e^-} = \rho_{p^+}$ .
- (c) Derive the equality  $\beta\mu_i = \beta f_i + \log(\rho_i \Lambda_i^3)$  from the expression  $\beta F_i = \beta N_i f_i + N_i \log(\rho_i \Lambda_i^3) - N_i$ . Here,  $F_i$  is the free energy of species  $i$ ,  $\beta = 1/(k_B T)$  with  $T$  the temperature and  $k_B$  Boltzmann's constant,  $N_i$  is the number of particles of species  $i$ ,  $\mu_i$  the associated chemical potential,  $\Lambda_i$  the thermal wavelength, and  $f_i$  the 'excess' (non-ideal) free-energy per particle, which includes contributions from the ground-state energy and internal degrees of freedom.
- (d) Show using (c) and properties of partition functions that

$$\frac{\rho_{e^-} \rho_{p^+}}{\rho_H} = \frac{\Lambda_H^3}{\Lambda_{e^-}^3 \Lambda_{p^+}^3} \exp(\beta [f_H - f_{p^+} - f_{e^-}]); \quad (5.18)$$

$$\approx \left( \frac{2\pi m_{e^-} k_B T}{h^2} \right)^{3/2} \exp(\beta [f_H - f_{p^+} - f_{e^-}]), \quad (5.19)$$

with  $m_{e^-}$  the electron mass and  $h$  Planck's constant. Explain in a few words why the approximation in the second line is justified.

- (e) Now we define the ionization energy to be  $\chi_i$  that part of  $f_{p^+} - f_{e^-} - f_H$  that comes from the ionization energy only. Assume that the remainder of the degrees of freedom can be captured by an excess partition function  $Z_i$  for each respective term. Show that this leads to the Saha equation

$$\frac{\rho_{e^-} \rho_{p^+}}{\rho_H} = \left( \frac{2\pi m_{e^-} k_B T}{h^2} \right)^{3/2} \frac{2Z_{p^+}}{Z_H} \exp(-\beta \chi_i). \quad (5.20)$$

Explain in a few words what the physical interpretation of the factor 2 is in Eq. (5.20).

- (f) It turns out that to good approximation in a star,  $Z_H = 2$  (ground state) and  $Z_{p^+} = 1$ . For hydrogen we have that  $\chi_i \approx 13.6$  eV. Estimate the temperature at which point you would expect half the hydrogen atoms to be ionized and comment on — using only a few words — whether this situation is applicable to the surface of a star, which you can assume is at 5000 K (our sun).
- (g) The above basic estimate is quite inaccurate. You can refine it assuming charge conservation  $\rho_{e^-} = \rho_{p^+}$  and particle preservation, defining the total density as  $\rho = \rho_H + \rho_{p^+} + \rho_{e^-}$ . Show that this leads to

$$\frac{\rho_{e^-}^2}{\rho - 2\rho_{e^-}} = \left( \frac{2\pi m_{e^-} k_B T}{h^2} \right)^{3/2} \exp(-\beta \chi_i). \quad (5.21)$$

This can be solved for  $\rho_{e^-}$  in general. Here, you may consider  $\rho_{e^-} = \rho/3$  with  $\rho \approx 2.3 \cdot 10^{16} \text{ m}^{-3}$  (photosphere) and  $m_{e^-} \approx 9.1 \cdot 10^{-31} \text{ kg}$ . Determine the temperature at which the photosphere assumes this degree of ionization. you should find about  $10^4$  K, which is much smaller than our estimate in (f) and readily attainable for stars hotter than our sun.

<sup>1</sup>We refer the interested reader to chapter 8 of "An Introduction to Modern Stellar Astrophysics" by Carroll and Ostlie for more information.



## Chapter 6

# Phase Diagrams

A phase diagram depicts the limits of stability of the various *stable* phases in a *thermodynamic* system at equilibrium, with respect to variables such as: temperature, pressure, density, composition, *etc.* For example, on the phase diagram of water, we would expect to see regions of a solid (ice), liquid (water), and gas (water vapor). The former phase is characterized by a crystalline (periodic) positional ordering of the constituents, while the latter two have an amorphous structure. This observation can be generalized to most single-component simple elements or compounds, which typically exhibit these three characteristic phases of matter.

A typical phase diagram in the pressure-temperature ( $pT$ ) representation is shown in the left-hand panel to Fig. 6.1. The phase diagram depicts regions of stability of a solid phase, a liquid phase, and a gas phase. Additionally, two extra points are indicated on this plot: (i) The *triple point*, where all three phases occur at the same state point and (ii) the *critical point*, where the distinction between a liquid and gas disappears. At the moment, all possible solid phases are grouped together, although in practice a system may also have phase transitions between various solid phases characterized by different underlying crystal structures. For instance, ice is one of 18 (presently) known forms of crystalline water.

A question that arises when examining Fig. 6.1 is: What is the distinction between a liquid and a gas? Both phases are characterized by an irregular positioning of the constituents with the difference between the two being simply the density; a liquid has a higher density than a gas. It will turn out that it is not possible to determine with certainty in which of the two phases a system is, without knowing more about the phase diagram, as we will argue in this chapter and return to in Chapter 13. The critical point on the phase diagram is the point where the density difference between the liquid phase and the gas phase disappears.

We can see this more clearly in the density-temperature ( $\rho T$ ) representation, see the right-hand panel to Fig. 6.1. Note that in this representation, large parts of the phase diagram are occupied by *coexistence* regions, *i.e.*, places where two phases occur simultaneously. For example, a large gas-liquid coexistence is seen, and there are also respective gas-solid, solid-liquid, and solid-fluid regions. A well-known example of such coexistence is that of water and ice at 0 °C. We have indicated a fourth phase in this plot: a fluid. The fluid appears above the critical temperature, where the presently rather nebulous distinction between a liquid and a gas disappears. The curves enclosing the phase coexistence region are called binodals, within the region, spinodal curves are also found, which we will return to in this chapter.

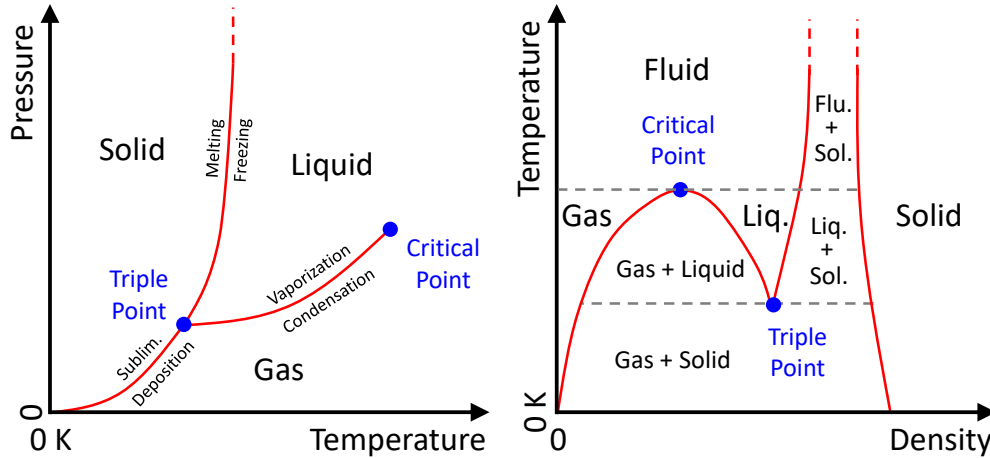


Figure 6.1: Phase diagram of a typical single-component system, *i.e.*, for an element or a simple compound. The temperature-pressure (left) and density-temperature (right) representation. In the former representation, we see that: at low temperature, the solid phase is stable; for moderate temperature and pressure, the liquid phase is stable; and for high temperature, the gas phase is stable. The limits of stability of the three phases are shown using red curves. Next to these lines the type of phase transformation is listed, with “Sublim.” standing for sublimation. Two extra points of interest are marked in blue: the triple point and the critical point. In the density-temperature representation of the phase diagram (right), the phase which appears above the critical point is typically called a fluid. Abbreviations for solid (Sol.), liquid (Liq.), and fluid (Flu.) appear in some places on this plot. The regions marked with two phases are unstable, here the system phase separates.

The remainder of this set of lecture notes will deal mostly with predicting and understanding phase diagrams, *i.e.*, predicting which phases are stable for a given state point. We will also describe in detail the phase transformations between these stable phases. To give a first taste of the consequences of a phase transition, we will conclude our excursion into the realm of quantum mechanics with a discussion of Bose-Einstein condensation.

## 6.1 Criteria for Coexistence

In this section, we derive the conditions for coexistence from the second law of thermodynamics. Consider a closed system of  $N$  identical particles in a volume  $V$  and with energy  $U$ . Assume that this system has two competing phases labeled 1 and 2, with associated free energies. Suppose phase 1 consists of  $N_1$  particles in a volume  $V_1$  and phase 2 consists of  $N_2$  particles in a volume  $V_2$ , see Fig. 6.2. The total energy of phase 1 is  $U_1$  while the total energy of phase 2 is  $U_2$ . Since the total number of particles is  $N$ , we can immediately write that  $N = N_2 + N_1$ . Similarly, we have  $V = V_2 + V_1$  and  $U = U_2 + U_1$ .

From the second law of thermodynamics, we have that the total entropy ( $S = S_1 + S_2$ ) is a maximum at equilibrium. At a maximum, we have  $dS = 0$ . Hence,  $dS/dU_1 = 0$ ,  $dS/dV_1 = 0$ , and  $dS/dN_1 = 0$ . Rewriting the internal energy differential to one for the entropy

$$dS = \frac{1}{T}dU + \frac{p}{T}dV - \frac{\mu}{T}dN, \quad (6.1)$$

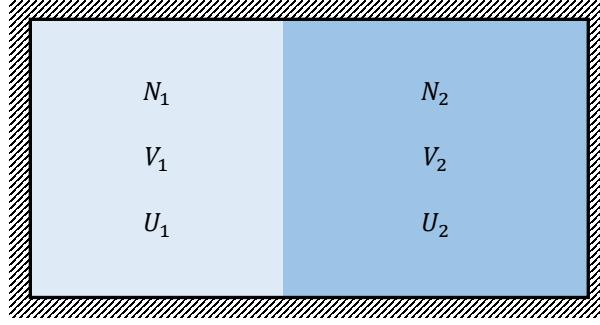


Figure 6.2: Sketch of two coexisting phases 1 and 2 in a closed system. In this case the total number of particles  $N = N_2 + N_1$ , the volume  $V = V_2 + V_1$ , and energy  $U = U_2 + U_1$  are fixed.

allows us to obtain

$$\begin{aligned}
 0 &= \left( \frac{\partial S}{\partial U_1} \right)_{V_1, V_2, N_1, N_2, U} = \left( \frac{\partial S_1}{\partial U_1} \right)_{V_1, N_1} + \left( \frac{\partial S_2}{\partial U_1} \right)_{V_2, N_2} ; \\
 &= \left( \frac{\partial S_1}{\partial U_1} \right)_{V_1, N_1} - \left( \frac{\partial S_2}{\partial U_2} \right)_{V_2, N_2} ; \\
 &= \frac{1}{T_1} - \frac{1}{T_2}, \tag{6.2}
 \end{aligned}$$

where we have used the fact that  $dU = dU_1 + dU_2 = 0$ . From the last line of Eq. (6.2) we have  $T_1 = T_2$ , which is commonly called thermal equilibrium.

Similarly, we can show that the condition  $dS/dV_1 = 0$  implies that  $p_1 = p_2$  (mechanical equilibrium) and that  $dS/dN_1 = 0$  implies that  $\mu_1 = \mu_2$  (chemical equilibrium; sometimes called mass equilibrium). Note that following a similar argument, we can show that  $(dU)_{S, V, N} = 0$  in equilibrium. These conditions also hold for any number of phases which are in equilibrium, *i.e.*,  $T_1 = T_2 = T_3 = \dots$ , *etc.*

## 6.2 Closer Look at Coexistences

As we saw in the right-hand panel to Fig. 6.1, phase diagrams often consist of two different types of regions: single phase regions and regions where two or more phases coexist. To examine in more detail how one might construct such a phase diagram, let us assume we have a free energy per volume as shown in the left-hand panel to Fig. 6.3. Note that for the remainder of this discussion we will assume that we work at fixed temperature  $T$  and simplify the notation by leaving out any reference to  $T$ .

We will be studying coexistence between two phases that are in contact, therefore, we know *a priori* that they must have the same temperature. Furthermore, we assume that at a number density  $\rho = N/V$  the system divides into two phases with number densities  $\rho_1$  and  $\rho_2$ , respectively, also see Fig. 6.3. Let us denote the fraction of the system at a number density  $\rho_1$  as  $x$ , *i.e.*, if  $V$  is the total volume of the system and  $V_1$  is the volume at number density  $\rho_1$ , then  $x = V_1/V$ . If  $V_2$  is the volume of the system with a density of  $\rho_2$ , then we also have  $V_2/V = (1 - x)$ . Furthermore, if  $N_1$  and  $N_2$  are the number of particles at densities  $\rho_1$  and  $\rho_2$  respectively, then the total density of the system is given by

$$\rho = \frac{N}{V} = \frac{N_1 + N_2}{V} = \frac{N_1 V_1}{V_1 V} + \frac{N_2 V_2}{V_2 V} = \rho_1 x + \rho_2 (1 - x). \tag{6.3}$$

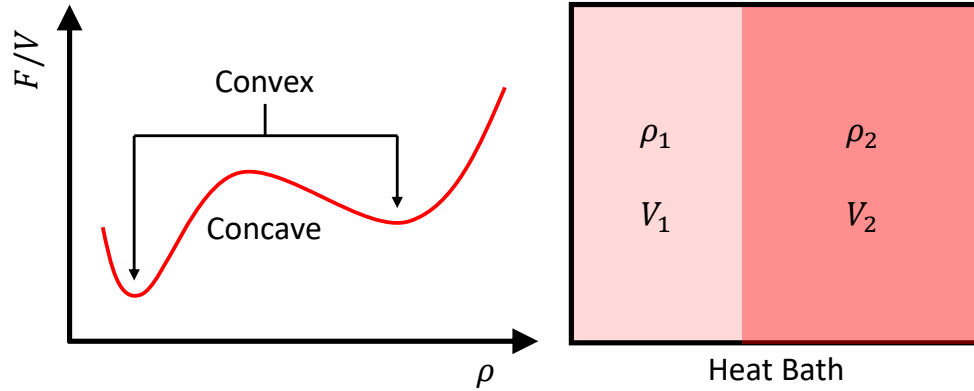


Figure 6.3: (left) Approximate free energy per volume  $F/V$  as a function of the density  $\rho$ . The free energy has two convex regions corresponding to two phases with different densities. (right) Cartoon of a system with two coexisting phases that this  $F/V$  curve can result in. One phase has density  $\rho_1$  in a volume  $V_1$ , *e.g.*, a gas, and one has density  $\rho_2$  in a volume  $V_2$ , which could, *e.g.*, be a coexisting liquid.

Rearranging the above expression we obtain

$$x = \frac{\rho - \rho_2}{\rho_1 - \rho_2}. \quad (6.4)$$

Additionally, the free energy per volume of the system is an intensive variable, *i.e.*, if we double the system size,  $F/V$  remains unchanged. Hence we can write

$$F(N, V) = V f(\rho). \quad (6.5)$$

The total free energy of the system with coexisting phases with densities  $\rho_1$  and  $\rho_2$ , respectively, is then given by

$$F_{\text{co}}(N, V) = V_1 f(\rho_1) + V_2 f(\rho_2), \quad (6.6)$$

which yields a total free energy per volume for the entire system:

$$f_{\text{co}}(\rho) = x f(\rho_1) + (1 - x) f(\rho_2). \quad (6.7)$$

Note that the subscript “co” is used to indicate Eq. (6.7) provides the free energy of the system with a phase coexistence.

Substituting Eq. (6.4) into Eq. (6.7), we obtain

$$f_{\text{co}}(\rho) = \left( \frac{\rho - \rho_2}{\rho_1 - \rho_2} \right) f(\rho_1) + \left( \frac{\rho - \rho_1}{\rho_2 - \rho_1} \right) f(\rho_2), \quad (6.8)$$

which is simply a linear function of  $\rho$ . Specifically, if  $\rho = \rho_2$ , we have  $f_{\text{co}}(\rho) = f(\rho_2)$ , while if  $\rho = \rho_1$ , we have  $f_{\text{co}}(\rho) = f(\rho_1)$ . For  $\rho$  between  $\rho_2$  and  $\rho_1$ , Eq. (6.8) describes a straight line. Several examples for different choices of  $\rho_1$  and  $\rho_2$  are depicted in Fig. 6.4. To summarize, when there is a coexistence between phases with densities  $\rho_1$  and  $\rho_2$  in a system with a number density  $\rho$ , then the free energy per volume as a function of the density is a straight line with endpoints at  $f_{\text{co}}(\rho) = f(\rho_2)$  and  $f_{\text{co}}(\rho) = f(\rho_1)$ .

Note that we have made no comment regarding the minimum free energy at  $\rho$  thus far. From thermodynamics, we know that the equilibrium phase will have the lowest free energy. Hence, at a given  $\rho$ ,

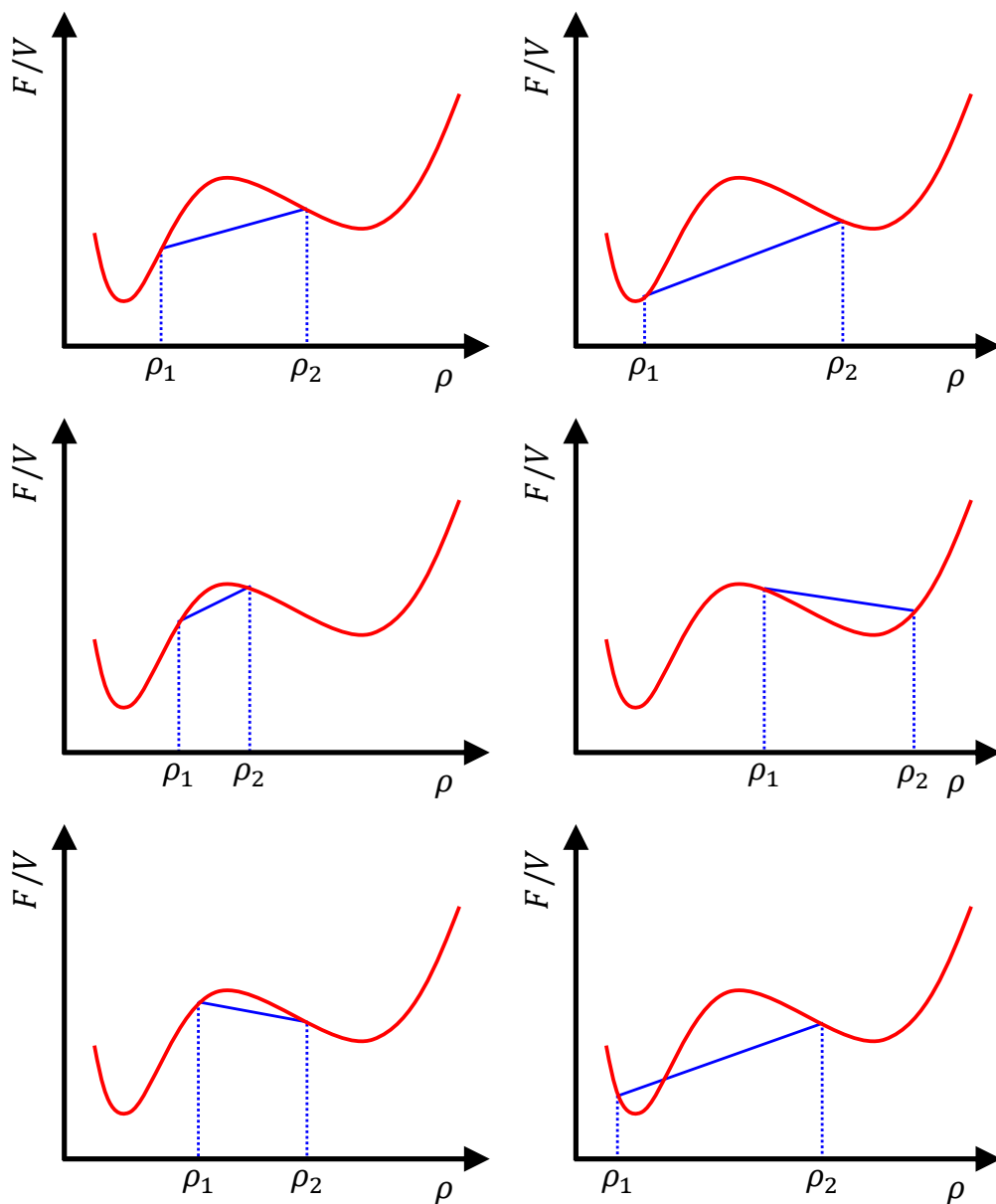


Figure 6.4: Red curves indicate the approximate free energy per volume  $F/V$  as a function of density  $\rho$  for a homogeneous system. By homogeneous system we mean that the entire system has a single density given by  $\rho$ . Solid blue lines indicate  $F/V$  as a function of  $\rho$  assuming that the system consists of a coexistence between phases with densities  $\rho_1$  and  $\rho_2$  (indicated by the dashed blue lines). The six plots correspond to different choices of  $\rho_1$  and  $\rho_2$ .

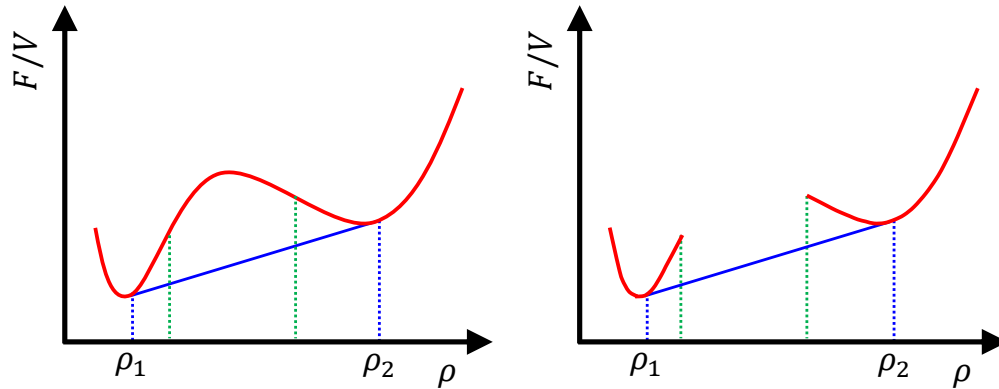


Figure 6.5: Common-tangent construction (solid blue line) for the approximate free energy per volume  $F/V$  as a function of density  $\rho$  (red curve). (left) The common tangent does *not* connect the two minima in the free energy! The coexistence densities  $\rho_1$  and  $\rho_2$  are indicated using the dashed blue lines. In equilibrium, we have coexistence for  $\rho_1 < \rho < \rho_2$ . The dashed green lines indicate the inflection points to  $F/V$ , where the free energy per volume transitions from convex to concave. (right) The same construction, now corrected for the ‘forbidden’ concave region to the  $F/V$ . This highlights the separation between phase 1 and phase 2, as we will label the low- and high-density phase, respectively.

we are interested in determining how to choose  $\rho_1$  and  $\rho_2$  such that the free energy ( $f_{\text{co}}$ ) is minimized. One way to solve this problem would be to write the free energy per volume as a function of  $\rho$ ,  $\rho_1$ , and  $\rho_2$ , and find the minimum for each value of  $\rho$  as a function of  $\rho_1$  and  $\rho_2$ . However, we can also examine Fig. 6.4 to intuit a graphical solution to this problem.

Figure 6.5 shows that below  $\rho_1$ , the free energy is always minimized if the entire system is in phase 1. Above  $\rho_2$ , the solution also appears trivial: the energy is minimized when the entire system is in phase 2. Between these two points, however, the free energy per volume is minimized by the line which is tangent to both regions. Hence, the system is in coexistence when we can draw a line tangent to the free energy at two different densities. This construction is often referred to as a *common-tangent construction*. Interestingly, from this common tangent, we also recover mechanical and chemical equilibrium. It will be left as an exercise to show that the common-tangent construction here ensures that (i) the pressures in both phases are equal and (ii) that the chemical potentials in the two phases are equal. The points where the common-tangent touches the free energy, give the coexistence densities and are also referred to as *binodal* points. When such binodal points are obtained for multiple temperatures, the coexistence region in a  $\rho T$  phase diagram may be mapped out. This coexistence region is delimited by two curves, which are appropriately called binodals.

Note that in our derivation we have ignored contributions from the interface between phases 1 and 2. For the purpose of this analysis we are, in fact, free to ignore the interface, since we are only interested in the thermodynamic limit (*i.e.*,  $N \rightarrow \infty$ ). We will explore in an exercise why we are allowed to do this. There is additional richness to the representation in Fig. 6.5, which we will turn to next.

### 6.3 Equilibrium and Metastability

Let  $A$  be a general notation for the ‘relevant free energy’ describing a system, *e.g.*,  $A$  could be  $U$ ,  $F$ , or  $\Omega$ . In equilibrium, the free energy assumes an extremal value, *i.e.*,  $dA = 0$ . A stable equilibrium requires that

$$(\Delta A)_{\mathbf{x}} > 0, \quad (6.9)$$

for all small displacements away from equilibrium, where  $\mathbf{x}$  denotes the associated variables. In other words, any deviations from the equilibrium will increase the free energy; it is a minimum of  $A$ . For example, if the variables are  $N$ ,  $V$ , and  $S$ , then the relevant free energy is simply the total energy  $U$ , and we have the stability condition

$$(\Delta U)_{S,V,N} > 0. \quad (6.10)$$

Turning back to the general free energy  $A$ , we thus require that around a stable equilibrium

$$(\Delta A)_{\mathbf{x}} = (d^2 A)_{\mathbf{x}} + (d^3 A)_{\mathbf{x}} + \dots > 0. \quad (6.11)$$

For small enough displacements, the quadratic term will dominate, hence in addition to the requirement  $(dA)_{\mathbf{x}} = 0$ , for an equilibrium to be stable we must also have  $(d^2 A)_{\mathbf{x}} \geq 0$ . This is simply a higher-dimensional, differential-form analogy to the standard requirements on the minimum of a scalar function.

#### 6.3.1 Isothermal Compressibility

Next, we will put this insight to use to determine the properties of the *isothermal compressibility*, a measure of the relative volume change of a material to an applied pressure. In the  $(N, V, T)$  ensemble, equilibrium requires

$$(\Delta F)_{N,V,T} > 0, \quad (dF)_{N,V,T} = 0, \quad (d^2 F)_{N,V,T} \geq 0, \quad (6.12)$$

where  $F$  is the Helmholtz free energy. Next, we assume that we have a system such that the number of particles  $N$ , volume  $V$ , and temperature  $T$  are fixed. Now, let us split the system into two subsystems (1) and (2), in a fashion reminiscent to the one shown in Fig. 6.2. Here, we split the system in half for the number of particles, such that:  $N_1 = N_2 = N/2$  and  $dN_1 = dN_2 = 0$ . For the volumes, we apply a small perturbation, such that:  $V_1 = V/2 + dV_1$  and  $V_2 = V/2 + dV_2$ . Clearly, we must have that

$$dV = dV_1 + dV_2 = 0. \quad (6.13)$$

Using the above expressions, we may write

$$\begin{aligned} (d^2 F)_{N,V,T} &= d^2 F_1 + d^2 F_2 \\ &= \frac{1}{2} \left( \left( \frac{\partial^2 F_1}{\partial V_1^2} \right)_{N,T} dV_1^2 + \left( \frac{\partial^2 F_2}{\partial V_2^2} \right)_{N,T} dV_2^2 \right), \\ &= \frac{1}{2} dV_1^2 \left( \left( \frac{\partial^2 F_1}{\partial V_1^2} \right)_{N,T} + \left( \frac{\partial^2 F_2}{\partial V_2^2} \right)_{N,T} \right). \end{aligned} \quad (6.14)$$

We can use standard thermodynamic identities to rewrite terms appearing in the above as

$$\left( \frac{\partial^2 F}{\partial V^2} \right)_{N,T} = - \left( \frac{\partial p}{\partial V} \right)_{N,T} = \frac{1}{K_T V}, \quad (6.15)$$

where  $K_T$  is the isothermal compressibility. We thus find that

$$d^2F = \frac{1}{2}dV_1^2 \left( \frac{1}{K_{T,1}V_1} + \frac{1}{K_{T,2}V_2} \right), \quad (6.16)$$

and using  $(d^2F)_{N,V,T} \geq 0$ , we finally arrive at

$$\left( \frac{1}{K_{T,1}V_1} + \frac{1}{K_{T,2}V_2} \right) \geq 0. \quad (6.17)$$

However, this must hold for any division into subsystems and  $V_1 > 0, V_2 > 0$ , so that  $K_T \geq 0$  in a stable system. A similar argument can be used to show that the heat capacity is non-negative, this will be done in one of the exercises.

### 6.3.2 Convexity of the Free Energy

Returning to the free energy of a system, let us consider the condition  $d^2F > 0$  away from the minimum. Note that at no point during the derivation in Section 6.3.1, we made use of the condition  $dF = 0$ . This implies that even away from the minimum  $K_T > 0$ , whenever  $d^2F > 0$ . Conversely,  $K_T < 0$ , when  $d^2F < 0$ , *i.e.*, the system has a negative compressibility! This means that it is favorable to make denser parts of the system more dense, and dilute parts of the system more dilute. In other words, the system is completely unstable. Consequently,  $F$  *must* be a convex function of  $V$  in systems that are not necessarily at the minimum in the free energy, but which are at least *conditionally* stable or *metastable*.

Note that our favorite approximate free energy — the one plotted in Figs. 6.3, 6.4, and 6.5 — does not satisfy this criterion. This is why we have made careful use of the term “approximate”. The well-defined variant of this free energy is shown in the right-hand panel to Fig. 6.5 and removes the concave part. This region (negative compressibility) is bounded by two dashed green lines, and the associated densities are typically referred to as *spinodal* points. These necessarily lie between the binodal points. Similarly they trace out curves called spinodals in a  $\rho T$  phase diagram, which delimit the region of unconditional instability for the system to phase separate.

In the coming chapters, we will encounter many free energies that are locally non-convex, which derive from approximative methods for determining the free energy of the physical system being modeled. An additional concept arises in these approximate theories: Is there a difference between the unstable locally convex and non-convex parts of the free energy? It turns out that the curvature of the free energy gives rise to a change in the systems dynamics<sup>1</sup>. Between the two spinodals, even the smallest of fluctuations will destabilize a homogeneous system and cause it to instantaneously phase separate. Because thermal fluctuations occur across space, *spinodal decomposition* of the system leads to distinct, sometimes intercalating patterns. However, outside the spinodal region, *i.e.*, between  $\rho_1$  and the left-most green line in Fig 6.5 or between the right-most green line and  $\rho_2$  in the same figure, *i.e.*, in the region between the binodal and spinodal curve, the system can remain in a metastable equilibrium for some time. That is, a significantly large fluctuation is required to cause the system to reach the equilibrium state. In this part of the phase diagram and in the metastable state, small nuclei of the stable phase constantly form and disappear. Only when these grow out to sufficient size, by a favorable arrangement of particles, can the stable phase nucleate. You are undoubtedly familiar with this phenomenon from the way supercooled water rapidly freezes by inserting needle. Here, the needle is the source of the substantial (non-thermal) fluctuation that drives the water into its thermodynamically preferred state. We will revisit this situation in Chapter 15.

<sup>1</sup>The dynamics can be described by the Cahn-Hilliard formalism, but a full discussion thereof unfortunately goes beyond the scope of these notes.

## 6.4 Common Tangent in a Single-Component System

In Section 6.1, we examined the thermodynamic conditions required for two phases to coexist in equilibrium and in Section 6.2 we saw that such a coexistence could be determined *via* a common-tangent construction. Here, we go backwards and derive a common-tangent construction, starting from the equilibrium conditions

- the temperature in the two phases is equal ( $T_1 = T_2$ ),
- the pressure in the two phases is equal ( $p_1 = p_2$ ),
- the chemical potential in the two phases is equal ( $\mu_1 = \mu_2$ ).

The common-tangent construction we derive in this section, is for the free energy  $F$  as a function of volume  $V$ , rather than  $F/V$  as a function of  $\rho$ . However, these two constructions are completely equivalent, as can be readily shown using basic calculus.

Let us assume that we know the Helmholtz free energy in both phases, *i.e.*, the  $F$  at constant  $T$ ,  $N$ , and  $V$ . From the definition of  $F$ , we have in phase 1 that

$$\frac{\partial F_1(N, V, T)}{\partial V} = -p_1, \quad (6.18)$$

and similarly in phase 2

$$\frac{\partial F_2(N, V, T)}{\partial V} = -p_2. \quad (6.19)$$

However, in equilibrium we also have  $p_1 = p_2$ , implying

$$\left. \frac{\partial F_1(N, V, T)}{\partial V} \right|_{V=V_1^{\text{coex}}} = \left. \frac{\partial F_2(N, V, T)}{\partial V} \right|_{V=V_2^{\text{coex}}}. \quad (6.20)$$

Consequently, the slope of the free energy  $F$  as a function of  $V$  must be equal in coexisting phases. This is the first part to obtaining a common-tangent construction. The tangents are equal, but we still need to show that coexisting phases are described by a *single* or “common” tangent line. This means that the  $F$ -axis intercepts of the two tangent lines through the respective coexistence points must be the same, as they then define the same line.

The chemical potential in phase 1 (for a single-component system) is simply the Gibbs free energy in phase 1 divided by the number of particles in the system, *i.e.*,  $\mu = G_1/N$ . Hence

$$\mu_1(N, V, T) = \frac{1}{N} (F_1(N, V, T) + p_1 V) = \frac{1}{N} \left( F_1(N, V, T) - \frac{\partial F_1(N, V, T)}{\partial V} V \right), \quad (6.21)$$

and similarly

$$\mu_2(N, V, T) = \frac{1}{N} (F_2(N, V, T) + p_2 V) = \frac{1}{N} \left( F_2(N, V, T) - \frac{\partial F_2(N, V, T)}{\partial V} V \right), \quad (6.22)$$

where we have used  $\partial F/\partial V = -p$ . In equilibrium, we also have  $\mu_1 = \mu_2$ , so that

$$F_1(N, V_1^{\text{coex}}, T) - \left. \frac{\partial F_1(N, V, T)}{\partial V} \right|_{V=V_1^{\text{coex}}} V_1^{\text{coex}} = F_2(N, V_2^{\text{coex}}, T) - \left. \frac{\partial F_2(N, V, T)}{\partial V} \right|_{V=V_2^{\text{coex}}} V_2^{\text{coex}}. \quad (6.23)$$

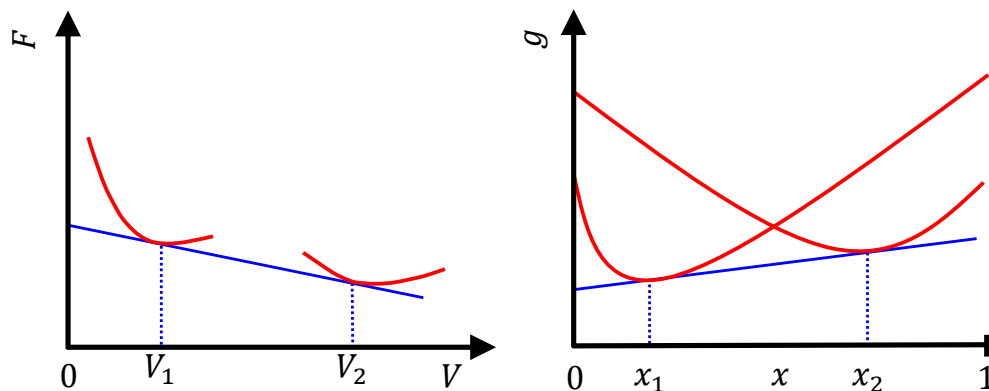


Figure 6.6: Common-tangent constructions for (left) the Helmholtz free energy  $F$  as a function of volume  $V$  and (right) the Gibbs free energy per particle  $g$  as a function of the composition  $x$  in a binary mixture. The free energy curves are indicated in red, the common tangent in blue, and the coexistence points using the dashed lines. In the left panel, the slope of the common tangent gives the pressure in both phases. The chemical potential is also the same in both phases and this is related to the  $F$ -axis intercept.

Note that either side of Eq. (6.23) represents exactly the intercept of the tangent line to the  $F$ -axis. Namely, the function value minus the slope times the position with respect to  $V = 0$ . Hence,  $\mu_1 = \mu_2$  implies that the intercepts of tangents to  $F_1$  and  $F_2$  as a function of  $V$  must be equal for phases 1 and 2 to be in coexistence, which in turn implies the existence of a *common tangent*.

To summarize, the two tangent lines to the free energy as a function of volume at the two coexistence points should have both the same slope (due to equal pressures) and the same intercept (due to equal chemical potentials). As a result, the coexistence points can be found by a common-tangent construction, which is demonstrated in the left-hand panel to Fig. 6.6. When we know a range of isotherms similar to the one shown in Fig. 6.6, we can determine the phase diagram associated with this system.

## 6.5 Coexistence in a Binary Mixture

In the previous sections, we examined coexistence in a single-component system. Many relevant systems instead consist of a mixture of different particles. Here, we address coexistence in such a system.

Let us consider the simplest situation first. Assume that we have a two component mixture and that we have  $N^i$  particles of type  $i \in \{a, b\}$ , as we will indicate using superscripts. The *entire system* can be in one of two phases, 1 and 2, which we will indicate using subscripts (to avoid confusion with exponents). Thus, the number of particles of species  $a$  in phase 2 is denoted  $N_2^a$  and so on. For example, we could have a homogeneous distribution of two types of gas molecule throughout space above the critical temperature. By lowering the temperature, our example system phase separates, due to the interaction rules between the molecular species. This leads to a phase that is rich in species  $a$  and poor in species  $b$  (phase 1), coexisting with a phase that is rich in  $b$  and poor in  $a$  (phase 2).

The conditions for thermodynamic equilibrium of the two phases require that the temperature, pressure, and chemical potentials for the two species are equal in both phases. Specifically, we have that (assuming

a homogeneous temperature  $T$ ):

$$p(\rho_1^a, \rho_1^b, T) = p(\rho_2^a, \rho_2^b, T); \quad (6.24)$$

$$\mu^a(\rho_1^a, \rho_1^b, T) = \mu^a(\rho_2^a, \rho_2^b, T); \quad (6.25)$$

$$\mu^b(\rho_1^a, \rho_1^b, T) = \mu^b(\rho_2^a, \rho_2^b, T), \quad (6.26)$$

where  $\rho_j^i$  is the density of species  $i$  in phase  $j$ ,  $p$  is the pressure, and  $\mu^i$  is the chemical potential of species  $i$ . It should be clear that there we do not work with partial pressures — the effective pressure of a molecular species in a mixture, if it instead occupied the volume by itself — as the presence of both species contributes to the pressure in one phase. Think in terms of non-ideal gasses, for instance, to see why such a cross coupling should be present. However, the two phases can be viewed as chambers separated by permeable membranes, which means that particles of species  $a$  and  $b$  can be exchanged across the boundary. This implies that the chemical potentials of the individual species must be equal to have coexistence between two phases. The interaction between the species is accounted for in the dependencies of these parameters on the phase composition.

To determine phase coexistence, we turn to the Gibbs free energy. This is an extensive variable and so it scales with the total number of particles in the system ( $N$ ) as

$$G(N^a, N^b, p, T) = Ng(x, p, T), \quad (6.27)$$

where  $g(x, p, T)$  is the Gibbs free energy per particle, and we have introduced the compositional parameter  $x = N^a/N$ . Since the chemical potentials are related to the Gibbs free energy by

$$\mu^i(x) = \left( \frac{\partial G}{\partial N^i} \right)_{N^{j \neq i}, p, T}, \quad (6.28)$$

they can be written

$$\mu^a(x) = g(x) + (1-x)g'(x); \quad (6.29)$$

$$\mu^b(x) = g(x) - xg'(x), \quad (6.30)$$

with the prime indicating the partial derivative with respect to  $x$ . Applying the chemical equilibrium relations expressed in Eqs. (6.25) and (6.26), we obtain

$$g'_{p_1}(x_1) = g'_{p_2}(x_2); \quad (6.31)$$

$$g'_{p_1}(x_1) = \frac{g_{p_1}(x_1) - g_{p_2}(x_2)}{x_1 - x_2}, \quad (6.32)$$

where the subscripts indicate the phase in which  $g$  is evaluated, which we additionally distinguished from the compositional labelling here for clarity. Summarizing, phase coexistence happens when for some  $x_1$  and  $x_2$ , the slopes of the Gibbs free energy per particle for both phases (at constant temperature and pressure) are equal, *and* the lines tangent to the free energy through both these points. That is, there is a common tangent to the relevant  $g$ , see the right-hand panel to Fig. 6.6. Another way to think about this common-tangent construction is that the system as a whole always tries to minimize the total free energy. Thus, for a given composition  $x$ , the system will choose a linear combination of phases 1 and 2 such that the total Gibbs free energy is minimized. Graphically, such a minimum corresponds to a common-tangent construction.

## 6.6 Phase Transitions

Up to this point, we have only examined phase transitions which are associated with coexistence, *i.e.*, the phase transition between a liquid and a gas involved going through a *coexistence region* where both

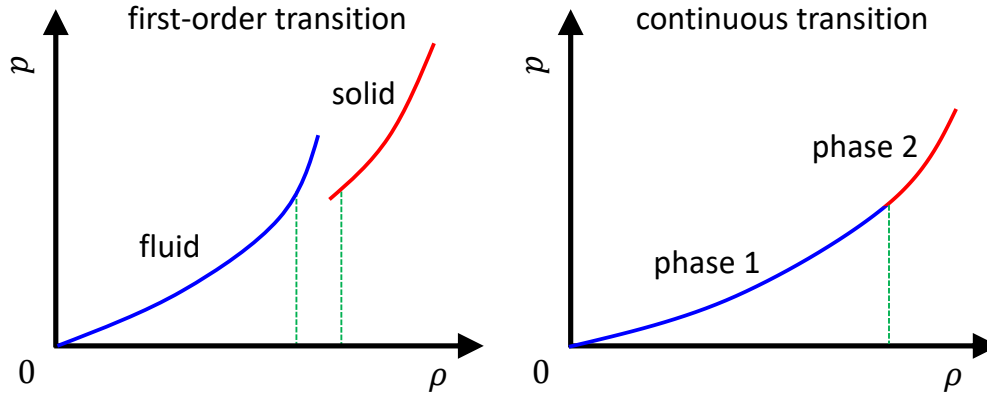


Figure 6.7: Typical equation of state, *i.e.*, pressure  $p$  as a function of density  $\rho$ , for a system with (left) a first-order phase transition and (right) a continuous phase transition. Blue and red indicate the different phases and green dashed lines coexistence densities (left), the transition point (right).

phases were present. This is not always the case. Phase transitions are often divided into two categories: *first-order* phase transitions and *continuous* phase transitions.

### 6.6.1 First-Order Phase Transitions

The phase transitions involving a coexistence region, as we have been examining in detail thus far in this chapter, are what we call first-order phase transitions. In the left-hand panel to Fig. 6.7, we plot the pressure  $p$  as a function of density  $\rho = N/V$  for a typical first-order phase transition. Such a curve is also commonly referred to as an *equation of state* (EoS). From this plot we can clearly see that there is a discontinuity in the first derivative of the free energy, because  $\partial F/\partial V = -p$ . The “first-order” in the name refers to the discontinuity in this derivative, which is what gives rise to the coexistence. Note additionally that the low- and high-density “branches” of the EoS extend beyond the coexistence densities/pressures. This is because the phases can be made metastable, without being unconditionally unstable at the same time. Snapshots of a system in coexistence are shown in Fig. 6.8.

### 6.6.2 Continuous Phase Transitions

The first derivative in a continuous phase transition does not show a jump. This can express itself in a nearly smooth equation of state, as shown in the right-hand panel to Fig. 6.7. To find a signature of such a phase transition, we have to go to higher-order derivatives of the free energy. Continuous phase transitions are also frequently classified by the exact derivative which is discontinuous, *i.e.*, second-order phase transitions, third-order phase transitions, *etc.* Labeling a phase transition according to the discontinuity in its derivative dates back to Ehrenfest. For the purpose of this set of notes, the more modern convention will be assumed: second- and higher-order phase transitions will be grouped under the label continuous phase transitions<sup>2</sup>.

<sup>2</sup>There are quite a few subtleties here that you will encounter as you progress in your study of physics. In particular, the role that symmetries and topology play in classifying a phase transition. It is therefore, at least for now, best to stick to the convention of continuous versus discontinuous / first-order in characterizing transitions.

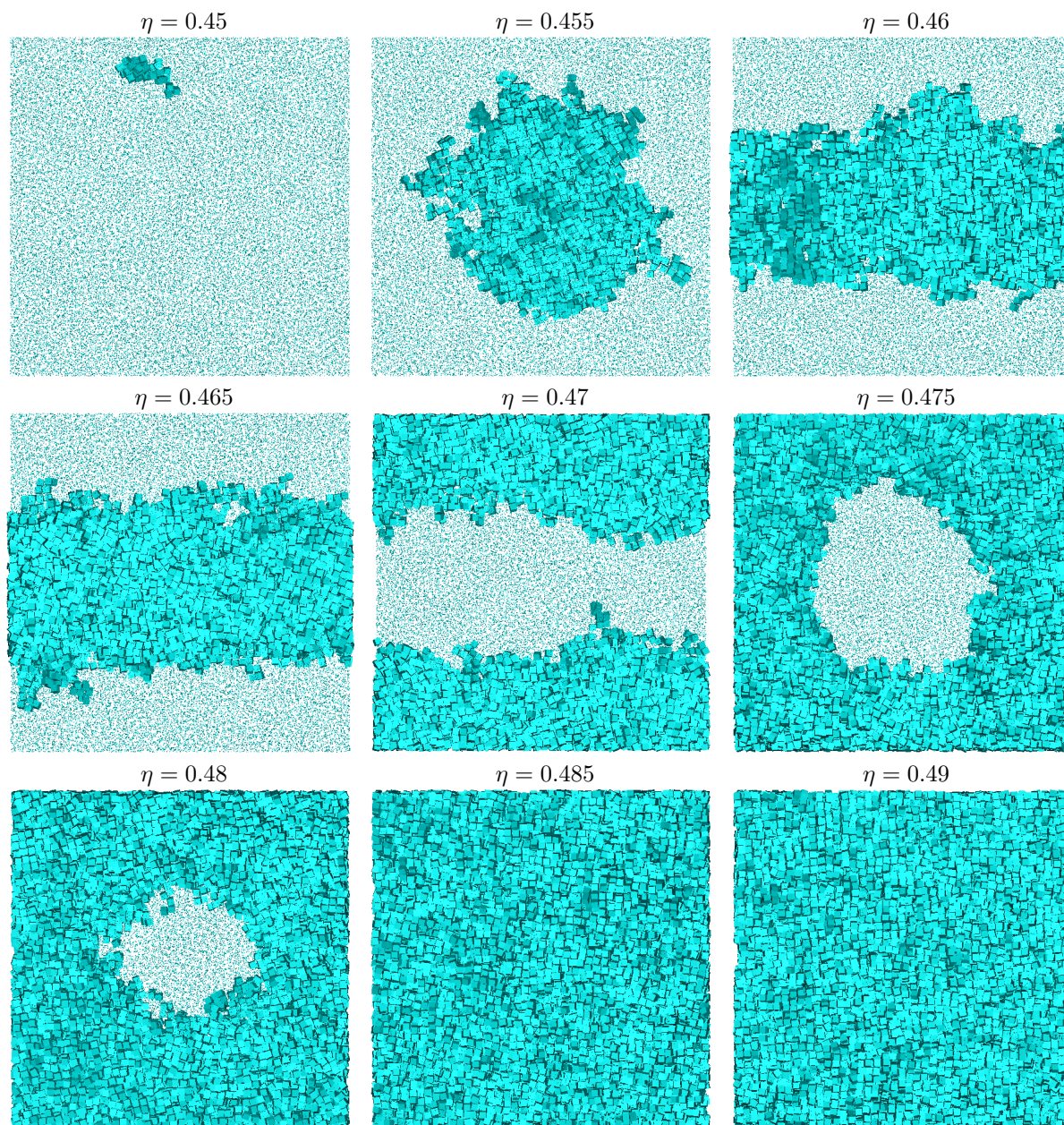


Figure 6.8: Coexistence between a fluid and solid phase in hard cubes for a range of densities in the coexistence region. Solid-like cubes are rendered large, whilst liquid-like cubes are rendered small. The system is, however, monodisperse. Note that this system does not have attractions, yet it still phase separates. We will return to this point in Chapter 14. Data kindly provided by F. Smallenburg.

It should be further noted that a jump is not the only condition for identifying a continuous phase transition. A divergence of a quantity, such as the heat capacity, can also signal a continuous phase transition. We will see that continuous phase transitions generally have associated with them a divergence of a length scale in a system, *i.e.*, local correlations becoming long-ranged. Hence, we find it appears the same on all length scales. The meaning of this will become apparent over the course of the following chapters. This scale-invariant property of continuous phase transitions makes them amenable to a mathematical technique referred to as renormalization group theory. This is one of the cornerstones of modern theoretical physics and a small inroad toward this theory will be made in Chapter 10.

## 6.7 A Phase Transition involving Quantum Statistics

We have thus far spoken about classical systems. The situation is not very different in quantum systems, when it comes to the phase-transition formalism. In this section, we will consider the continuous phase transition associated with Bose-Einstein condensation.

We pick up from our analysis of the Bose gas in Chapter 4. Recall that a non-interacting boson gas satisfies the Bose-Einstein statistics. The chemical potential satisfies  $\mu < 0$ , which implies that the fugacity  $z \in [0, 1)$ . Let us first consider a limitation of using the density of states as defined in Eq. (4.54). In Chapter 4, we only examined the high-temperature limit, in which it is reasonable to expect that the bosons are distributed over multiple energy levels, as we indeed found. However, due to their ability to be in the same state, many bosons will fall into the ground state as the temperature is lowered. The DoS provided in Eq. (4.54)  $\propto \sqrt{E}$ . This scaling seems to imply that there is no state with energy  $E = 0$ . However, there is a crucially important state at  $E = 0$ , namely the (single-particle) ground state. We did not have this ground state accounted for in our density-of-states expression, due to the approximations we used in deriving it. Fortunately, because  $z \ll 1$  in the high-temperature limit, the results in Chapter 4 are valid, despite the reduction. Here, we correct for the omission. Bose-Einstein statistics inform us that the occupancy of the ground state is

$$n_0 = g_s (z^{-1} - 1)^{-1}, \quad (6.33)$$

where we have accounted for the possible spin-based degeneracy  $g_s$ .

Taking the ground state into account for the our analysis at low temperatures, the total number of particles, as originally described in Eq. (4.55), becomes

$$N = g_s \frac{V}{\Lambda^3} \frac{2}{\sqrt{\pi}} \int_0^\infty dx \frac{x^{1/2}}{z^{-1}e^x - 1} + g_s \frac{z}{1-z} = g_s \frac{V}{\Lambda^3} g_{3/2}(z) + g_s \frac{z}{1-z}. \quad (6.34)$$

Here, we have introduced  $x = \beta E$  and defined a family of functions that have the form

$$g_n(z) = \frac{1}{\Gamma(n)} \int_0^\infty dx \frac{x^{n-1}}{z^{-1}e^x - 1}. \quad (6.35)$$

These are the Bose-gas equivalent of the  $f_n$  that we found for the Fermi gas. Similarly, we find that  $g_{5/2}$  appears in the expression for the energy (4.56).

Before we move onto the mathematical analysis of this expression, we should comment on the physical interpretation of the result. On the right-hand side of Eq. (6.34), we have a term that accounts for the number of particles found in the excited states, which scales with the volume. That is, the term is extensive. The number of particles in the ground-state as captured by the second term on the right-hand side, however, is (seemingly) intensive. Thus, we conclude that the number of particles in the

ground state typically does not significantly contribute to  $N$ . We have purposefully used the vague term “seemingly”, as this does not hold in general. When the system is sufficiently cooled, particles are forced into the ground state. In this case, the ground-state term becomes extensive. The transition between intensive scaling and extensive scaling marks the formation of the Bose-Einstein condensate. We will make this picture more mathematically rigorous next.

It should be noted that we have obtained the  $g_n$  by converting a sum into an integral *via* the DoS. Now we will convert the  $g_n$  back to a sum — albeit with a different index — which will help us evaluate the (energy) density:

$$\begin{aligned} g_n(z) &= \frac{z}{\Gamma(n)} \int_0^\infty dx x^{n-1} e^{-x} \sum_{m=0}^\infty z^m e^{-mx}; \\ &= \frac{1}{\Gamma(n)} \sum_{m=1}^\infty \frac{z^m}{m^n} \int_0^\infty du u^{n-1} e^{-u}; \\ &= \sum_{m=1}^\infty \frac{z^m}{m^n}. \end{aligned} \tag{6.36}$$

Here, the integral in the second line is nothing more than the gamma function, hence the final result. The function  $g_n$  is called a polylog and is a monotonically increasing function with  $z$ . It coincides with the Riemann zeta function  $\zeta(n)$  for  $z = 1$ . For  $n = 3/2$ , we have that  $\zeta(3/2) \approx 2.612$ . N.B. This is likely the first time that you will see the zeta function appear in a physics context. It will not be the last, if you delve into the realm of theoretical physics. To the best of the author’s knowledge, there is nothing profound about the appearance of this function here.

Returning to the analysis of the low-temperature limit, we note that when  $T \downarrow 0$  the fugacity  $z = \exp(\beta\mu) \uparrow 1$ . The reasoning was given in Chapter 4, where we discussed the requirements on maintaining a constant density in the grand-canonical ensemble under these conditions. In brief, constant  $N$  necessitates that  $\mu$  goes to zero faster than  $T$ . We recognize that  $z \uparrow 1$  in Eq. (6.34) is problematic. That is, the ground-state term on the right-hand side diverges, which is in contradiction with a finite and constant value of  $N$  as per our equality. Simultaneously, the excited-state term vanishes, as  $\Lambda \propto T^{-1/2}$  and the integral tends toward  $\zeta(3/2) \approx 2.612$ . The intuition is that — in the limit, but not necessarily at the transition temperature — the excited states become nearly devoid of particles, while the ground state contains nearly all  $N$  particles. Clearly, to ensure this and avoid the divergence, we must ensure that  $z$  does not reach the value 1. If we want to fully occupy the ground state (for fixed  $N$ ), the scaling  $g_s z / (z - 1)$  suggest that  $z$  must tend to  $1 - g_s/N$ , but that it may not exceed this threshold. This can be achieved by simultaneously letting the chemical potential tend to zero faster than the inverse temperature increases. It will turn out that there is a finite value of  $T$ , for which  $z$  reaches this value in 3D. The answer is different for spatial dimensions other than three, as partly explored in Exercise Q49.

How do we now determine at which temperature BEC occurs? First, we should consider the physical intuition. At the start of Chapter 4, we remarked that quantum effects would not play a role provided  $\Lambda \ll \rho^{-1/3}$ . That is, the inter particle spacing should exceed the quantum coherence length, as specified by the De Broglie wavelength. Clearly, BEC is predicated on the quantum nature of bosons, so it is reasonable to expect that the De Broglie wavelength should grow to at least the inter-particle spacing to observe it. Substituting  $\ll$  by  $=$  and solving for  $T$  ( $\Lambda \propto T^{-1/2}$ ), will give us an estimate for the transition temperature

$$T_c \approx \frac{h^2 \rho^{2/3}}{2\pi m k_B}. \tag{6.37}$$

However, in the above expression there is no reference to degeneracy. We have thus identified a scaling

with density, but we have not quite reached the final result.

We can do slightly better than this coarse estimate by using Eq. (6.34). We have just used the ground-state term on the right-hand side of Eq. (6.34) to establish the low-temperature limit to  $z$ . Examining instead the excited-state term, we assume we are at a low (but sufficiently high) temperature that we may assume that all particles are in the excited state. This approximation is reasonable above the transition temperature, as the number of particles in the ground state remains intensive in this region. We then approximate the integral over the Bose-Einstein statistics for the excited state using its zero-temperature value of  $\zeta(3/2)$ . This is permitted, because the integral does not vary strongly near  $T = 0$ . The resulting expression involving  $N$  can then be solved for  $T$ , as the temperature dependence only remains present in  $\Lambda$ . Carrying out the necessary manipulations results in

$$T_c = \left( \frac{2\pi\hbar^2}{k_B m} \right) \left( \frac{\rho}{g_s \zeta(3/2)} \right)^{2/3}, \quad (6.38)$$

which is more precise than our original estimate for  $T_c$  and involves the degeneracy. The accuracy of this approximation is revealed in Fig. 6.9, which shows the numerically determined value of  $z$  as a function of the reduced temperature  $T/T_c$  for  $g_s/N = 0.001$ .

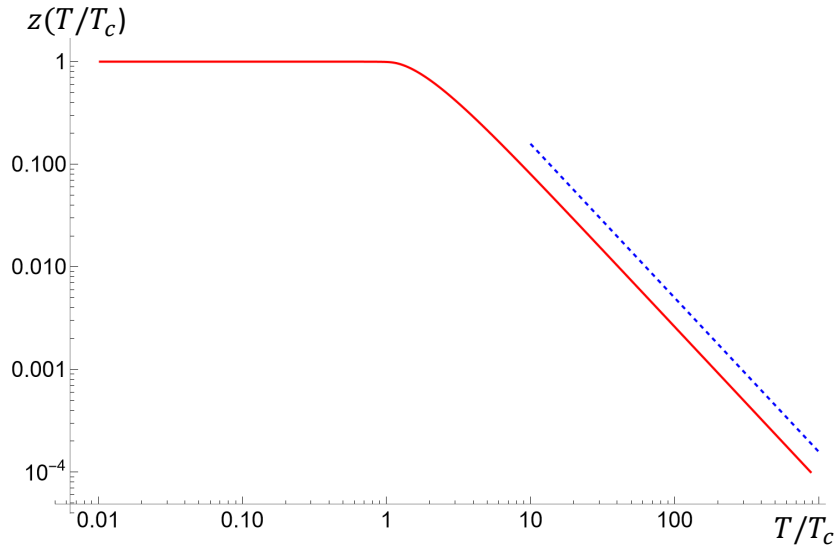


Figure 6.9: The fugacity  $z$  as a function of the reduced temperature  $T/T_c$  (red), where  $T_c$  is as in Eq. (6.38). The dashed blue line shows the dependency  $z \propto t^{-3/2}$ , which sets in at high temperature. At low temperatures,  $z$  tends to a constant slightly smaller than  $1 \approx 1 - g_s/N$ . In this numerically computed  $z$  curve, we used  $g_s/N = 0.001$ .

To demonstrate that this temperature indeed defines a phase transition, we can consider the heat capacity. However, first we examine the pressure using  $\Omega = -pV$ . It follows that

$$\beta p = \frac{g_s}{\Lambda^3} g_{5/2}(z) - \frac{g_s}{V} \log(1 - z), \quad (6.39)$$

where the second term accounts for the ground-state contribution. This function is smooth on  $z \in [0, 1 - g_s/N]$ , indicating that there is no first-order phase transition. Turning to the energy density, we

find that

$$\frac{E}{V} = \frac{3}{2} g_s \frac{k_B T}{\Lambda^3} g_{5/2}(z), \quad (6.40)$$

where there is no ground-state contribution, because we set that energy level to  $E = 0$ . The associated (constant-volume) heat-capacity per volume is given by

$$\begin{aligned} \frac{C_V}{V} &= \frac{15}{4} g_s \frac{k_B}{\Lambda^3} g_{5/2}(z) + \frac{3}{2} g_s \frac{k_B T}{\Lambda^3} \frac{\partial g_{5/2}}{\partial z}(z) \frac{\partial z}{\partial T}; \\ &= \frac{15}{4} g_s \frac{k_B}{\Lambda^3} g_{5/2}(z) + \frac{3}{2} g_s \frac{k_B T}{\Lambda^3} \frac{g_{3/2}(z)}{z} \frac{\partial z}{\partial T}. \end{aligned} \quad (6.41)$$

The subtleties come from the term  $\partial z / \partial T$  and we will discuss these next, in order to demonstrate that the scaling of the heat capacity on either side of  $T_c$  is different.

The derivative of  $z$  with respect to  $T$  in Eq. (6.41) is interesting. For  $T < T_c$ ,  $z \approx 1 - g_s/N$  (a constant, as also revealed by Fig. 6.9) and the derivative should approximately vanish. This implies

$$C_V \approx \frac{15}{4} g_s \frac{k_B}{\Lambda^3} \zeta(5/2) \propto T^{3/2}. \quad (6.42)$$

For  $T > T_c$  the scaling is  $z \propto T^{-3/2}$ , because we are working at constant density, as we argued in Chapter 4. Thus, we expect the derivative to contribute and working out the scaling, it is easy to find the heat capacity tends toward a constant. This constant should be  $3Nk_B/2$  using the method of counting degrees of freedom. In addition, monotonicity of the  $g_n$  combined with the fact that  $\partial z / \partial T < 0$  in this regime, indicates that  $C_V$  is a decreasing function. Now, we have that  $C_V$  increases with temperature away from  $T = 0$  and beyond  $T_c$  it decreases. Clearly,  $C_V$  has a maximum somewhere around  $T_c$ .

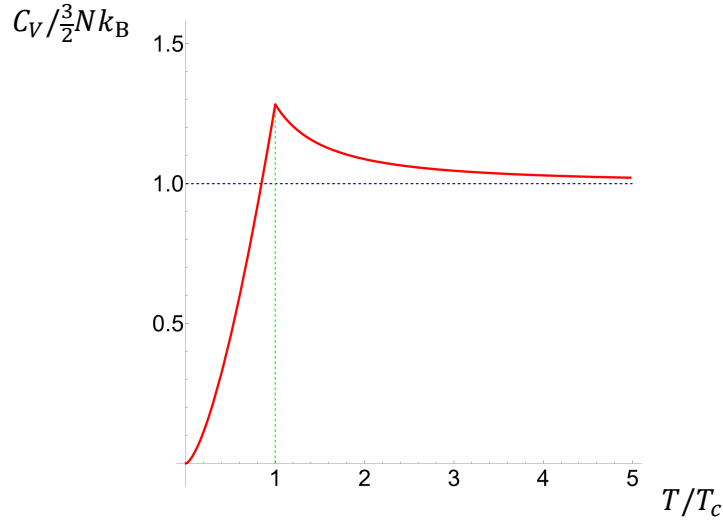


Figure 6.10: The constant-volume heat-capacity  $C_V$  of an ideal Bose gas as a function of the temperature  $T$ . Note that the function is continuous at the critical temperature  $T_c$ , but that it has a discontinuous derivative. The behavior near  $T_c$  follows from our derivation in the main text. Here, the full curve was solved for numerically using  $z = 1$  below the transition.

We can do more than this. If we were to approach  $T_c$  from above, we know using Eq. (6.34) that  $g_{3/2}(z) \approx \rho\Lambda^3$ , because we can ignore the contributions of the ground state. We can also Taylor expand  $g_{3/2}(z)$  around  $z = 1$  to gain a feeling for its behavior (scaling) around  $T_c$ . The Taylor expansion point is sensible, as we can infer from Fig. 6.9 that in the thermodynamic limit, we have a kink in  $z(T/T_c)$  at  $T = T_c$ . That is, we transition from  $z = 1$  ( $T < T_c$ ) to something decreasing in  $t$ . The expansion is analytically involved — it can, however, be straightforwardly done with an algebraic manipulation software such as `Mathematica` — but eventually leads to the form

$$g_{3/2}(z) \approx \zeta(3/2) + 2\sqrt{\pi}\sqrt{1-z} + \dots, \quad (6.43)$$

where we have confirmed our intuition in approximating the integral at low temperature, as  $\zeta(3/2)$  is the leading-order term. Together with our previous relation, the expansion allows us to write

$$\begin{aligned} z &\approx 1 - \frac{1}{4\pi} (\zeta(3/2) - \Lambda^3 \rho)^2; \\ &= 1 - \frac{\zeta(3/2)^2}{4\pi} \left( \left[ \frac{T}{T_c} \right]^{3/2} - 1 \right)^2; \\ &\approx 1 - \frac{9\zeta(3/2)^2}{16\pi} \left( \frac{T - T_c}{T_c} \right)^2. \end{aligned} \quad (6.44)$$

Note that here we see a feature of power-law departure away from a critical point.

Substituting this expression into Eq. (6.40) and taking a derivative with respect to temperature, we arrive at the following

$$C_V = \frac{15}{4} \frac{\zeta(5/2)}{\zeta(3/2)} N k_B T_c \begin{cases} \left( \frac{T}{T_c} \right)^{3/2} & T < T_c \\ 1 & T = T_c \\ 1 - \left( \frac{9}{20\pi} \frac{\zeta(3/2)^3}{\zeta(5/2)} - \frac{3}{2} \right) \left( \frac{T}{T_c} - 1 \right) & T > T_c \end{cases}, \quad (6.45)$$

which holds close to  $T = T_c$  to first order. This expression clearly has a kink, but not a divergence as one might expect on the basis of our intuition for phase transitions, when we think about the Ising model, see Chapter 7. The associated (full) expression for the heat capacity — in the thermodynamic limit — is shown in Fig. 6.10. Note that the curve shown in this figure is continuous, as we would have expected on the basis of Eq. (6.45). However, its derivative will not be, which is one of the hallmarks of a phase transition. That is, we have a phase transition from a phase wherein bosons occupy many states to a ‘condensed’ phase, wherein nearly all particles are in the ground state: the *Bose-Einstein condensate*. As the constant-volume heat-capacity can be related to a second-order derivative of a thermodynamic potential, this transition is indeed continuous. It will turn out that Bose-Einstein condensation can be classified as a second-order transition *via* a theoretical analysis that goes beyond the notes.

## 6.8 Exercises

### Q38. Equilibrium Conditions

Use the second law of thermodynamics to show that in equilibrium  $p_1 = p_2$  (mechanical equilibrium) and that  $\mu_1 = \mu_2$  (chemical equilibrium) for a single-component system.

### Q39. Heat Capacity (Again)

Show that the heat capacity  $C_V = T(\partial S/\partial T)_{V,N}$  is always greater than or equal to zero for a stable system. Start by writing the heat capacity in terms of  $U$  and the natural variables of the internal energy.

### Q40. Coexistence: Surface versus Volume

Assume that we have two phases in coexistence, labeled 1 and 2. Explain why or show why we can ignore the contributions from the interface between phases 1 and 2, when we are deriving the equilibrium conditions for coexistence between the two phases. Provide a scaling argument. Hint: For coexistence we are interested in the thermodynamic limit ( $N \rightarrow \infty$ ).

### Q41. Equilibrium: One Component from David Chandler (*Introduction to Modern Physics*)

Consider a single component system with two possible phases: one labeled 1 and one labeled 2. When the material is in phase 1, the equation of state is given by

$$\beta p = a(\beta) + b(\beta)\beta\mu \quad (6.46)$$

where  $\beta = 1/(k_B T)$ , and  $a(\beta)$  and  $b(\beta)$  are positive functions of  $\beta$ . In the 2 phase, the equation of state is given by

$$\beta p = c(\beta) + d(\beta) (\beta\mu)^2, \quad (6.47)$$

where  $c(\beta)$  and  $d(\beta)$  are positive functions of  $\beta$  and  $d > b$  and  $c < a$ . Determine the density change ( $\rho_2 - \rho_1$ ) that occurs when the material undergoes a phase transition from phase 1 to phase 2; assume that the density  $\rho_1$  is smaller than  $\rho_2$  at coexistence. Also determine the pressure at which the transition occurs. Hint: The Gibbs-Duhem equation might be useful. The final answer for both questions should be an expression of  $a$ ,  $b$ ,  $c$ ,  $d$ , and  $\beta$  only.

### Q42. Coexistence from a Common-Tangent Construction

Show that the common-tangent construction as depicted in the right-hand panel to Fig. 6.5:

- (a) ensures that the pressures in the coexisting phases are equal.
- (b) ensures that the chemical potentials in the coexisting phases are equal.

This should follow the line of argument set out in Section 6.4, but for  $F/V$  as a function of  $\rho$ , rather than  $F$  as a function of  $V$ .

### Q43. Phase Diagram

A theorist develops an approximate theory to calculate the free energy of the system. The free energy that she finds, is shown in Fig 6.11 for four different temperatures. Note that here she has plotted  $F/V$  as a function of the density  $\rho = N/V$ . Use the four plots to sketch a phase diagram of the system.

### Q44. The Maxwell Equal-Area Rule

In this exercise, we examine the construction of binodals attributed to Maxwell, who considered the presence of an unstable region in the van-der-Waals (vdW) equation of state (EoS). We will

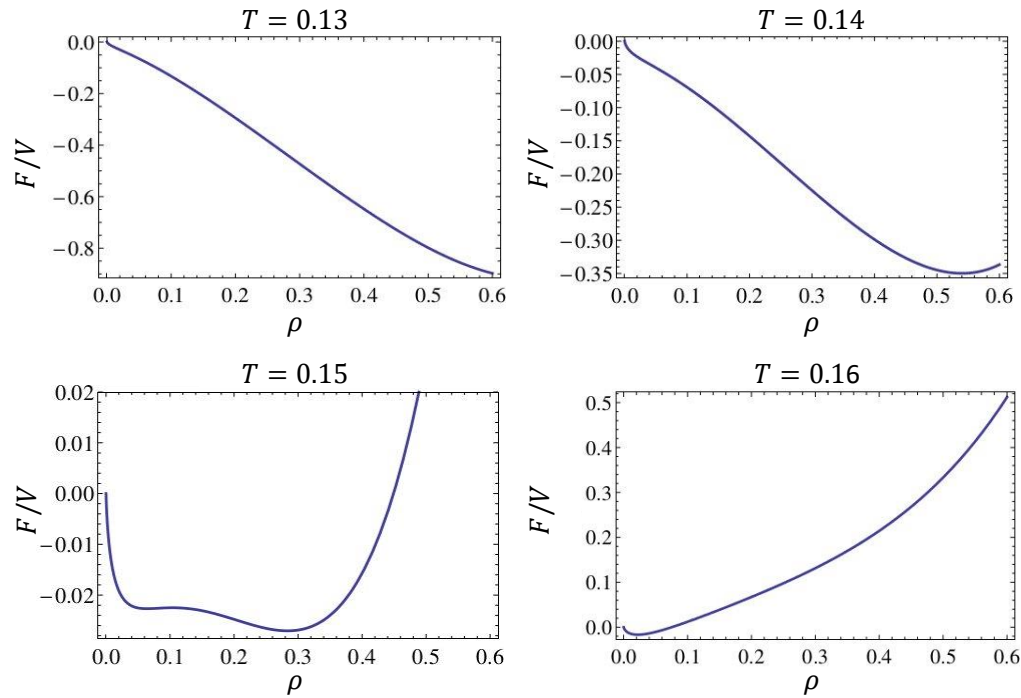


Figure 6.11: The approximate Helmholtz free energy per volume  $F/V$  as a function of density  $\rho$  for four values of the (reduced) temperature  $T$ .

return to the vdW gas in Chapter 13, for the purpose of this exercise we only require to know the shape of the isotherms. The vdW EoS is given by  $\beta p = \rho/(1 - b\rho) - \beta a\rho^2$ , with  $\rho = N/V$  the particle number density,  $b$  an excluded volume per particle, and  $a$  a measure for attraction between particles.

- Rewrite the above EoS to obtain  $(v-p)$  isotherms, *i.e.*, the pressure  $p$  as a function of the volume per particle  $v = V/N$ .
- Sketch a  $(v-p)$  isotherm below the critical temperature  $T < T_c$ . Indicate an approximate lower bound for  $v$  in terms of the vdW gas parameters. Label your axes!
- Why should one replace the “wiggly part” of the isotherms with  $T < T_c$ ? By what should it be replaced?
- Maxwell argued that  $p_{\text{eq}}$  must be chosen such that within the wiggle the areas between the constant pressure line and the isotherm are equal. This leads to the expression

$$\int_{v_g}^{v_l} dv (p(v) - p_{\text{eq}}) = 0, \quad (6.48)$$

where integration takes place between the two coexistence volumes per particle, labelled  $g$  and  $l$  for gas and liquid, respectively. Use the definition of the pressure to rewrite  $p(v)$  in terms of the free energy and evaluate the above integral to obtain  $-p_{\text{eq}} = (f(v_l) - f(v_g)) / (v_l - v_g)$ , where  $f = F/N$  is the free energy per particle.

- (e) Explain how this proves that the Maxwell equal-area rule is equivalent to the common tangent.
- (f) There is a preference for the common-tangent construction over the equal-area rule. Explain what is problematic with the equal-area rule, referencing the spinodal region.

**Q45. The Phases of Ouzo**

When you mix Ouzo (a Greek alcoholic spirit, comprised of alcohol, water, and essential oils that give it an anise flavor) with a small amount of water, you obtain a turbid (cloudy) suspension. An experimentalist has obtained the following ternary phase diagram for this situation, see Fig. 6.12.

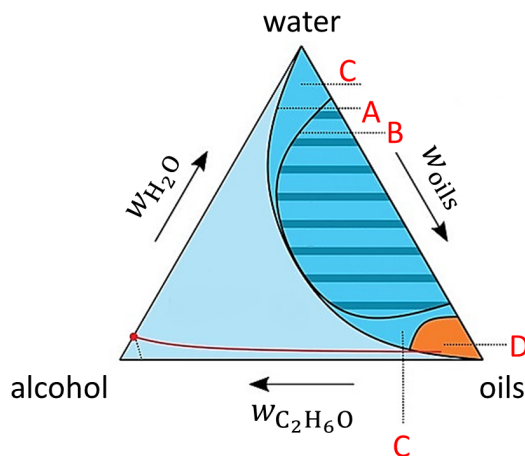


Figure 6.12: A phase diagram for an ouzo-like mixture of oils, water, and alcohol.

The ternary phase diagram has the pure phases at each corner, the two-phase diagrams at each edge, with the arrows indicating the increasing (weight) fraction of one of the phases, and the three-phase states in the body of the triangle.

- (a) What lines do A and B represent?
- (b) What characterizes the spinodal curve?
- (c) What characterizes the striped region? What do you expect the order of the phase transition to be from the lower-left (lightest-blue) region to the orange region (D)? That is, when moving along the red line from left to right?
- (d) Where is the critical point located?

**Q46. More on Phase Diagrams** from David Chandler (*Introduction to Modern Physics*)

A hypothetical experimentalist measures the hypothetical equation of state for a substance near the liquid-solid phase transition. She finds that over a limited range of temperatures and densities, the liquid phase can be characterized by the following formula for the Helmholtz free energy per unit volume:

$$F/V = \frac{1}{2}a(T)\rho^2 \quad (6.49)$$

where  $\rho$  is the number density and  $a(T)$  is a function of the temperature given by  $a(T) = \alpha/T$  with  $\alpha$  a constant. Similarly, in the solid phase she finds

$$F/V = \frac{1}{3}b(T)\rho^3 \quad (6.50)$$



**Q48. Broken Spring**

It is found that when stretched to a certain length, a particular spring breaks. Before the spring breaks, *i.e.*, for small extensions, the free energy is given by

$$\frac{A}{M} = \frac{1}{2}kx^2 \quad (6.51)$$

with  $x$  the length per unit mass and  $M$  the mass of the spring. The free energy  $A = U - TS$  obeys  $dA = -SdT + fdL + \mu dM$ , with  $f$  the tension and  $L$  the length. After breaking, the free energy is given by

$$\frac{A}{M} = \frac{1}{2}h(x - x_0)^2 + c. \quad (6.52)$$

The constants  $k$ ,  $h$ ,  $x_0$ , and  $c$  are all independent of  $x$  but do depend on  $T$ . Furthermore, we assume  $k > h$ ,  $c > 0$ , and  $x_0 > 0$  for all  $T$ .

- Determine the equation of state  $f = f(T, x)$  for the spring at small and large extensions.
- Similarly, determine the chemical potentials  $\mu$ .
- Show that  $\mu = \frac{A}{M} - fx$
- Find the force that at given temperature will break the spring.
- Determine the discontinuous change in  $x$  when the spring is breaks.
- Is this like a first order phase transition or second order phase transition?

**Q49. Bose-Einstein Condensation in 2D?**

Write down the grand partition function  $\Xi(V, T, z)$  for the two-dimensional (2D) ideal Bose Gas. From  $\Xi$  calculate the mean particle density  $\rho = \langle N \rangle / V$  as a function of the fugacity  $z$  and the temperature  $T$ . Show that the 2D ideal Bose gas does not condense. This calculation should confirm your suspicions from Exercise Q27.

**Q50. Two Types of Boson: Conserved and Non-Conserved**

There are two types of bosons: conserved bosons (like helium-4 atoms) and non-conserved bosons (like photons). The goal of this problem is to develop an intuitive understanding of the difference between those two types.

Conserved bosons remain in existence (on all relevant time scales), while non-conserved bosons can appear or disappear. For non-conserved bosons the chemical potential is typically 0; but, in special cases, it can take other values. For conserved bosons, when the temperature changes, the chemical potential needs to adjust to guarantee that the particle number remains constant (conserved). Note, however, that in both cases the chemical potential can never become larger than the single-particle-ground-state energy, which is usually chosen as reference energy  $\epsilon_0 = 0$ .

- Start by writing down the particle number  $N$  in integral form with density of states  $g(\epsilon)$  and Bose-Einstein distribution  $f(\epsilon)$ . Draw the functions of the integrand; that is, draw  $f(\epsilon)$ ,  $g(\epsilon)$ , but also  $f(\epsilon)g(\epsilon)$ .
- For non-conserved bosons, answer the following questions:
  - What happens to the particle number  $N$  if you increase/decrease the temperature  $T$ ?
  - What happens to  $N$  if you increase/decrease the chemical potential  $\mu$ ?
  - Can non-conserved bosons undergo a Bose-Einstein condensation? Hint: consider conserved bosons first.

- (iv) Is the distribution of non-conserved bosons at high temperatures well described by the Maxwell-Boltzmann distribution? Hint: consider conserved bosons first.
- (b) For conserved bosons, answer the following questions:
  - (i) What happens to the chemical potential  $\mu$  if you increase/decrease the temperature  $T$ ?
  - (ii) What happens when the chemical potential is at the single-particle-ground-state energy  $\mu = \epsilon_0$  and you decrease the temperature? Where do particles accumulate and what does it have to do with Bose-Einstein condensation?
  - (iii) What happens to  $e^{\beta\mu}$  in the limit of large temperature? Show that in this case, the Bose-Einstein distribution can be well approximated by the Maxwell-Boltzmann distribution.

# Chapter 7

## The Ising Model

In this chapter, we will learn about the Ising model, named after Ernst Ising, which dates back to 1920. The model was proposed by Wilhelm Lenz as a simple model for ferromagnetism and solved in one dimension by his student Ernst Ising. We will study several approaches to obtaining analytic expressions for its behavior here. It was later solved by Lars Onsager in two dimensions, which we will touch upon, but remains unsolved in three dimensions. In the years since the model was first developed, it has seen wide use. Not only is it suited to describe systems of spins, but the concept of universality allows it to be applied to an amazing variety of systems including, *e.g.*, protein folding, biological membranes, and social behavior. We will comment on universality further in Chapter 10. Additionally, since the Ising model has been solved analytically in one and two dimensions, it provides valuable insight into the properties of phase transitions for any (theoretical) physicist.

### 7.1 Introducing the Model

Consider a set of  $N$  particles on a lattice. Assume that each particle can take on two states, which we will call spin and label using  $S_i$ : “up” spins give  $S_i = +1$  and “down” spins  $S_i = -1$ . If these spins only interact with their nearest neighbors and are placed in an external field, we can write a simple Hamiltonian for the system as

$$\mathcal{H} = -\frac{J}{2} \sum_{i=1}^N \sum_j' S_i S_j - H \sum_{i=1}^N S_i, \quad (7.1)$$

where  $J$  is the coupling between the spins and  $H$  is an external field. The  $\sum_j'$  indicates a sum of the  $j$  nearest neighbors of particle  $i$ . The factor of  $1/2$  is included so that each pair of spins is only counted once. Note that this notation is not unique, there are many different notations used in literature to denote a sum over nearest neighbors.

Looking more closely at the two terms which occur in Eq. (7.1), we see that for  $J > 0$ , the first term is minimized when the spins on sites  $i$  and  $j$  are pointing in the same direction. This is the situation encountered in a ferromagnet, see Fig. 7.1. If  $J < 0$ , the interaction is minimized when neighboring spins point in opposite directions, as in an antiferromagnet, see Fig. 7.1. The second term appearing in Eq (7.1) is the coupling between the spins and the external magnetic field. When  $H > 0$  this term is minimized when the spins point in the direction of the field; for  $H < 0$  the energy is minimized when the spins point in the direction opposite to the field.

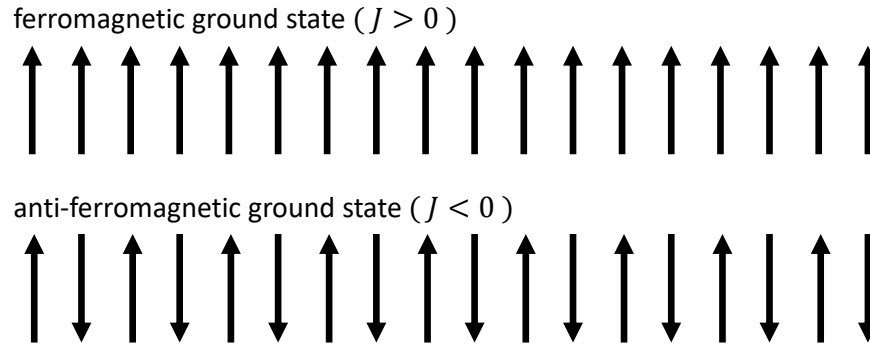


Figure 7.1: Ground states of the Ising model depend on the sign of the spin-field coupling parameter  $J$ . Positive values of  $J$  (top) correspond to ferromagnetic behavior and negative values of  $J$  (bottom) to anti-ferromagnetic behavior.

## 7.2 Intuition for the Zero-Field Behavior

In this section, we will focus on the zero field limit, *i.e.*,  $H = 0$ . We will come back to the system with an external field in Section 7.5. Let us begin by examining what we expect to happen when varying the temperature; we will consider  $J > 0$  here. At high temperatures, the spins should be disordered, as the interaction energy is small compared to the thermal energy. At zero temperature, we know that the system will be in its ground state, with all the spins aligned, *i.e.*, the lowest energy state. However, we do not know *a priori* whether there is a finite temperature, below which the system spontaneously orders. More specifically, we can ask whether there is a *critical* temperature (denoted  $T_c$ ) where the system undergoes a phase transition from a disordered state to an ordered state.

We characterize the system's order by examining the average magnetization. The net magnetization is defined as

$$M = \sum_{i=1}^N S_i, \quad (7.2)$$

while the average magnetization is given by

$$m = \frac{M}{N}. \quad (7.3)$$

In the ground state, *i.e.*,  $T = 0$ , all the spins are aligned and the magnetization is given by  $M = N$ . At high temperatures, the spins are not aligned, and the average value of the magnetization is simply  $M = 0$ . So what about finite temperature?

Let us first examine the Ising model in one dimension with  $N$  spins. Because there is no field, it is equally favorable to have all spins pointing up or down, the only source of deviations away from the ground state comes from defects. A single defect is formed when the right-hand side of the spin chain has an opposite magnetization to that of the left-hand side, see Fig. 7.2, with the defect being localized at the disconnection point. Note that a single flipped spin constitutes two defects, one on either side of the flipped spin, and is energetically even less favorable than the defect state shown in Fig. 7.2. We thus find that in one dimension, a single defect removes all correlations between the left- and right-hand side of the chain. That is, it would not be possible to grow a single, system spanning cluster with even a single flipped spin.

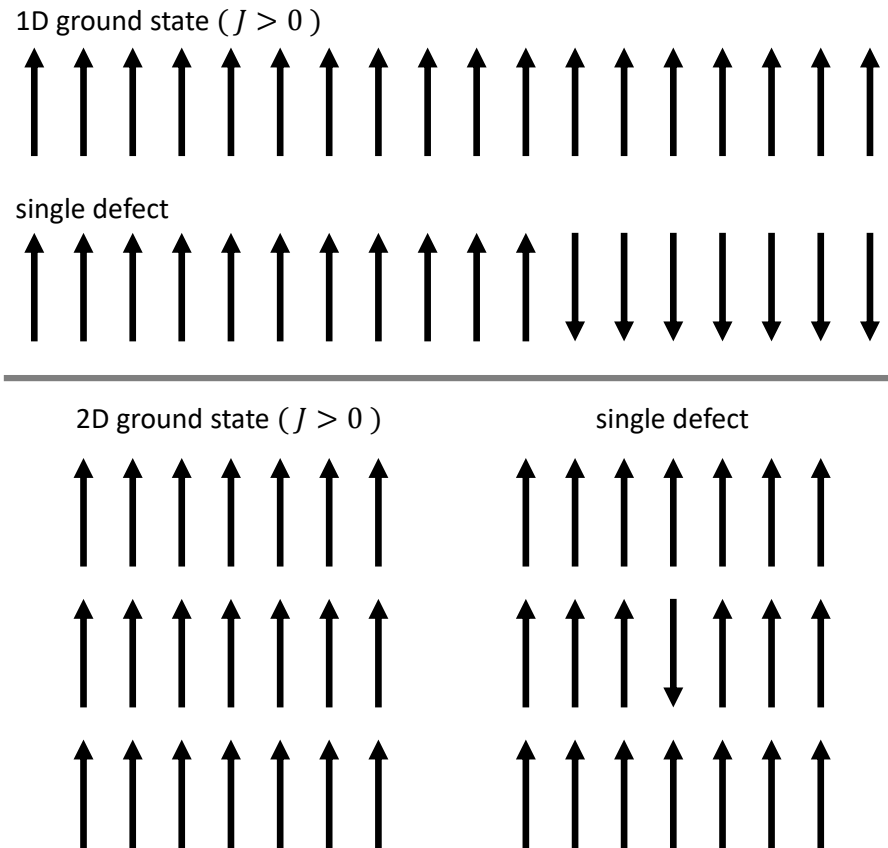


Figure 7.2: Defects in the ferromagnetic Ising model ( $J > 1$ ). (top) One-dimensional Ising model ground state and a state with a single defect. The defect disconnects the right-hand side of the spin chain from its left-hand side. (bottom) Two-dimensional Ising ground state (left) and a state with a single defect (right). In contrast to the one-dimensional case, the spins neighboring the defect can remain pointing upwards, since they each interact with three other neighbors which point up. Hence, the defect does not appear to have a long-range effect on the ordering in the system.

This might not immediately present itself as a problem, because the two half spaces in Fig. 7.2, are essentially very large in the thermodynamic limit, *i.e.*, when  $N \rightarrow \infty$ . However, at any non-zero temperature we expect to have a finite fraction of all spins flipped. This means that at any  $T > 0$ , the string of spins will be subdivided into a number of different regions with spins “up” and “down”. Spins know only about their nearest neighbors, so that the length of these domains is random. That is, there is no energetic penalty for having a longer or shorter domain with spins pointing opposite to those of its neighboring domains. Therefore, we cannot distinguish this defect-rich state from a state with random magnetization. Hence, there is no phase transition from a disordered to an ordered system. While not exactly a hard proof, our intuition in this case is accurate, we will show shortly.

We can also examine the two-dimensional Ising model in a similar fashion. If we start in the ground state and introduce a single defect, see Fig 7.2, the remaining spins on all sides of the flipped spin are still connected to three up-pointing spins. Hence, the energy is minimized if they stay pointing upwards. In other words, a cluster can survive a single defect spin and hence we expect that the system would be able to stay ordered for a range of finite temperatures. It therefore seems likely that the system will undergo a phase transition at a finite temperature. Again, while this is not a hard proof, it does indicate the behavior of the 2D system will be significantly different from the 1D case. Our intuition will again turn out to be correct and a similar argument holds for three (and higher) dimensions.

### 7.3 Zero-Field Ising Model in One Dimension

We will now solve the zero-field 1D Ising model exactly. We start by writing down the partition function

$$\begin{aligned}
 Z(N, \beta) &= \sum_{S_1} \sum_{S_2} \dots \sum_{S_N} e^{-\beta \mathcal{H}(S_1, S_2, \dots, S_N)}; \\
 &= \sum_{S_1} \sum_{S_2} \dots \sum_{S_N} e^{\frac{\beta J}{2} \sum_{i=1}^N \sum_j' S_i S_j}; \\
 &= \sum_{S_1} \sum_{S_2} \dots \sum_{S_N} e^{\beta J (S_1 S_2 + S_2 S_3 + \dots + S_{N-1} S_N)}; \\
 &= \sum_{S_1} \sum_{S_2} \dots \sum_{S_N} e^{\beta J S_1 S_2} e^{\beta J (S_2 S_3 + \dots + S_{N-1} S_N)}; \\
 &= \sum_{S_2} \dots \sum_{S_N} \left[ \sum_{S_1} e^{\beta J S_1 S_2} \right] e^{\beta J (S_2 S_3 + \dots + S_{N-1} S_N)}. \tag{7.4}
 \end{aligned}$$

The expression in square brackets can now be solved exactly by summing over  $S_1 = \pm 1$ :

$$\left[ \sum_{S_1} e^{\beta J S_1 S_2} \right] = e^{\beta J S_2} + e^{-\beta J S_2} = 2 \cosh(\beta J S_2). \tag{7.5}$$

However, since  $S_2$  can only take on values of +1 and -1, and since  $\cosh(x) = \cosh(-x)$ , we can simplify the above expression to

$$\left[ \sum_{S_1} e^{\beta J S_1 S_2} \right] = 2 \cosh(\beta J) \tag{7.6}$$

which is independent of  $S_2$ . Hence, the partition function becomes

$$\begin{aligned}
Z(N, \beta) &= 2 \cosh(\beta J) \sum_{S_2} \dots \sum_{S_N} e^{\beta J(S_2 S_3 + \dots + S_{N-1} S_N)}; \\
&= 2 \cosh(\beta J) \sum_{S_3} \dots \sum_{S_N} \left[ \sum_{S_2} e^{\beta J S_2 S_3} \right] e^{\beta J(S_3 S_4 + \dots + S_{N-1} S_N)}; \\
&= (2 \cosh(\beta J))^2 \sum_{S_3} \dots \sum_{S_N} e^{\beta J(S_3 S_4 + \dots + S_{N-1} S_N)}; \\
&= \dots; \\
&= (2 \cosh(\beta J))^{N-1} \sum_{S_N} 1; \\
&= 2 (2 \cosh(\beta J))^{N-1}. \tag{7.7}
\end{aligned}$$

From the partition function, we can determine the Helmholtz free energy

$$\begin{aligned}
F(N, \beta) &= -\frac{1}{\beta} \log Z(N, \beta); \\
&= -\frac{1}{\beta} \log \left( 2 (2 \cosh(\beta J))^{N-1} \right); \\
&= -\frac{1}{\beta} [\log 2 + (N-1) \log (2 \cosh(\beta J))]. \tag{7.8}
\end{aligned}$$

Finally, in the thermodynamic limit, *i.e.*,  $N \rightarrow \infty$ , we have

$$F(N, \beta) = -\frac{N}{\beta} \log (2 \cosh(\beta J)). \tag{7.9}$$

As discussed in Chapter 6, for there to be a phase transition, there must be a discontinuity in a derivative (1st derivative, 2nd derivative, *etc.*) of  $F$ . Clearly,  $F$  is perfectly smooth, so there is *no* phase transition in the 1D Ising model with  $H = 0$ . This holds for both signs of  $J$ , so that our intuition of Section 7.2, also holds for the antiferromagnetic 1D Ising model.

## 7.4 Zero-Field Ising Model in Two and Three Dimensions

The Ising model in two dimensions was solved in the 1940s by Lars Onsager. The partition function for the two-dimensional Ising model (at zero field) is given by

$$Z(N, \beta) = [2 \cosh(2\beta J) \exp(I)]^N \tag{7.10}$$

where

$$I = \frac{1}{\pi} \int_0^{\pi/2} d\phi \log \left( \frac{1}{2} \left[ 1 + (1 - \kappa^2 \sin^2 \phi)^{1/2} \right] \right), \tag{7.11}$$

with  $\kappa = 2 \sinh(2\beta J) / \cosh^2(2\beta J)$ . While we will not do so here, it is possible to show that the above partition function leads to a spontaneous magnetization for  $T$  below  $T_c = 2J / (k_B \log(1 + \sqrt{2})) \approx 2.27J/k_B$  where  $k_B$  is Boltzmann's constant. Above  $T_c$  the system is disordered. Hence, there is a phase transition in the 2D Ising model. As we will explore later, it turns out that this phase transition is an example of a second-order phase transition. In a second-order phase transition, the phase transition is characterized by a discontinuity in the second-order derivative of the free energy.

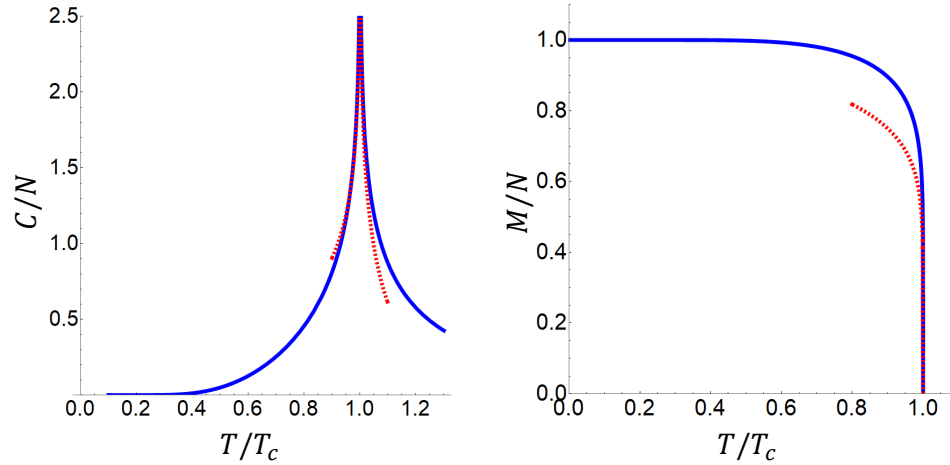


Figure 7.3: Critical phenomena in the zero-field, two-dimensional Ising model. (left) The heat capacity per particle  $C/N$  as a function of the temperature  $T$  normalized by the critical temperature  $T_c$ . (right) The magnetization per particle  $M/N$  as a function of  $T/T_c$ . The full solution by Onsager is shown in thick blue, while the asymptotic behavior near the critical point is given by dashed red lines.

The heat capacity was also determined by Onsager and is given by

$$\frac{C}{N} = \frac{1}{N} \left( \frac{\partial \langle E \rangle}{\partial T} \right)_{H=0} \approx \frac{8k_B}{\pi} (\beta J)^2 \log \left| \frac{1}{T - T_c} \right|, \quad (7.12)$$

where the approximation holds close to the critical point. A plot is shown in the left-hand panel to Fig. 7.3. Note that this plot shows that the heat capacity is singular. This means that a divergence in the heat capacity is also sufficient to have a continuous phase transition, provided there are no discontinuities in lower-order derivatives of the free energy<sup>1</sup>. The magnetization for  $T < T_c$  is given by

$$\frac{M}{N} \propto (T_c - T)^\beta, \quad (7.13)$$

with  $\beta = 1/8$ , see the right-hand panel to Fig. 7.3.

The three-dimensional Ising model still has not been solved analytically. However, numeric work on the system has found that there is also a phase transition in the 3D Ising model, which is similar to that of the 2D system, and that the corresponding critical temperature is approximately  $4.52J/k_B$ . Near the critical temperature, the heat capacity has the form

$$\frac{C}{N} \propto |T - T_c|^{-\alpha} \quad (7.14)$$

with  $\alpha \approx 0.1096$ . For  $T < T_c$ , the magnetization is given by

$$\frac{M}{N} \propto (T - T_c)^\beta, \quad (7.15)$$

with  $\beta \approx 0.32653$ . The numbers come from [Campostrini, *et al.*, Phys. Rev. E **65**, 066127 (2002)]. The exponents  $\alpha$  and  $\beta$  are referred to as *critical exponents* and are typically used to characterize the phase

<sup>1</sup>Note, we have also previously seen a finite, but spiked heat capacity for Bose-Einstein condensates in Chapter 6, which had power-law behavior near its critical point.

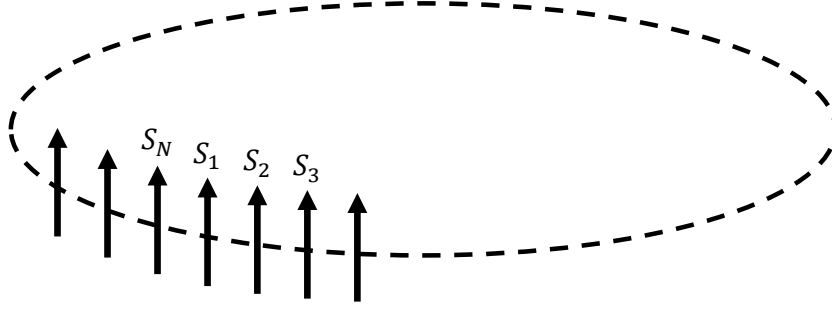


Figure 7.4: Sketch of the 1D Ising model with  $N$  spins and periodic boundary conditions.

transition. This characterization is not simply used in discussing the Ising model, but rather critical points in general, as we will return to in Chapter 12.

## 7.5 Transfer Matrix Method for 1D Ising Model with Field

In this section, we consider Eq. (7.1) when the field  $H \neq 0$ . It might appear at first glance that we should be able to solve this in a similar manner as was taken in Section 7.3. However, this is not the case. The method we will apply to determine an expression for the free energy is often referred to as the *transfer matrix method*. This method was first used by Kramers and Wannier in 1941, and was later used by Onsager to solve the field-free Ising model in 2D.

We start by rewriting the Hamiltonian in a symmetric representation, specifically

$$\mathcal{H} = -J \sum_{i=1}^N S_i S_{i+1} - \frac{H}{2} \sum_{i=1}^N (S_i + S_{i+1}). \quad (7.16)$$

Here, we use *periodic* boundary conditions, namely  $S_{N+1} = S_1$ , see Fig. 7.4. This contrasts with our solution approach for the Ising model without a field, where we used *open* boundary conditions. The partition function for this system is given by

$$\begin{aligned} Z(\beta, H) &= \sum_{S_1} \sum_{S_2} \cdots \sum_{S_N} e^{\beta \sum_{i=1}^N (J S_i S_{i+1} + \frac{H}{2} (S_i + S_{i+1}))}; \\ &= \sum_{S_1} \sum_{S_2} \cdots \sum_{S_N} \prod_{i=1}^N e^{\beta (J S_i S_{i+1} + \frac{H}{2} (S_i + S_{i+1}))}; \\ &= \sum_{S_1} \sum_{S_2} \cdots \sum_{S_N} \prod_{i=1}^N T_{S_i, S_{i+1}}, \end{aligned} \quad (7.17)$$

where we have defined

$$T_{S_i, S_{i+1}} = e^{\beta (J S_i S_{i+1} + \frac{H}{2} (S_i + S_{i+1}))}. \quad (7.18)$$

Hence,  $\mathbf{T}$  can be looked at as a matrix with the elements

$$T_{1,1} = e^{\beta(J+H)}; \quad (7.19)$$

$$T_{1,-1} = e^{-\beta J}; \quad (7.20)$$

$$T_{-1,-1} = e^{\beta(J-H)}; \quad (7.21)$$

$$T_{-1,1} = e^{-\beta J}. \quad (7.22)$$

We know from matrix algebra that the square of matrix  $\mathbf{A}$  with matrix elements  $A_{i,j}$  can be written

$$(\mathbf{A}^2)_{i,j} = (\mathbf{A}\mathbf{A})_{i,j} = \sum_k A_{i,k}A_{k,j}. \quad (7.23)$$

Therefore we can rewrite the partition function further as

$$\begin{aligned} Z(\beta, H) &= \sum_{S_1} \sum_{S_3} \sum_{S_4} \cdots \sum_{S_N} \left( \sum_{S_2} T_{S_1, S_2} T_{S_2, S_3} \right) T_{S_3, S_4} \cdots T_{S_N, S_1}; \\ &= \sum_{S_1} \sum_{S_3} \sum_{S_4} \cdots \sum_{S_N} T_{S_1, S_3}^2 T_{S_3, S_4} \cdots T_{S_N, S_1}; \\ &= \sum_{S_1} T_{S_1, S_1}^N; \\ &= \text{Tr}(\mathbf{T}^N), \end{aligned} \quad (7.24)$$

where  $\text{Tr}(\mathbf{A})$  is the trace of matrix  $\mathbf{A}$ . Again, from matrix algebra, we know that the trace of a matrix is simply the sum of its eigenvalues<sup>2</sup>. Moreover, if the eigenvalues of a matrix  $\mathbf{A}$  are  $\lambda_+$  and  $\lambda_-$ , then the eigenvalues of  $\mathbf{A}^N$  are  $\lambda_+^N$  and  $\lambda_-^N$ .

The eigenvalues of  $\mathbf{T}$  can be determined by solving

$$\left| \begin{pmatrix} T_{1,1} - \lambda & T_{1,-1} \\ T_{-1,1} & T_{-1,-1} - \lambda \end{pmatrix} \right| = 0, \quad (7.25)$$

where  $|\mathbf{A}|$  denotes the determinant of matrix  $\mathbf{A}$ . Hence,

$$\begin{aligned} 0 &= (T_{1,1} - \lambda)(T_{-1,-1} - \lambda) - T_{1,-1}T_{-1,1}; \\ &= \lambda^2 - \lambda(T_{1,1} + T_{-1,-1}) + T_{1,1}T_{-1,-1} - T_{1,-1}T_{-1,1}; \\ &= \lambda^2 - \lambda(e^{\beta(J+H)} + T_{-1,-1}) + T_{1,1}T_{-1,-1} - T_{1,-1}T_{-1,1}; \\ &= \lambda^2 - 2\lambda e^{\beta J} \cosh(\beta H) + 2 \sinh(2\beta J), \end{aligned} \quad (7.26)$$

which is just a quadratic equation with solutions

$$\lambda_{\pm} = e^{\beta J} \cosh(\beta H) \pm (e^{-2\beta J} + e^{2\beta J} \sinh^2(\beta H))^{1/2}. \quad (7.27)$$

The full free energy per spin is then given by

$$\begin{aligned} \frac{\beta F(\beta, H)}{N} &= -\frac{1}{N} \log(\lambda_+^N + \lambda_-^N); \\ &= -\frac{1}{N} \left( \log \left( \frac{\lambda_+^N + \lambda_-^N}{\lambda_+^N} \right) + \log \lambda_+^N \right); \\ &= -\frac{1}{N} \left( \log \left( 1 + \left( \frac{\lambda_-}{\lambda_+} \right)^N \right) + \log \lambda_+^N \right). \end{aligned} \quad (7.28)$$

<sup>2</sup>In fact, it is always the sum of the elements on the diagonal, but this sum is invariant under rotations, which is what the orthogonalizing matrices that put  $\mathbf{A}$  into its diagonal form represent.

However, from Eq. (7.27), we have that  $\lambda_+ > \lambda_-$  always. Therefore, in the limit of large  $N$ ,  $(\lambda_-/\lambda_+)^N$  goes to zero and the expression for the reduced free energy per particle in the thermodynamic limit reads

$$\frac{\beta F}{N} = -\log \lambda_+. \quad (7.29)$$

Filling in  $\lambda_+$  and simplifying, we obtain

$$\beta F(\beta, H) = -\beta N J - N \log \left( \cosh(\beta H) + (e^{-4\beta J} + \sinh^2(\beta H))^{1/2} \right). \quad (7.30)$$

Once we have the free energy, we can calculate the other thermodynamic properties of the system. For example, the magnetization is given by

$$M(\beta, H) = - \left( \frac{\partial F}{\partial H} \right)_T = \frac{N \sinh(\beta H)}{(e^{-4\beta J} + \sinh^2(\beta H))^{1/2}}. \quad (7.31)$$

Note that the free energy in Eq. (7.30) indeed reduces to Eq. (7.8) in the zero-field limit. The same limit is not useful for the magnetization.

## 7.6 Exercises

### Q51. Gas on a Lattice

Consider a simplified model for a gas. Assume that the gas consists of atoms which sit at lattice sites (the lattice has  $M$  sites and there are  $N \leq M$  particles). Furthermore, assume that each lattice site can have at most a single gas particle. Neighboring particles interact with energy  $\epsilon$  according to the following Hamiltonian:

$$\mathcal{H} = \frac{\epsilon}{2} \sum_{i=1}^M \sum_j' n_i n_j, \quad (7.32)$$

where  $n_i$  is 1 if there is a single particle on site  $i$  or 0 if there is no particle. Note that the sum is over the number of sites  $M$ , which is a bit strange. The number of particles  $N$  is the relevant parameter for a Hamiltonian, so naively one would expect a Hamiltonian that depends on the position of the  $N$  particles. Hint: Does it matter if you sum over the number of (occupied) sites instead?

- Write the grand canonical partition function for the lattice gas model in one dimension. Note: You should not try and evaluate this, but just write down the expression.
- Using the substitution  $S_j = 2n_j - 1$ , show that this is equivalent to the canonical partition function for the Ising model with a field.
- You have seen that there is a mapping between the canonical Ising model and the grand-canonical lattice gas. Discuss in a *few* words what having a continuous phase transition in the 2D Ising model implies for the transition in the lattice gas. Reference your understanding of a general gas-liquid phase diagram to see where this mapping may be most useful.

This exercise is a setup toward the concept of universality as we will discuss in Chapter 12.

### Q52. Transfer Matrix for a Spin-1 Model

Consider a 1D system of spins  $S_i$  which can have values  $-1, 0, 1$ . Assume that the spins interact via the Hamiltonian

$$\mathcal{H} = -K \sum_i S_i S_{i+1}, \quad (7.33)$$

where  $K$  is the coupling constant and assume  $K > 0$ .

- What is the transfer matrix for this problem?
- What are the eigenvalues? Using Mathematica is probably wise.
- Plot the eigenvalues using Mathematica. Which is the largest eigenvalue? Note that regardless of  $K$ , it is always the same eigenvalue which is largest.
- What is the partition function in the thermodynamic limit?
- What is the resulting free energy?

### Q53. Ising Model with Nearest-Neighbor and Next-Nearest-Neighbor Interactions

The zero-field Ising model with nearest and next-nearest neighbor interactions can be written

$$\mathcal{H} = -J_{nn} \sum_{i=1}^{N-1} S_i S_{i+1} - J_{nnn} \sum_{i=1}^{N-2} S_i S_{i+2}. \quad (7.34)$$

The partition function for this system can be shown to be

$$\frac{1}{N} \log Z \propto \log \left[ e^{\beta J_{nnn}} \cosh(\beta J_{nn}) + \{ e^{-2\beta J_{nnn}} + e^{2\beta J_{nnn}} \sinh^2(\beta J_{nn}) \}^{1/2} \right]. \quad (7.35)$$

- (a) Write down the free energy per particle.  
 (b) Show that

$$\langle S_i S_{i+1} \rangle = \frac{\sinh(\beta J_{nn})}{[\exp(-4\beta J_{nnn}) + \sinh^2(\beta J_{nn})]^{1/2}}. \quad (7.36)$$

- (c) Show that  $\langle S_i S_{i+2} \rangle =$

$$1 - \frac{2 \exp(-4\beta J_{nnn})}{[\exp(-4\beta J_{nnn}) + \sinh^2(\beta J_{nn})]^{1/2} [\cosh(\beta J_{nn}) + (\exp(-4\beta J_{nnn}) + \sinh^2(\beta J_{nn}))^{1/2}]}. \quad (7.37)$$

- (d) What are  $\langle S_i S_{i+1} \rangle$  and  $\langle S_i S_{i+2} \rangle$  in the limit as  $J_{nnn} \rightarrow 0$ .  
 (e) What are  $\langle S_i S_{i+1} \rangle$  and  $\langle S_i S_{i+2} \rangle$  in the limit as  $J_{nn} \rightarrow 0$ .

#### Q54. Random Mixing and the Ising Model

Consider the Ising model for a ferromagnet with an external field  $H$  given by

$$\mathcal{H} = -\frac{J}{2} \sum_i \sum_j' S_i S_j - H \sum_i S_i \quad (7.38)$$

where  $H > 0$ . Define the number of “up” spins as  $N_+$  and the number of “down” spins as  $N_-$ . Then the total number of spins in this system is given by  $N = N_+ + N_-$ . Furthermore, define the number of pairs of neighboring spins with both spins up to be  $N_{++}$ , one up and one down to be  $N_{+-}$ , and both down to be  $N_{--}$ . Finally, assume *periodic boundary conditions*, that is to say, that the last spin in the chain (in any direction) is paired with the first spin in the chain. Hence, if the system is one dimensional, and there are three spins in the chain, then there are also three spin pairs.

- (a) Find  $a$ ,  $b$ ,  $c$ , and  $d$  such that

$$zN_+ = aN_{++} + bN_{+-}; \quad (7.39)$$

$$zN_- = cN_{--} + dN_{+-}, \quad (7.40)$$

where  $z$  is the number of neighbors of each lattice site. For simplicity, assume that in 2D we have a square lattice where each spin has 4 neighbors, and in 3D we have a cubic lattice, where each spin has 6 neighbors. (In 1D, each spin has two neighbors). Note that a single spin can be part of multiple pairs and that  $a$ ,  $b$ ,  $c$ , and  $d$  are constants and *not* functions of  $z$ .

- (b) Show that the Hamiltonian, for a fixed number of spins  $N$ , can be rewritten in terms of  $N_+$  and  $N_{++}$  as

$$\mathcal{H} = -J \left( \frac{1}{2} zN - 2zN_+ + 4N_{++} \right) - H(2N_+ - N). \quad (7.41)$$

- (c) In the random mixing approximation, we assume that the probability of finding a spin up is given simply by  $p = \frac{1+L}{2}$ , and the probability of finding a spin down is  $q = \frac{1-L}{2}$ . Show that the Hamiltonian (within this approximation) can then be written

$$\mathcal{H} = -\frac{1}{2} J L^2 zN - H L N, \quad (7.42)$$

- (d) Within the above approximation, the partition function of the system becomes

$$Z(\beta) = \sum_L g(L) e^{\beta N (\frac{1}{2} z J L^2 + H L)}, \quad (7.43)$$

where  $g(L)$  is the multiplicity factor associated with a particular value of  $L$  and is given by  $g(L) = N! / ((Np)!(Nq)!)$ . Explain why this is the multiplicity.

- (e) Show that the value of  $L$  that maximizes the summand in Eq. (7.43), is given by  $L = L^*$  with  $L^*$  given by

$$\frac{1}{2} \log \left( \frac{1 + L^*}{1 - L^*} \right) = \beta (z J L^* + H). \quad (7.44)$$

Hint: You will need to use Stirling's approximation.

- (f) Approximating the partition function by its value at  $L^*$ , determine the free energy and the internal energy, and show that the entropy takes the value

$$S(H, \beta) = -N k_B (p^* \log p^* + q^* \log q^*) = -N k_B (p^* \log p^* + (1 - p^*) \log(1 - p^*)), \quad (7.45)$$

where  $p^* = p(L^*)$  and  $q^* = q(L^*)$ .

- (g) Explain how this is equivalent to a mean-field approximation, see Chapter 8 for additional details on this approximation.

#### Q55. Infinite-Range Ising Model

The Ising model that we have examined so far always has *nearest-neighbor* interactions. Here, we examine what happens when the interaction range becomes infinite. Specifically, consider an Ising model with infinite-range interactions such that each spin interacts equally strongly with all other spins. The Hamiltonian of this system is given by

$$\mathcal{H} = -c \sum_{i < j} S_i S_j - H \sum_i S_i, \quad (7.46)$$

where  $c$  measures the interaction strength. Let  $L = N^{-1} \sum_i S_i$ , and rewrite the Hamiltonian in terms of  $L$ . Show that in the limit of  $N \rightarrow \infty$  and  $c \rightarrow 0$ , with the limits taken such that  $Nc$  is kept constant, this gives the random mixing Hamiltonian from Exercise Q54 with  $Nc = Jz$ . Interpret this result.

# Chapter 8

## Mean-Field Theory

In this chapter, we cover mean-field theory. This is an approximative approach for describing systems with a known Hamiltonian, but for which an exact partition function is not available or cannot be readily derived. At its core, mean-field theory isolates a single object, for instance a single spin in the Ising model, and treats it exactly. However, this object's interactions with the rest of the system are treated 'on average'. In terms of the Ising model, this could, *e.g.*, be the single spin coupling to the average orientation of the spins in the rest of the system. In other words, the system described by an exact many-body partition function is approximated by ignoring correlations between the objects, which results in a one-body partition function that approximates the behavior in the real system. This will become more clear when we examine our first example.

### 8.1 Mean-Field Ising Model

The one- and two-dimensional Ising models can be solved exactly, but the three-dimensional Ising model has yet to be solved (and cannot be generally solved). In addition, as we already saw from the expressions for the 2D Ising model, the analytic expressions that one obtains may not be that insightful or analytically tractable. Nonetheless, we are still interested in the phase-transitions of the Ising model and we will use mean-field theory to make progress, see Fig. 8.1 for a cartoon of the procedure. Our one-body description focusses on a single spin, hence we expect the mean-field Hamiltonian to be of the form

$$\mathcal{H} = \sum_i H_{\text{eff}} S_i, \quad (8.1)$$

where  $H_{\text{eff}}$  is the average field acting on spin  $i$ .

An equivalent way of describing mean-field theory is simply to rewrite the Hamiltonian ignoring correlations between the "objects" we treat exactly. To see explicitly how this works, we write the spins  $i$  as

$$S_i = \langle S \rangle + \delta S_i, \quad (8.2)$$

where  $\langle S \rangle$  is the average spin of the system and  $\delta S_i$  is the difference between the spin  $S_i$  and the average. We can then rewrite  $S_i S_j$  in the following manner:

$$\begin{aligned} S_i S_j &= (\langle S \rangle + \delta S_i)(\langle S \rangle + \delta S_j), \\ &= \langle S \rangle^2 + \langle S \rangle (\delta S_i + \delta S_j) + \delta S_i \delta S_j. \end{aligned} \quad (8.3)$$

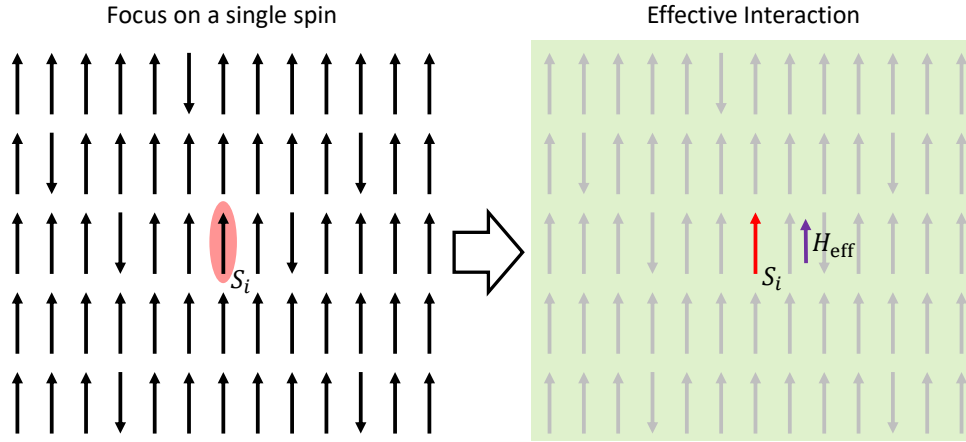


Figure 8.1: Cartoon showing a mean-field approximation for a two-dimensional Ising spin system. (left) We focus on a single spin  $S_i$  (red outline). (right) The rest of the system is treated as an effective field (green outline). When this process is repeated for all of the particles in the system, the resulting Hamiltonian will be of the form  $\mathcal{H} = H_{\text{eff}} \sum_i S_i$ .

The approximation in mean-field theory ignores correlations between spins; hence within this approximation  $S_i S_j$  becomes

$$S_i S_j \approx \langle S \rangle^2 + \langle S \rangle (\delta S_i + \delta S_j). \quad (8.4)$$

Finally, rewriting  $\delta S_i$  and  $\delta S_j$  in terms of  $S_i$  and  $S_j$ , see Eq. (8.2), we obtain

$$S_i S_j \approx \langle S \rangle (S_i + S_j) - \langle S \rangle^2. \quad (8.5)$$

Putting this back into the Hamiltonian for the Ising model we obtain

$$\begin{aligned} \mathcal{H} &= -\frac{J}{2} \sum_i \sum_j' S_i S_j; \\ &\approx -\frac{J}{2} \sum_i \sum_j' \left( \langle S \rangle (S_i + S_j) - \langle S \rangle^2 \right); \\ &\approx \frac{JNz}{2} \langle S \rangle^2 - \tilde{H} \sum_i S_i, \end{aligned} \quad (8.6)$$

where we have summed over the nearest neighbors  $j$ ;  $z$  is the number of nearest neighbors around a single spin and  $\tilde{H}$  is given by

$$\tilde{H} = Jz \langle S \rangle. \quad (8.7)$$

The average spin  $\langle S \rangle$  is the magnetization per particle, which we will denote  $m \equiv M/N = \langle S \rangle$ .

Now, we want to use Eq. (8.6) to determine whether or not there is a phase transition in the Ising model, and if it exists, determine the mean-field prediction for the transition temperature  $T_c$ . As discussed in the introduction to the Ising model, there is a phase transition if there exists a finite temperature where the magnetization becomes non-zero, *i.e.*, when the system orders. Hence, we now use the Hamiltonian

given in Eq. (8.6), *i.e.*, the mean-field approximation to the original Hamiltonian, to calculate the magnetization per particle (canonical ensemble):

$$\begin{aligned} m &= \langle S_i \rangle = \frac{\sum_{S_1} \sum_{S_2} \cdots \sum_{S_N} S_i \exp(-\beta\mathcal{H})}{\sum_{S_1} \sum_{S_2} \cdots \sum_{S_N} \exp(-\beta\mathcal{H})}; \\ &= \tanh(\beta J z m). \end{aligned} \quad (8.8)$$

Equation (8.8) is called a *self-consistent equation*, since the magnetization (on the left-hand side) is a function of itself. While we cannot solve this expression analytically, we can solve it graphically.

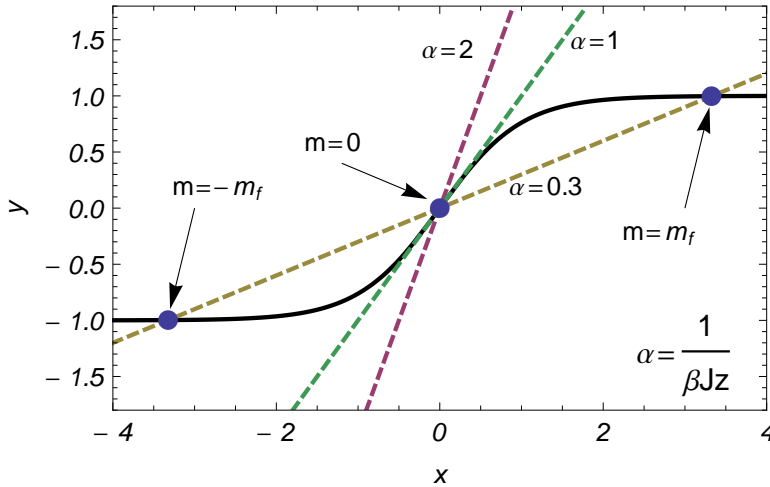


Figure 8.2: Graphical solution to the self-consistent mean field approximation to the Ising model as given by Eq. (8.8). The solid black line corresponds to  $y = \tanh(x)$  while the dashed lines correspond to  $y = x/(\beta J z) \equiv \alpha x$  for various choices of  $\beta J z$ . Note that for  $\alpha > 1$ , there is only the trivial solution  $m = 0$  while when  $\alpha < 1$  there are three possible solutions  $m = 0$ ,  $m = m_f$  and  $m = -m_f$ . The two solutions at  $m = \pm m_f$  are equivalent and simply represent states with the spins predominately pointing either “up” or “down”.

To solve Eq. (8.8) graphically, we first rewrite the expression. Letting  $x = \beta J z m$  we have

$$\frac{x}{\beta J z} = \tanh(x). \quad (8.9)$$

In Fig. 8.2 we plot  $y = \tanh(x)$  as well as  $y = x/(\beta J z)$ , for various choices of  $\beta J z$ ; the crossings of the two curves indicate solutions to Eq. (8.8). We see that for small  $\beta J z$  (the fraction is larger than 1), there is only a single solution corresponding to  $m = 0$ . However, as we lower the temperature, *i.e.*, increase  $\beta$  and thereby decrease the fraction, eventually there arise three possible solutions:  $m = 0$ ,  $m = m_f$  and  $m = -m_f$ . Here, the value of  $m_f$  is determined by the graphical solution (or numerically). The solutions  $m = m_f$  and  $m = -m_f$  are equivalent solutions and are simply a result of the “up/down” symmetry of the zero-field Ising model. This graphical solution, however, still leaves us with a dilemma: which of the two solutions ( $m = 0$  or  $|m| = |m_f|$ ) should we use when the coupling is large ( $\beta J z > 1$ )? If the answer is  $m = 0$  then we would conclude that there is no disorder to order transition in the Ising model. However, if there exists a temperature for which we go from  $m = 0$  to  $m = m_f$  then we could conclude that mean-field theory predicts a phase transition in the Ising model. In order to answer this question, we have to determine which solution corresponds to the minimum in the free energy.

The free energy per spin is obtained using the much reduced expression for the mean-field partition sum

$$\begin{aligned} f &= -\frac{1}{\beta} \log \left( \sum_{S_i=\pm 1} e^{\beta J z m S_i - (1/2)\beta J z m^2} \right); \\ &= -\frac{1}{\beta} \log \left( e^{\beta J z m - (1/2)\beta J z m^2} + e^{-\beta J z m - (1/2)\beta J z m^2} \right). \end{aligned} \quad (8.10)$$

The free-energy difference between  $m = 0$  and  $m = m_f$  is given by

$$\begin{aligned} \Delta f &= \int_0^{m_f} dm \frac{\partial f}{\partial m}; \\ &= \frac{1}{\beta} \int_0^{m_f} dm (\beta J z m - \beta J z \tanh(\beta J z m)). \end{aligned} \quad (8.11)$$

Using our previous change of variable  $x = \beta J z m$ , we obtain

$$\begin{aligned} \Delta f &= \frac{1}{\beta} \int_0^{m_f/\beta J z} dx \left( \frac{1}{\beta J z} x - \tanh(x) \right); \\ &= \frac{1}{\beta} (A_{\text{linear}} - A_{\text{tanh}}), \end{aligned} \quad (8.12)$$

where  $A_{\text{linear}}$  is the area under the dashed line in Fig. 8.2 from the  $m = 0$  point to the  $m = m_f$  point while  $A_{\text{tanh}}$  is the area under the tanh-function for the same range in  $m$ . For all cases where there is more than a single solution to Eq. (8.8), the area under the linear line is less than under the tanh-function. Consequently,  $A_{\text{linear}} < A_{\text{tanh}}$  and  $\Delta f < 0$  for this range in  $\beta$ , and the solution corresponding to  $m = m_f$  has a lower free energy. We conclude that mean-field theory predicts the system to be ordered for all temperatures where the graphical solution in Fig. 8.2 finds more than one solution. The transition temperature  $T_c$  is the temperature associated with the transition between a single solution and three solutions to Eq. (8.8). This transition occurs when  $\beta J z = 1$ , so that the transition temperature predicted by mean-field theory is  $k_B T_c = J z$ . For the 2D square-lattice Ising model, we have that  $z = 4$ , which means that the mean-field approximation overestimates the critical temperature, which according to Onsager is given by  $T_c \approx 2.27 J/k_B$ . This overestimate makes sense, as correlations between spins, which have been ignored in mean-field theory, should become relevant when the system becomes ordered. In the coming chapters, we will see just how important they are.

One should note that we have made no reference to the dimension of the system in the entire mean-field treatment of the Ising model. Hence, our prediction of a phase transition is independent of dimension. However, as we saw in Chapter 7, an exact treatment of the Ising model finds *no* phase transition in the one-dimensional Ising model, hence the mean-field treatment fails to capture the 1D behavior. It will be left as an exercise to explain why this is the case.

## 8.2 Cell Theory for a Hard-Sphere Crystal

The study of the free energy of crystalline phases is another example where mean-field theory can be applied. The specific form of mean-field theory that we consider in this section is referred to as *cell theory*. The naming will become clear as we cover the example of a hard-sphere crystal. Hard spheres are one of the simplest model systems that exhibits a liquid to crystal phase transition (first order), and they are called ‘hard’ spheres, because their interaction potential is given by

$$\beta U = \begin{cases} 0 & r > \sigma \\ \infty & r < \sigma \end{cases}, \quad (8.13)$$

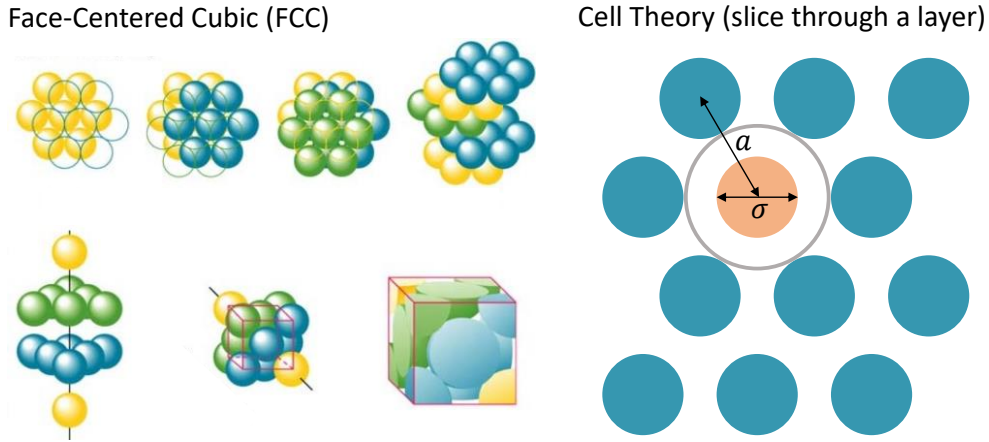


Figure 8.3: Cell theory for a the face-centered cubic (FCC) crystal formed by hard spheres, adapted from original by the University of Washington. (left) Representation of the FCC crystal showing several cut planes and 3D dimensional views to indicate the stacking of the spheres and the cubic nature of the unit cell. (right) Two-dimensional hexagonal arrangement of spheres in a single layer from a FCC crystal. In our mean-field approximation we calculate the partition function for the light colored disk assuming that the other particles all remain at their lattice sites. Note that  $\sigma$  is the diameter of a sphere and  $a$  is the spacing between the centers of mass of nearest particles.

where  $r$  is the 3D distance between the particles and  $\sigma$  is the particle diameter.

The crystal phase which is stable for a hard sphere system can be shown to be a face centered cubic crystal, as depicted in the left-hand panel to Fig. 8.3. In this case, the object we treat exactly is a single hard sphere. We assume that the other spheres are located at their “ideal” lattice positions. Hence, we can write the partition function as a product of volumes, that is

$$Z_N = \prod_{i=1}^N \frac{V_i}{\Lambda^3} \quad (8.14)$$

where  $V_i$  is the free volume in which the center of mass particle  $i$  can move assuming all the other particles are frozen to their lattice sites. This is sketched in the right-hand panel to Fig. 8.3. The sphere of interest is thus confined to a single “cell” of the idealized crystal.

For a face centered cubic lattice, all nearest neighbors are a distance  $a$  from the target particle. We make the additional assumption that the center of mass can only move within a sphere of radius  $a - \sigma$ . In reality, the volume in which the center of mass can move is not exactly spherical, but as you can judge from Fig. 8.3, this is a fairly decent approximation. The free volume per particle is then given by

$$V_i = \frac{4\pi}{3} (a - \sigma)^3. \quad (8.15)$$

Using the above expression and the approximate partition function, we obtain the mean-field free energy

$$\begin{aligned} \beta F &= -\log(Z_N); \\ &= -N \log \left( \frac{4\pi}{3} \left( \frac{a - \sigma}{\Lambda} \right)^3 \right). \end{aligned} \quad (8.16)$$

We will now reduce this free-energy expression further by using scaling arguments. When all the spheres are touching, *i.e.*, when the system is in its *close-packed* arrangement, the number density is  $\sigma^3 \rho_{\text{cp}} = \sigma^3 N/V = \sqrt{2}$ , where  $N$  is the number of particles in a volume  $V/\sigma^3$ . The lattice spacing scales with the close-packed density as

$$a^3 \rho = \sigma^3 \rho_{\text{cp}}, \quad (8.17)$$

so that we can rewrite the free energy as

$$\beta F = -N \log \left( \frac{4\pi}{3} \left( \left( \frac{\rho_{\text{cp}}}{\rho} \right)^{1/3} - 1 \right)^3 \frac{\sigma^3}{\Lambda^3} \right). \quad (8.18)$$

From the free energy we can directly calculate the pressure:

$$\beta P \sigma^3 = -\beta \frac{\partial F}{\partial V}, \quad (8.19)$$

which gives us the mean-field equation of state. We will explore this concept further in the exercises.

## 8.3 Exercises

### Q56. Binary Lattice Gas

Consider a binary gas of particles (labeled  $A$  and  $B$ ) at temperature  $T$  where the particles are restricted to moving on a simple cubic lattice. Note that in a simple cubic lattice, each lattice site has 6 neighbors. Assume that the lattice has  $M$  lattice sites. Assume that the density of particles of type  $A$  is  $\rho_A$  and that the density of particles of type  $B$  is  $\rho_B$ . Also assume that the particles do not interact with any of the other particles of the same species at all, but if two particles of different species are on the same site or on adjacent sites (horizontally or vertically), they repel, leading to an interaction energy  $\epsilon$ . The total number of particles is  $N = N_A + N_B$ , with  $N_i$  the number of particles of type  $i$ . In this exercise, we will explore the phase transitions for this system using a mean-field approximation, and as such ignore all correlations between the particle positions.

- Given a homogeneous density  $\rho_B$  of particles of species  $B$ , what is the average energy of a single particle of species  $A$ ? And what is the average energy  $\langle E \rangle$  of the entire system?
- Within such a simple mean-field approximation, what is the canonical partition function of the full system?
- Define the composition  $x$  of the system is the fraction of particles that belongs to species  $A$ :  $x = N_A/(N_A + N_B)$ . Show that the Helmholtz free energy can be written as

$$\frac{\beta F(N, x, V, T)}{N} = x \log x + (1 - x) \log(1 - x) + Kx(1 - x) + \log V_0 \rho - 1, \quad (8.20)$$

where  $\rho = (N_A + N_B)/V$  is the total density and  $V_0$  is a unit of lattice volume, and  $K$  is a function of  $\beta$ ,  $\epsilon$  and  $\rho$ .

Now consider a large system containing this binary gas at composition  $x = 1/2$ , so  $N_A = N_B = N/2$ . We divide this system into two parts, marked 1 and 2. Both subsystems have the same volume  $V_1 = V_2 = V/2$  and contain the same number of particles  $N_1 = N_2 = N/2$ , so they have the same total density  $\rho$ . However, the two subsystems can have different compositions  $x_1$  and  $x_2$ , and therefore also different numbers of particles of each species ( $N_{A,1}$  and  $N_{A,2}$  can be different from  $N_{B,1}$  and  $N_{B,2}$ ). The total free energy can then be written as a function of either  $x_1$  or  $x_2$ . In terms of  $x_1$ , the total free energy is given by

$$f(x_1) = \frac{\beta F}{N} = x_1 \log x_1 + (1 - x_1) \log(1 - x_1) + Kx_1(1 - x_1) + \log V_0 \rho - 1. \quad (8.21)$$

- Show that  $x_1 = 1/2$  is always an extremum of this free energy. Explain what this means.

Expanding the free energy around  $x_1 = 1/2$  up to fourth order gives the following:

$$f(x_1) \simeq C + (2 - K) \left( x_1 - \frac{1}{2} \right)^2 + \frac{4}{3} \left( x_1 - \frac{1}{2} \right)^4. \quad (8.22)$$

Here,  $C$  is independent of  $x_1$ . All higher order terms in the expansion are positive even powers of  $(x_1 - 1/2)$ . We can see this as a Landau expansion of the order parameter  $m = x_1 - 1/2$ , we will discuss these in detail in Chapter 9.

- Sketch the Landau free energy for this system for (i)  $T > T_c$ , (ii)  $T = T_c$ , and (iii)  $T < T_c$ , where  $T_c$  is the critical temperature.

- (f) Sketch the order parameter  $m$  as a function of temperature  $T$ , associated with the global minimum of the Landau free energy.
- (g) What type of phase transition occurs in this system? Explain.
- (h) What is the value of  $K$  associated with the phase transition?
- (i) What does the system look like for  $T > T_c$ ? What does the system look like for  $T < T_c$ ? That is, describe the phases associated with the phase transition.
- (j) In this exercise we used an approximate method to determine the phase behavior of this system. Describe one way in which we could improve this approximation. There are many possible correct answers to this question.

### Q57. Improved Mean-Field Theory for the Ising Model

By explicitly taking into account nearest neighbors, we can make a better mean-field approximation for the Ising model. In this approximation, instead of zooming in on a single spin, we consider a cluster of spins consisting of a central spin  $s_0$  and its  $q$  nearest neighbors. The rest of the system is approximated by an effective field with field strength  $B_{\text{eff}}$ . We assume that there is no external field. Since  $s_0$  only interacts with its nearest neighbors, it does not couple to  $B_{\text{eff}}$ . Thus, the effective Hamiltonian for the cluster is given by:

$$\mathcal{H}_c = -(Js_0 + B_{\text{eff}}) \sum_{j=1}^q s_j. \quad (8.23)$$

- (a) Explicitly calculate the partition function  $Z_c$  for the cluster in one and two dimensions ( $q = 2, 4$ ). Show that both cases can be expressed as

$$Z_c = 2^q \cosh^q(j+b) + 2^q \cosh^q(-j+b). \quad (8.24)$$

Note that  $b = \beta B_{\text{eff}}$  and  $j = \beta J$ .

- (b) Calculate  $\langle s_0 \rangle$  and  $\langle s_1 \rangle$ , and show that:

$$\langle s_0 \rangle = \frac{2^q}{Z_c} (\cosh^q(j+b) - \cosh^q(-j+b)); \quad (8.25)$$

$$\langle s_1 \rangle = \frac{2^q}{Z_c} (\sinh(j+b) \cosh^{q-1}(j+b) + \sinh(-j+b) \cosh^{q-1}(-j+b)). \quad (8.26)$$

- (c) Rewrite  $\langle s_1 \rangle$  to show that

$$\langle s_1 \rangle = \langle s_0 \rangle + \frac{2^q e^{-j}}{Z_c} (\cosh^{q-1}(-j+b)e^b - \cosh^{q-1}(j+b)e^{-b}). \quad (8.27)$$

Hint:  $\sinh(x) = \cosh(x) - \exp(-x) = -\cosh(x) + \exp(x)$ .

- (d) Since the system is translation invariant, we know that  $\langle s_0 \rangle = \langle s_1 \rangle$ . The only freedom we have to satisfy this equation is in the value of  $B_{\text{eff}}$ . Show that

$$\frac{\cosh^{q-1}(\beta(J + B_{\text{eff}}))}{\cosh^{q-1}(\beta(J - B_{\text{eff}}))} = \exp(2\beta B_{\text{eff}}). \quad (8.28)$$

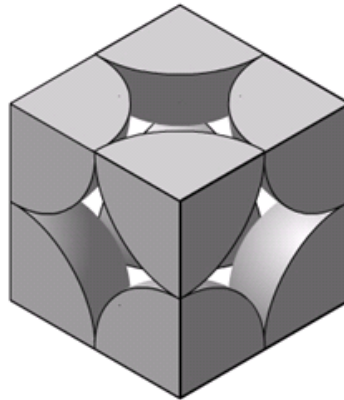
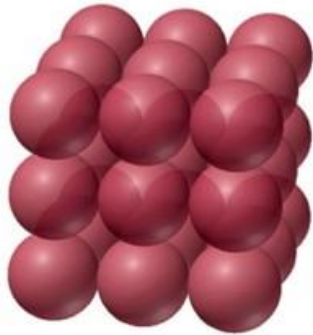
- (e) Note that  $B_{\text{eff}} = 0$  is always a solution of the above equation. What are the limits of the left-hand and right-hand sides of this equation for  $B_{\text{eff}} \rightarrow \infty$ ? Argue that if the slope of the left-hand side (as a function of  $B_{\text{eff}}$ ) is greater than  $2\beta$  at  $B_{\text{eff}} = 0$ , there will be another solution at finite  $B_{\text{eff}}$ .

- (f) Set the slope of the left-hand side to  $2\beta$  with  $B_{\text{eff}} = 0$ , and calculate  $k_B T_c / J$  for one and two dimensions in this case. Explain why this can be used to determine the critical temperature  $T_c$ . Are the results better than for the mean-field approximation including only a single spin?

**Q58. Hard Sphere Crystals: FCC versus Simple-Cubic Ordering**

Some atomic and colloidal particles can be modelled by hard spheres. Hard spheres have a simple interaction potential: the energy of the system is zero when there are no overlaps of the spheres, and infinity when there is an overlap. At high densities and low temperatures, atomic and colloidal systems form crystals. Here we explore which crystal structure is most stable for hard spheres. Two of the possible crystalline phases include simple cubic and face-centered cubic, see Fig. 8.4. Using cell theory, we can approximate the free energy of these different crystals.

simple cubic:



face-centered cubic:

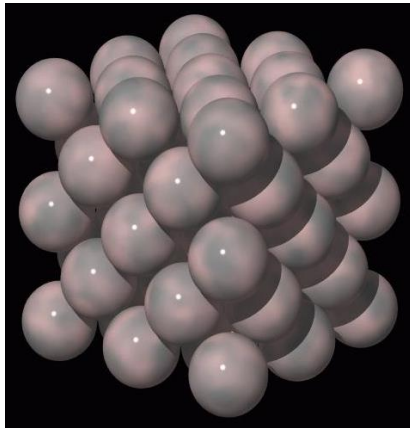


Figure 8.4: Simple-cubic and face-centered-cubic lattice (left) and their respective unit cells (right).

- (a) What is the highest packing fraction possible for hard spheres organized on an FCC lattice? a simple cubic lattice? Note that the packing fraction is the amount of space occupied by the spheres. Assume that the spheres have diameter  $\sigma$ .
- (b) Use cell theory to determine the free energy of both an FCC and simple cubic lattice of hard spheres as a function of the number density  $\rho\sigma^3 = N/V$ .

- (c) Show that within cell theory the hard sphere FCC crystal has a lower free energy than the hard sphere simple cubic crystal. Note: You may want to plot the free energies using Mathematica.

**Q59. Vacancies in Crystals of Hard Disks**

Some two-dimensional (2D) colloidal systems may be modelled as hard disks with diameter  $\sigma$ . These have a simple overlap potential: the energy of the system is zero, when there are no overlaps, and infinity, when there is an overlap. The area packing fraction  $\eta$  of a system is the ratio of area occupied by disks to the total area  $A$ , *i.e.*,  $\eta = \pi\sigma^2 N/(4A)$ , with  $N$  the number of disks. In 2D cell theory, the partition function of the system can be written as  $Z_N = \prod_{i=1}^N (A_i/\Lambda^2)$ , where  $A_i$  is the free area accessible to a single particle and  $\Lambda$  is the thermal wavelength.

- (a) Show that the highest area packing fraction ( $\eta_{cp}$ ) possible for hard disks on a hexagonal lattice is given by  $\pi/(2\sqrt{3})$ . And that when the disks are organized on a simple square lattice it is  $\pi/4$ .
- (b) Explain how to use a mean-field approximation to compute  $A_i$  as a function of  $\eta$ ; you may want to make a sketch. You should arrive at  $A_i \approx \pi(a - \sigma)^2$  with  $a$  the lattice spacing. Does it matter whether you do this for a square or hexagonal crystal?
- (c) Show that within cell theory the hard-disk hexagonal crystal has a lower free energy than that of the simple-square crystal. Why is that expected?

Assume that the Helmholtz free energy of the perfect hexagonal crystal is given by  $F_{\text{perf}}(N = M, A, T)$ , where  $M$  is the number of lattice sites and  $T$  is the temperature. Note that in a perfect crystal, the number of lattice sites  $M$ , is the same as the number of particles  $N$ . Additionally, assume that the Helmholtz free energy associated with changing a specific particle into a vacancy, *i.e.*, removing that specific particle, is given by  $f_{\text{vac}}(\rho_M, T)$ , where  $\rho_M = M/A$ . Define  $N_{\text{vac}}$  as the number of vacancies, such that  $M = N + N_{\text{vac}}$  and  $N_{\text{vac}} \ll M, N$ . Finally, we assume that the vacancies do not interact with each other and that they are randomly distributed throughout the crystal.

- (d) Argue that  $Z_{\text{vac}} = \binom{M}{N_{\text{vac}}} \exp(-\beta N_{\text{vac}} f_{\text{vac}})$  and provide the Helmholtz free energy of the system with vacancies.

Lastly, assume that the equation of state is not affected by the presence of vacancies. In other words, the pressure  $P(M, N, A, T)$  is not dependent on  $N_{\text{vac}}$ . The Gibbs free energy is then given by

$$\beta G(M, N, P, T) = \beta N \mu_{\text{perf}}(P, T) + \beta(M - N) \mu_{\text{vac}}(P, T) + N \log \frac{N}{M} + (M - N) \log \frac{M - N}{M},$$

where  $\mu_{\text{perf}}(P, T)$  is the chemical potential of the perfect crystal and  $\mu_{\text{vac}} = \mu_{\text{perf}}(P, T) + \tilde{f}_{\text{vac}}(P, T)$ . Here,  $\tilde{f}_{\text{vac}}(P, T)$  equal to  $f_{\text{vac}}(\rho_M, T)$ , evaluated at  $\rho_M$  corresponding to  $P$  in a perfect crystal.

- (e) Demonstrate that  $\beta G(M, N, P, T)$  is as above and indicate where the assumptions are used.
- (f) When  $\mu_{\text{vac}}$  is approximately  $9k_B T$  (close to the melting point of the crystal), show that the equilibrium vacancy concentration is approximately  $\langle (M - N)/M \rangle = 1 \cdot 10^{-4}$ .

**Q60. Rotating-Spin System**

We consider a system that consists of unit-length spin vectors  $\mathbf{s}_i$ , which are free to rotate in the  $xy$ -plane. That is, unlike the Ising model for which the spins can point up or down along the

$y$ -axis, the spins in this model can be described by an angle  $\theta \in [-\pi, \pi]$  with respect to the  $x$ -axis. This angle is defined by  $\cos \theta_i = \mathbf{s}_i \cdot \hat{\mathbf{x}}$  with  $\hat{\mathbf{x}}$  the unit vector pointing along the  $x$ -axis and  $\cdot$  the inner product. The Hamiltonian for this system can be written as

$$\mathcal{H} = -\frac{J}{2} \sum_i \sum_j' \mathbf{s}_i \cdot \mathbf{s}_j - \sum_i \mathbf{h} \cdot \mathbf{s}_i = -\frac{J}{2} \sum_i \sum_j' \cos(\theta_i - \theta_j) - h \sum_i \cos \theta_i, \quad (8.29)$$

where  $\sum_j'$  indicates a sum over nearest neighbors, and  $\mathbf{h} \equiv h\hat{\mathbf{x}}$  is an external field pointing along the  $x$ -axis. For the first few subproblems, we will assume  $h = 0$  and that the sites are located on a one-dimensional (1D) chain.

- Assume a chain of  $N$  sites, which is not periodic. Sketch a few microstates.
- Demonstrate that the expression for the canonical partition sum  $Z(N, T)$  for this open-ended 1D chain —  $N$  is the total number of sites and  $T$  the temperature — can be written as

$$Z(N, T) = 2\pi \left( \int_{-\pi}^{\pi} d\theta \exp(\beta J \cos \theta) \right)^{N-1} \equiv (2\pi)^N I_0(\beta J)^{N-1}, \quad (8.30)$$

with  $\beta = 1/(k_B T)$ , where  $k_B$  is Boltzmann's constant,  $\theta$  is an auxiliary integration variable, and  $I_0$  is used for notational convenience (it is the modified Bessel function of the first kind).

- Compute the free energy per site  $f = \beta F/N$  in the thermodynamic limit. Compute the high-temperature limit of  $f$  and explain in a few words why your results make sense.
- Now assume a closed 1D chain, *i.e.*, periodic boundary conditions. Write down the transfer matrix belonging to angles  $\theta$  and  $\theta'$  for this problem. How is  $f$  (definition in part c) related to the eigenvalues of this matrix? Do not compute these eigenvalues!

We now consider the same rotating-spin model on a two-dimension (2D) square lattice of  $N$  spins. Assume  $h \neq 0$  from here on. Define  $z_i = \exp(\iota\theta_i)$  with  $i$  the index and  $\iota$  the imaginary unit. Let  $z_i = w + \delta z_i$  with  $w \equiv \langle z_i \rangle$  the statistical average.

- Write down the complex conjugate relations for  $z_i$  using the standard  $*$  notation. Show that  $\cos(\theta_i - \theta_j) = \text{Re}(z_i^* z_j)$ , with  $\text{Re}$  indicating the real part.
- Use the result from (e) to expand the Hamiltonian in Eq. (8.29) up to  $\mathcal{O}(\delta z^2)$ , *i.e.*, neglecting terms such as  $\delta z_i \delta z_j$ . Show that the mean-field Hamiltonian is given by:

$$\mathcal{H}^{\text{MF}} = 2JN|w|^2 - 2J \sum_i \text{Re}(w^* z_i + w z_i^*) - \frac{h}{2} \sum_i (z_i^* + z_i). \quad (8.31)$$

- Explain in a few words why the above free energy should be minimized when  $w$  points in the same direction as the external field, *i.e.*,  $w \in \mathbb{R}$  and, assuming  $h > 0$ ,  $w > 0$ . Show that this leads to

$$\mathcal{H}_{\text{min}}^{\text{MF}} = 2JNw^2 - (h + 4Jw) \sum_i \cos \theta_i, \quad (8.32)$$

The corresponding mean-field free energy per site is given by

$$f_{\text{min}}^{\text{MF}} = 2\beta Jw^2 - \log(2\pi I_0(\beta(h + 4Jw))). \quad (8.33)$$

Minimizing Eq. (8.33) leads to  $w = I_1(\beta(h + 4Jw))/I_0(\beta(h + 4Jw))$ , with  $I_1$  the derivative with respect to the argument of  $I_0$ .

- (h) What kind of equation is this for  $w$  and what role does  $w$  serve in describing the phase transition? Explain in a few words.
- (i) Based on the above analysis, do you think the 2D rotating-spin model has a phase transition? Explain why using only a few words.

### Q61. Variational Mean-Field Theory

In this exercise, we will cover the variational approach to the development of mean-field theory. This makes more rigorous the formalism covered in the main text. The derivation holds both in the discrete and continuous case. We will therefore use the trace ( $\text{Tr}$ ) notation in this exercise, which simply signifies the sum or integral over all possible states. So for instance the canonical partition function (or sum) is given by  $Z = \text{Tr} \exp(-\beta\mathcal{H})$ , where  $\beta$  is the inverse thermal energy and  $\mathcal{H}$  is the Hamiltonian describing the system.

To start off, we will consider a result from probability theory. Let  $x \in \mathbb{R}$  be a random variable with associated probability density function  $P(x)$ . That is  $\int_{\mathbb{R}} dx P(x) = 1$ . Let  $\langle x \rangle = \int_{\mathbb{R}} dx xP(x)$  be the first moment of the distribution. Then we have that  $\langle e^x \rangle \geq e^{\langle x \rangle}$ . This is a specific application of Jensen's inequality.

- (a) Show that the above exponential inequality holds. Hint use the result  $e^x \geq 1+x$  for all  $x \in \mathbb{R}$  and start from  $e^{x-\langle x \rangle}$ .

Now consider any classical probability distribution  $\rho$  satisfying  $\text{Tr}\rho = 1$ .

- (b) Use the definition of the partition function in terms of the Helmholtz free energy  $F$  to show that  $F \leq \text{Tr}\rho\mathcal{H} + k_{\text{B}}T\text{Tr}\rho \log \rho$ . The first term on the left-hand side is simply the average of the Hamiltonian with respect to the distribution  $\rho$  and can also be written as  $\langle \mathcal{H} \rangle_{\rho}$ .
- (c) Give an interpretation to the second term on the right-hand side. The resulting expression is also known as the Bogliubov inequality.
- (d) What happens when we assume that  $\rho = \exp(-\beta\mathcal{H})/Z$ ?

The inequality gives a handle on how to approximate the free energy of a system of interest. A functional form with some free (unspecified) parameters is chosen to approximate  $\rho$ . The inequality is subsequently minimized with respect to the free parameters to obtain the optimal approximation. Mean-field theory is obtained by assuming a distribution  $\rho$  that can be factorized into a product of independent single particle distributions. That is, if  $\rho_i$  is the probability distribution belonging to the degrees of freedom of particle  $i$ , then the mean-field distribution reads

$$\rho = \sum_i \rho_i. \quad (8.34)$$

One route toward choosing an appropriate  $\rho_i$  requires the use of an order parameter, see Chapter 9 for more information. The other is to choose another non-interacting Hamiltonian  $\mathcal{H}_0$  and minimize with respect to it.

We will take the latter route for the Ising model

$$\mathcal{H} = -\frac{J}{2} \sum_{i=1}^N \sum_j' S_i S_j - H \sum_{i=1}^N S_i. \quad (8.35)$$

Let  $\mathcal{H}_0 = -h \sum_i S_i$  with  $h$  our free parameter. We have that the partition function for this Hamiltonian is  $Z_0 = 2^N \cosh^N(\beta h)$ .

- (e) Show that this implies  $\langle \mathcal{H} \rangle_0 = -N [z\beta J \langle S_i \rangle_0^2 + \beta H \langle S_i \rangle_0]$ , with  $z$  the number of nearest neighbors as before and the subscript 0 denoting the average with respect to the Boltzmann-based probability density coming from  $\mathcal{H}_0$ .
- (f) Recall the expression for  $\langle S_i \rangle_0$  and compute  $k_B T \text{Tr} \rho \log \rho$ .
- (g) Minimize the resulting right-hand side of the inequality with respect to  $h$  to obtain a familiar expression.



# Chapter 9

## Landau Theory

Thus far, we have discussed two different types of phase transitions, namely first-order phase transitions and continuous phase transitions. A first-order phase transition is characterized by a discontinuity in the first derivative of the free energy, with an  $n$ th-order ( $n > 1$  implies continuous) phase transition having a discontinuity in the  $n$ th derivative. First-order phase transition is special in a sense, as one of the discontinuities appears in the equation of state. This implies that such a phase transition can exhibit phase coexistence, see Chapter 6. Hence, one of the most fundamental problems associated with phase transitions is identifying whether it is first-order or continuous. Specifically, it would be extremely valuable if we were able to write down a simple theory that allows us to determine the order of the transition. Landau addressed this question with a mean-field theory in 1937, the result of which today is commonly referred to as Landau theory, which is the subject of this chapter.

### 9.1 Introduction

In Landau theory, we assume that a phase transition can be characterized by an *order parameter* that measures the degree of ordering in the system. For instance, if we were looking at the ferromagnetic transition of the Ising model, we would use the magnetization; for a system which displays a phase transition between a fluid and a phase separated liquid-gas mixture, the order parameter could be the density difference between the liquid and the gas:  $\rho_l - \rho_g$ . Each transition will have its own order parameter and there might be multiple order parameters that equivalently describe a single transition, *e.g.*, there are various ways to measure crystalline structure for a solid-to-solid transition. Frequently, the order parameter is chosen such that it is zero in the disordered phase and non-zero in the ordered phase. There are, however, cases where it is simpler to relax this condition.

Critical to the understanding of order parameters is that these are quantities that emerge by setting the state variables. However, be very careful, they are *not* the same as the state variables! This is readily seen when considering the magnetization in the Ising model, which results from picking a temperature (and coupling parameter). The difference becomes somewhat muddled when we consider, for instance, a density difference  $\Delta\rho$  between a gas and a liquid, as one would set  $N$ ,  $V$ , and  $T$  in a system that phase separates, *i.e.*, density and temperature. The distinction is that the density gap emerges  $\delta\rho$  by setting  $\rho$  and  $T$ ; this is not the same as the  $\rho$  you imposed. In addition, the gas-liquid transition is a bit unusual, as the density gap can only be defined *a posteriori*, knowing that the system phase separates by a first-order transition.

One of the main assumptions in Landau theory is that we can expand the relevant free energy of disordered phase in terms of the order parameter. We emphasize here that this is an assumption and it is most definitely not obvious that we *can* do this. In fact, near a critical point, such as we encountered for the Ising model in Chapter 7, the free energy cannot be written in this form. In Chapter 10 we will study a method, which can be used to study the behavior *at* and close to critical points. However, despite the evident shortcomings of such an expansion, the Landau expansion of the free energy turns out to be extremely useful in understanding phase transitions. Specifically, we write for the expansion

$$f(T, m) = f_o(T) + a(T)m + b(T)m^2 + c(T)m^3 + d(T)m^4 + \dots, \quad (9.1)$$

where  $a, b, c, d, \dots$  are the coefficients associated with the expansion and  $m$  is the order parameter. For a given system, the coefficients are chosen such that they respect the symmetry of the disordered phase. We will return to the concept of symmetry in last sections of this chapter, but it is this which lies at the heart of the usefulness of Landau theory.

Before continuing, let us examine Eq. (9.1) more closely. In this equation, we have not made any reference to the volume, strength of a magnetic field, *etc.* For simplicity, they have been intentionally left out of this expression, since the relevant variables depend on the system in question. However, we assume that all these variables are fixed such that we are looking at the free energy for a given *single* state point, *e.g.*, for a given temperature. The only variable — in the equation sense; not in the thermodynamic sense — left is the order parameter  $m$ . Hence, we are comparing the free energy of different possible phases at the *same* state point. For example, in the Ising model this means that we are comparing states with different levels of magnetization (disordered and ordered) for a given temperature, field, and coupling. Going back to what we know from thermodynamics, the stable phase will be the phase with the lowest free energy, which can be obtained by studying the behavior of  $f$  in Eq. (9.1) as a function of  $m$ .

From our definition of the order parameter, the disordered phase always occurs at  $m = 0$ . Thus, it follows that there must be a minimum in the free energy at  $m = 0$  for  $T > T_c$ , *i.e.*,  $\partial f / \partial m|_{m=0} = 0$ . Hence, the linear term in the expansion must be zero:  $a = 0$ . Furthermore, since  $m = 0$  corresponds to a stable phase for  $T > T_c$ , we must have  $f(T, m = 0)$  be a local minimum, *i.e.*,  $\partial^2 f / \partial m^2|_{m=0} > 0$  hence  $b > 0$  for  $T > T_c$ .

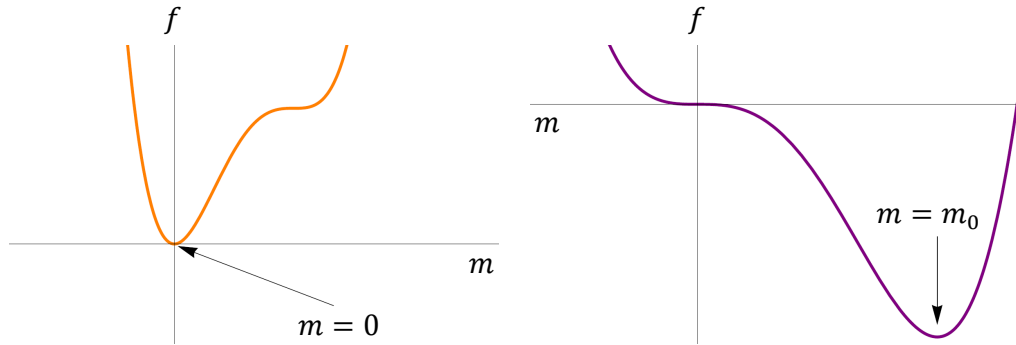


Figure 9.1: Examples of Landau free energies with a single minimum. (left) The minimum is located at  $m = 0$ , hence at the state point corresponding to this Landau free energy, we would predict the disordered phase to be stable. (right) The minimum is located at  $m = m_0 \neq 0$ , hence in this state point, the ordered phase is stable.

Now, let us consider some of the possibilities which may arise when we look at example expressions for the Landau free energy. In the left-hand panel to Fig. 9.1 we see a Landau free energy, for which there is a single minimum located at  $m = 0$ . Hence, the stable phase in this case will be the disordered phase. In the right-hand panel to Fig. 9.1, we have the opposite scenario, there is a single minimum, but in this case it is at  $m = m_0$ . This constitutes an example of a stable ordered phase.

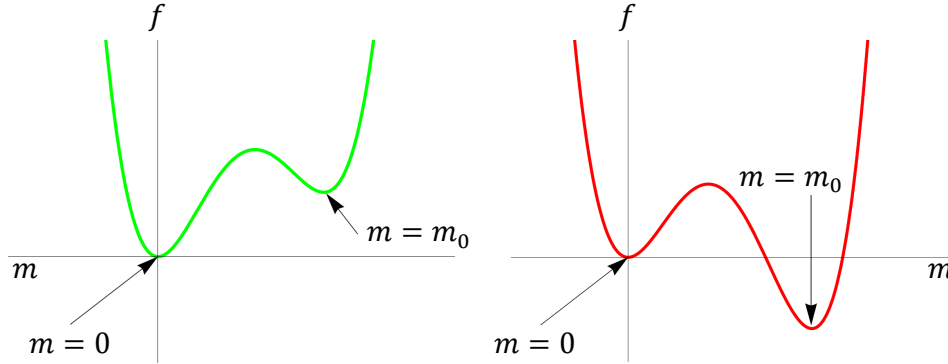


Figure 9.2: Examples of Landau free energies with two minima. (left) A state point for which the disordered phase  $m = 0$  is stable and the ordered phase  $m = m_0$  is metastable. (right) A state point with the opposite stability conditions.

However, the situation is not always this simple. Sometimes the Landau free energy has more than one minimum, such as in Fig. 9.2. In both cases, the stable phases are still easy to identify. In the left-hand panel, the disordered phase corresponds to the global minimum in the free energy, so that the disordered phase is stable. Equivalently, in the right-hand panel, the global minimum occurs at  $m = m_0$ , which means that the ordered phase characterized by  $m = m_0$  is stable. The “local” minima occurring in these plots are generally referred to as extra minima or metastable states. Note also that because  $f$  in Eq. (9.1) is dependent on an order parameter, *not* on state variables, you *cannot* and must *never* perform a common-tangent construction on the Landau free energy!

To quickly summarize, if we were able to write a Landau expansion of the free energy, we would be able to determine which state was stable at each state point. This still does not answer the question we set out to solve: Can we say something about the type of the phase transition (first order or continuous) by the form of the Landau free energy? In the following two sections we are going to examine two “case studies” in the hope of answering this question. In the last sections of this chapter, we see how Landau theory can be applied by writing the Landau free energy of two models, namely the Ising model and a new system which we have not yet encountered: liquid crystals.

## 9.2 Case 1: A Continuous Phase Transition

For the moment, let us assume that the free energy of the disordered phase can be written approximately

$$f(T, m) \approx b(T)m^2 + d(T)m^4. \quad (9.2)$$

where we have made the temperature dependence explicit and we assume  $d(T) > 0$  for all  $T$ . In principle, all of the coefficients of the Landau free energy could be temperature dependent, however, we will find

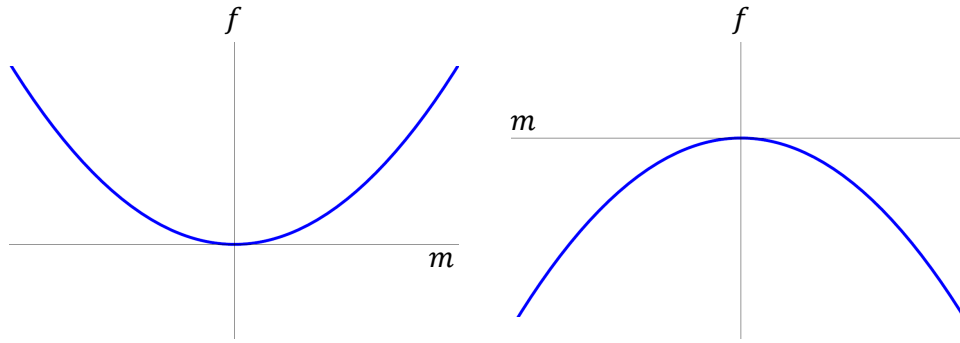


Figure 9.3: A zoom-in on the Landau free energy near  $m = 0$ . (left) For  $b(T) > 0$  corresponding to  $T > T_c$ , the shape implies that the disordered phase is stable or metastable. (right) The opposite situation with  $b(T) < 0$  corresponding to  $T < T_c$ ; the disordered phase is neither stable nor metastable.

it useful for the purpose of studying the type of phase transition to only examine the temperature dependence of  $b(T)$  and assume that the others are temperature independent, *i.e.*,  $d(T) = d$ .

The assumption that  $d > 0$  ensures that the free energy goes to infinity as  $m$  goes to infinity in both the positive and negative directions, *i.e.*, the global minimum is found for a finite  $m$ . The minima of Eq. (9.2) are given by  $m = 0$  for  $b(T) > 0$  and  $m = \pm\sqrt{-b(T)/2d}$  for  $b(T) < 0$ . If we zoom in on the minimum around  $m = 0$ , we see that changing the sign of  $b(T)$  from positive to negative takes it from being a stable or metastable state, *i.e.*, at least a local minimum in the free energy, to being completely unstable. If we identify the temperature associated with changing the sign of  $b(T)$  to be  $T_c$  then we can approximate  $b(T)$  by  $b(T) \approx b'(T - T_c)$  where  $b'$  is a positive constant. Thus for  $T > T_c$ ,  $b(T) > 0$  and the disordered phase is (meta)stable, while for  $T < T_c$  the disordered phase is not stable, see Fig. 9.3. With this rewrite, the minima are given by  $m = \pm\sqrt{-b'(T - T_c)/2d}$ . The free energies for  $T > T_c$ ,  $T = T_c$  and  $T < T_c$  are shown in Fig. 9.4. The minimum as a function of  $T - T_c$  continuously goes away from  $m = 0$ . As a result, the global minimum in the free energy goes continuously away from  $m = 0$ , a clear signature of a continuous phase transition.

Note also that due to the symmetry of the problem, there are two global minima. This could, for instance, correspond to the two solutions associated with spins pointed up and spins pointed down in the Ising model. Additionally, note that the Ising model is an example of a system which obeys this symmetry. We can go even further here and look at the properties of the order parameter *near* the critical temperature  $T_c$ . Here, our Landau theory predicts that the order parameter behaves as

$$m \propto (T_c - T)^{1/2}. \quad (9.3)$$

Hence, we predict the critical exponent  $\beta = 1/2$ .

### 9.3 Case 2: A First-Order Phase Transition

In this case, let us assume that we have a system for which the Landau free energy is given by

$$f(T, m) \approx b(T)m^2 - c(T)m^3 + d(T)m^4. \quad (9.4)$$

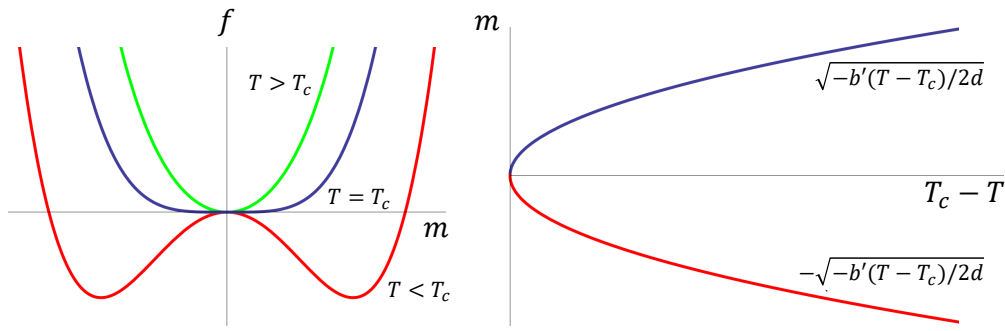


Figure 9.4: (left) Free energy as a function of  $m$  where the Landau free energy is given by Eq. (9.2). (right) Minima of the Landau free energy as a function of temperature with respect to the critical temperature  $T - T_c$ . Note that the minimum goes away from  $m = 0$  continuously. This is an example of a continuous phase transition. Note that for  $T < T_c$  two minima appear, due to the symmetry in this problem. This could, for instance, correspond to the Ising model where one minimum would correspond to all spins pointing “up” while the other minimum would correspond to all spins pointing “down”.

where  $c(T) > 0$  and  $d(T) > 0$ . Again for simplicity, let us assume that both  $c$  and  $d$  are not temperature dependent. Additionally, as in the previous case, the disordered phase becomes completely unstable when the sign of  $b(T)$  changes from positive to negative. This time we will call this temperature  $T_0$  and write  $b(T) \approx b'(T - T_0)$ . Remembering that a minimum requires  $\partial f/\partial m = 0$  and  $\partial^2 f/\partial m^2 > 0$ , we find that for  $b(T) > 9c^2/32d$  there is only a single minimum located at  $m = 0$ . This situation changes at  $b(T) = 9c^2/32d$  where a second minimum appears at  $m = m_f$  corresponding to an ordered state, see Fig. 9.5. The temperature associated with the appearance of this extra minimum we denote as  $T_1$ .

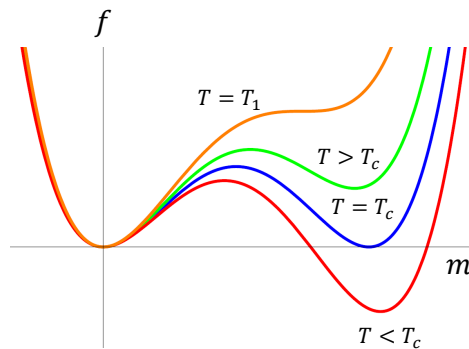


Figure 9.5: Landau free energy given by Eq. 9.4 as a function of  $m$  for a range of temperatures. For  $T > T_1$  the only minimum corresponds to the disordered state. For  $T_0 < T < T_1$ , there are two minima, but the disordered state ( $m = 0$ ) is the global minimum. Hence, the disordered state is stable, while the ordered state is metastable. At  $T_c$  we see a jump in the global minimum from the disordered state to the ordered state. Hence, at  $T_c$ , we see a first-order phase transition between the disordered state ( $m = 0$ ) and the state characterized by the minimum at finite  $m$ .

For the region  $c^2/4d < b(T) < 9c^2/32d$  there continue to be two minima located at  $m = 0$  and  $m = m_f$ , respectively. However, within this range the free energy at  $m = 0$  is always less than the free energy at  $m = m_f$  and so the disordered state is stable. However, at  $b(T) = c^2/4d$ , the global minimum in the free energy jumps discontinuously from  $m = 0$  to  $m = m_f$ . This discontinuity is a signature of a first-order phase transition, and we define the temperature associated with this transition to be  $T_c$ . Finally, at  $T = T_0$  the sign of  $b$  changes and the disordered phase is no longer even metastable, *i.e.*, there is only a single minimum present in the Landau free energy corresponding to the ordered phase.

## 9.4 Example: Zero-Field Ising Model

An order parameter which distinguishes between the disordered state and the ferromagnetic state is the magnetization  $m$ . As we have seen in Chapter 7, the magnetization is zero in the disordered state and non-zero in the ordered state. We will now consider a minimal Landau expansion that satisfies these considerations. The role of symmetry in eliminating certain expansion coefficients, will take the center stage in this example.

For the Ising model, we know that the free energy must be the same under a *global* flip of all spins, because the (zero-field) Hamiltonian is invariant under this operation. The magnetization, however, changes sign ( $m \rightarrow -m$ ) under a global spin flip. Thus, a Landau free energy expansion describing the Ising model should satisfy:  $f(T, m) = f(T, -m)$ . This can only be the case when the expansion exclusively has terms even in  $m$ :

$$f(T, m) = b(T)m^2 + dm^4 + \dots \quad (9.5)$$

Finally, the free energy must go to infinity as  $m$  goes towards both plus and minus infinity. As we saw in Cases 1 and 2, the coefficient  $b(T)$  changes sign when the disordered phase is no longer stable nor metastable. Consequently, we know that the free energy must contain at least a fourth-order power in  $m$ . When we assume  $d > 0$ , we can terminate the expansion at  $m^4$ , which leads to

$$f(T, m) \approx b(T)m^2 + dm^4. \quad (9.6)$$

This constitutes the minimal Landau expansion that satisfies the underlying microscopic symmetry property of the Ising model.

Referencing the form we studied in Case 1, we immediately see that this expansion describes a second-order phase transition. Hence, considering only the underlying microscopic symmetries, we have predicted that the phase transition in the Ising model is second order. A natural question would now be: What if we added further even terms, would the order of the transition change? One of the exercises will show you that this is indeed the case. Clearly, one should exercise caution in using Landau theory and interpreting its result.

Along that line of thinking, we should remark that from Eq. (9.3) we obtain a critical exponent of  $\beta = 1/2$ . This is clearly not the right value for two- and three-dimensional Ising models, also see Chapter 7. As a mean-field description, Landau theory lacks predictive power near the critical point, so this is not unexpected.

## 9.5 Example: Isotropic to Nematic Phase Transition

Typically, when picturing a gas, liquid, or even a crystal, we imagine arrangements of spherically symmetric particles. In a gas, liquid, or fluid, the particles are not ordered, but to a good approximation

randomly distributed throughout space. In a crystal, the particles are situated on a lattice, *i.e.*, they are positionally ordered. If we know the average position of a particle at one site of a lattice, we can fairly accurately infer the positions of the other particles. Similar observations can be made about the phases of particles that interact *via* a spherically symmetric pair potential. By such a pair potential, we mean that if particle 1 is at position  $\mathbf{r}_1$  and the position of particle 2 is given by  $\mathbf{r}_2$ :  $\phi(\mathbf{r}_1, \mathbf{r}_2) = \phi(|\mathbf{r}_1 - \mathbf{r}_2|)$ .

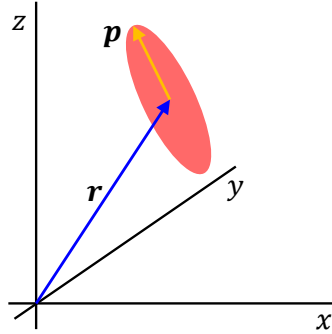


Figure 9.6: Cartoon of an ellipsoid showing the position of its center of mass  $\mathbf{r}$  together with a vector defining its orientation  $\mathbf{p}$ . Note that both are required to fully describe the particle.

However, there are many situations which can arise where the interaction potential is *not* spherically symmetric. One way to introduce anisotropy into the pair potential is simply to consider non-spherical particles, we will return to this topic in Chapter 17. Then the interaction potential between the two particles will depend on both the orientation of the particles, as well as their center-to-center distance. One of the simplest examples of a non-spherical particle is an ellipsoid. Here, we denote its center of mass by  $\mathbf{r}$  and its orientation by  $\mathbf{p}$ , see Fig. 9.6.

Extra phases compared to those associated with spherically symmetric potentials emerge as a consequence of the added rotational degrees of freedom needed to describe the ellipsoid. In particular, we encounter situations that have neither orientational nor positional order, the *isotropic* phase, see Fig. 9.7a. When the particles are globally aligned along a director  $\mathbf{n}$ , but do not possess positional order, the system is in the *nematic* phase, see Fig. 9.7b. The particles can be orientationally ordered, as well as positionally ordered into layers, which is called a *smectic* phase, see Fig. 9.7c. Finally, we can have full positional and orientational order, the *crystal* phase, see Fig. 9.7d. The difference between a smectic and a crystal is that in the smectic the ellipsoids are disordered in orthogonal direction, *i.e.*, the layers are fluid-like.

Here, we study the isotropic to nematic phase transition in ellipsoids. In both these phases, the particles are not positionally ordered. The main difference is found in the orientational order, absent in the isotropic phase and present in the nematic phase. Specifically, in the nematic phase, the particles on average point in a specific direction, which we will denote by the unit vector  $\mathbf{n}$ . For this transition, we do not have an immediate inroad to a symmetry argument. In fact, we do not even have an order parameter, yet, so let us define that first.

To describe this system, we require an order parameter  $m$  which is zero in the case where the particles are not orientationally ordered and non-zero when the particles point along the director  $\mathbf{n}$ . As a first attempt, we might try something like  $m_{\text{trial}} = 1/N \sum_i \mathbf{p}_i \cdot \mathbf{n}$  where  $\mathbf{p}_i$  is a unit vector which indicates the orientation of the  $i$ th particle, and  $N$  is the number of particles in the system. However, the symmetry

of the particle is such that we cannot distinguish between a particle pointing in the  $\mathbf{n}$  direction from a particle pointing in the  $-\mathbf{n}$ . Hence, we need the order parameter to also be equivalent for  $\mathbf{n}$  and  $-\mathbf{n}$ . One way to accomplish this is to take the square of the dot product:  $m_{\text{square}} = \langle 1/N \sum_i (\mathbf{p}_i \cdot \mathbf{n})^2 \rangle = \cos^2(\theta)$ , where  $\theta$  is the angle between  $\mathbf{n}$  and  $\mathbf{p}_i$ . However, we still have a problem: we want the order parameter to be *zero* in the disordered phase and nonzero in the ordered phase. To calculate the expected value of the order parameter in the disordered phase we write

$$m_{\text{square}} = \frac{1}{4\pi} \int_0^{2\pi} d\phi \int_0^\pi d\theta \sin\theta \cos^2(\theta) = \frac{1}{3}, \quad (9.7)$$

which means that  $m_{\text{square}}$  is not zero in the disordered phase. We can correct this however, by subtracting this part from our order parameter. We are now left with  $m \propto 1/N \sum_i (\cos^2(\theta) - 1/3)$ . Finally, although not strictly necessary, we can choose  $m$  such that its maximum value is 1. Note that this does not change the behavior in the disordered phase, but it is typically done in literature and so we will do the same here. We thus obtain the definitive order parameter for the isotropic-nematic transition

$$m = \frac{1}{N} \sum_i \frac{1}{2} (3 \cos^2(\theta) - 1). \quad (9.8)$$

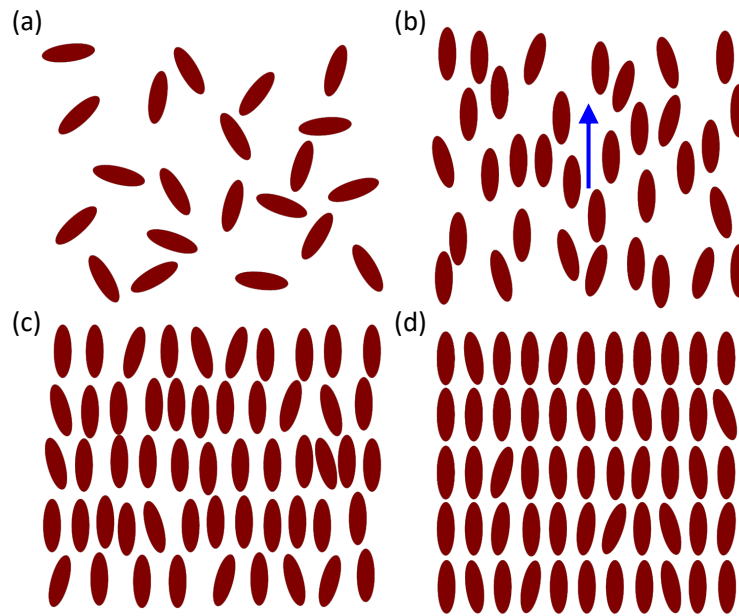


Figure 9.7: Possible phases for ellipsoidal particles. (a) The *isotropic* phase is characterized by the absence of positional and orientational order. (b) The *nematic* phase possesses average orientational order, but no positional order. The particles are orientated in the direction of the blue arrow, which represents the nematic director  $\mathbf{n}$ . (c) The *smectic* phase has orientational order along  $\mathbf{n}$  and positional order in one direction, *i.e.*, it is layered in one direction and disordered (positionally) in the orthogonal planes. (d) The *crystal* phase possesses both threefold positional order and orientational order.

Now that we have an order parameter for the isotropic to nematic phase transition, we would like to write down the free energy. We know that there should be two possible minima in the free energy (depending

on the temperature), one when the system is disordered and one when the system is ordered. Unlike in the Ising model, here we keep both the even and odd ordered terms. Hence, up to fourth order we obtain

$$f(T, m) \approx b(T)m^2 - cm^3 + dm^4, \quad (9.9)$$

with  $c$  and  $d$  positive;  $c$  is positive since there should be some lowering of the free energy for aligned ellipsoids while  $d$  is positive to ensure that the free energy goes to infinity for  $m \rightarrow \pm\infty$ . We conclude that the free energy is of the form that studied in case 2. This Landau theory therefore describes a first-order phase transition between the isotropic phase and the nematic phase. This turns out to be accurate, as we shall see using Onsager theory in Chapter 17.

But wait, what symmetry argument motivates this? Is the ellipsoid not also front-aft symmetric? Why do we not therefore eliminate the odd  $m^3$  term? This is not the case, because flipping each ellipsoid individually is not a natural symmetry operation on the entire space inhabited by the ellipsoids. The *global* symmetries that preserve the ellipsoid Hamiltonian are rotations. However, these do not impose constraints on the existence of an  $m^3$  term, as the nematic director rotates along with the entire system, leaving our  $m$  invariant as well. In the case of the Ising model, the global operation did not leave its  $m$  invariant, *i.e.*,  $m \rightarrow -m$  in that case.

The above line of argument may not be entirely satisfactory, as we only touch upon the concept of symmetry in these notes, rather than formalize it. However, we hope to have given you a flavor of what Landau theory is and why researchers would be enthusiastic about a method that allows for the prediction of the order of a phase on the basis of symmetries that leave the Hamiltonian invariant.

## 9.6 Exercises

### Q62. Landau Theory and the Ising model

- Starting from the mean-field expression for the free energy of the Ising model without a field, show that the Landau expansion is of the form of Case 1.
- What is the transition temperature associated with this Landau expansion. How does it compare to the transition temperature we determined from mean field theory?

### Q63. Landau Theory from Pathria and Beale (*Statistical Mechanics*)

Consider a system where the Landau free energy can be expanded as

$$f(T, m) = rm^2 + sm^4 + um^6 \quad (9.10)$$

where  $u > 0$ . Define  $\alpha = -(3ur)^{1/2}$ ,  $\gamma = -(4ur)^{1/2}$ , and  $\xi = (r/u)^{1/4}$ . Then as we did when we considered the two possible cases, characterize the phase transition associated with this expansion. Proceed along the following route:

- Plot the function using Mathematica for several different values of  $r$ ,  $s$  and  $u$ . What types of phase transitions seem possible for this Landau free energy?
- What are the five possible minima associated with this Landau free energy?
- Show that for  $r > 0$  and  $s > \alpha$ ,  $m_0 = 0$  is the only real solution.
- Show that for  $r > 0$  and  $\gamma < s \leq \alpha$ ,  $m_0 = 0$  or  $\pm m_1$ , where

$$m_1^2 = \frac{-s + \sqrt{(s^2 - \alpha^2)}}{3u}. \quad (9.11)$$

However, the minimum of  $f$  at  $m_0 = 0$  is lower than the minimum at  $m_0 = \pm m_1$ , so the global minimum is at  $m_0 = 0$ .

- Show that for  $r > 0$  and  $s = \gamma$ ,  $m_0 = 0$  or  $\pm \xi$ . Now, the minimum of  $f$  at  $m_0$  is of the same height as the ones at  $m_0 = \pm \xi$ , so a nonzero spontaneous magnetization is as likely to occur as the zero one.
- Show that for  $r > 0$  and  $s < \gamma$ ,  $m_0 = \pm m_1$ . Explain how this indicates a first-order phase transition. Note that the line  $s = \gamma$ , with  $r > 0$  is generally referred to as a “line of first-order phase transitions”.
- Show that for  $r = 0$  and  $s < 0$ ,  $m_0 = \pm(2|s|/3u)^{1/2}$ .
- Show that for  $r < 0$ ,  $m_0 = \pm m_1$  for all  $s$ . As  $r \rightarrow 0$ ,  $m_1 \rightarrow 0$  if  $s$  is positive.
- Show that for  $r = 0$  and  $s > 0$ ,  $m_0 = 0$  is the only solution. Explain why the line with  $r = 0$  and  $s$  positive is a line of second order phase transitions?

### Q64. Simple Model for the Isotropic to Nematic Phase Transition

In this exercise, we examine a simple model system that undergoes an isotropic-like to nematic-like phase transition. We consider a system of particles on a square lattice. Each particle covers  $L$  lattice sites, arranged in a line. There are two species of particles  $A$  and  $B$ , oriented horizontally and vertically, respectively, see Fig. 9.8.

All  $A$  particles are identical and all  $B$  particles are identical. Whenever two particles overlap, they have an interaction energy of  $\epsilon > 0$ . Particles that do not overlap have an interaction energy of 0. Note that each particle can interact with multiple other particles, even at the same lattice site. Assume there are  $N_A$  particles of species  $A$  and  $N_B$  particles of species  $B$ , in a volume  $V$  at temperature  $T$ , so that the number density of the two species are  $\rho_A = N_A/V$  and  $\rho_B = N_B/V$ . Additionally, assume periodic boundary conditions.

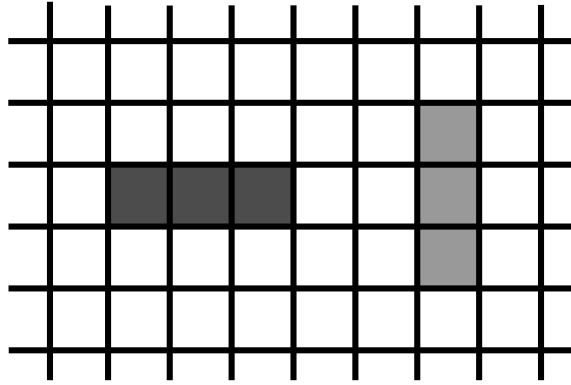


Figure 9.8: A horizontal  $A$ -type particle (left) and a vertical  $B$ -type particle (right) for  $L = 3$ .

- (a) We begin by getting a feeling for the system:
- (i) Sketch all the configurations where an  $A$  particle overlaps with an  $A$  particle for the case where  $L = 3$ . Assuming that all particles are homogeneously spread over the system, argue within a mean-field approximation that the average potential energy of an  $A$  particle due to its interaction with other  $A$  particles is given by  $U_{AA} = (2L - 1)\rho_A\epsilon$ .
  - (ii) Assuming that the  $B$  particles are also homogeneously spread over the system, argue that the average potential energy of a  $B$  particle due to its interaction with other  $B$  particles is similarly given by  $U_{BB} = (2L - 1)\rho_B\epsilon$ .
  - (iii) Sketch all the configurations where an  $A$  particle overlaps with a  $B$  particle for the case where  $L = 3$ . Still within the mean-field approximation, *i.e.*, where we assume that the particles of both species are homogeneously spread over the system, argue that the average potential energy of an  $A$  particle due to its interaction with the  $B$  particles is given by  $U_{AB} = L^2\rho_B\epsilon$ .
- (b) Using your results from parts (a), show that the energy of this system within the mean-field approximation is given by

$$U = \frac{1}{2}L^2\epsilon(N_A\rho_B + N_B\rho_A) + L\epsilon(N_A\rho_A + N_B\rho_B) - \epsilon\frac{(N_A\rho_A + N_B\rho_B)}{2}. \quad (9.12)$$

- (c) Assuming that  $\epsilon = 0$ , what is the canonical partition function  $Z(N_A, V, T)$  for the  $A$  type particles? For the  $B$  type particles ( $Z(N_B, V, T)$ )? For the combined system of  $A$  and  $B$  ( $Z(N_A, N_B, V, T)$ )? Note that when  $\epsilon = 0$ , both the  $A$  and  $B$  species act like ideal gases.
- (d) For  $\epsilon \neq 0$  what is the canonical partition function  $Z(N_A, N_B, V, T)$  for the system within the mean field approximation described in (a)?
- (e) Using the partition function from part (d), calculate the Helmholtz free energy  $F(N_A, N_B, V, T)$ . Make the substitution that  $x = N_A/N$  to obtain the free energy as a function of  $F(x, N, V, T)$ . Show that this free energy is given by

$$\begin{aligned} \frac{\beta F(x, N, V, T)}{N} &= \log(\rho) - 1 + (1 - x)\log(1 - x) + x\log x \\ &\quad + \beta\rho\epsilon \left( L^2(1 - x)x + L(2x^2 - 2x + 1) - x^2 + x - \frac{1}{2} \right), \end{aligned} \quad (9.13)$$

where  $x = N_A/N$ , and  $\rho = N/V$ , with  $N = N_A + N_B$ .

- (f) Assume now that the particles can freely change identity between species  $A$  and  $B$ , at no additional free energy cost. Argue that in this case, in equilibrium

$$\frac{\partial F(x, N, V, T)}{\partial x} = 0. \quad (9.14)$$

Show that  $x = 1/2$  is always an extremum of the free energy. What does the system look like when  $x = 1/2$ ? Is this an ordered phase or a disordered phase? Explain.

- (g) If we substitute  $m = x - 1/2$  into the Helmholtz free energy, and expand around  $m = 0$  we obtain a Landau free energy

$$\frac{\beta F}{N} = C + (-\beta\rho\epsilon - \beta L^2\rho\epsilon + 2\beta L\rho\epsilon + 2)m^2 + \frac{4m^4}{3} + \frac{32m^6}{15} + \mathcal{O}(m^7) \quad (9.15)$$

where  $C$  is a constant. Using this Landau free energy, at what temperature does a phase transition occur in this system? What type of phase transition is it (continuous or discontinuous)? Explain.

### Q65. Mixing on a Square Lattice

Consider a square lattice. On a square lattice, each lattice site has four nearest neighbors. Assume that each lattice site can be in one of three different states, which we will label  $A$ ,  $B$ , and  $C$ . Assume that the interaction between lattice sites is such that the contribution to the energy is zero when nearest neighbor lattices are in different states, while it is  $-J$  when they are in the same state. The Hamiltonian for this system can be written

$$H = -\frac{J}{2} \sum_i \sum_j' \delta_{\sigma_i, \sigma_j}, \quad (9.16)$$

where  $\sum_j'$  indicates a sum over nearest neighbors,  $\sigma_i$  represents the state of the lattice site, *i.e.*, it can be either  $A$ ,  $B$ , or  $C$ , and  $\delta_{\sigma_i, \sigma_j}$  is the Kronecker delta function defined by

$$\delta_{\sigma_i, \sigma_j} = \begin{cases} 0 & \text{if } \sigma_i \neq \sigma_j \\ 1 & \text{if } \sigma_i = \sigma_j \end{cases}. \quad (9.17)$$

Note that if there is a phase transition in this system, it will be between a phase where the system consists of an equal number of lattice sites in states  $A$ ,  $B$ , and  $C$ , while in the ordered phase, one of the three will be more likely. For simplicity, in this problem we will assume that the ordered state consists of more  $A$  lattice sites than either  $B$  or  $C$ . Here, we want to use the random mixing approximation (a form of mean-field theory) to study the phase behavior of this system. Within the random mixing approximation, the states of all lattice sites are uncorrelated. Define  $p_A$  to be the probability that a particular lattice site is in state  $A$ ,  $p_B$  the probability that it is in state  $B$ , and  $p_C$  the probability that it is in state  $C$ . Note that in the disordered state,  $p_A = p_B = p_C$ .

- (a) Argue why, in both the ordered and disordered phases,  $p_B = p_C = (1 - p_A)/2$ .  
 (b) What is the expected potential energy in the system for a given value of  $p_A$ ?  
 (c) What is the entropy for given value of  $p_A$ ?  
 (d) Show that, within the random mixing approximation, the free energy of the system can be written

$$\frac{\beta F}{N} = -K \left( p_A^2 + \frac{1}{2}(1 - p_A)^2 \right) + p_A \log(p_A) + (1 - p_A) \log \left( \frac{1 - p_A}{2} \right), \quad (9.18)$$

where  $K = 2\beta J$ , and  $N$  is the number of lattice sites.

- (e) In the disordered phase,  $p_A = 1/3$ . Define an order parameter  $m$  such that  $m = \frac{3}{2}(p_A - 1/3)$ . Note that it is 0 in the disordered phase and non-zero in the ordered phase. Rewrite the free energy in terms of  $m$ . Show that the Landau expansion for the free energy can then be written

$$\frac{\beta F}{N} = -\log(3) - \frac{K}{3} + \left(1 - \frac{2}{3}K\right)m^2 - \frac{m^3}{3} + \frac{m^4}{2} + \mathcal{O}(m^5). \quad (9.19)$$

- (f) Using the Landau free energy, determine the transition temperature for this system. Is the phase transition continuous or discontinuous? Explain.



## Chapter 10

# Real-Space Renormalization Group

In Chapter 7, we saw that for the 2D Ising model there is a logarithmic divergence of the heat-capacity as a function of the temperature  $T$  near the critical point, *i.e.*, the temperature  $T = T_c$  for which the phase transition takes place. The magnetization exhibits a power-law behavior in  $T$  near this point. Divergences and power-law behavior are a common feature of systems that undergo a continuous phase transition. Unfortunately, the 2D Ising model is rather involved to study and the 1D Ising model has no finite-temperature phase transition. In this chapter, we will therefore consider another (simple) model that has such a phase transition: site percolation. This model will allow us to gain intuition into the features of a critical system that underlie these divergences. It will turn out that these are correlations and a loss of ‘scale’ in the system. A more precise definition of the concept of correlation will be given in Chapter 11. However, the notion of scale invariance will be all that is required to set up the theoretical machinery to study the critical point, as we will see.

In most cases in physics, we extract information from complicated systems by first determining which length scales are important. This allows us to coarse grain the model so that we can treat the system correctly with respect to these important length scales: such procedures typically lead to perturbation theories. However, at critical points scale invariance interferes with this paradigm: there is no set scale around which to perturb the system. Scale invariance also means that the system has self-similarity. That is, if there is no intrinsic scale, then the system must ‘look similar’ irrespective of the size we are considering. Here, we introduce a completely different and rather beautiful method for studying continuous phase transitions that exploits this scale invariance: renormalization-group theory (RG).

RG was developed in the early 1970s by Kenneth Wilson, and its importance was recognized with the 1982 Nobel Prize in Physics. Wilson’s Nobel lecture can be found on the Nobel Prize website. RG has been applied to an enormous variety of systems. It should be mentioned that RG is more of a way of looking at a system than a method in itself. That is, the exact implementation will depend on the system in question. Hence, the main goal of this chapter is to give the reader a flavor for what is possible within the RG framework.

### 10.1 Site Percolation

The *percolation transition* is an example of a geometric phase transition, and it is sometimes referred to as the percolation threshold. The term *percolation* refers to a system-spanning quality of some quantity

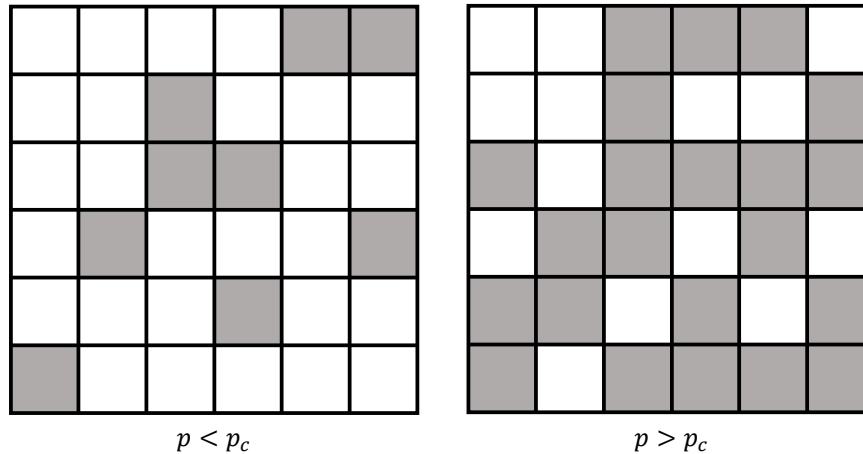


Figure 10.1: A square lattice where grey squares are occupied and white ones are not. On the left, we see that the occupied squares do not percolate the system, while in the system on the right they do. Here,  $p$  is the probability of coloring a square grey.

of interest. Let us assume that we have a 2D square lattice with periodic boundary conditions, *e.g.*, see Fig. 10.1. Each block on the lattice is either occupied or unoccupied. In this percolation model we assume that each block is occupied with a probability  $p$ . Note that we assume that the blocks do not interact. Then there exists a probability  $p_c$  above which the occupied blocks will percolate the lattice, *i.e.*, form a connected path from left to right and/or top to bottom, and below which they do not. This probability is referred to as the percolation transition or percolation threshold. Where the threshold lies exactly depends on the specific choice of percolation. One could imagine demanding that only a path from left to right to exist, though for this system here unidirectional percolation coincides with bidirectional percolation in the thermodynamic limit.

In Fig. 10.2, typical configurations are shown for various system sizes of a system below, at, and above the percolation threshold, with occupied sites in the same cluster indicated by the same color. Here, clusters are determined by the requirement that any two occupied sites that share a horizontal or vertical border are in the same cluster. Note that the structure of the clusters is special at the critical point. The structure appears frayed and it is not easy (or even possible) to order the snapshots by size, without zooming into the smallest scale of a single site for reference. This lack of intrinsic order is a characteristic of scale invariance as at each scale the system is self-similar, *i.e.*, it looks like itself. You may have already encountered scale invariance in studying fractal systems. It is possible to assign a fractal-like quality to systems at the critical point. This will impact how they behave, more so than their microscopic interaction rules, as we will see in Chapter 12.

Let us now gain a feeling for RG by applying it to calculate the phase transition in this system. To do so, we need to make a mapping between the original blocks and a new set of *super blocks*, which are simply groupings of blocks. The mapping we choose is shown in Fig. 10.3. Note that this mapping is only an approximation. That is, we make a choice for what we consider connecting and what we do not. The consequence is that our outcome for percolation depends on the choice. We now look at the behavior of the system as we apply consecutive renormalization steps, each corresponding to the mapping in Fig. 10.3. Each step can be thought of as ‘zooming out’: we look at the system at a larger length scale. Since at the critical point the system looks the same at all length scales, we will look for

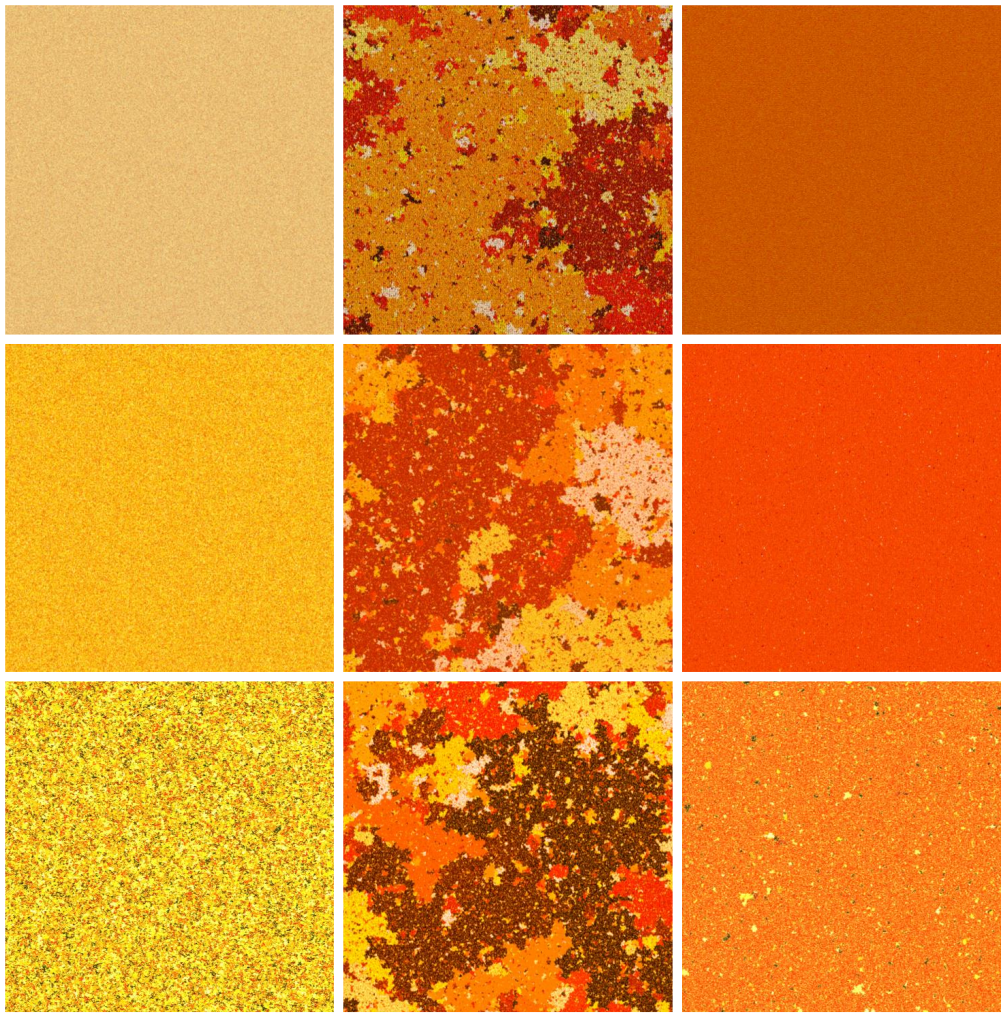


Figure 10.2: Example of critical behavior in a percolation model, see Section 10.1. Sites are considered occupied or empty with a probability  $p$  and  $(1 - p)$ , respectively. The sites are then clustered based on nearest neighbors, and sites belonging to the same cluster have been given the same color. Below the critical point, for  $p = 0.45$  (left column), there are no system-spanning clusters, as revealed by the small streaks representing clusters in the highest-magnification (bottom row); from top to bottom the magnification increases by a factor of 5 for each row. Above the critical point, for  $p = 0.63$  (right column), there is a system spanning cluster. The smallest zoom-in shows little islands of unoccupied sites within it. However, at the critical point  $p = p_c \approx 0.592746$  (middle column), the relative size of the clusters compared to the box does not change noticeably. The system looks similar on all length scales. Yellow hues correspond to empty sites, clusters are indicated with reds.

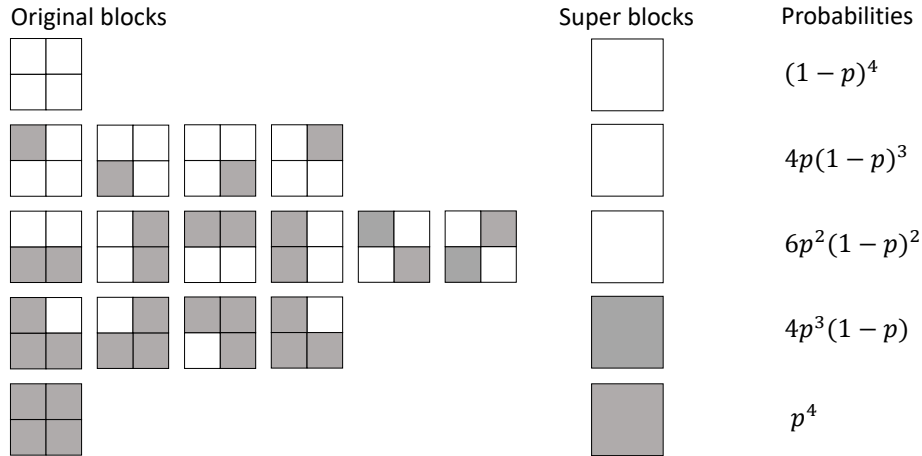


Figure 10.3: Graphical representation of the renormalization-group transformation that we are using for the percolation system. In the column titled *Original blocks* we have the system before a RG step, while the mapping for that set of blocks is shown in the column *Super blocks*. The probability of finding the super blocks is provided in terms of the original probability  $p$  for being occupied in the last column.

values of  $p$  where this zooming out does not change the structure of the system. The implication is that we are searching for that point where the structure is self-similar, which is exactly the property of the critical phase. In detecting this point, we are thus able to localize the phase transition.

We proceed in this direction by determining a relationship between the probabilities of the original blocks being occupied ( $p$ ) and the super blocks being occupied ( $p'$ ):

$$p' = R(p). \quad (10.1)$$

These probabilities are also shown in Fig. 10.3. When we sum the total probabilities for the occupied super blocks we obtain the following:

$$R(p) = p^4 + 4p^3(1 - p). \quad (10.2)$$

To determine the probabilities for which the system looks the same at all length scales, we look for the fixed points associated with Eq. (10.1). Since  $R(p)$  is given by Eq. (10.2), Eq. (10.1) is simply a polynomial, which we can solve exactly, either by hand, using Mathematica, or numerically. We obtain three fixed points:  $p^* = 0$ ,  $1$  and  $(1/6)(1 + \sqrt{13}) \approx 0.767592$ . In Fig. 10.4, we summarize the RG procedure. The top panel shows that a system with  $p < p_c$  will become less populated by making super blocks, while for  $p > p_c$  it will become more populated (middle panel). This leads to the RG flow diagram shown in the bottom panel, which indicates the three fixed points, two stable ones at  $p^* = 0$  and  $p^* = 1$  and an unstable fixed point at  $p = p_c$ . The arrows depict the direction of flow from  $p$  to  $p'$  that occurs when performing a renormalization step in the two regions. We observed that  $p^* = p_c$  corresponds to the only non-trivial fixed point, and is therefore the percolation threshold.

The mapping described in Fig. 10.3 is only an approximation. This should be clear from the fact that our RG theory predicts another value of  $p_c$  than we used in Fig. 10.2. The result is dependent on the way the RG procedure is set up, *i.e.*, RG makes errors by introducing a specific super block format. Figure 10.5 shows an example of two original blocks side-by-side which are not system spanning, but a two resulting super blocks that do. The mapping we used does not properly address these configurations.

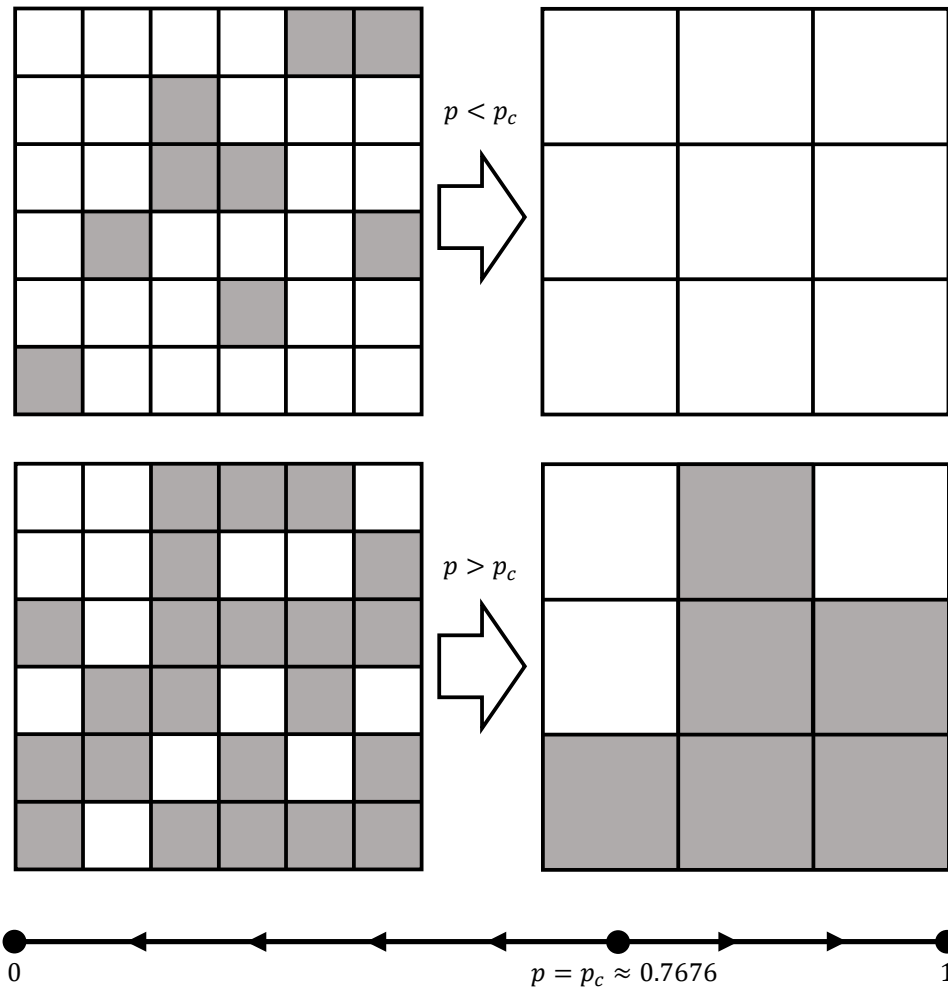


Figure 10.4: Graphical example of a single renormalization step for a system below the percolation transition (top) and above the percolation transition (middle). The associated RG flow diagram for the square lattice with the mapping show in Fig. 10.3 is shown at the bottom. The value  $p = p_c = (1/6)(1 + \sqrt{13}) \approx 0.7676$  represents an unstable fixed point, with the flow going toward 0 and 1 to the left and right of this point.

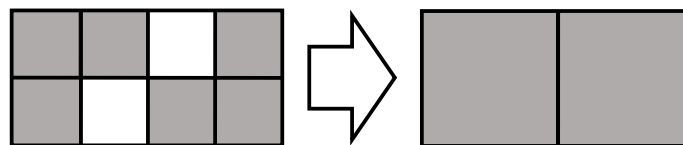


Figure 10.5: Graphical example of one of the errors introduced by the renormalization transition described in Fig. 10.3. The system on the left does not percolate while the system on the right does.

Summarizing, we have shown an example of RG in action and how it can be used to determine the critical point. We have also come to the realization that RG is an approximative procedure, which exploits the nature of the critical phase, but which is not going to give the exact point where the transition occurs.

## 10.2 RG for the Zero-Field 1D Ising Model

As we mentioned in the introduction to this chapter, there are many different ways to use renormalization-group theory to examine a critical point. In this section, we will see a slightly different implementation of RG in the context of the Ising model. We will first carry out the mathematics, which will seem out of the blue, before discussing what the underlying thought process is.

Referring back to Chapter 7, we see that the canonical partition function of the zero-field Ising model can be written as

$$\begin{aligned}
 Z(N, \beta) &= \sum_{S_1} \sum_{S_2} \dots \sum_{S_N} e^{-\beta \mathcal{H}(S_1, S_2, \dots, S_N)}; \\
 &= \sum_{S_1} \sum_{S_2} \dots \sum_{S_N} e^{\frac{\beta J}{2} \sum_{i=1}^N \sum_j' S_i S_j}; \\
 &= \sum_{S_1} \sum_{S_2} \dots \sum_{S_N} e^{\beta J (S_1 S_2 + S_2 S_3 + \dots + S_{N-1} S_N)}. \tag{10.3}
 \end{aligned}$$

For notational convenience, let us define  $K = \beta J$ . Then we have

$$\begin{aligned}
 Z(N, K) &= \sum_{S_1} \sum_{S_2} \dots \sum_{S_N} e^{K(S_1 S_2 + S_2 S_3 + \dots + S_{N-1} S_N)}; \\
 &= \sum_{S_1} \sum_{S_2} \dots \sum_{S_N} e^{K(S_1 S_2 + S_2 S_3)} e^{K(S_3 S_4 + S_4 S_5)} \dots; \\
 &= \sum_{S_1} \sum_{S_3} \dots \sum_{S_N} \left( \sum_{S_2} e^{K(S_1 S_2 + S_2 S_3)} \right) \left( \sum_{S_4} e^{K(S_3 S_4 + S_4 S_5)} \right) \dots \tag{10.4}
 \end{aligned}$$

Performing the sum of the even spins, *i.e.*,  $S_2 = \pm 1$ ,  $S_4 = \pm 1$ , *etc.*, we obtain

$$Z(N, K) = \sum_{S_1} \sum_{S_3} \dots \sum_{S_N} \left( e^{K(S_1 + S_3)} + e^{-K(S_1 + S_3)} \right) \left( e^{K(S_3 + S_5)} + e^{-K(S_3 + S_5)} \right) \dots \tag{10.5}$$

Now, in a renormalization group treatment, we would like this evened-out partition function, which now depends on  $N/2$  particles, to be of the same form as the original partition function, which concerned  $N$  particles. In other words, we want the result the same after eliminating half of the degrees of freedom. Explicitly, we would like to be able to write

$$Z(N, K) = g(K) Z(N/2, K') \tag{10.6}$$

where  $g(K)$  is an as-of-yet-unknown function. Next, we would be able to do the same thing for  $Z(N/2, K')$ , which leads to

$$Z(N/2, K') = g(K') Z((N/2)/2, K''), \tag{10.7}$$

and so on. Equation (10.6) thus defines a recursion relation for  $Z(N, K)$ . The procedure we are following here is also often referred to as a decimation-based RG transformation<sup>1</sup>, and this is visualized in Fig. 10.6.

<sup>1</sup>Note that ‘decimation’ does not solely refer to ‘reduction’ by 10% in its historic context.

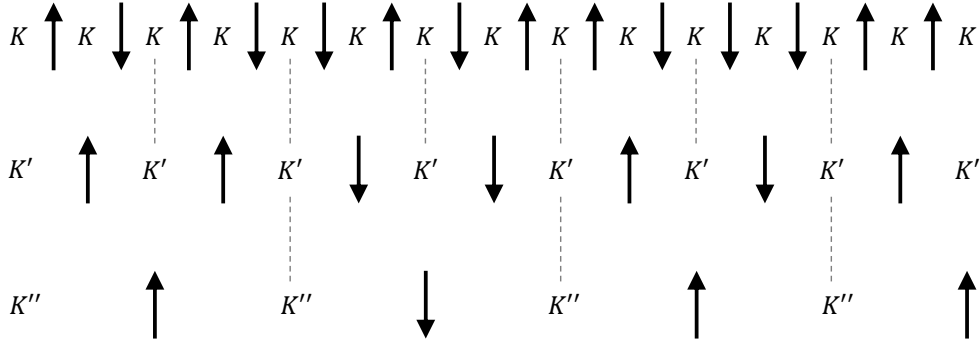


Figure 10.6: Visualization of the decimation procedure for the zero-field, one-dimensional Ising model. From top to bottom, we show two recursion steps in for the RG.

Examining Eq. (10.5), we note that the relation described by Eq. (10.6) is obeyed if

$$e^{K(S'+S'')} + e^{-K(S'+S'')} = f(K)e^{K'(S'S'')}. \quad (10.8)$$

Specifically, if we use Eq. (10.8), the new partition function can be written as

$$Z(N, K) = [f(K)]^{N/2} Z(N/2, K'). \quad (10.9)$$

Now, we are left with two unknowns in Eq. (10.9):  $f(K)$  and  $K'$ . However, note that we have only four possible choices for sets of  $S'$  and  $S''$ . We can have  $S' = S'' = \pm 1$  and  $S' = -S'' = \pm 1$ . Substituting  $S' = S'' = \pm 1$  into Eq. (10.8) we obtain

$$e^{2K} + e^{-2K} = f(K)e^{K'}, \quad (10.10)$$

which simplifies to

$$2 \cosh(2K) = f(K)e^{K'}. \quad (10.11)$$

In the case where  $S' = -S'' = \pm 1$ , Eq. (10.8) reduces to

$$2 = f(K)e^{-K'}. \quad (10.12)$$

We now have two independent equations, namely Eqs. (10.11) and (10.12), and two unknowns  $K'$  and  $f(K)$ . Solving this system results in

$$f(K) = 2 \cosh^{1/2}(2K), \quad (10.13)$$

and

$$K' = \frac{1}{2} \log [\cosh(2K)]. \quad (10.14)$$

Note that at this stage, we can already partially solve for a fixed point, namely one to Eq. (10.14). Unsurprisingly,  $K^* = 0$  and  $K^* = \infty$  are the only fixed points for the parameter  $K$ . The former is attractive and stable, corresponding to the high-temperature limit, the latter is unstable and corresponds to the limit  $T \downarrow 0$ . This makes sense, as we know that the 1D Ising model should not undergo a phase transition and that the fully aligned state, which can only exist at zero temperature, is unstable to small increases in the temperature. The associated RG recursion and flow are shown in the left-hand panel

to Fig. 10.7. The right-hand panel to Fig. 10.7 shows the corresponding result for the 2D Ising model, which does have a fixed point. The recursion relation for this model is given by the logical extension of the 1D decimation scheme

$$K'_{2D} = \frac{3}{8} \log [\cosh (4K_{2D})]. \quad (10.15)$$

The graphical representation in Fig. 10.7 immediately suggests a criterion for stability of a fixed point, namely based on the value of the derivative at  $K^*$ . This can be generalized to more complex flows.

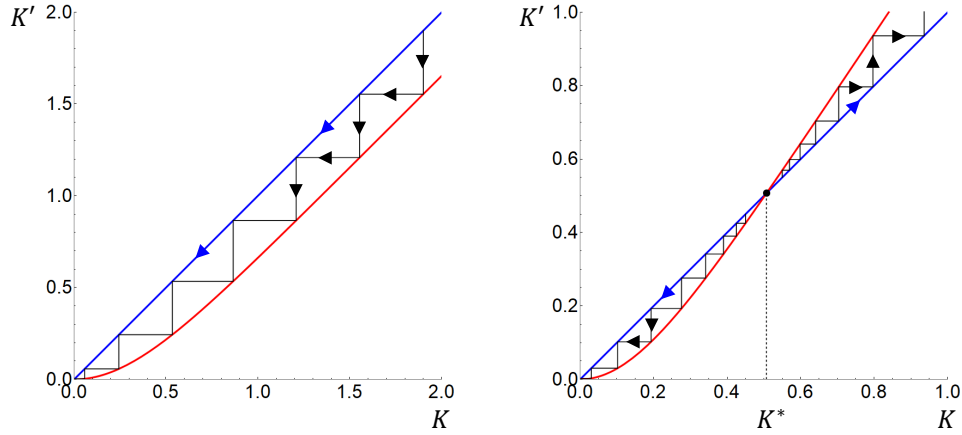


Figure 10.7: RG for the zero-field 1D (left) and 2D (right) Ising model. The recursion relation (red curve) is shown using the staircase construction (black line) for some initial choice of  $K$ , with the direction of the flow indicated using the black arrows. The 1D RG transformation only has two fixed points  $K^* = 0$  and  $K^* = \infty$ , the former being stable. 2D RG has a third fixed point, indicated using a black dot, which is non-trivial and unstable. This corresponds to a fixed-point value of  $K^* \approx 0.507$ , as indicated by the dashed line. The blue line  $K = K'$  is an RG flow together with the blue arrows indicating the direction; the full construction is provided here to give additional insight in the recursion process.

We could stop at this point, as we have recovered our physical intuition. However, we have technically not completed the full RG argument, since we do not have an expression for the partition function or free energy in terms of  $K$  yet. Recall that the free energy is extensive, *i.e.*, proportional to the number of particles in the system and it may therefore be written as

$$\beta F(N, K) = -\log (Z(N, K)) = -N f_1(K). \quad (10.16)$$

Note that the function  $f_1(K)$  depends only on  $K$  and *not* the number of particles in the system. This is a special result, because it implies that features of the single particle interactions are washed out in favor of some effective measure that accounts for the structure of the system, *i.e.*, its self-similarity at the critical point. Combining Eqs. (10.16) and (10.9) we obtain

$$f_1(K) = \frac{1}{2} \log (f(K)) + \frac{1}{N} \log (Z(N/2, K')). \quad (10.17)$$

However, from Eq. (10.16) we also have

$$\log (Z(N/2, K')) = \frac{N}{2} f_1(K'). \quad (10.18)$$

which allows us to eliminate the explicit dependence on the partition function and rewrite Eq. (10.17) to

$$f_1(K) = \frac{1}{2} \log(f(K)) + \frac{1}{2} f_1(K'). \quad (10.19)$$

Using Eqs. (10.19) and (10.13), we can further express  $f_1(K')$  in terms of  $f_1(K)$  and  $K$  only

$$f_1(K') = 2f_1(K) - \log\left(2 \cosh^{1/2}(2K)\right). \quad (10.20)$$

Here, the factor of 2 is due to the decimation length scale we have employed. This procedure, originally by American researcher Leo Philip Kadanoff, can also be applied to larger sets of spins, say of length  $s$ , which implies that factors of  $s$  would naturally appear in the above expressions. Equations (10.14) and (10.20) together comprise the renormalization-group equations. In the exercises, we will go through these calculations ourselves.

### 10.3 Exercises

#### Q66. Vertical Spanning Cluster

Consider a square lattice, for which squares can be occupied with probability  $p$ . Assume that a cell spans if there is a vertically spanning cluster in a  $2 \times 2$  superblock RG argument. Show that  $R(p) = 2p^2(1-p)^2 + 4p^3(1-p) + p^4$ . Find the corresponding nontrivial fixed point.

#### Q67. Renormalization in 3x3

Enumerate all the possible spanning configurations for a cell on a square lattice where the “super blocks” are  $3 \times 3$  instead of  $2 \times 2$  as we did in the notes. Assume that a cell is occupied if a cluster spans the cell both vertically and horizontally. Determine the probability of each configuration and find the renormalization transformation  $R(p)$ . What are the fixed points? Explain the significance of the fixed points. Hint: Use the computer to tabulate these configurations.

#### Q68. Renormalization on a Triangular Lattice

Assume that particles can move on a two-dimensional (2D) triangular lattice and that they are not able to overlap. The particles can occupy sites with probability  $p$ . Take hexagonal groupings of 7 lattice sites as the “super blocks” for a renormalization group argument, see Fig. 10.8. A super block is filled whenever *at least* 4 of its 7 sites are occupied by particles. Compute the non-trivial fixed point of this RG recursion.

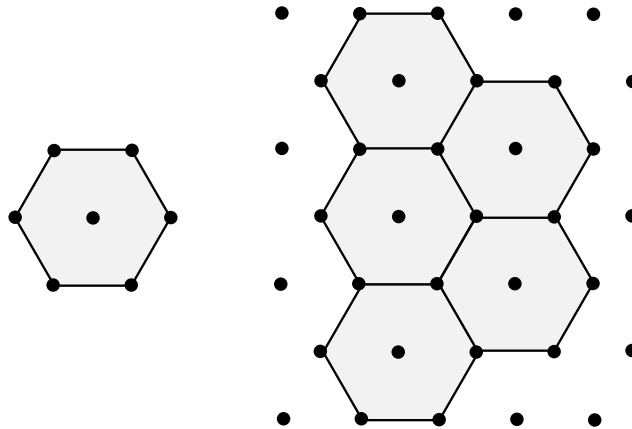


Figure 10.8: (left) A single super block is comprised of 7 sites. (right) Several super blocks superimposed on the triangular lattice being subjected to real-space renormalization.

#### Q69. Recursive relations for Ising model

We can also solve Eqs. (10.14) and (10.20) for  $K$  and  $f_1(K)$  as a function of  $K'$  to obtain

$$K = \frac{1}{2} \operatorname{arccosh}\left(e^{2K'}\right); \quad (10.21)$$

$$f_1(K) = \frac{1}{2} \log(2) + \frac{1}{2} K' + \frac{1}{2} f_1(K'). \quad (10.22)$$

K	Renormalization Group $f_1(K)$	Exact $f_1(K)$
0.010000	0.693147	0.693197
0.100333	0.698147	0.698172
0.327447	0.745814	0.745826
0.636247	0.883204	0.883210
0.972709	1.106299	1.106302
1.316710	1.386078	1.386080
1.662637	1.697968	1.697968
2.009049	2.026876	2.026877
2.355582	2.364536	2.364536
2.702146	2.706633	2.706633
3.048717	3.050963	3.050963

Table 10.1: Evaluation of the renormalization group recursion relations associated with Eqs. (10.21) and (10.22). The exact solution can be evaluated from Eq. (7.9). Note that a small error in the initial guess of  $K$  and  $f_1(K)$  leads to increasingly smaller errors in the sequential evaluations.

The reason for this rewrite is stability. How does this affect the direction of the flow? In order to see how the RG equations work, generate the first few lines from Table 10.1. As an initial condition we have chosen  $K = 0.01$  and  $f_1(0.01) \approx \log 2$ . Why is this a sensible choice?

**Q70. RG for the 1D Ising Model with an External Field** from David Chandler (*Introduction to Modern Physics*)

Consider the one-dimensional Ising model with an external magnetic field. With suitably reduced variables, the canonical partition function is

$$Z(K, h, N) = \sum_{S_1} \sum_{S_2} \dots \sum_{S_N} \exp \left[ h \sum_{i=1}^N S_i + K \sum_{i=1}^{N-1} S_i S_{i+1} \right]. \quad (10.23)$$

Assume periodic boundary conditions.

- (a) Show that by summing over all the even spins

$$Z(K, h, N) = [f(K, h)]^{N/2} Z(K', h', N/2), \quad (10.24)$$

where

$$h' = h + \frac{1}{2} \log \left[ \frac{\cosh(2K + h)}{\cosh(-2K + h)} \right]; \quad (10.25)$$

$$K' = \frac{1}{4} \log \left[ \frac{\cosh(2K + h) \cosh(-2K + h)}{\cosh^2(h)} \right], \quad (10.26)$$

and

$$f(K, h) = 2 \cosh(h) \left[ \frac{\cosh(2K + h) \cosh(-2K + h)}{\cosh^2(h)} \right]^{1/4}. \quad (10.27)$$

- (b) Discuss the flow pattern for the renormalization equations,  $h' = h'(h, K)$ ,  $K' = K'(K, h)$ , in the two-dimensional parameter space  $(K, h)$ .

(c) Start with the estimate that at  $K = 0.01$ ,

$$f_1(0.01, h) \simeq f_1(0, h), \quad (10.28)$$

and follow the flow of the RG transformation for several values of  $h$ .

# Chapter 11

## Correlation Length and Functions

Before we can continue with our analysis of the critical point, we need to discuss correlation. This will enable us to distinguish between various forms of critical behavior in Chapter 12. We have run into this concept a few times during this course. For example, we used a lack of correlation to argue that there is no phase transition in the zero-field 1D Ising model. We also encountered the concept of correlations in our discussion of mean-field theory, where we purposefully made the approximation to ignore these. This greatly simplified the theoretical description. However, this simplification came at a price, as mean-field theory predicts a phase transition for the zero-field 1D Ising model. Thus, clearly, there are cases where we must deal with correlations in the system in order to describe it accurately. Continuing this line of thought, it should also come as no surprise that self-similarity at the critical point is a strong indicator of (divergent) correlation.

In this chapter<sup>1</sup>, we will make the concept of correlations — generally speaking statistical associations, which are not necessarily causal — more precise and discuss correlation functions and their relation to phase transitions. We will also introduce a new concept: *correlation length* as a means to quantify spatial correlation<sup>2</sup>. Correlation length can be understood as follows. Imagine cutting a material up into smaller pieces. Most of the time, if you cut it up, the smaller pieces behave much the same as the “whole”. However, if we cut it up sufficiently small, the properties of the material will change. The length scale associated with this change is associated with the *correlation length*. In addition, this length depends on external conditions, such as the temperature, pressure, *etc.* This will become more clear shortly as we discuss several physical examples.

### 11.1 Statistical Association and Causation

You may have previously encountered the concept of correlation in a statistics course. This describes a statistical relation between two random variables. For example, if you measure the temperature and the total sales of ice cream over a period of time in a certain region, you will likely find that as one goes up so does the other. That is, the two quantities are positively correlated. It will not be a perfect trend, as there will be some fluctuations having to do with your finite sample set, *i.e.*, the statistical

---

<sup>1</sup>We note that a nice introduction to phase transitions and critical phenomena is provided in the book by John Cardy “Scaling and Renormalization in Statistical Physics”. Parts of this chapter are inspired by the discussion in his book.

<sup>2</sup>The temporal equivalent is the *decorrelation time* as for time-dependent quantities one is often interested in how quickly correlations are lost with respect to some initial state.

nature of your measurement. Now imagine a similar graph of the number of shark attacks as a function of temperature. These can also be shown to be positively correlated; more people tend to go swimming as the temperature of the water increases. This then implies that when you graph the number of ice cream sales against shark attacks there will also be a positive correlation. Clearly, the latter is a case of correlation not implying causation.

In physics, we typically wish to have a more useful notion of correlation, which is why the correlations we study are often associated with a microscopic quantity of interest. For example, in a molecular system, we can look at correlations in the positions of particles, as we will do next. In the case of the Ising model, we examine correlations in the orientation of the spins separated by a given number of lattice sites. In both cases, we will find that the correlations that we measure contain important information about the microscopic organization in the system. This is directly tied into its structure, which relates to the nature of its phases, as well as ultimately the associated transitions between these. Thus, here, we are interested in correlations for which the causation is baked into their form.

## 11.2 Correlations and Ordering

Correlations and correlation functions play an important role in phase identification. Phases are often distinguished by ordering in various degrees of freedom they possess. In this section, we will have a first look at this for the case of a simple fluid, a system which we will study in much greater detail in Chapter 13. We will gain an impression of the topic, before moving onto the 1D Ising model, for which things are generally easier to compute.

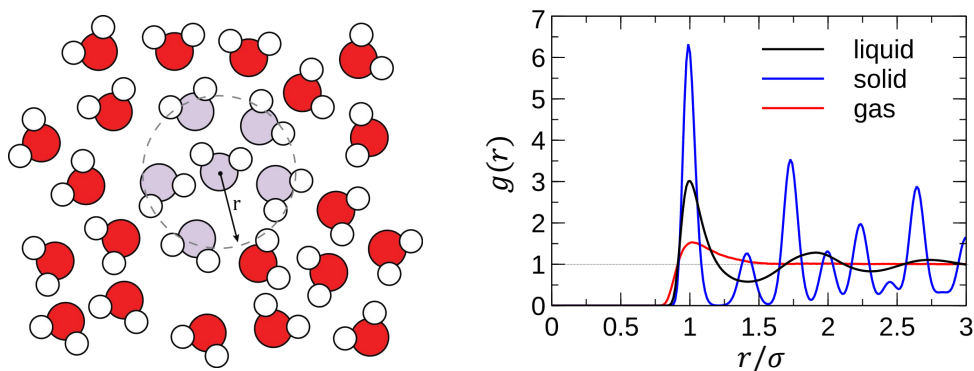


Figure 11.1: The radial distribution function for three phases of water, adapted from figures by Christophe Rowley. (left) Determining the number of molecules that are a distance  $r$  away from a chosen molecule, *i.e.*, the number of molecules of which the center is in the shell with radius  $r$  and infinitesimal width  $dr$ . (right) The resulting (averaged) radial distribution function  $g(r)$  for the gas, liquid, and solid phase. The main text explains what  $g(r)$  measures.

If we consider a fluid and a crystal, clearly there is a difference, which is associated with the organization of particles. The fluid has little positional order, while the crystal is periodic<sup>3</sup>. But that does not mean there is no positional ordering in the fluid. How can we properly assess this?

<sup>3</sup>The situation can also become more complicated. For instance, in the case of liquid crystals there is both positional and orientational ordering: the isotropic system had neither, while the nematic phase had orientational ordering but no positional ordering. The smectic phase even has orientational and partial positional order.

Let us take a single fluid particle, then on average other fluid particles are arranged in ‘shells’ around this particle, as the molecules in the fluid cannot (fully) interpenetrate, see the left-hand panel to Fig. 11.1. That is, knowledge of the position of a single molecule imposes limitations on where the other molecules can be, at least locally. We can quantify this by determining a histogram of the number of particles found at a radial distance  $r$  away from a particle of choice. When we average this over all particles in the system, we can obtain a smooth curve in the thermodynamic limit. We expect the number of particles in a bin to increase with  $r$ , and thus the function that we have obtained shows a similar trend. This volumetric scaling can be divided out to arrive at the radial distribution function  $g(r)$ , shown in the right-hand panel to Fig. 11.1; note it tends to 1 due to the normalization. We will define  $g(r)$  exactly in Chapter 14 and provide the simple relation between the radial distribution function and the pair-correlation function for the fluid and gas phase. In a few words the relation is as follows. If you know the vector-based positional correlation between a pair of particles, and the environment is homogeneous, then taking one particle as the frame of reference and radially averaging gives  $g(r)$ . Thus, we will use  $g(r)$  as a stand in for the proper pair correlation function. If you do not enjoy this level of hand-waving descriptiveness, please page ahead to Chapter 14.

It should be obvious that for a gas there is no real structure, beyond that particles cannot be at the same position; the density is too low to promote shell formation. This is expressed by a nearly flat  $g(r)$  which is zero in the region where the particles overlap. The small bump in  $g(r)$  indicates that you are slightly more likely to find a particle one diameter away from the center of another, because they cannot overlap. For a typical fluid we see a set of peaks that decrease in height. This implies that some distances are more common than others, *i.e.*, the particles are arranged in shells around our central one. These give the peaks, while the valleys correspond to the mid-points between shells which do not readily accommodate the presence of a particle, due to exclusions. Note that the height of the peaks decreases with distance, implying that the system has only a short-range correlation. Or, in other words, the shells become more spread out, as the particles have significant freedom to move in a fluid, leading to loss of correlation. We can now readily imagine that the correlation length in the gas and fluid phase is associated with the decay of the peaks. It turns out that this decay is exponential and thus leads to a single natural length scale.

The behavior in the gas and fluid is distinct from that in a(n idealized) crystal, where the correlations do not decay to zero, even at very long distances. That is, in a crystal the particles organize themselves onto a lattice, such that knowledge of a single unit cell gives information on the position of a particle many unit cells away. As a result, the correlations in a crystal are often called *long-range*. However, it should be understood that long-range correlations do *not* have to stem from long-range interactions! Even a system as simple as hard spheres can undergo a disordered-to-ordered (fluid-crystal) transition as the density is increased.

From the above it should be clear that correlations and correlation functions give us another way to characterize phases, as well as phase transitions, beyond the description provided by order parameters. Types of ordering are usually divided into three groups: (i) short-ranged ordering where the correlations decay rapidly to zero (typically exponentially), (ii) long-ranged ordering where the correlations decay to a constant, and (iii) quasi-long ranged order where the correlations decay *slowly* (typically algebraically) to zero. The slow-decaying correlations can, for instance, be found in the 2D hexatic phase that lies between a fluid and a crystal of hard disks moving in a plane, see, for example, the work by Thorneywork *et al.* [Phys. Rev. Lett. **118**, 158001 (2017)]. A phase transition should be sought in a change of the correlation, or equivalently in the behavior of the correlation length; let us turn to this aspect next.

### 11.3 First-Order and Continuous Phase Transitions

As we discussed previously, for instance in Chapter 6, at a phase transition, the macroscopic behavior of a system can change abruptly when the external conditions are varied continuously. When the phase transition takes place discontinuously (also known as first-order phase transition), the two states on either side of the transition coexist at the transition. Each of the two coexisting states has its own macroscopic properties and typically a finite amount of correlation. Adding to the observations in the previous section, even in a crystal close to coexistence the correlation is finite, due to the presence of defects. Thus, in a first-order phase transition, we expect a finite value of the correlation length, with some signature of the presence of a phase transition.

For a continuous phase transition, however, the result is markedly different. To illustrate this, consider the 2D or 3D Ising model without an external field. If we smoothly lower the temperature, the system abruptly changes a disordered to an ordered state at a temperature  $T_c$ . This is associated with a change in the average magnetization: above  $T_c$  the average magnetization is zero, while below  $T_c$ , the magnetization is finite. In other words, the spins point up and down and randomly and intuitively there should be limited correlation above  $T_c$ , while below  $T_c$  the spins are aligned and there is more significant correlation in the system. Yet, looking at it like this, there does not appear to be a major difference between a first-order and continuous phase transition. So what makes the continuous transition special?

The order parameter characterizing the system does not have a jump. The system accomplishes this by being a single phase that has features of both the disordered and the ordered phase at the critical point. This phase is often referred to as the *critical phase*. The critical phase has features of both phases on all length scales, as has been visualized for the site-percolation model in Chapter 10. This leads to correlations over all length scales. For every piece of ordered phase, you will encounter some order at some larger length scale, and *vice versa*. The correlation length for such a structure turns out to be divergent, as we will compute for the Ising model in the next section. This divergent correlation length is a general property of continuous phase transitions and together with the structure of the system it gives an inroad towards describing these systems theoretically.

### 11.4 Correlation Function for the 1D Ising Model

Now that we have set the stage for our analysis, let us turn to defining correlation functions for the Ising model. In Chapter 7, we studied the one-dimensional Ising model, and discovered that it was fairly easy to solve exactly. Hence, it seems a reasonable starting point for an introduction to correlation length<sup>4</sup>.

For a ferromagnetic system, it is logical to study the *spin-spin* correlation function defined by

$$G(i, j) = \langle S_i S_j \rangle - \langle S_i \rangle \langle S_j \rangle, \quad (11.1)$$

which measures the degree of correlation between spins at sites  $i$  and  $j$ . This definition is an extension of the concept of variance you have encountered in probability theory. We expect  $G(i, j)$  to be a useful quantity, as at infinite temperature, knowing the orientation of a spin at  $i$  does not inform us of the orientation of a spin at  $j$ ,  $G(i, j)$  is identically zero. In the ground state (all spins up or all down), knowing the spin at  $i$  implies that we know the spin at  $j$ , and  $G(i, j)$  is also uniformly zero. Anywhere in between, there will be some finite range of decay of the correlation, as the interaction tends to align neighboring spins. We will quantify this range next.

---

<sup>4</sup>The development of this section follows closely the discussion in Pathria and Beale, “Statistical Mechanics”.

Because in the 1D Ising model only the ground state is fully ordered, we have that  $\langle S_i \rangle = 0$  for any  $T > 0$ . Thus, we can reduce Eq. (11.1) to

$$G(i, j) = \langle S_i S_j \rangle. \quad (11.2)$$

Now recall from Chapter 7 that we can write the partition function of the Ising model as

$$Z(N, \beta) = \sum_{S_1} \sum_{S_2} \dots \sum_{S_N} \prod_{i=1}^{N-1} e^{\beta J S_i S_{i+1}}. \quad (11.3)$$

Next, we generalize this expression such that the pairwise interaction parameter  $J$  becomes site dependent:  $J_i$ . This will allow us to perform a mathematical trick, as we will see shortly. In this case, the partition function becomes

$$Z(N, \beta) = \sum_{S_1} \sum_{S_2} \dots \sum_{S_N} \prod_{i=1}^{N-1} e^{\beta J_i S_i S_{i+1}}. \quad (11.4)$$

These sums can be carried out in exactly the same manner as we did in Chapter 7 resulting in

$$\frac{1}{N} \log Z(N, \beta) = \log 2 + \frac{1}{N} \sum_{i=1}^{N-1} \log (\cosh(\beta J_i)). \quad (11.5)$$

To see what the trick is about, note that

$$\langle S_k S_{k+1} \rangle = \frac{1}{Z(N, \beta)} \left( \frac{1}{\beta} \frac{\partial}{\partial J_k} \right) Z(N, \beta) = \left( \frac{1}{\beta} \frac{\partial}{\partial J_k} \right) \log Z(N, \beta). \quad (11.6)$$

You can see that by taking the derivative of Eq. (11.4) and noting that the second term above becomes the definition of the average of  $S_k S_{k+1}$ . Hence, applying the derivative to the evaluated partition function of Eq. (11.5), the correlation function for *nearest neighbors* becomes

$$G_{nn}(k, k+1) = \langle S_k S_{k+1} \rangle = \tanh(\beta J_k). \quad (11.7)$$

Note that  $S_i^2 = 1$  for all  $i$ , therefore

$$S_k S_{k+p} = S_k S_{k+1} S_{k+1} S_{k+2} S_{k+2} \dots S_{k+p-1} S_{k+p}. \quad (11.8)$$

We can now expand the (*not* nearest neighbor) spin-spin correlation function as follows

$$\begin{aligned} G(k, k+p) &= \langle S_k S_{k+p} \rangle = \langle (S_k S_{k+1})(S_{k+1} S_{k+2}) \dots (S_{k+p-1} S_{k+p}) \rangle; \\ &= \frac{1}{Z(N, \beta)} \left( \frac{1}{\beta} \frac{\partial}{\partial J_k} \right) \left( \frac{1}{\beta} \frac{\partial}{\partial J_{k+1}} \right) \left( \frac{1}{\beta} \frac{\partial}{\partial J_{k+2}} \right) \dots \left( \frac{1}{\beta} \frac{\partial}{\partial J_{k+p-1}} \right) Z(N, \beta); \\ &= \prod_{i=k}^{k+p-1} \tanh \beta J_i. \end{aligned} \quad (11.9)$$

However, in the case of the simple Ising model that we studied in Chapter 7, we had  $J_i = J$ , *i.e.*, the coupling constant was not site dependent. Consequently, the spin-spin correlation function reduces to

$$G(k, k+p) = \tanh^p(\beta J). \quad (11.10)$$

We now define the *correlation length*  $\xi$  by writing Eq. (11.10) in the form

$$G(k, k+p) = e^{-p/\xi}, \quad (11.11)$$

which assumes that there is a single, natural length scale in the system over which (on average) the system loses the information that a spin at a given site  $k$  is pointing in a certain direction. This assumption leads to the following expression for the correlation length

$$\xi = \frac{1}{\log(\coth(\beta J))}. \quad (11.12)$$

In the limit of low temperature, *i.e.*, when  $\beta J \gg 1$ , the correlation length simplifies to

$$\xi \approx \frac{1}{2} e^{2\beta J}, \quad (11.13)$$

which implies that as  $T$  goes to 0,  $\xi$  diverges. This is consistent with what we found in Chapter 7. In particular we found that the 1D Ising model (at zero field) did not have a phase transition, and more specifically, that the 1D Ising model was ordered only when  $T = 0$ , *i.e.*, any thermal fluctuation is sufficient to disorder the system.

There is a subtlety here, however. At the start of this section, we noted that  $G(i, j) = 0$  for  $T = 0$ . In our analysis, a divergent correlation length  $\xi$  reintroduced in Eq. (11.11) would lead to a value of  $G(i, j) = 1$ , *i.e.*, the infinite correlation length crushes any finite positional difference in the exponent. This seems in contradiction, until we note that for  $T = 0$ ,  $\langle S_i \rangle \neq 0$ , which we assumed in the above calculation. In general, the correlation function in an ordered material does not decay to zero. For example, in the 2D Ising model finite temperature defects below  $T_c$  imply a finite value of  $0 < \langle S \rangle \leq 1$ . However, we know  $G(i, i) = 1$  and that spins close to our central spin are more likely to be pointed in the same direction. The decay toward the finite limiting value of  $G$  defines the correlation length in this case. Note that there is a second divergence of  $\xi$  as the temperature is lowered to  $T = 0$  for the 2D Ising model, as the correlation function flattens with the defects becoming further spaced out. In the 1D Ising model,  $T_c$  and  $T = 0$  pathologically coincide.

## 11.5 Correlations and Mean-Field Theory for the Ising Model

In the mean-field-theory Ising model, we have ignored correlations between the spins in a *homogeneous* system. It is, however, possible to make local variants of Landau theory (Ginzburg-Landau) and compute correlation functions for the Ising model in this manner using path integrals. This falls under the domain of Statistical Field Theory and goes beyond the scope of these notes. As such, we will not derive the Ising correlation function within the mean-field approximation, but just list and discuss the results here.

First, note that  $G(i, j)$  depends only on the distance between spins  $i$  and  $j$ . Hence, we can write  $G(i, j) = G(r)$ . Then, the correlation function for the Ising model in  $d$  dimensions can be written

$$G(r) \propto \left(\frac{a^2}{\xi r}\right)^{(d-2)/2} K_{(d-2)/2}(r/\xi), \quad (11.14)$$

where the correlation length is given by  $\xi = a(c'/t)^{1/2}$ , with  $a$  the effective lattice constant,  $c'$  a number of order unity which depends on the exact structure of the lattice, and  $K_\mu(x)$  a modified Bessel function. Additionally,  $t = (T - T_c)/T_c$ , with  $T_c$  the transition temperature. In three dimensions ( $d = 3$ ), the Bessel function is given by:

$$K_{1/2}(r/\xi) = e^{-r/\xi} \sqrt{\frac{\pi\xi}{2r}}. \quad (11.15)$$

The correlation function then reduces to:

$$G(r) = \frac{a}{r} \sqrt{\frac{\pi}{2}} e^{-r/\xi}. \quad (11.16)$$

As  $T$  approaches  $T_c$ , the correlation length  $\xi \propto (T - T_c)^{-1/2}$  diverges. Thus, correlations in the system occur at *all* length scales. This is typical of continuous phase transitions. Note that this scaling defines a critical exponent, which we will return to in Chapter 12. Lastly, note that the above expressions reveal that there is a short-ranged (relative to the exponential decay) power-law component to the correlation function. This is a result that holds in general.

## 11.6 Exercises

### Q71. Correlations and Eigenvalues of the Transfer Matrix

As we will prove in exercise Q72, the correlation length can also be found using the eigenvalues of the transfer matrix, whenever a system is amenable to such a method for obtaining an exact form of the partition function. Here, we will first show this to be true for the 1D Ising model by evaluating the expression for the transfer-matrix-based correlation length:

$$\xi = \left( \log \frac{\lambda_+}{\lambda_-} \right)^{-1}, \quad (11.17)$$

where  $\lambda_+$  is the largest eigenvalue and  $\lambda_-$  is the second largest eigen value of the transfer matrix  $\mathbf{T}$ . That is, in general, an  $N \times N$  transfer matrix has  $N$  eigenvalues  $\lambda_i$ , for which we require  $\lambda_+ > \lambda_- > \dots > \lambda_N$ . In the case of the 1D Ising model there are only 2 eigenvalues, see Eq. (7.27). Perform the necessary algebraic manipulations to recover the expression in Eq. (11.13). Hint: Note the condition on the magnetic field that results in Eq. (11.13). Plot how the correlation length departs from this zero-field result for several values of  $H$ .

### Q72. The Transfer-Matrix Method

In this exercise, we will show that Eq. (11.17) holds for a general partition function that can be decomposed by a transfer-matrix approach. Let  $\mathcal{H}$  be a Hamiltonian, which depends on interactions between  $N$  particles on a lattice that can all assume the same  $k$  states, labelled here as  $m$ . Then we may write the Hamiltonian as follows

$$\mathcal{H} = \sum_{i=1}^N \sum_{j=1}^N m_i C_{m_i m_j} m_j + \sum_{i=1}^N f_{m_i} m_i. \quad (11.18)$$

Here,  $C_{m_i m_j}$  indicates the coupling between states  $m_i$  and  $m_j$  and  $f_{m_i}$  represents interaction of state  $m_i$  with an external field.

- What would the form of  $m$ ,  $C$ , and  $f$  have to be in order to recover the 1D Ising model?
- Write down the partition function for the general model.

Next, we assume that the labeling  $i$  corresponds to some 1D positional ordering with fixed separation on a ring, *i.e.*, there are periodic boundary conditions. In addition, we assume that there are only nearest-neighbor interactions and that the field is homogeneous across space. In this case, we can use the transfer-matrix approach.

- Start by transforming the system to an orthonormal representation of the  $m_i$ . That is, the  $s$ th possible value of  $m_i$  is identified with the unit vector  $\hat{e}_s$  of length  $k$ , where the  $s$ th element is 1 and the rest is zero. What is the expression for  $m_i$  in terms of these unit vectors, assume that there is a diagonal matrix  $\mathbf{M}$  that brings the orthonormal basis into the regular basis. Write down  $\mathcal{H}$  in the matrix form, as well as the partition function in this new basis.
- Let  $\mathbf{T}_i$  denote the  $i$ th transfer matrix for this model. Show that the individual terms in the partition sum are given by  $\hat{e}_i^T \mathbf{T}_i \hat{e}_{i+1}$ , where the superscript  $T$  denotes transposition. Provide an expression for the full transfer matrix. Use the properties of the unit vectors to show that the partition function may be written

$$Z_N = \sum_{e_1} \hat{e}_1^T \left( \prod_{i=1}^N \mathbf{T}_i \right) \hat{e}_1 = \text{Tr} \left( \prod_{i=1}^N \mathbf{T}_i \right). \quad (11.19)$$

Finally, assume that all  $\mathbf{T}_i$  are the same, *i.e.*, write  $\mathbf{T}$ . Introduce the orthogonal matrices  $\mathbf{O}$  by which  $\mathbf{T}$  can be diagonalized, *i.e.*,  $\mathbf{T} = \mathbf{O}\mathbf{\Lambda}\mathbf{O}^T$  with  $\mathbf{\Lambda}$  the diagonal matrix with eigenvalues  $\lambda_+ > \lambda_- > \dots > \lambda_k$ . We will now compute the correlation between particles that 1 and  $L$ , which are a reduced distance  $L$  apart. We are now in a position to derive the correlation length.

- (e) What is entailed in the assumption that all  $\mathbf{T}_i$  are the same?  
 (f) Write down the expression for the correlation function  $\langle m_1 m_L \rangle$  in terms of the partition function  $Z_N$  and the Hamiltonian  $\mathcal{H}$  in our orthonormal basis.  
 (g) Rewrite this using the transfer matrices to read

$$\langle m_1 m_L \rangle = \frac{\sum_{\{e_i\}} m_1 \hat{e}_1^T \mathbf{T} \hat{e}_2 \cdots \hat{e}_{L-1}^T \mathbf{T} \hat{e}_L m_L \hat{e}_L^T \mathbf{T} \hat{e}_{L+1} \cdots \hat{e}_N^T \mathbf{T} \hat{e}_1}{\sum_{i=1}^k \lambda_i^N}, \quad (11.20)$$

and reshape this to

$$\langle m_1 m_L \rangle = \frac{\sum_{v_1} \sum_{v_L} \left( m_1 \mathbf{v}_1^T \mathbf{\Lambda}^L \mathbf{v}_L \right) \left( m_L \mathbf{v}_L^T \mathbf{\Lambda}^{N-L} \mathbf{v}_1 \right)}{\sum_{i=1}^k \lambda_i^N}, \quad (11.21)$$

where the  $\mathbf{v}$  are eigenvectors to  $\mathbf{\Lambda}$  and the sums are over the elements.

- (h) Take the thermodynamic limit to reveal

$$\lim_{N \uparrow \infty} \langle m_1 m_L \rangle = \tilde{m}_+ \tilde{m}_+ + \sum_{k \neq +} \left( \frac{\lambda_k}{\lambda_+} \right)^L \tilde{m}_k \tilde{m}_+, \quad (11.22)$$

where  $\tilde{m}_i = \sum_{q=1}^k m_q \mathbf{v}_q^T \mathbf{v}_i$ , *i.e.*, the value of  $m$  with respect to the eigenvectors of  $\mathbf{T}$ .

- (i) Argue that analogously, in the thermodynamic limit,  $\langle m_j \rangle = \tilde{m}_+$  and that consequently the correlation function reads

$$G(L) = \lim_{N \uparrow \infty} (\langle m_1 m_L \rangle - \langle m_1 \rangle \langle m_L \rangle) = \sum_{k \neq +} \left( \frac{\lambda_k}{\lambda_+} \right)^L \tilde{m}_k \tilde{m}_+. \quad (11.23)$$

- (j) Finally, take the limit  $L \uparrow \infty$  of the function  $-(1/L) \log G(L)$  to obtain  $\xi^{-1}$  and thereby recover the result in Eq. (11.17).



## Chapter 12

# Critical Exponents and Universality

In Chapter 10, we discovered that continuous phase transitions are special in the sense that there is a scale invariance. This gave us a handle on how to compute the critical point (approximatively) using RG theory and obtain expressions for the free energy and partition function at this point. The latter were dependent on the self-similar structure of the system, rather than on the interaction details. This then implies that near a critical point, many properties of a system are largely independent of the microscopic details of the interactions between the individual particles. Admittedly, that is an oversimplification, as the 2D and 3D Ising models have different critical exponents and are therefore not quite the same in this regard. However, it turns out that there are systems that appear vastly different from a microscopic perspective, which nonetheless possess the same critical exponents. These systems are said to belong to the same *universality class*. In this chapter, we will briefly explore what this means.

### 12.1 The Ising Model and the Gas-Liquid System

Many physical quantities associated with systems that have continuous phase transitions display power-law behavior in the vicinity of the critical point. It is customary to introduce two dimensionless variables to describe this type of response, namely:

- the *reduced temperature* defined as  $t = (T - T_c) / T_c$  ;
- the *reduced external field* defined  $h = \beta H$  .

Using these definitions, we can write down the following five critical exponents for the Ising model:

$\alpha$ : For  $h = 0$  the *specific heat* scales as

$$C \propto \begin{cases} A |t|^{-\alpha} & (t > 0) \\ A' |t|^{-\alpha'} & (t < 0) \end{cases}, \quad (12.1)$$

for which it can be shown that  $\alpha = \alpha'$ . Note that  $A$  is not typically equal to  $A'$ , but (we will not show this in these notes) renormalization-group theory predicts that the ratio  $A/A'$  is the

same for members of the universality class. For the 2D Ising model  $\alpha = 0$ , which implies that the divergence is not power-law. There is a lower-order divergence, however, which is logarithmic in nature, as we have seen previously for the 2D Ising model in Chapter 7. For the 3D Ising model the exponent is given by  $\alpha = 0.11008$ .

$\beta$ : The *spontaneous magnetization* is given by

$$\lim_{h \downarrow 0} M \propto (-t)^\beta, \quad (12.2)$$

for  $t < 0$ . That is, the magnetization is defined for temperatures smaller than the critical temperature. For the 2D and 3D Ising models  $\beta = 1/8$  and  $0.326419$ , respectively.

$\gamma$ : For  $h = 0$  the *susceptibility* follows the power law

$$\chi \equiv \lim_{H \downarrow 0} \left( \frac{\partial M}{\partial H} \right)_T \propto \begin{cases} |t|^{-\gamma} & (t > 0) \\ |t|^{-\gamma'} & (t < 0) \end{cases}. \quad (12.3)$$

It follows from renormalization-group theory that  $\gamma = \gamma'$ . For the 2D and 3D Ising models  $\gamma = 7/4$  and  $1.237075$ , respectively.

$\delta$ : The *magnetization* at the critical temperature, *i.e.*, when  $t = 0$ , follows the power law

$$M \propto |h|^{1/\delta}. \quad (12.4)$$

For the 2D and 3D Ising models  $\delta = 15$  and  $4.78984$ , respectively.

$\nu$ : The *correlation length* ( $\xi$ ) at zero field  $h = 0$  scales as

$$\xi \propto |t|^\nu. \quad (12.5)$$

For the 2D and 3D Ising models  $\nu = 1$  and  $0.629971$ , respectively. Above and below the critical point the power may be different in general, *i.e.*, there can be a  $\nu$  and  $\nu'$ . Note that the correlation length is related to the asymptotic behavior of the correlation function associated with the fluctuations in the local magnetization by

$$G(r) = \frac{e^{-r/\xi}}{r^{-(d-2+\eta)}}, \quad (12.6)$$

with  $d$  the dimension of space and  $\eta$  another critical exponent, given by  $\eta = 1/4$  and  $0.036298$  for the 2D and 3D Ising models, respectively.

In the case of a system that undergoes a gas-liquid phase transition, we can determine the same critical exponents. This might require some explanation. The liquid-gas transition is a first-order transition, after all. However, recall from Chapter 6 that there is a temperature, the critical temperature  $T_c$ , above which the distinction between a gas and a liquid vanishes. The phase above this temperature is referred to as a fluid. At the critical temperature, the density gap between gas and liquid vanishes and the transition between the two becomes continuous. Therefore, we can examine critical exponents for a gas-liquid phase transition, provided we are in the rather special case of  $T = T_c$ .

Clearly, our variables need to be changed to suit the system. The pressure with respect to the critical pressure  $P - P_c$  takes the place of the applied field  $H$ . The magnetization  $m$  is replaced by  $\rho_l - \rho_c$ , where  $\rho_l$  is the density of the liquid and  $\rho_c$  is the density at the critical point. We now find

- $\alpha$ : The specific heat is given by  $C_V \propto |t|^{-\alpha}$  when  $\rho_l = \rho_c$ .
- $\beta$ : The shape of the coexistence curve in the vicinity of the critical point is given by  $(\rho_l - \rho_g) \propto (-t)^\beta$  for  $t < 0$ .
- $\gamma$ : The zero-field susceptibility is replaced by the isothermal compressibility, which behaves as follows near the critical point  $k_T \propto |t|^{-\gamma}$ .
- $\delta$ : The magnetization at the critical temperature is replaced with

$$|P - P_c|_{t=0} \propto |\rho_l - \rho_c|^\delta, \quad (12.7)$$

which describes the shape of the critical isotherm in the vicinity of the critical point.

- $\nu$ : The correlation length has the same shape as that of the ferromagnet. However, the correlation function is now a density-density rather than spin-spin correlation function.

Interestingly, the experimentally obtained critical exponents for argon are  $\alpha = 0.108 \pm 0.010$ ,  $\beta = 0.339 \pm 0.006$ ,  $\gamma = 1.20 \pm 0.002$ , and  $\eta = 0.045 \pm 0.010$ , from which it follows  $\delta \approx 4.5$  and  $\nu \approx 0.62$  [Anisimov *et al.*, Sov. Phys. JETP **49**, 844 (1979)]. Similar analyses have been performed on xenon, carbon dioxide, and hydrogen [Green *et al.*, Phys. Rev. Lett. **8**, 1113 (1967)], which led to comparable numbers. Lastly, for the archetypal Lennard-Jones simulation model, see Chapter 13 for more information, the following numbers were obtained:  $\alpha \approx 0.11$ ,  $\beta = 0.3285(7)$ ,  $\gamma \approx 1.23$ ,  $\delta \approx 4.7$ ,  $\nu = 0.63(4)$ , and  $\eta = 0.043$  [Watanabe *et al.*, J. Chem. Phys. **136**, 204102 (2012)]. Here, we have used scaling relations

$$\nu d = 2 - \alpha = 2\beta + \gamma = \beta(\delta + 1) = \gamma \frac{\delta + 1}{\delta - 1}; \quad (12.8)$$

$$2 - \eta = \frac{\gamma}{\nu} = d \frac{\delta - 1}{\delta + 1}, \quad (12.9)$$

to obtain the numbers that were not provided, as indicated using  $\approx$  signs. We will touch upon the concept of scaling relations in one of the exercises.

The take-away message is that there are only a finite number of exponents and these are not fully independent. The startling conclusion is that the critical behavior of the 3D Ising model, which is a lattice-based description of (anti)ferromagnetism, and a general off-lattice molecular system undergoing gas-liquid phase separation have the same critical exponents! Or in other words, these seemingly different systems behave identically near the critical point and therefore belong to the same *universality class*. The transition to the Bose-Einstein condensate in a Bose gas belongs to a different class.

## 12.2 Landau Theory Critical Exponents

Next, we consider Landau theory and examine what this theory has to say about criticality. Assume we have a system where the Landau expansion consists of  $m^2$  and  $m^4$  terms, in an external field  $h$ . Then, the Landau free energy can be written

$$f(t, m) = -hm + b(t)m^2 + dm^4 \quad (12.10)$$

where  $d$  is a positive constant,  $t = (T - T_c)/T_c$ , and we can approximate  $b(t) = b't$ . In Chapter 9, we studied the case where the external field  $h$  was zero and found this expansion represents a system with

a continuous phase transition. When  $h = 0$ , we can calculate the equilibrium value of  $m$  by finding the minimum of  $f$ . Taking the derivative with respect to  $m$  gives us

$$-h + 2b'tm + 4dm^3 = 0. \quad (12.11)$$

When  $h = 0$  and  $t < 0$ , *i.e.*, in the ordered phase, the above expression implies that the magnetization scales as  $m \propto (-t)^{1/2}$ , which yields the exponent  $\beta = 1/2$ . The zero-field susceptibility ( $h \rightarrow 0^+$ ) is given by

$$\chi = \lim_{h \downarrow 0} \left( \frac{\partial h}{\partial m} \right)_t^{-1} = \frac{1}{2b't + 12dm^2}. \quad (12.12)$$

When  $t > 0$ , the system is disordered and  $m = 0$ . Hence, the zero-field susceptibility is given by

$$\chi \propto \frac{1}{2b't} \quad (12.13)$$

implying the  $\gamma = 1$ . In contrast, when  $t < 0$ , *i.e.*, when the system is ordered, the magnetization scales as  $m = \sqrt{b'|t|/2d}$ . The positive root is chosen, since we are assuming that  $h \downarrow 0$ . In this limit, we obtain

$$\chi \propto \frac{1}{4b'|t|}, \quad (12.14)$$

and therefore  $\gamma' = 1$ . Lastly, at the critical temperature,  $t = 0$ , the magnetization can be read off from Eq. (12.11), which gives us

$$m \propto \left( \frac{h}{4d} \right)^{1/3}, \quad (12.15)$$

and  $\delta = 3$ . Using the scaling relations we can summarize the critical exponents for the Landau expression of Eq. (12.10) as:  $\alpha = 0$ ,  $\beta = 1/2$ ,  $\gamma = 1$ , and  $\delta = 3$ . The values of  $\nu$  and  $\eta$  depend on the dimension of the system and cannot be obtained in pure Landau theory. It turns out that this Landau theory is in the same universality class as the four-dimensional Ising model. This might not be entirely surprising as a mean-field theory should become better as the dimensionality increases.

## 12.3 Exercises

### Q73. Critical Exponents from Pathria and Beale (*Statistical Mechanics*)

Consider a system with a Landau free energy given by

$$f(t, m) = -hm + r(t)m^2 + um^6, \quad (12.16)$$

with  $u$  a positive constant and  $t = (T - T_c)/T_c$ . Approach the tri-critical (three-phase critical) point along the  $r$ -axis by setting  $r(t) = r't$ . Show that the critical exponents are  $\beta = 1/4$ ,  $\gamma = 1$ , and  $\delta = 5$ . What is the value of  $\alpha$ ?

### Q74. Rushbrook Inequality

Consider the internal energy  $U(S, B)$  for a magnetic system subject to a field  $B$  in the thermodynamic limit, where  $S$  is the entropy. We have that the differential of  $U$  is given by  $dU = TdS - MdB$  with  $M$  the magnetization and  $T$  the temperature. We define the constant-temperature magnetic susceptibility

$$\chi_T = \left( \frac{\partial M}{\partial B} \right)_T, \quad (12.17)$$

and the specific heat at constant field strength

$$c_B = T \left( \frac{\partial S}{\partial T} \right)_B. \quad (12.18)$$

(a) Show that the follow equality holds

$$\chi_T (c_B - c_M) = T \left( \frac{\partial M}{\partial T} \right)_B^2, \quad (12.19)$$

using the magnetic analogue of a Maxwell relation. Here,  $c_M$  is the specific heat at constant magnetization, which is defined analogously to  $c_B$ . Hint: You need to make use of Maxwell's relations, Legendre transforms, and the tripple-product rule.

(b) Use stability of the system to write down the inequality for  $c_B$ , namely  $c_B > (T/\chi_T) (\partial M/\partial T)_B^2$  from Eq. (12.19).

(c) Assume  $H = 0$  and  $t < 0$  and plug in the near-critical power-law expansions for the  $M$ ,  $c_B$ , and  $\chi_T$  to obtain  $\alpha' + 2\beta + \gamma' \geq 2$ .

Further inequalities may be derived from the convexity of the free energy, such as the Griffiths inequality  $\alpha' + \beta(\delta + 1) \geq 2$ . Proving the equalities requires a more sophisticated approach.



## Chapter 13

# Classical Non-Ideal Gases and Dilute Fluids

The classical ideal-gas laws  $pV = Nk_{\text{B}}T$  and  $E = \frac{3}{2}Nk_{\text{B}}T$ , see Chapter 4, do not hold for real gases at finite density  $\rho = N/V$ , because there are interactions between the atoms or molecules comprising the gas. In theoretical descriptions of such systems, it is often assumed that the interactions are *pairwise additive*, *i.e.*, the interaction energy is a sum of terms characterized by a pair potential  $\phi(\mathbf{r}_i - \mathbf{r}_j)$  that depends on the relative coordinates of particle  $i$  and  $j$ . For simple fluids the pair potential is radially symmetric, which means that the Hamiltonian can be written as

$$\mathcal{H}(\mathbf{\Gamma}) = \sum_{i=1}^N \frac{\mathbf{p}_i^2}{2m} + \sum_{i<j}^N \phi(r_{ij}), \quad (13.1)$$

with  $r_{ij} = |\mathbf{r}_i - \mathbf{r}_j|$  the radial distance between particle  $i$  and  $j$  and  $\mathbf{\Gamma}$  the full  $6N$ -dimensional phase-space coordinates, as in Chapter 3. Radial symmetry is a good approximation for the noble gases, and a fair approximation for small molecules like  $\text{CH}_4$  (methane),  $\text{N}_2$ , and  $\text{O}_2$ . The typical form of  $\phi(r)$  for such simple atomic systems is depicted in Fig. 13.1.

Over the years, many empirical ‘laws’ have been introduced to account for the deviations from ideality for systems with real interactions. One of the most fundamental of these is due to Kamerlingh-Onnes, who introduced, on empirical grounds, the virial expansion for the pressure. It is written as

$$p(\rho, T) = k_{\text{B}}T (\rho + B_2(T)\rho^2 + B_3(T)\rho^3 + \dots), \quad (13.2)$$

where the temperature dependent virial coefficients  $B_n(T)$  can be obtained by fitting to the observed deviations from ideal-gas behavior. In this chapter, we will *derive* the functional form of Eq. (13.2) using the ensemble formalism developed in previous chapters, and find explicit expressions for the virial coefficients in terms of the interaction potential between the particles.

### 13.1 Features of Atomic Gases

Atomic gases have many properties that are intriguing from a general physics perspective, *e.g.*, their flow and dynamics. However, for the purpose of an equilibrium classical statistical mechanics description, two features emerge as the most relevant:

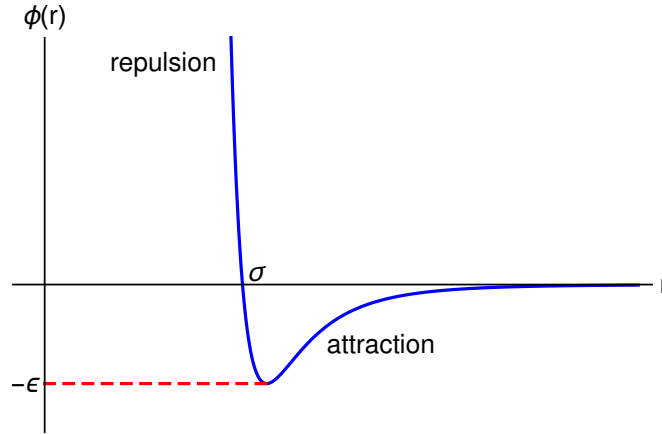


Figure 13.1: Typical pair potential  $\phi$  as a function of the particle separation  $r$  for molecules of ‘diameter’  $\sigma$  comprising a simple fluid.  $\epsilon$  sets the attraction strength.

- The interaction is steeply repulsive for  $r \lesssim \sigma$ , with  $\sigma$  a measure for the diameter of the particle. For simple fluids  $\sigma$  is typically 2 to 5 Å. This short-ranged repulsion is due to Pauli exclusion (and Coulomb repulsion) between outer shell electrons of two particles in close proximity.
- The interaction is attractive for  $r \gtrsim \sigma$ , with Van der Waals interactions  $\phi(r) \propto -r^{-6}$  when  $r \gg \sigma$ . These attractions are caused by correlated (induced) dipole fluctuations between the two particles. The range over which these attractions are appreciable is typically  $\simeq 2\sigma$ . The depth of the minimum,  $-\epsilon$ , that occurs at  $r \simeq \sigma$ , depends on the chemical species.

Physically, one wishes to capture these salient features of the molecular interactions using relatively simple potentials, as we will return to shortly. The question we will address in this chapter is how to relate microscopic interactions to macroscopic observables such as the pressure, and to phenomena such as liquid condensation.

## 13.2 Simple Interaction Models

A convenient, successful, and famous parameterization for molecular interactions is the Lennard-Jones form that is commonly encountered in numerical simulations of atomistic systems:

$$\phi_{\text{LJ}}(r) = 4\epsilon \left[ \left( \frac{\sigma}{r} \right)^{12} - \left( \frac{\sigma}{r} \right)^6 \right], \quad (13.3)$$

which gives good agreement with many experiments by adjusting the well depth  $\epsilon$  and ‘size’  $\sigma$ . The term with exponent 12 captures the short-ranged repulsive nature, but this value of the exponent has no physical motivation; it (still) is simply computationally efficient to compute. A less realistic, but an analytically more tractable form is the square-well potential

$$\phi_{\text{sw}}(r) = \begin{cases} \infty & r < \sigma \\ -\epsilon & \sigma < r < \lambda\sigma \\ 0 & r > \lambda\sigma \end{cases}, \quad (13.4)$$

where  $\sigma$  denotes the hard-core diameter and where  $\lambda > 1$  is a measure for the range of the attractive well. Another important potential is the hard-sphere potential

$$\phi_{\text{HS}}(r) = \begin{cases} \infty & r < \sigma \\ 0 & r > \sigma \end{cases}, \quad (13.5)$$

where  $\sigma$  is the hard-sphere diameter. The hard-sphere system does not contain any attraction, but does describe the short-ranged atomic repulsions crudely. Neglecting attractions may seem unphysical at first sight, but we will see that the hard-sphere fluid plays a crucial role as a reference zeroth-order approximation in perturbation theory of liquids, where the attractions are treated as a small modification of the purely repulsive short-ranged interactions. The hard-sphere fluid itself is also extremely interesting, as it undergoes a fluid-solid phase transition that is exclusively driven by entropy. For this reason the hard-sphere fluid has been of great theoretical importance. Moreover, due to advances in the synthesis of colloidal particles — mesoscopic solid particles with diameter in the range from 1 nm to 1  $\mu\text{m}$  — experimental realizations of hard-sphere systems actually exist in the form of colloidal suspensions.

### 13.3 Van der Waals Theory

In his 1873 thesis, Van der Waals proposed two corrections to the ideal-gas law  $p = Nk_{\text{B}}T/V$  that address the repulsive/attractive character of simple atomic liquids. Firstly, he argued that the actual volume available to a molecule is smaller than the total volume  $V$  of the container, because the finite diameter (or volume) of each molecule excludes some volume, say  $b$ , to all the others. Secondly, he argued that the attractions between the molecules reduce the pressure  $p$  by an amount  $-a\rho^2$ , where  $a > 0$  is a measure of the strength of the attractions. Taking these two mean-field-like approximations into consideration, Van der Waals wrote

$$p = \frac{Nk_{\text{B}}T}{V - Nb} - a\rho^2 = \frac{\rho k_{\text{B}}T}{1 - \rho b} - a\rho^2 = \frac{k_{\text{B}}T}{v - b} - \frac{a}{v^2}, \quad (13.6)$$

where  $v = 1/\rho = V/N$  is the volume per particle and  $a$  and  $b$  are phenomenological parameters. Note that the very existence of molecules was not generally accepted in Van der Waals' days, and their interactions were not understood in a modern sense, as this requires knowledge of quantum mechanics. Nonetheless, Van der Waals got the essential features of short-ranged repulsions (giving the excluded volume  $b$ ) and the long-ranged attractions (parameterized by  $a$ ) right. Moreover, his splitting of these two effects into two separate contributions is fully consistent with the perturbation theory about a hard-sphere reference fluid, as we will see later.

Figure 13.2 shows a plot of the pressure as a function of density at several temperatures, the curves follow from Van der Waals' expression [Eq. (13.6)]. At sufficiently high temperatures,  $T > T_c$ , the pressure increases monotonically with density, whereas at low enough temperatures,  $T < T_c$ , there is a density regime with  $(\partial p/\partial \rho)_T < 0$ . The critical isotherm, at temperature  $T_c$ , separates these two regimes, and shows a point of inflection with zero slope at the critical density  $\rho_c$ . The critical point  $(\rho_c, T_c)$  follows from the conditions

$$\left. \begin{aligned} \left(\frac{\partial p}{\partial \rho}\right)_{T_c} &= 0 \\ \left(\frac{\partial^2 p}{\partial \rho^2}\right)_{T_c} &= 0 \end{aligned} \right\} \implies \begin{aligned} \rho_c b &= 1/3 \\ k_{\text{B}}T_c &= \frac{8a}{27b}. \end{aligned} \quad (13.7)$$

This result will be worked out in detail in one of the exercises. As discussed in Chapter 6, a negative slope in the isotherm  $p(\rho)$ , *i.e.*, a negative compressibility, signifies a thermodynamic instability. That

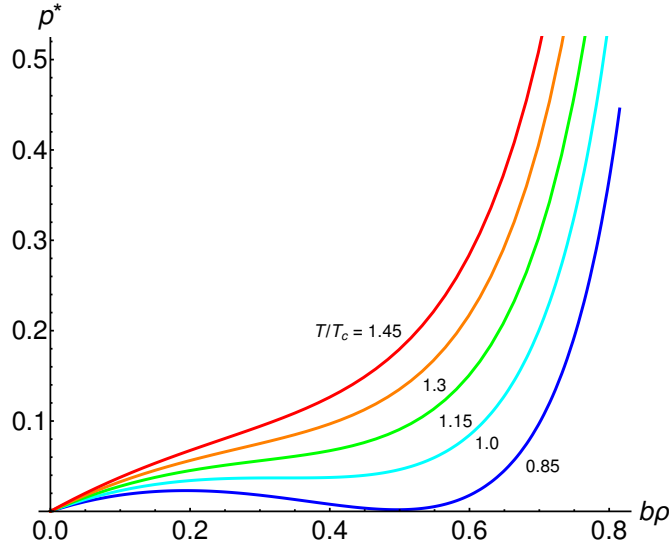


Figure 13.2: The reduced Van der Waals' pressure  $p^* = b^2 p/a$  as a function of the reduced density  $\rho b$  for temperatures  $T$  above, at, and below the critical temperature  $T_c$ , as indicated by the labeling.

is, this is an example of an approximative free energy mentioned in that chapter. Critical exponents can also be derived for the Van der Waals model, but we will not do so here.

We will now determine the Helmholtz free energy for this system. From  $p = -(\partial F/\partial V) = -f + \rho(\partial f/\partial \rho)_T$ , with  $f = F/V$  the free-energy density, it follows from a straightforward integration that

$$f_{\text{VdW}} \equiv \frac{F_{\text{VdW}}}{V} = \rho k_B T \left( \log \frac{\rho \Lambda^3}{1 - b\rho} - 1 \right) - a\rho^2, \quad (13.8)$$

where the integration constant is chosen such that the ideal-gas free energy is obtained in the limit  $\rho \rightarrow 0$ . A plot of  $f_{\text{VdW}}$ , in reduced units, is shown in Fig. 13.3.

Note that the convexity of the free energy is directly related to the slopes of the equation of state in Fig. 13.2, since

$$\left( \frac{\partial p}{\partial \rho} \right)_T = \frac{\partial}{\partial \rho} \left( -f + \rho \left( \frac{\partial f}{\partial \rho} \right)_T \right)_T = \rho \left( \frac{\partial^2 f}{\partial \rho^2} \right)_T. \quad (13.9)$$

A negative compressibility is therefore equivalent to a concave part in  $f(\rho)$ . Recall from Chapter 6 that the set of points  $\rho(T)$  for which  $(\partial^2 f/\partial \rho^2)_T = 0$  is called the *spinodal*. The spinodal densities at  $T = 0.85T_c$  are indicated by the arrows in Fig. 13.3. Following the common-tangent methodology described in Chapter 6, the full phase diagram of this system can now be determined. This will be left as an exercise for the reader.

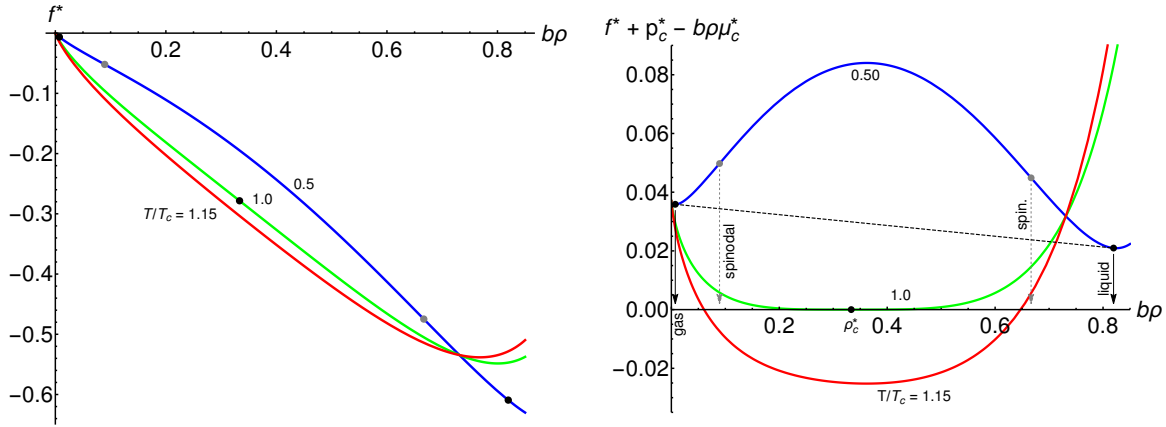


Figure 13.3: The reduced Van der Waals' free-energy density  $f^* = b^2 f/a$  ( $\Lambda = b^{1/3}$ ) as a function of the reduced density  $\rho b$ . The function is plotted for three temperatures  $T$  above ( $T = 1.15T_c$ ), at ( $T = T_c$ ), and below ( $T = 0.5T_c$ ) the critical temperature  $T_c$ , as indicated using the labeling. The left-hand graph shows regular form of the reduced free-energy density. The position of the coexistence points (black) and the inflection points (gray) is indicated using points. The right-hand graph shows the same data, but the reduced free-energy density is now shifted by the reduced critical pressure  $p_c^*$  and a linear form involving the reduced critical chemical potential  $\mu_c^*$  has been added. The latter makes it slightly easier to see the common-tangent line for the sub-critical free energy. Note that this form implies that at the critical point, the common-tangent coincides with the  $b\rho$ -axis and that the critical point is located on this axis, as indicated using  $\rho_c^*$ .

## 13.4 Virial Expansion

For later reference we also calculate the density expansion of the excess (with respect to the ideal gas contribution) Helmholtz free-energy density

$$\frac{F - F_{\text{id}}}{Vk_{\text{B}}T} = f - f_{\text{id}} = f_{\text{ex}} = \sum_{n=2}^{\infty} C_n(T)\rho^n, \quad (13.10)$$

with  $C_n(T)$  the coefficients to be determined. Note the subtle difference in the way we define  $f$  here with respect to in Eq. (13.8). Recalling that  $p/k_{\text{B}}T = -f + \rho(\partial f/\partial \rho)_T$ , we have

$$\frac{p - p_{\text{id}}}{k_{\text{B}}T} = -f_{\text{ex}} + \rho \left( \frac{\partial f_{\text{ex}}}{\partial \rho} \right)_T = \sum_{n=2}^{\infty} (n-1)C_n(T)\rho^n, \quad (13.11)$$

which in combination with the virial expansion for the pressure, Eq. (13.2), yields

$$C_n(T) = \frac{B_n(T)}{n-1} \quad n \geq 2. \quad (13.12)$$

The Helmholtz free energy can thus be written as

$$\frac{F}{Vk_{\text{B}}T} = f = \rho \log(\rho\Lambda^3) - \rho + B_2(T)\rho^2 + \frac{B_3(T)}{2}\rho^3 + \dots \quad (13.13)$$

### 13.4.1 The Mayer Expansion

Here, we examine a theoretical foundation for the virial expansion and develop theoretical expressions for the virial coefficients. To begin, we consider a gas described by a Hamiltonian of the form (13.1) in a fixed volume  $V$ . It turns out to be convenient to consider this system grand canonically, *i.e.*, at fixed temperature  $T$  and fixed chemical potential  $\mu$ ; or equivalently at fixed inverse thermal energy  $\beta = 1/k_{\text{B}}T$  and the thermal-volume-weighted fugacity  $\tilde{z} = \exp[\beta\mu]/\Lambda^3$ . The starting point of our analysis is the grand-canonical partition function, which takes the form

$$\begin{aligned}\Xi(\mu, V, T) &= \sum_{N=0}^{\infty} \frac{\exp[\beta\mu N]}{N!\Lambda^{3N}} \int_V d\mathbf{r}^N \exp \left[ -\beta \sum_{i<j}^N \phi(r_{ij}) \right]; \\ &= \sum_{N=0}^{\infty} \frac{\tilde{z}^N}{N!} Q(N, V, T); \\ &\equiv 1 + Q_1 \tilde{z} + \frac{1}{2} Q_2 \tilde{z}^2 + \frac{1}{3!} Q_3 \tilde{z}^3 + \dots,\end{aligned}\tag{13.14}$$

where we defined the configurational integral

$$Q_N \equiv Q(N, V, T) = \int_V d\mathbf{r}^N \exp \left[ -\beta \sum_{i<j}^N \phi(r_{ij}) \right].\tag{13.15}$$

Combining Eq. (13.14) with the Taylor expansion  $\log(1+x) = \sum_{n=1}^{\infty} \frac{(-1)^{n+1}}{n} x^n$ , and collecting terms with the same power of  $\tilde{z}$ , we can write

$$\log \Xi = V \sum_{j=1}^{\infty} b_j \tilde{z}^j,\tag{13.16}$$

where the first few coefficients are given explicitly by

$$b_1 = \frac{1}{V} Q_1 = 1;\tag{13.17}$$

$$b_2 = \frac{1}{2!V} (Q_2 - Q_1^2);\tag{13.18}$$

$$b_3 = \frac{1}{3!V} (Q_3 - 3Q_2 Q_1 + 2Q_1^3);\tag{13.19}$$

$$b_4 = \frac{1}{4!V} (Q_4 - 4Q_3 Q_1 - 3Q_2^2 + 12Q_2 Q_1^2 - 6Q_1^4).\tag{13.20}$$

Even though the expressions for  $b_j$  become more cumbersome as  $j$  increases, it is possible to write down a general formula for  $b_j$  in terms of the  $Q_i$ s; we will not do that here as we focus on the first few terms only. Note that we implicitly assumed that the expansion of Eq. (13.16) exists. Generally speaking, convergence of the Mayer function is not guaranteed and care needs to be taken when moving very far away from the low-density limit or using long-ranged potentials.

Inserting the expansion of Eq. (13.16) into the expressions for  $p(\tilde{z}, T) = k_{\text{B}}T(\log \Xi)/V$  and  $N = \tilde{z}(\partial \log \Xi / \partial \tilde{z})_T = \rho(\tilde{z}, T)V$  yields

$$p(\tilde{z}, T) = k_{\text{B}}T \sum_{j=1}^{\infty} b_j \tilde{z}^j;\tag{13.21}$$

$$\rho(\tilde{z}, T) = \frac{\tilde{z}}{V} \frac{\partial \log \Xi}{\partial \tilde{z}} = \sum_{j=1}^{\infty} j b_j \tilde{z}^j.\tag{13.22}$$

Now we have both  $p$  and  $\rho$  as a power series in  $\tilde{z}$ , whereas much experimental data involves the density dependence of the pressure, *e.g.*, see Eq. (13.2). It is our task now to eliminate  $\tilde{z}$  between the Eqs. (13.21) and (13.22). This can be accomplished algebraically by writing

$$\tilde{z} = a_1\rho + a_2\rho^2 + a_3\rho^3 + \cdots, \quad (13.23)$$

where the yet unknown coefficients  $a_j$  follow by inserting Eq. (13.23) into Eq. (13.22) and equating the resulting coefficients of each power of  $\rho$  on both sides of the equation. This gives

$$a_1 = 1; \quad (13.24)$$

$$a_2 = -2b_2; \quad (13.25)$$

$$a_3 = -3b_3 + 8b_2^2. \quad (13.26)$$

Higher-order terms become more complicated but are, in principle, tractable as well, though probably using a computer to keep track of all the coefficients. Inserting the density expansion of  $\tilde{z}$ , given by the Eq. (13.23) and the above  $a_i$ , into the fugacity expansion of  $p$ , Eq. (13.21), yields a density expansion of the pressure as phenomenologically provided in Eq. (13.2), but now with explicit expressions for the virial coefficients,

$$B_2(T) = -b_2; \quad (13.27)$$

$$B_3(T) = 4b_2^2 - 2b_3. \quad (13.28)$$

These expressions will be worked out in detail below.

### 13.4.2 The Second Virial Coefficient $B_2(T)$

The second virial coefficient is given by

$$\begin{aligned} B_2(T) &= -b_2; \\ &= -\frac{1}{2V} \left( \int d\mathbf{r}_1 d\mathbf{r}_2 (\exp[-\beta\phi(r_{12})] - 1) \right) \\ &= -\frac{1}{2} \int d\mathbf{r} f(r), \end{aligned} \quad (13.29)$$

where we used translational invariance of the pair interaction, ignored (small) surface effects that arise when  $\mathbf{r}_1$  and/or  $\mathbf{r}_2$  are close to the wall of the container, and where we introduced the Mayer function (named after the couple that first performed this analysis)

$$f(r) = \exp[-\beta\phi(r)] - 1. \quad (13.30)$$

We have now expressed the lowest-order correction to the ideal-gas pressure in terms of the pair interaction  $\phi(r)$ . The Mayer function is temperature dependent, and is shown in Fig. 13.4 for the Lennard-Jones potential (13.3).

We first remark that  $f(r)$  for  $r < \sigma$  is rather insensitive to the details of  $\phi(r)$ ; it equals  $-1$  as long as  $\phi(r) \gg k_B T$ . At  $r \approx \sigma$ , the Mayer function changes sign quite abruptly, goes through a positive maximum and decays to zero as  $f(r) \simeq -\beta\phi(r)$  for  $r \gg \sigma$ . The latter implies that  $B_2$  exists, *i.e.*, is finite, if  $\phi(r)$  decays to zero more rapidly than  $r^{-3}$ . This convergence criterion excludes application of the Mayer theory to the important cases of Coulombic fluids (electrolytes, ionic liquids, plasmas, *etc.*), as well as dipolar fluids (water, magnetic colloids). However, systems interacting through, *e.g.*, Lennard-Jones,

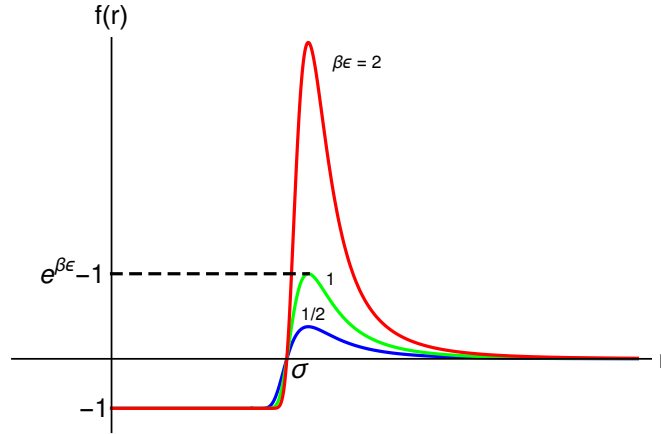


Figure 13.4: Mayer function  $f(r)$  for the Lennard-Jones potential, at several values of the reduced temperature (inverse thermal energy)  $\beta\epsilon$ .

square-well, hard-sphere, and screened-Coulomb potentials, can be treated within this framework. Note that the temperature dependence of  $f(r)$  implies that  $B_2(T)$  can change sign at the Boyle temperature  $T_B$ , *i.e.*,  $B_2(T_B) = 0$ . At low temperatures  $T < T_B$ , we have  $B_2(T) < 0$ , signifying that the Van der Waals attractions reduce the pressure with respect to the ideal-gas pressure. At temperature  $T > T_B$  the hard-core repulsions increase the pressure beyond the ideal-gas pressure.

### 13.4.3 The Third Virial Coefficient $B_3(T)$

The third virial coefficient is calculated as follows.

$$\begin{aligned}
 B_3(T) &= 4b_2^2 - 2b_3; \\
 &= -\frac{1}{3V} [(Q_3 - 3Q_2Q_1 + 2Q_1^3) - 3Q_1^{-1}(Q_2 - Q_1^2)^2]; \\
 &= -\frac{1}{3V} [Q_3 - 3Q_1^{-1}Q_2^2 + 3Q_1Q_2 - Q_1^3]; \\
 &= -\frac{1}{3V} \int d\mathbf{r}_1 d\mathbf{r}_2 d\mathbf{r}_3 \left( \exp[-\beta(\phi_{12} + \phi_{13} + \phi_{23})] - 3\exp[-\beta(\phi_{12} + \phi_{13})] + 3\exp[-\beta\phi_{12}] - 1 \right); \\
 &= -\frac{1}{3} \int d\mathbf{r}_1 d\mathbf{r}_3 f(r_{12})f(r_{13})f(r_{23}), \tag{13.31}
 \end{aligned}$$

where we used the shorthand notation  $\phi_{ij} = \phi(r_{ij})$ , the fact that  $Q_1 = V$ , and that  $\mathbf{r}_i$  are dummy integration variables. The product of three Mayer functions in Eq. (13.31) implies that  $B_3(T)$  involves three particles, and since  $f(r_{ij})$  vanishes, if particle  $i$  and  $j$  are separated, the product will vanish unless all three particles are simultaneously close to each another.

### 13.4.4 Higher-Order Virial Coefficients and Diagrams

The analysis of higher-order virial coefficients becomes increasingly difficult, and the expressions increasingly involved. To keep track of the bookkeeping a pictorial technique has been developed, whereby integrals of Mayer functions are represented by *cluster diagrams*. These diagrams, or graphs, consist of

points (representing coordinates  $\mathbf{r}_i$ ,  $\mathbf{r}_j$ , *etc.*) and lines connecting points (representing  $f(r_{ij})$ ). Using this we can write

$$B_2(T) = -\frac{1}{2V} \int d\mathbf{r}_1 d\mathbf{r}_2 \text{---} \bullet \bullet ; \quad (13.32)$$

$$B_3(T) = -\frac{1}{3V} \int d\mathbf{r}_1 d\mathbf{r}_2 d\mathbf{r}_3 \text{---} \triangle ; \quad (13.33)$$

$$B_4(T) = -\frac{1}{8V} \int d\mathbf{r}_1 d\mathbf{r}_2 d\mathbf{r}_3 d\mathbf{r}_4 \left( 3 \text{---} \square + 6 \text{---} \square_{\text{diag}} + \text{---} \square_{\text{diag2}} \right); \quad (13.34)$$

It has been proven that all diagrams appearing in the integrand of the virial coefficients are *doubly connected*, *i.e.*, are still connected when *any* point and all of its associated lines are removed. This means that diagrams like the following



do not occur. We remark that in most of the literature the integral symbol and the integral measure  $d\mathbf{r}_1 \cdots d\mathbf{r}_n$  are ignored when the diagrams are defined, and often even the prefactors, such as the “3” and the “6” into the expression for  $B_4$ , are absorbed in the definitions. We will not pursue this here.

The number of diagrams for  $B_n$  increases rapidly with  $n$ , *e.g.*, 468 in  $B_7$ . For the hard-sphere potential (diameter  $\sigma$ )  $B_2$ ,  $B_3$ ,  $B_4$  are known analytically,

$$B_2 = \frac{2\pi}{3} \sigma^3 \equiv b_0; \quad (13.35)$$

$$B_3 = \frac{5\pi^2}{18} \sigma^6 = \frac{5}{8} b_0^2; \quad (13.36)$$

$$B_4 = \left( -\frac{89}{280} + \frac{219\sqrt{2}}{2240\pi} + \frac{4131}{2240\pi} \arccos\left(\frac{1}{\sqrt{3}}\right) \right) b_0^3; \quad (13.37)$$

$$\simeq 0.28695 b_0^3, \quad (13.38)$$

while higher-order terms have been calculated by various numerical techniques, *e.g.*, by Monte Carlo integration methods

$$B_5 = 0.1097(3) b_0^4; \quad (13.39)$$

$$B_6 = 0.0386(4) b_0^5; \quad (13.40)$$

$$B_7 = 0.0138(4) b_0^6. \quad (13.41)$$

The convergence of the hard-sphere virial expansion can be judged from Fig. 13.5, where the numbers label the second, third, *etc.* virial approximation, and where the full curve is the ‘exact’ result, which was obtained using Metropolis Monte Carlo simulations.

Obviously, the deviations between the exact equation of state and the truncated virial expansions become more pronounced as the packing fraction  $\eta = (\pi/6)\rho\sigma^3$  increases, and the 7th-order expansion gives a good account up to moderate packing fractions, say  $\eta \simeq 0.3$ . More recent studies have computed

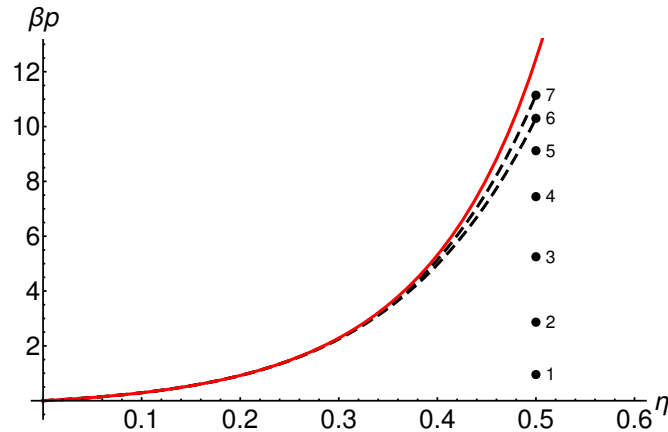


Figure 13.5: Equation of state of hard-sphere fluid as a function of the dimensionless density  $\eta = (\pi/6)\rho\sigma^3$  (the packing fraction). The red solid line is an exact result from simulations.

coefficients up to the 12th order [R.J. Wheatley, Phys. Rev. Lett. **110**, 200601 (2013)]. Nonetheless, we may conclude from Fig. 13.5 that the virial expansion is *not* suitable to describe liquids quantitatively. This is because a typical liquid density is  $\eta \simeq 0.5$  and many terms will need to be computed at great expense to describe this with sufficient accuracy, whilst there exist other, more efficient ways to treat such dense fluids. Another reason why the virial expansion is cumbersome when applied to liquids is that the virial coefficients are generally  $T$ -dependent, so that lengthy calculations must be performed at many values of  $T$ . This contrasts the hard-sphere case, where the virial coefficients are temperature independent. For these reasons other methods have been devised to deal with dense liquids.

The virial expansion is, nevertheless, a valuable tool in the study of dilute or moderately dense gases. For instance, much of our knowledge of atomic pair potentials stems from measurements of virial coefficients. Although we focused on the application of the virial expansion to a one-component, classical, monoatomic gas, it is possible to extend these results to more components and polyatomic molecules, as well as describe quantum effects. We will return to the two former in Chapter 17.

## 13.5 Exercises

### Q75. Van der Waals Equation of State

The van der Waals equation of state  $p(\rho)$  is given by

$$p(\rho) = \frac{Nk_{\text{B}}T}{V - Nb} - a\rho^2 \quad (13.42)$$

where  $N$  is the number of particles,  $V$  is the volume,  $k_{\text{B}}$  is Boltzmann's constant,  $\rho$  is the density,  $p$  is the pressure, and  $a$ ,  $b$  are phenomenological constants.

- Explain in your own words what  $a$  and  $b$  are. Explain in what way this is a mean-field approximation. Argue why both  $a$  and  $b$  are positive constants.
- Use Mathematica and plot the equation of state for different values of  $a$  and  $b$ . Notice that for fixed  $a$  and  $b$ , the shape of the equation of state changes as the temperature changes.
- Write the isothermal compressibility in terms of the density  $\rho$ . Recall that the isothermal compressibility is always positive in stable systems. Argue that this implies that there are  $T$  where, for a range of densities, the equation of state describes an 'unstable' system.
- Using your observations from part (c), argue that the critical point can be determined from setting

$$\left(\frac{\partial p}{\partial \rho}\right) = 0 \quad \text{and} \quad \left(\frac{\partial^2 p}{\partial \rho^2}\right) = 0. \quad (13.43)$$

- Show that the critical point is given by

$$k_{\text{B}}T_c = \frac{8a}{27b} \quad \text{and} \quad \rho_c b = \frac{1}{3}. \quad (13.44)$$

- Use the isothermal compressibility to determine the spinodals. Note: You may wish to use Mathematica to solve this.
- Determine the free energy assuming that in the limit of  $\rho \rightarrow 0$  it is that of the ideal gas.
- Let  $a = 1$  and  $b = 1$ , then plot the free energy for various temperatures. Identify in each plot if there is a coexistence region or not.
- Using the free energies from part (h), determine the phase diagram for this system.

### Q76. Dieterici's Equation

Assume that a gas obeys Dieterici's equation of state

$$\beta p \left(\frac{1}{\rho} - b\right) = e^{-\beta a \rho}, \quad (13.45)$$

where  $p$  is the pressure,  $\rho = N/V$  with  $N$  the number of particles and  $V$  the volume, and  $a$  and  $b$  are coefficients that set the properties of the gas.

- Show that in the low-density limit Dieterici's equation of state reduces to that of the Van der Waals gas and provide the expression for the third virial coefficient.
- Interpret the 'improvement' made to the Van der Waals gas by the exponential term on the right-hand side of Dieterici's equation of state equation using a few words.

- (c) Sketch three isotherms of  $p$  as a function of  $v = V/N$  for the Dieterici's equation of state above, at, and below the critical temperature  $T_c$ , respectively, indicating which is which. Label your axes and indicate the spinodal points.
- (d) Show that  $k_B T_c = a/(4b)$ , the critical pressure is given by  $p_c = a/(4b^2 e^2)$ , and critical volume per particle is  $v_c = 2b$ . Here  $k_B$  denotes the Boltzmann constant.

The isothermal compressibility can also be defined in terms of  $v$  and reads

$$\kappa_T = -\frac{1}{v} \left( \frac{\partial v}{\partial p} \right)_{T,N}. \quad (13.46)$$

- (e) Describe in a few words what happens with  $\kappa_T$  when you cross a spinodal curve for  $T < T_c$ .
- (f) Introduce  $t = k_B(T - T_c)$  and expand the compressibility around  $t = 0$  and  $v = v_c$ . What is the value of the critical exponent  $\gamma$ , *i.e.*,  $\kappa_T \propto |t|^{-\gamma}$ ? Describe in a few words what feature of the system leads to this behavior.

#### Q77. The Mayer Expansion for Nonideal Gases

The Mayer expansion for nonideal gases is derived from the grand canonical partition function  $\Xi(\tilde{z}, V, T) = \sum_{N=0}^{\infty} \tilde{z}^N Q_N(V, T)/N!$ , with  $\tilde{z}$  the thermal-volume-weighted fugacity and  $Q_N(V, T)$  the configuration integral of  $N$  particles.

- (a) Define the coefficients  $b_j$  by  $\log \Xi = V \sum_{j=1}^{\infty} b_j \tilde{z}^j$ , and give  $b_1, \dots, b_4$  in terms of  $Q_1, \dots, Q_4$ .
- (b) Calculate  $Q_1, Q_2, b_1$  and  $b_2$  in terms of  $V$  and the pair potential  $\phi(r)$ .
- (c) How are the pressure  $p$  and the density  $\rho$  related to  $\Xi(\tilde{z}, V, T)$ ? Give  $p(\tilde{z}, T)$  and  $\rho(\tilde{z}, T)$  in terms of  $b_j$  and  $\tilde{z}$ .
- (d) Invert  $\rho(\tilde{z}, T)$  using the Ansatz  $\tilde{z} = a_1 \rho + a_2 \rho^2 + a_3 \rho^3 + \dots$ , and give the first three terms of the  $\rho$ -expansion of  $p$ . Identify the second and third virial coefficient in terms of the  $b_j$ 's.

#### Q78. Virial Coefficients of Hard Spheres

In this problem we examine the virial coefficients for hard spheres.

- (a) Calculate  $B_2$  for the hard-sphere (HS) system (diameter  $\sigma$ ). Does  $B_2$  depend on  $T$ ? Argue that  $B_2$  is half the volume where the center of a second sphere cannot be because of the presence of the first, *i.e.*, that  $B_2$  is half the pairwise excluded volume.
- (b) Calculate  $B_3$  for hard spheres of diameter  $\sigma$ . Hint: Consider and calculate the lens-shaped overlap volume  $v(r_{12})$  of two spheres ("1" and "2") of radius  $\sigma$  at center-to-center separation  $0 \leq r_{12} \leq \sigma$ ; this is the volume in which the center of sphere "3" must be in order to overlap with "1" and "2" simultaneously.
- (c) Check that  $B_2 = 4v_0$  and  $B_3 = 10v_0^2$  for hard spheres, with  $v_0$  the volume of the spheres, and use this to show that virial expansion for the pressure  $P$  of a hard sphere system of density  $\rho$  at temperature  $T$  can be written as  $Pv_0/k_B T = \eta(1 + 4\eta + 10\eta^2 + \mathcal{O}(\eta^3))$ , where  $\eta = \rho v_0$  is the so-called packing fraction. Give an interpretation of  $\eta$ .
- (d) Estimate on the basis of (c) for which  $\eta$  the deviation from the ideal-gas pressure is (i) a factor 1.1 (so the deviation is 10%) and (ii) a factor 2.

#### Q79. The Second Virial Coefficient of Square-Well Potentials

In this problem we examine the second virial coefficient of square-well potentials. Calculate the second virial coefficient  $B_2(T)$  of a square-well (SW) fluid with hard-core diameter  $\sigma$ , well depth  $-\epsilon < 0$ , and well width  $\lambda\sigma$  with  $\lambda > 1$ ). Compare/check the limiting cases  $\epsilon \rightarrow 0$  and  $\lambda \rightarrow 1$  against the hard-sphere result.

**Q80. The Second Virial Coefficient of for Long-Ranged Potentials**

Here we consider the second virial coefficient in the case of long-ranged potentials.

- (a) Define the reduced second virial coefficient of the Lennard-Jones (LJ) fluid as  $B^* = B_2^{LJ} / B_2^{HS}$ , where  $B_2^{LJ,HS}$  is the second virial coefficient of the LJ, HS system with the same  $\sigma$ . Give an expression for  $B^*(T^*)$  as a function of the reduced temperature  $T^* = k_B T / \epsilon$ . The (dimensionless) integral cannot be calculated analytically, but easily numerically.
- (b) The pair potential  $\phi(r)$  must decay to zero sufficiently fast with increasing  $r$  for  $B_2$  to be finite. Show, for the case that  $\phi(r) \propto r^{-n}$  for  $r \rightarrow \infty$ , that  $B_2$  only exists provided  $n > d$  with  $d$  the spatial dimensionality. Does  $B_2^{LJ}$  exist in  $d = 3$ ? Does  $B_2$  exist for Coulomb interactions in  $d = 3$ ?



## Chapter 14

# Classical Dense Fluids

The simplest way to take into account the effect of interactions between the particles, is through a low-density (virial) expansion such as in Eq. (13.2). In terms of the pair potential such an approach yields for the second virial coefficient

$$B_2(T) = \frac{1}{2} \int d\mathbf{r} (1 - \exp[-\beta\phi(r)]), \quad (14.1)$$

but expressions for higher-order coefficients, say beyond  $B_5$  or so, become hopelessly complicated. In fact, analytic calculations of  $B_3$  are already far from trivial. The rapidly increasing complexity of higher-order virial coefficients prohibits practical applications of the virial expansion to dense fluids such as molecular liquids. In fact, the problem is not only practical but also fundamental, as it is not guaranteed that the radius of convergence of the virial series is sufficiently enough to include the high densities of interest. Moreover, the virial expansion does not take into account the true nature of a liquid, in which each molecule constantly interacts strongly with all its neighbors. That is, this route approximates the liquid as ‘small groups’ of particles in vacuum, rather than as a small group embedded in a liquid comprised of other similar molecules.

In order to obtain better expressions for the thermodynamics of dense fluids, we have to explicitly take into account the structure of the fluid. The structure of the fluid is captured by correlation functions such as the structure factor and  $n$ th-order real-space correlation functions, with the second-order being the pair-correlation function that we encountered in Chapter 11. In this chapter, we will examine these correlation functions, and using Ornstein-Zernike theory, we will explore the behavior of dense fluids.

### 14.1 Structure Factor

Experimentally it is possible (and common practice) to measure *correlations* in a gas or liquid by neutron or X-ray scattering. Imagine a sample of gas or liquid irradiated by a coherent X-ray beam, say, of wavelength  $\lambda$ . The wavevector of the incident radiation is called  $\mathbf{k}_i$ , with  $|\mathbf{k}_i| = 2\pi/\lambda \equiv k$  the wavenumber. Due to the presence of particles in the sample, radiation will be scattered in all directions, and its intensity  $I(\theta)$  can be detected far from the sample as a function of the angle  $\theta$  with respect to the incident beam, as illustrated in Fig. 14.1.

Scattered radiation in a particular direction  $\theta$ , with outgoing wavevector  $\mathbf{k}_o$ , satisfies  $|\mathbf{k}_o| = k$  for

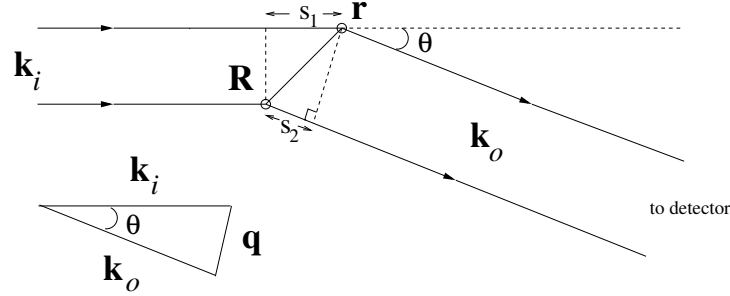


Figure 14.1: Schematic setup of a scattering experiment, indicating incoming and outgoing wave vectors  $\mathbf{k}_i$  and  $\mathbf{k}_o$ , respectively, as well as the scattering angle  $\theta$ .

elastic scattering. Consider now the path-length difference  $\Delta s = s_2 - s_1$  between the path “source  $\rightarrow \mathbf{R} \rightarrow$  detector”, with  $\mathbf{R}$  an arbitrary point in the sample, and the path “source  $\rightarrow \mathbf{r} \rightarrow$  detector”, where  $\mathbf{r}$  is the position of a scattering particle. It follows from the geometry that  $ks_1 = \mathbf{k}_i \cdot (\mathbf{r} - \mathbf{R})$  and  $ks_2 = \mathbf{k}_o \cdot (\mathbf{r} - \mathbf{R})$ . From this the phase difference  $\Delta\psi$  of the two paths at the detector is obtained as

$$\Delta\psi = \frac{2\pi\Delta s}{\lambda} = k\Delta s = (\mathbf{k}_o - \mathbf{k}_i) \cdot (\mathbf{r} - \mathbf{R}) = \mathbf{q} \cdot (\mathbf{r} - \mathbf{R}), \quad (14.2)$$

where we defined the momentum transfer  $\mathbf{q} \equiv \mathbf{k}_o - \mathbf{k}_i$  in the scattering process. The contribution from this particle to the field amplitude  $\mathcal{A}$  at the detector is proportional to  $\exp[i\Delta\psi]$ . The total amplitude at the detector is given by the contribution from all particles, and can be written as

$$\mathcal{A}(\theta) \propto \sum_{j=1}^N \exp[i\mathbf{q} \cdot (\mathbf{r}_j - \mathbf{R})], \quad (14.3)$$

for some static configuration of  $N$  particles in the irradiated volume. The measured intensity is the ensemble or time average of the squared modulus of the amplitude, and can be written as

$$I(\theta) = \langle |\mathcal{A}(\theta)|^2 \rangle \propto \left\langle \sum_{j,k}^N \exp[i\mathbf{q} \cdot \mathbf{r}_{jk}] \right\rangle \propto S(q), \quad (14.4)$$

where  $\mathbf{r}_{jk} = \mathbf{r}_j - \mathbf{r}_k$ , and where the *structure factor*  $S(q)$  is defined as

$$S(q) \equiv \left\langle \frac{1}{N} \sum_{j,k}^N \exp[i\mathbf{q} \cdot \mathbf{r}_{jk}] \right\rangle = 1 + \left\langle \frac{1}{N} \sum_{j \neq k}^N \exp[i\mathbf{q} \cdot \mathbf{r}_{jk}] \right\rangle. \quad (14.5)$$

Note that  $q$  is directly related to  $\theta$  through  $q \equiv |\mathbf{q}| = 2k \sin(\theta/2)$  from elementary geometry. It is implicitly assumed that the fluid of interest is homogeneous and isotropic, so that only the modulus  $q$  is relevant and not the direction of  $\mathbf{q}$ . A typical liquid structure factor is shown in Fig. 14.2.

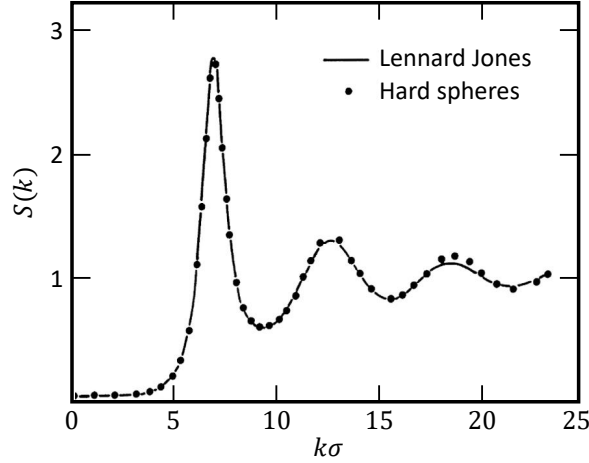


Figure 14.2: Structure factor of a Lennard-Jones fluid close to its triple point ( $\rho\sigma^3 = 0.844$ ,  $k_{\text{B}}T/\epsilon = 0.72$ ), and that of a hard-sphere fluid close to freezing ( $\eta = 0.495$ ), as obtained from computer simulations. Image adapted from [J.P. Hansen and I.R. McDonald, *Theory of Simple Liquids*, Academic Press, 2nd ed. (1990)].

## 14.2 The Pair-Correlation Function

A key role in these theories describing dense fluids is played by the real-space distribution functions

$$\rho^{(1)}(\mathbf{r}) = \left\langle \sum_{i=1}^N \delta(\mathbf{r} - \mathbf{r}_i) \right\rangle; \quad (14.6)$$

$$\rho^{(2)}(\mathbf{r}, \mathbf{r}') = \left\langle \sum_{i=1}^N \sum_{j \neq i}^N \delta(\mathbf{r} - \mathbf{r}_i) \delta(\mathbf{r}' - \mathbf{r}_j) \right\rangle, \quad (14.7)$$

which are called the one-particle distribution and the pair distribution function, respectively. Higher-order distributions can be defined accordingly, but we do not need them here because we restrict attention to pairwise interactions. The angular brackets in Eqs. (14.6) and (14.7) denote an ensemble average, either canonical or grand canonical.  $\rho^{(1)}(\mathbf{r})$  is a measure for the probability density that a particle is present at position  $\mathbf{r}$ . Because of the normalization  $\int d\mathbf{r} \rho^{(1)}(\mathbf{r}) = N$ , we see that  $\rho^{(1)}(\mathbf{r})$  is the local density, and equals  $\rho = N/V$  in a homogeneous bulk system.  $\rho^{(2)}(\mathbf{r}, \mathbf{r}')$  is called the pair distribution function, and is a measure for the probability that there is a particle at position  $\mathbf{r}$  and *another* one at  $\mathbf{r}'$  *simultaneously*. Within the canonical ensemble, we obtain from Eq. (14.7) that

$$\begin{aligned} \rho^{(2)}(\mathbf{r}, \mathbf{r}') &= \frac{1}{Q_N} \int d\mathbf{r}^N \exp[-\beta\Phi(\mathbf{r}^N)] \left( \sum_{i=1}^N \sum_{j \neq i}^N \delta(\mathbf{r} - \mathbf{r}_i) \delta(\mathbf{r}' - \mathbf{r}_j) \right); \\ &= \frac{N(N-1)}{Q_N} \int d\mathbf{r}^N \exp[-\beta\Phi(\mathbf{r}^N)] \delta(\mathbf{r} - \mathbf{r}_1) \delta(\mathbf{r}' - \mathbf{r}_2); \\ &= \frac{N(N-1)}{Q_N} \int d\mathbf{r}_3 \cdots d\mathbf{r}_N \exp[-\beta\Phi(\mathbf{r}, \mathbf{r}', \mathbf{r}_3, \cdots, \mathbf{r}_N)]. \end{aligned} \quad (14.8)$$

Recall the definition of the configuration integral

$$Q_N = Q(N, V, T) = \int d\mathbf{r}^N \exp[-\beta\Phi(\mathbf{r}^N)]. \quad (14.9)$$

At sufficiently long distances  $|\mathbf{r} - \mathbf{r}'|$  these probabilities become uncorrelated, and we have  $\rho^{(2)}(\mathbf{r}, \mathbf{r}') \rightarrow \rho^{(1)}(\mathbf{r})\rho^{(1)}(\mathbf{r}')$ . In isotropic, homogeneous systems such as liquids and gases we can use translational invariance to define the *radial distribution function*  $g(r)$  by

$$\rho^{(2)}(\mathbf{r}, \mathbf{r}') = \rho^2 g(|\mathbf{r} - \mathbf{r}'|). \quad (14.10)$$

Note that  $\rho g(r)$  is the average particle density at a distance  $r$  from a fixed particle. Also note that  $\lim_{r \rightarrow \infty} g(r) = 1$ . For systems with pairwise additive interactions, the thermodynamics follows completely from  $g(r)$ , that is from  $g(r; \rho, T)$  in the canonical ensemble or from  $g(r; \mu, T)$  in the grand canonical ensemble. There are three independent routes from  $g(r)$  to thermodynamics, *viz.*

1. Virial route:

$$p = \rho k_B T - \frac{\rho^2}{6} \int d\mathbf{r} r \phi'(r) g(r); \quad (14.11)$$

2. Caloric route:

$$\frac{E}{V} = \frac{3}{2} \rho k_B T + \frac{\rho^2}{2} \int d\mathbf{r} \phi(r) g(r); \quad (14.12)$$

3. Compressibility route:

$$k_B T \left( \frac{\partial \rho}{\partial p} \right)_T = 1 + \rho \int d\mathbf{r} (g(r) - 1). \quad (14.13)$$

The virial and caloric route follow straightforwardly from the canonical partition function of a pairwise additive system, as will be shown in one of the problems. The compressibility route is necessarily derived grand canonically, and follows directly from the normalization  $\int d\mathbf{r} d\mathbf{r}' \rho^{(2)}(\mathbf{r}, \mathbf{r}') = \langle N(N-1) \rangle = \langle N^2 \rangle - \langle N \rangle$  and Eq. (3.23).

Knowledge of  $g(r)$  does not only lead to the thermodynamics of the fluid, but also to the structure factor  $S(q)$  (that can be measured in scattering experiments). The relation between  $S(q)$  and  $g(r)$  is obtained as follows

$$\begin{aligned} S(q) &\stackrel{(14.5)}{=} 1 + \left\langle \frac{1}{N} \sum_{i \neq j}^N \exp[i\mathbf{q} \cdot \mathbf{r}_{ij}] \right\rangle; \\ &= 1 + \frac{1}{NQ_N} \int d\mathbf{r}^N \exp[-\beta\Phi(\mathbf{r}^N)] \sum_{i \neq j}^N \exp[i\mathbf{q} \cdot \mathbf{r}_{ij}]; \\ &= 1 + \frac{1}{N} \int d\mathbf{r}_1 d\mathbf{r}_2 \exp[i\mathbf{q} \cdot \mathbf{r}_{12}] \left( \frac{N(N-1)}{Q_N} \int d\mathbf{r}_3 \cdots d\mathbf{r}_N \exp[-\beta\Phi(\mathbf{r}^N)] \right); \\ &\stackrel{(14.8)}{=} 1 + \frac{1}{N} \int d\mathbf{r}_1 d\mathbf{r}_2 \exp[i\mathbf{q} \cdot \mathbf{r}_{12}] \rho^{(2)}(\mathbf{r}_1, \mathbf{r}_2); \\ &\stackrel{(14.10)}{=} 1 + \rho \int d\mathbf{r} \exp[i\mathbf{q} \cdot \mathbf{r}] g(r), \end{aligned} \quad (14.14)$$

*i.e.*,  $S(q)$  is essentially the Fourier transform of  $g(r)$ . Since  $g(r)$  approaches unity for large  $r$  it is convenient to rewrite Eq. (14.14) as

$$S(q) = 1 + \rho \int d\mathbf{r} \exp[i\mathbf{q} \cdot \mathbf{r}] (g(r) - 1) + (2\pi)^3 \rho \delta(\mathbf{q}), \quad (14.15)$$

where the last term is irrelevant as long as the scattering angle  $\theta$ , and hence the scattering vector  $\mathbf{q}$ , do not vanish. Clearly, we can also invert Eq. (14.14) with the result

$$\rho g(r) = \frac{1}{(2\pi)^3} \int d\mathbf{q} (S(q) - 1) \exp[i\mathbf{q} \cdot \mathbf{r}], \quad (14.16)$$

which can be used to deduce  $g(r)$  from a measurement of  $S(q)$ . Typical  $g(r)$ s for dense fluids are shown in Fig. 14.3.

For later reference we define the *potential of mean force*  $w(r; \rho, T)$  by

$$w(r_{12}) = -k_B T \log g(r_{12}) \iff g(r_{12}; \rho, T) = \exp[-\beta w(r_{12}; \rho, T)]. \quad (14.17)$$

This name stems from the fact that the gradient  $-\nabla_i w(r_{12})$  is the average force  $\mathbf{f}(r_{12})$  acting on particle 1, keeping 1 and 2 fixed and averaging over all the others,

$$\begin{aligned} \nabla_1 w(\mathbf{r}_{12}) &\stackrel{(14.17)}{=} \frac{-k_B T}{g(r_{12})} \nabla_1 g(r_{12}); \\ &\stackrel{(14.8)}{=} \frac{\int d\mathbf{r}_3 \cdots d\mathbf{r}_N \exp[-\beta \Phi(\mathbf{r}^N)] (-\nabla_1 \Phi(\mathbf{r}^N))}{\int d\mathbf{r}_3 \cdots d\mathbf{r}_N \exp[-\beta \Phi(\mathbf{r}^N)]}; \\ &\equiv \langle \mathbf{f}(r_{12}) \rangle. \end{aligned} \quad (14.18)$$

### 14.3 Ornstein-Zernike Theory

Because of the importance of  $g(r)$  in the theory of strongly interacting, dense fluids, many approaches have been devised to calculate (approximations to) this function, either analytically or numerically. Methods go by the names of ‘‘Kirkwood integral equation’’, ‘‘BBGKY hierarchy’’, and ‘‘Ornstein-Zernike’’ theory. The latter one will be discussed here heuristically. Rigorous derivations require extensive graph analysis and functional techniques that are too involved for the present course.

It is convenient to define the *total correlation function*

$$h(r_{12}) = g(r_{12}) - 1, \quad (14.19)$$

which is a measure for the ‘influence’ of molecule 1 on molecule 2 a distance  $r_{12}$  away. In 1914, Ornstein and Zernike proposed to split this influence into two contributions, a direct part and an indirect part. The direct contribution is *defined* to be given by what is called the *direct correlation function*, denoted  $c(r_{12})$ . The indirect part is due to the direct influence of molecule 1 on a third molecule, labeled 3, which in turn influences molecule 2, directly and indirectly. Clearly, this indirect effect must be weighted by the density of particle 3, and averaged over all its possible positions. Mathematically this decomposition can be written as

$$h(r_{12}) = c(r_{12}) + \rho \int d\mathbf{r}_3 c(r_{13}) h(r_{32}), \quad (14.20)$$

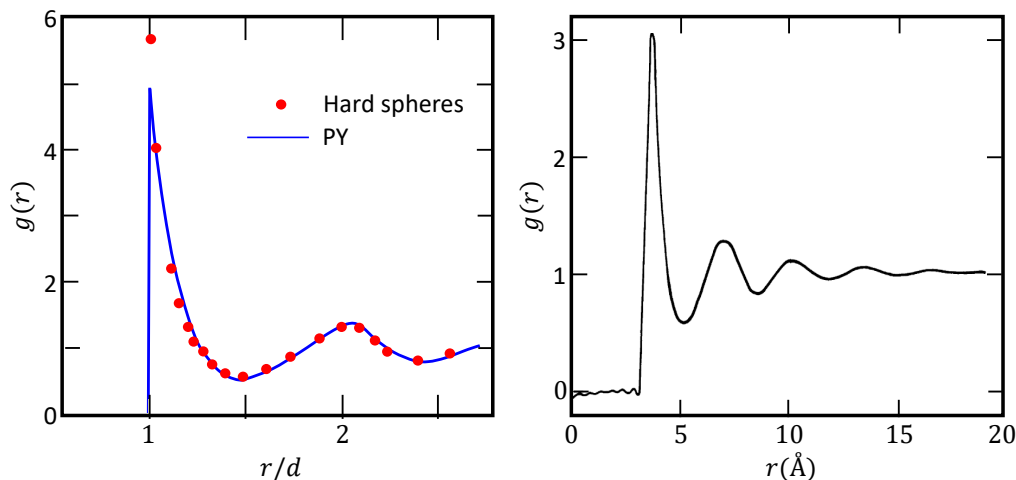


Figure 14.3: Radial distribution functions  $g(r)$ . (left) Dense hard-sphere fluid at volume fraction  $\eta = 0.49$  showing excellent agreement between exact simulation results and the theoretical result based on the Percus-Yevick closure. (right) Radial distribution function of triple-point liquid Argon (85 K) as measured by neutron scattering. The ripples at small  $r$  are artifacts of the data analysis. The large number of oscillations in  $g(r)$  is indicative of being close to a critical point. Images adapted from [J.P. Hansen and I.R. McDonald, *Theory of Simple Liquids*, Academic Press, 2nd ed. (1990)].

which is called the Ornstein-Zernike (OZ) equation. It can be viewed as the defining equation for the direct correlation function  $c(r)$ . One may also argue, however, that we have rewritten a function we wish to calculate,  $h(r)$ , in terms of another function that we do not know,  $c(r)$ . In that sense Eq. (14.20) can be viewed as a single equation with two unknowns, which can only be solved provided another relation between  $c(r)$  and  $h(r)$  is given. Such an additional relation is called the *closure*. The power of the decomposition given by Ornstein and Zernike is that approximate closures can be given, that allow for explicit calculation of  $c(r)$  and  $h(r)$  at a given density and temperature.

Before discussing an example of such a closure, we remark that the OZ equation (14.20) can be rewritten in terms of the Fourier transforms  $\hat{h}(q)$  and  $\hat{c}(q)$  of  $h(r)$  and  $c(r)$ , respectively, as

$$\hat{h}(q) = \hat{c}(q) + \rho \hat{c}(q) \hat{h}(q), \quad (14.21)$$

from which we obtain that

$$\hat{c}(q) = \frac{\hat{h}(q)}{1 + \rho \hat{h}(q)} \quad \text{and} \quad \hat{h}(q) = \frac{\hat{c}(q)}{1 - \rho \hat{c}(q)}. \quad (14.22)$$

From Eqs. (14.15) and (14.22) we find that  $\hat{c}(q)$  is related to the structure factor through

$$S(q) = \frac{1}{1 - \rho \hat{c}(q)}. \quad (14.23)$$

A very successful and relatively simple closure is named after Percus and Yevick (PY). It consists of the *approximation* that

$$c(r) \stackrel{\text{PY}}{\approx} g(r)(1 - \exp[+\beta\phi(r)]). \quad (14.24)$$

The physical motivation behind the PY closure is as follows. First we note that the direct correlation  $c(r)$  can be seen as the difference between the (total) pair correlation  $g(r) \equiv \exp[-\beta w(r)]$ , see Eq. (14.17), and an *indirect* term  $g_{\text{ind}}(r)$ . This indirect term, which is *defined* as  $g_{\text{ind}}(r) = g(r) - c(r)$ , is now *approximated* as  $g_{\text{ind}}(r) = \exp[-\beta(w(r) - \phi(r))] = g(r) \exp[+\beta\phi(r)]$ , *i.e.*, as the Boltzmann factor of  $w(r) - \phi(r)$ . Equation (14.24) then follows readily. Having in mind that  $w(r)$  is the (total) potential of mean force, while  $\phi(r)$  is the pair potential, this approximation indeed captures the idea that the indirect contribution is *not* due to direct pair interactions. Other, more technical motivations for the PY closure can also be given, *e.g.*, in terms of ignoring some subclasses of diagrams in the diagrammatic expansion of  $c(r)$ , but this is beyond the present goals.

The OZ equation (14.20) with the PY closure (14.24) constitutes two independent equations that can be solved for the two unknown functions  $h(r)$  and  $c(r)$ , at least in principle. In practice this can often only be done numerically, but for the important case of the hard-sphere potential (13.5) analytic results have been found. It is instructive to consider the PY closure (14.24) for the hard-sphere case explicitly, as it can be rewritten as

$$\begin{cases} g(r) = 0, & r < \sigma \\ c(r) = 0, & r > \sigma \end{cases}, \quad (14.25)$$

where  $\sigma$  is the hard-sphere diameter. This closure reflects the idea that for hard spheres the direct correlation  $c(r)$  indeed vanishes if there is no direct hard-core overlap (this is an approximation, however). Independently from each other Wertheim and Thiele showed, in 1963, that the PY closure to the OZ equation of a hard-sphere fluid (diameter  $\sigma$ ) at the dimensionless density  $\eta = (\pi/6)\rho\sigma^3$  (*i.e.*, the packing fraction) yields for the direct correlation function

$$c(r) = \begin{cases} \frac{-(1+2\eta)^2 + 6\eta(1+\frac{1}{2}\eta)^2\left(\frac{r}{\sigma}\right) - \frac{1}{2}\eta(1+2\eta)^2\left(\frac{r}{\sigma}\right)^3}{(1-\eta)^4} & r < \sigma \\ 0 & r > \sigma \end{cases}. \quad (14.26)$$

This can be analytically Fourier transformed, from which the structure factor follows using Eq. (14.23). Unfortunately,  $g(r)$  cannot be written down analytically, but a numerical Fourier transform of  $S(q)$  is straightforward, and from Eq. (14.14)  $g(r)$  follows. The result is in very good agreement with computer simulations of  $g(r)$  of hard spheres for  $0 < \eta \lesssim 0.5$ . This is illustrated in the left-hand panel to Fig. 14.3.

Since the hard-sphere fluid freezes at  $\eta \approx 0.494$ , the PY closure is accurate in the whole fluid regime of hard spheres. In one of the problems we will calculate that the explicit form (14.26) for  $c(r)$  leads to the pressure  $p_c$  via the compressibility route (14.13), and to  $p_v$  via the virial route (14.11), where

$$\frac{p_c}{\rho k_B T} = \frac{1 + \eta + \eta^2}{(1 - \eta)^3} \quad \text{and} \quad \frac{p_v}{\rho k_B T} = \frac{1 + 2\eta + 3\eta^2}{(1 - \eta)^2}. \quad (14.27)$$

The difference between these two expressions increases with increasing  $\eta$ , but both give good account of the pressure that results from simulations. The (slight) inconsistency that results from the different routes is due to the PY approximation; an exact theory would lead to fully consistent thermodynamics. It turns out that the linear combination  $p_{CS} = (2p_c + p_v)/3$ , which is named after Carnahan and Starling, is indistinguishable from the simulations up to  $\eta = 0.5$ ,

$$\frac{p_{CS}}{\rho k_B T} = \frac{1 + \eta + \eta^2 - \eta^3}{(1 - \eta)^3}. \quad (14.28)$$

In one of the problems it will be worked out that the Helmholtz free energy,  $F_{CS}$ , that follows from  $p_{CS}$  reads

$$\frac{F_{CS}}{N k_B T} = \log \rho \Lambda^3 - 1 + \frac{4\eta - 3\eta^2}{(1 - \eta)^2}, \quad (14.29)$$

where the first two terms are ideal gas terms, see Eq. (4.3), and the last one the excess term due to the hard-sphere interactions.

Because a typical triple point density,  $\rho_{\text{tr}}$ , of a simple fluid like argon satisfies  $\rho_{\text{tr}}\sigma^3 \approx 1$ , it is interesting to compare the triple-point structure with that of hard spheres at  $\rho\sigma^3 \simeq 1$ , *i.e.*,  $\eta \simeq 0.5$ . Figure 14.3 shows such a comparison: the structure of a real dense fluid (argon) is qualitatively similar to that of a dense hard-sphere fluid! This implies that the fluid structure is mainly determined by the short-ranged repulsions, while the attractions hardly affect the high-density structure. This notion is a crucial ingredient of the perturbation theory to be discussed in the next section.

## 14.4 Thermodynamic Perturbation Theory

We have seen that ensemble theory provides a formal framework to calculate thermodynamic properties starting from a microscopic Hamiltonian. Such a calculation always involves, in one way or another, the explicit calculation of the partition function, which is usually intractable analytically. Low-density expansions are possible, but these are typically not applicable in the regime of dense fluids. Here, we present a method that does allow for realistic calculations of the Helmholtz free energy  $F(N, V, T)$ , and hence the full thermodynamics, of dense fluids.

We consider a Hamiltonian of the form (3.1), and decompose the interaction part  $\Phi$ , formally, into a reference part  $\Phi_0$  and a perturbation  $\Phi_1$ . At this stage the decomposition is arbitrary, but a typical one would be to include the repulsions into  $\Phi_0$  and the attractions into  $\Phi_1$ . We define the auxiliary Hamiltonian

$$H_\lambda(\mathbf{\Gamma}) = \sum_{i=1}^N \frac{\mathbf{p}_i^2}{2m} + \Phi_0(\mathbf{r}^N) + \lambda\Phi_1(\mathbf{r}^N) \equiv H_0(\mathbf{\Gamma}) + \lambda\Phi_1(\mathbf{r}^N), \quad (14.30)$$

where  $H_0$  is the *reference Hamiltonian*, and  $\lambda \in [0, 1]$  a *coupling constant* or a *switching* parameter that switches  $H_\lambda$  from the reference Hamiltonian at  $\lambda = 0$  to the Hamiltonian of interest at  $\lambda = 1$ . The Helmholtz free energy  $F_\lambda$  of the system with Hamiltonian  $H_\lambda$  can be written as

$$\exp[-\beta F_\lambda(N, V, T)] = \frac{1}{N!h^{3N}} \int d\mathbf{\Gamma} \exp[-\beta H_\lambda(\mathbf{\Gamma})] = \frac{1}{N!\Lambda^{3N}} \int d\mathbf{r}^N \exp[-\beta\Phi_0(\mathbf{r}^N) - \beta\lambda\Phi_1(\mathbf{r}^N)]. \quad (14.31)$$

Taking the derivative with respect to  $\lambda$  on both sides of Eq. (14.31), and rearranging terms gives

$$\frac{\partial F_\lambda(N, V, T)}{\partial \lambda} = \frac{\int d\mathbf{r}^N \Phi_1(\mathbf{r}^N) \exp[-\beta(\Phi_0 + \lambda\Phi_1)]}{\int d\mathbf{r}^N \exp[-\beta(\Phi_0 + \lambda\Phi_1)]} \equiv \langle \Phi_1 \rangle_\lambda, \quad (14.32)$$

where the angular brackets  $\langle \cdot \rangle_\lambda$  denote the canonical ensemble average of systems with Hamiltonian  $H_\lambda$ . Using Eq. (14.32), the Helmholtz free energy of interest can be written

$$F(N, V, T) = F_0(N, V, T) + \int_0^1 d\lambda \langle \Phi_1 \rangle_\lambda, \quad (14.33)$$

with  $F_0$  the free energy of the reference system. Note that Eq. (14.33) is an exact result. Thermodynamic perturbation theory is based on a  $\lambda$ -expansion of the integrand of Eq. (14.33) about  $\lambda = 0$ . It follows

from Eq. (14.32) that

$$\begin{aligned}
\langle \Phi_1 \rangle_\lambda &= \frac{\int d\mathbf{r}^N \Phi_1 \exp[-\beta\Phi_0](1 - \beta\lambda\Phi_1 + \frac{1}{2}\beta^2\lambda^2\Phi_1^2 + \dots)}{\int d\mathbf{r}^N \exp[-\beta\Phi_0](1 - \beta\lambda\Phi_1 + \frac{1}{2}\beta^2\lambda^2\Phi_1^2 + \dots)}; \\
&= \frac{\langle \Phi_1 \rangle_0 - \lambda\beta\langle \Phi_1^2 \rangle_0 + \frac{1}{2}\lambda^2\beta^2\langle \Phi_1^3 \rangle_0 + \dots}{1 - \lambda\beta\langle \Phi_1 \rangle_0 + \frac{1}{2}\lambda^2\beta^2\langle \Phi_1^2 \rangle_0 + \dots}; \\
&= \langle \Phi_1 \rangle_0 - \lambda\beta(\langle \Phi_1^2 \rangle_0 - \langle \Phi_1 \rangle_0^2) + \frac{\lambda^2}{2}\beta^2\langle (\Phi_1 - \langle \Phi_1 \rangle_0)^3 \rangle_0 + \mathcal{O}(\lambda^3), \tag{14.34}
\end{aligned}$$

where  $\langle \cdot \rangle_0$  is a canonical average over the ensemble of reference systems. Using Eq. (14.33) we have

$$\beta F(N, V, T) = \beta F_0(N, V, T) + \beta\langle \Phi_1 \rangle_0 - \frac{\beta^2}{2}\langle (\Phi_1 - \langle \Phi_1 \rangle_0)^2 \rangle_0 + \mathcal{O}((\beta\Phi_1)^3). \tag{14.35}$$

This is often called the *high-temperature expansion*. This name is not entirely appropriate, since  $\beta$  does not only appear explicitly in the prefactors of the successive terms, but also implicitly in the average of the reference system.

Let us now focus on the case that  $\Phi(\mathbf{r}^N)$  can be written as a sum of pair potentials, with

$$\Phi_0(\mathbf{r}^N) = \sum_{i<j}^N \phi_0(r_{ij}) \quad \text{and} \quad \Phi_1(\mathbf{r}^N) = \sum_{i<j}^N \phi_1(r_{ij}), \tag{14.36}$$

*i.e.*, the pair potential of interest is  $\phi(r) = \phi_0(r) + \phi_1(r)$ . Then

$$\begin{aligned}
\langle \Phi_1 \rangle_\lambda &\stackrel{(14.32)}{=} \frac{N(N-1)}{2} \frac{\int d\mathbf{r}_1 d\mathbf{r}_2 \phi_1(r_{12}) d\mathbf{r}_3 \cdots d\mathbf{r}_N \exp[-\beta(\Phi_0 + \lambda\Phi_1)]}{\int d\mathbf{r}^N \exp[-\beta(\Phi_0 + \lambda\Phi_1)]}; \\
&\stackrel{(14.8)}{=} \frac{1}{2} \int d\mathbf{r}_1 d\mathbf{r}_2 \rho_\lambda^{(2)}(\mathbf{r}_1, \mathbf{r}_2) \phi_1(r_{12}) \stackrel{(14.10)}{=} \frac{V}{2} \rho^2 \int d\mathbf{r} g_\lambda(r) \phi_1(r), \tag{14.37}
\end{aligned}$$

where the last step only holds for uniform, isotropic systems in the thermodynamic limit. The Helmholtz free energy is

$$\begin{aligned}
F(N, V, T) &= F_0(N, V, T) + \frac{V\rho^2}{2} \int_0^1 d\lambda \int d\mathbf{r} g_\lambda(r) \phi_1(r); \\
&= F_0(N, V, T) + \frac{V\rho^2}{2} \int_0^1 d\lambda \int d\mathbf{r} [g_0(r) + \lambda g'_0(r) + \dots] \phi_1(r); \\
&= F_0(N, V, T) + \frac{V\rho^2}{2} \int d\mathbf{r} [g_0(r) + \frac{1}{2}g'_0(r) + \dots] \phi_1(r), \tag{14.38}
\end{aligned}$$

where  $g'_0(r) = (\partial g_\lambda(r)/\partial \lambda)_{\lambda=0}$ .

The crucial point of the perturbation theory for a dense liquid-like triple point Argon, *e.g.*, a liquid described by a pair potential of the form shown in the right-hand panel to Fig. 14.3, is that its radial distribution function  $g(r)$  hardly differs from that of the corresponding hard-sphere fluid, see the left-hand panel to that same figure. This implies that the decomposition

$$\phi_0(r) = \phi_{\text{HS}}(r) \quad \text{and} \quad \phi_1(r) = \phi(r) - \phi_{\text{HS}}(r) \tag{14.39}$$

is such that  $g'_0(r)$  (and also higher-order derivatives with respect to  $\lambda$ ) is small. Consequently, the free energy is given accurately by first-order perturbation theory about the hard-sphere reference fluid, *viz.*

$$\begin{aligned} F(N, V, T) &= F_{\text{HS}}(N, V, T) + \frac{V\rho^2}{2} \int d\mathbf{r} g_{\text{HS}}(r)(\phi(r) - \phi_{\text{HS}}(r)); \\ &= F_{\text{HS}}(N, V, T) + \frac{V\rho^2}{2} \int_{r>\sigma_{\text{HS}}} d\mathbf{r} g_{\text{HS}}(r)\phi(r), \end{aligned} \quad (14.40)$$

where we used that  $g_{\text{HS}}(r) = 0$  for  $r < \sigma_{\text{HS}}$ , the hard-sphere diameter. One can now use the Carnahan-Starling free energy of Eq. (14.29) as a very accurate representation of  $F_{\text{HS}}$ , and the PY radial distribution for  $g_{\text{HS}}(r)$ , to describe the thermodynamics of dense fluids quantitatively correctly. Note that there is some freedom to choose  $\sigma_{\text{HS}}$ .

## 14.5 Exercises

### Q81. Refresher on Fourier Transforms

The mathematics of this chapter relies heavily on Fourier transforms. In this exercise, you will consider several identities that are useful to the calculations that follow. We define the forward and backward Fourier transforms as

$$\hat{f}(\boldsymbol{\omega}) = \int d\mathbf{r} f(\mathbf{r}) e^{-i\boldsymbol{\omega} \cdot \mathbf{r}} \quad \text{and} \quad f(\mathbf{r}) = \frac{1}{(2\pi)^d} \int d\boldsymbol{\omega} \hat{f}(\boldsymbol{\omega}) e^{i\boldsymbol{\omega} \cdot \mathbf{r}}, \quad (14.41)$$

where  $d$  is the dimension of the vectors  $\mathbf{r}$  and  $\boldsymbol{\omega}$ .

- What are the Fourier transforms of: (i) The Gaussian function in 1D,  $\exp(-\alpha x^2)$  with  $\alpha > 0$  a constant? (ii) The Dirac distribution in 3D,  $\delta(\mathbf{r} - \mathbf{r}_0)$  with  $\mathbf{r}_0$  a fixed point? (iii) The Heaviside function  $\theta(x)$ , with  $\theta(x) = 0$  for  $x < 0$  and  $\theta(x) = 1$  for  $x > 0$ ? (iv) The 1D function  $x^n f(x)$  with  $f(x)$  a sufficiently smooth function that is itself Fourier transformable? Note: One of these is a trick question.
- What is the Fourier representation of the gradient of a function  $f(\mathbf{r})$  with  $\mathbf{r}$  a three-dimensional vector. And what is it for the Laplacian?
- Show that the convolution of two Fourier-transformable functions

$$h(x) = (f * g)(x) \equiv \int_{\mathbb{R}} dy f(y) g(x - y), \quad (14.42)$$

is given by the product of the Fourier transforms  $\hat{h}(\omega) = \hat{f}(\omega) \hat{g}(\omega)$ .

### Q82. Scattering and the Structure Factor

Consider the scattering set up shown in Fig. 14.1. The incoming radiation is coherent and monochromatic (wavelength  $\lambda$ ), the scattering is elastic, the scattering vector is  $\mathbf{q} = \mathbf{k}_o - \mathbf{k}_i$ , and the scattering angle is  $\theta$ .

- Show that the phase difference  $\Delta\psi$  of light that follows the two pathways towards the detector far from the sample is given by  $\Delta\psi = \mathbf{q} \cdot (\mathbf{r} - \mathbf{R})$ .
- Show that  $|\mathbf{q}| = (4\pi/\lambda) \sin(\theta/2)$ . This results indicates that the scattering angle and the (norm of the) scattering vector are one-to-one related for a given  $\lambda$  of the incoming beam.
- Show that the scattered intensity at angle  $\theta$  with respect to the incoming beam, for the case of a static configuration of  $N$  scatterers at positions  $\mathbf{r}_i$  in the sample, is proportional to  $\sum_{i,j}^N \exp(i\mathbf{q} \cdot \mathbf{r}_{ij})$ .
- Consider a perfect static cubic crystal with lattice spacing  $a$  without defects and without thermal excitations (no phonons). The crystal is perfectly aligned with the beam, *i.e.*,  $\mathbf{k}_i$  is parallel to a cartesian  $z$ -axis of the crystal, and the detector is in the  $xy$ -plane. Give a condition for wavevectors  $\mathbf{q} = (q_x, 0, q_z)$  for which a strong scattering (peak) is expected — this is an example of the Bragg condition for Bragg scattering giving rise to Bragg peaks.
- If the particles perform thermal motion during the scattering, *e.g.*, phonons in a crystal, diffusion in a liquid, or Brownian motion in a colloidal suspension, the scattering involves a thermal average. In this case, the intensity is proportional to  $S(q) = 1 + (1/N) \langle \sum_{i \neq j} \exp(i\mathbf{q} \cdot \mathbf{r}_{ij}) \rangle$  such that the Bragg peaks are smeared out. Calculate  $S(q)$  for an ideal gas.
- The length scale  $\ell$  that is ‘probed’ at wavenumber  $q$  is given by  $\ell = 2\pi/q$ . Show that length scales much larger than  $\lambda$  can be probed at small angles  $\theta$ . This is exploited in SAXS (small-angle X-ray scattering) measurements, where information on a length scale  $\ell \simeq 100\text{nm}$  can be obtained from X-rays with  $\lambda = 0.1\text{nm}$ . How small should the angle  $\theta$  then be?

**Q83. Hard spheres and  $g(r)$** 

A classical fluid with pair potential  $\phi(r)$  at density  $\rho$  and temperature  $T$  has a pressure  $p(\rho, T)$  given by Eq. (14.11),  $\beta p = \rho - (1/6)\rho^2 \int d\mathbf{r} \beta\phi'(r)rg(r)$ , with  $g(r)$  the radial distribution function.

- (a) It turns out that  $g(r) = \exp[-\beta\phi(r)]$  in the low-density limit  $\rho \rightarrow 0$ . Show, using integration by parts, that this is consistent with the *second virial* approximation  $\beta p = \rho + B_2(T)\rho^2$  with  $B_2 = (1/2) \int d\mathbf{r} (1 - \exp(-\beta\phi(r)))$ .

For hard spheres of diameter  $\sigma$  the radial distribution is discontinuous at  $r = \sigma$ , but one can show (not here) that it can be written as  $g(r) = \exp(-\beta\phi(r))y(r)$  with  $y(r)$  continuous.

- (b) Argue that  $d \exp[-\beta\phi(r)]/dr = \delta(r - \sigma)$ , and use this to show that the hard-sphere pressure can be written as  $\beta p = \rho(1 + 4\eta g(\sigma^+))$  with  $\eta = (\pi/6)\sigma^3\rho$  the packing fraction, and  $g(\sigma^+)$  the contact value  $g(r \downarrow \sigma)$ .
- (c) Use the Carnahan-Starling equation of state to calculate  $g(\sigma^+)$ , and evaluate it for  $\eta = 0.01$  and  $\eta = 0.5$ .

**Q84. The Three Routes from  $g(r)$  to Thermodynamics**

The three routes that lead from the radial distribution function to thermodynamics are called the *virial*, the *caloric*, and the *compressibility* route. The first two of these follow from the partition function  $Z(N, V, T) = Q(N, V, T)/N!\Lambda^{3N}$ , with  $Q(N, V, T) = \int_V d\mathbf{r}^N \exp[-\sum_{i<j}^N \phi(r_{ij})/k_B T]$  the configuration integral, and will be derived here.

- (a) Show first that  $\beta p = (\partial \log Q / \partial V)_{N, T}$ .

Taking the derivative in (a) w.r.t. the domain of integration of  $Q$  requires the following trick. Transform to scaled Cartesian coordinates  $s_{i\alpha} = r_{i\alpha}/V^{1/3}$ , i.e., such that  $d\mathbf{s}_i = d\mathbf{r}_i/V$  and  $\phi(r_{ij}) = \phi(s_{ij}V^{1/3})$ .

- (b) Show that the volume derivative gives rise to

$$\beta p = N/V - \frac{1}{6k_B T V} \int_V d\mathbf{r}_1 d\mathbf{r}_2 r_{12} \phi'(r_{12}) \rho^{(2)}(\mathbf{r}_1, \mathbf{r}_2). \quad (14.43)$$

Reduce this for a homogeneous and isotropic system to Eq. (14.11).

- (c) Show that  $E = \langle H \rangle = -(\partial \log Z / \partial \beta)_{N, V}$ , and rewrite this as Eq. (14.12).

Note that the virial and caloric route only hold for a pair-wise interaction Hamiltonian; the compressibility route is more generally valid.

**Q85. The Structure Factor and Ornstein-Zernike Theory**

In this exercise, we will develop a better feeling for the structure factor. The structure factor of a fluid is defined by

$$S(q) = 1 + \left\langle \frac{1}{N} \sum_{i \neq j}^N \exp(i\mathbf{q} \cdot \mathbf{r}_{ij}) \right\rangle, \quad (14.44)$$

with  $q = |\mathbf{q}|$ . The average is over a canonical ensemble.

- (a) Show that  $S(q) = 1 + (2\pi)^3 \rho \delta(\mathbf{q}) + \rho \int d\mathbf{r} \exp(i\mathbf{q} \cdot \mathbf{r}) h(r)$ , with  $h(r) = g(r) - 1$  the *total* correlation function and  $\rho = N/V$  the density. Hint: use that  $\int d\mathbf{r} \exp(i\mathbf{q} \cdot \mathbf{r}) / (2\pi)^3 = \delta(\mathbf{q})$  is a representation of the Dirac- $\delta$ .
- (b) Calculate  $S(q)$  for an ideal gas.

The Ornstein-Zernike equation  $h(r_{12}) = c(r_{12}) + \rho \int d\mathbf{r}_3 c(r_{13})h(r_{32})$  as given in Eq. (14.20) relates  $h(r)$  to the *direct* correlation function  $c(r)$  of a fluid at density  $\rho$ . Here  $r_{ij} = |\mathbf{r}_i - \mathbf{r}_j|$ . We define the Fourier transform  $\hat{h}(q) = \int d\mathbf{r} \exp(i\mathbf{q} \cdot \mathbf{r})h(r)$ , and likewise for  $\hat{c}(q)$ .

- (c) Show that  $\hat{h}(q) = \hat{c}(q) + \rho \hat{c}(q)\hat{h}(q)$ .  
 (d) Show that  $S(q) = (1 - \rho \hat{c}(q))^{-1}$ .  
 (e) We have already seen that  $g(r) = \exp(-\beta\phi(r))$  in the low- $\rho$  limit. Show that this is consistent with  $c(r) = \exp(-\beta\phi(r)) - 1 \equiv f(r)$  the Mayer function in this limit, and combine this with (d) to show for  $q \neq 0$  that  $S(q) = 1 + 24\eta[q\sigma \cos(q\sigma) - \sin(q\sigma)]/(q\sigma)^3 + \mathcal{O}(\eta^2)$  for hard spheres with diameter  $\sigma$  and packing fraction  $\eta = (\pi/6)\rho\sigma^3$ . What is the typical length scale?  
 (f) Check that the general identity  $\lim_{q \rightarrow 0} S(q) = k_B T (\partial\rho/\partial p)_T$  applied to the answer of (e) is consistent with the second-virial equation of state of hard spheres.

At higher densities a more accurate expression for  $c(r)$  is provided by PY theory, see Eq. (14.26), which results in  $g(r)$  as plotted in Fig. 14.1, giving quantitative agreement with ‘exact’ simulation results at densities as high as  $\eta = 0.49$ .

### Q86. Hard-Sphere Phase Diagram

Consider a mixture of hard spheres of diameter  $\sigma$ . The potential energy for a hard sphere system is given by

$$\beta U(r) = \begin{cases} 0 & r > \sigma \\ \infty & r \leq \sigma \end{cases} . \quad (14.45)$$

The packing fraction ( $\eta$ ) of the system is the amount of space occupied by the particles. Note: Feel free to use Mathematica to help solve this problem.

- (a) How is the number density  $\rho$  (the number of spheres per volume) related to the packing fraction  $\eta$ ?  
 (b) The equation of state for the hard sphere fluid is approximately

$$\frac{P_{\text{liq}}V}{Nk_B T} = \frac{1 + \eta + \eta^2 - \eta^3}{(1 - \eta)^3} . \quad (14.46)$$

What is the corresponding free energy? Hint: At very low packing fraction the hard sphere liquid acts like an ideal gas.

- (c) The hard sphere solid is a face-centered-cubic crystal. The equation of state of the hard sphere solid is well approximated by

$$\frac{P_{\text{sol}}V}{Nk_B T} = \frac{3}{1 - x} - 0.5921 \frac{x - 0.7072}{x - 0.601} \quad (14.47)$$

where

$$x = \frac{6\eta}{\pi\sqrt{2}} . \quad (14.48)$$

The excess free energy at a packing fraction  $\eta = 0.545$  is  $\beta F_{ex}/N = 5.91889$ . Note: the excess free energy is the difference between the free energy of the system and the free energy of an ideal gas. What is the free energy as a function of  $\eta$ ?

- (d) Using the free energies you just calculated, what equations would you need to solve to predict the coexistence between the liquid and solid in this system?

- (e) Using the result of part (d), what is the region of phase coexistence between the fluid and the solid as a function of  $\eta$ ?
- (f) What is the pressure at coexistence?
- (g) Which phase has the higher entropy at coexistence?
- (h) Sketch the resulting phase diagram.

**Q87. Equation of State for a Square-Well Fluid**

Consider a system with a square-well (SW) pair-interaction potential given by:

$$\phi_{\text{SW}}(r) = \begin{cases} \infty & r < \sigma \\ -\epsilon & \sigma \leq r \leq \lambda\sigma \\ 0 & r > \lambda\sigma \end{cases}, \quad (14.49)$$

with  $\lambda > 1$  a measure for the range of the attraction (strength  $\epsilon$ ) and  $r$  the center-of-mass separation between the particles. The equation of state (EoS) can be determined using a virial expansion at low densities. A more precise high-density EoS can be derived from the virial route.

- (a) Show that the pressure of the SW fluid is given by

$$\beta p_{\text{SW}} = \rho - \frac{\beta \rho^2}{6} \int_V dr r \phi'_{\text{SW}}(r) g_{\text{SW}}(r). \quad (14.50)$$

with  $\rho$  the particle number density,  $g_{\text{SW}}(r)$  the SW pair-correlation function and  $\phi'_{\text{SW}}(r)$  the derivative w.r.t.  $r$  of the pair potential.

- (b) Demonstrate that you can write:

$$\exp[-\beta \phi_{\text{SW}}(r)] = (1 - \exp(\beta\epsilon)) \Theta(r - \lambda\sigma) + \exp(\beta\epsilon) \Theta(r - \sigma), \quad (14.51)$$

where  $\Theta(x)$  is the Heaviside function, which has the property  $\Theta(x < 0) = 0$  and  $\Theta(x > 0) = 1$ .

- (c) Introduce  $e(r) = \exp[-\beta \phi_{\text{SW}}(r)]$  and  $y(r) = g_{\text{SW}}(r)/e(r)$  and use these functions to rewrite Eq. (14.50) in terms of these functions. Show that

$$\beta p_{\text{SW}} = \rho + \frac{2\pi\sigma^3}{3} \rho^2 [\exp(\beta\epsilon)y(\sigma) - \lambda^3 (\exp(\beta\epsilon) - 1) y(\lambda\sigma)], \quad (14.52)$$

and use this to obtain

$$\beta p_{\text{SW}} = \rho + \frac{2\pi\sigma^3}{3} \rho^2 [g_{\text{SW}}(\sigma^+) + \lambda^3 (g_{\text{SW}}(\lambda\sigma^+) - g_{\text{SW}}(\lambda\sigma^-))]. \quad (14.53)$$

with the plus and minus signs indicating the direction in which the limit to the value is taken, *i.e.*, from above and below, respectively.

Obtaining good contact values for  $g_{\text{SW}}(\lambda\sigma^+)$  is in general difficult. The square-well EoS can instead (more readily) be obtained by thermodynamic integration with respect to the hard-sphere (HS) reference. For this reference system, the reduced free energy is given by

$$f_{\text{HS}}(\eta) \equiv \beta \frac{\pi\sigma^3}{6} \frac{F_{\text{HS}}(\eta)}{V} = \eta \log \eta - \eta + \eta \frac{4\eta - 3\eta^2}{(1 - \eta)^2}, \quad (14.54)$$

in the Carnahan-Starling approximation, where we have ignored some constant offset.

- (d) State in a few words what the Carnahan-Starling approximation is.

- (e) Give an expression for  $\phi_*(r)$  which defines the perturbative pair potential by which the system goes from HS to SW interactions.
- (f) Derive that the thermodynamic perturbation of the HS fluid can be written as

$$f_*(\eta) = \frac{3\beta}{\pi\sigma^3}\eta^2 \int_{r>\sigma} d\mathbf{r} g_{\text{HS}}(r)\phi_{\text{SW}}(r), \quad (14.55)$$

where  $g_{\text{HS}}(r)$  is the HS pair-distribution function and  $f_{\text{SW}}(\eta) = f_{\text{HS}}(\eta) + f_*(\eta)$ .

- (g) Show that that Eq. (14.55) may be approximated as  $f_*(\eta) \approx -12\beta\epsilon\eta^2 g_{\text{HS}}(\sigma^+)$  when  $\lambda \approx 1$ .
- (h) State in a few words how you would obtain the contact value of the pair-distribution function  $g_{\text{HS}}(\sigma^+)$  for hard spheres at low densities.

Our rewrite may not seem to have solved much, as we still require the contact value of  $g_{\text{HS}}$ . However, in the Carnahan-Starling approximation

$$g_{\text{HS}}(\sigma^+) \approx \frac{1}{2} \frac{2-\eta}{(1-\eta)^3}. \quad (14.56)$$

- (i) Determine the differential equation for the reduced equation of state  $\beta \frac{\pi\sigma^3}{6} p_{\text{SW}}$  in terms of  $f_{\text{SW}}(\eta)$  as a function of  $\eta$ . Do not plug in expressions!
- (j) Taylor approximate the  $f_{\text{SW}}(\eta)$  up to  $\mathcal{O}(\eta^3)$  and show that in this low-density approximation  $\beta \frac{\pi\sigma^3}{6} p_{\text{SW}} \approx \eta + 4(1 - 3\beta\epsilon)\eta^2$  holds. Can the system phase separate?
- (k) Sketch a temperature  $T$ , density  $\rho$ , and coupling constant  $\lambda$  diagram, and explain using the diagram what the purpose of thermodynamic perturbation theory can be in this regard.

### Q88. Einstein Crystal and Thermodynamic Integration

The titular crystal consists of  $N$  particles at fixed equilibrium positions  $\mathbf{R}_i$ . Every particle is harmonically bound to a position by a spring with spring constant  $C$ , such that the Einstein Hamiltonian reads  $H_E = \sum_{i=1}^N H_i$  with  $H_i = \mathbf{p}_i^2/2m + C\mathbf{u}_i^2/2$  with  $m$  the mass,  $\mathbf{u}_i$  the displacement from equilibrium, and  $\mathbf{p}_i$  the momentum. The particles do not interact.

- (a) Calculate the Helmholtz free energy  $F_0(N, T)$  of this system. Does  $F$  depend on the  $\mathbf{R}_i$ ?
- (b) How does  $F$  depend on the value of  $C$ ? For which values of  $C$  does the free energy diverge? Does that make sense physically?

We are now interested in the free energy  $F(N, V, T)$  of a crystalline phase formed by hard spheres. We assume that the system is described by a Hamiltonian  $H = \sum_{i=1}^N \mathbf{p}_i^2/2m + \sum_{i<j}^N \phi(r_{ij})$ . Note that the particles are in principle free to move at low density. However, in the solid phase, they may be assumed to be effectively bound to cages through constraints imposed by their neighbors. The particles can rattle around in their cages about a well-defined center.

- (c) Use the Einstein crystal as a reference point to define a difference potential by which you can carry out thermodynamic integration on the system. Name your coupling constant  $\lambda$ . What is an appropriate choice for the center points to the Harmonic wells of the Einstein crystal? Why is the hard-sphere interaction problematic in setting up the difference potential? Provide your answers using only a *few* words.
- (d) Suppose we remove the hard-sphere interaction and we physically connect the particles to their closest lattice site. Explain in a *few* words what happens when  $\lambda \downarrow 0$ ?

- (e) If we keep the hard-sphere interaction, explain in a *few* words how you can effectively remove particle interaction by appropriately choosing value of  $C$  (assume a non-close-packed density).
- (f) Perform thermodynamic integration and show that

$$F = F_0 + \int_0^1 d\lambda \langle \Phi_1 \rangle_\lambda. \quad (14.57)$$

What is  $\Phi_1$  in this context? Your answer should follow from the insights you have gained above. What is the implicit assumption you make in setting  $F_0$  to your result from (a)?

## Chapter 15

# Gas-Liquid Interfaces and Classical Nucleation Theory

In the case of first-order phase transitions, we discovered that such systems have coexistences — for instance, in an  $NVT$  ensemble, we can have part of our system in the liquid phase and part of it in a gas phase; assuming we are in the coexistence region. However, we have completely neglected to discuss the *interface* between these two regions. In Exercise Q40 of Chapter 6, we argued that for a system in the thermodynamic limit, the surface free energy did not contribute to the free energy per particle in the system. However, there are cases where it can matter. In this chapter, we will examine the surface free energy for a gas-liquid interface, typically referred to as the surface tension. We then build upon this to discuss what happens inside the region of the phase diagram between the binodal and spinodal curves. This is the domain where there is an activation cost for going from one phase to another, as we have argued in Chapter 6. What happens within the spinodal region will also be touched upon, but a full theoretical description thereof goes beyond the scope of this course.

### 15.1 Free Energy of the Interface

We have seen that Eq. (13.8) for the Helmholtz free energy per unit volume predicts coexistence of a gas phase of density  $\rho_g$  and a liquid phase of density  $\rho_l$ , provided  $T < T_c$ . For a given temperature, the values for  $\rho_g$  and  $\rho_l$  follow from a common-tangent construction, or equivalently from the conditions of mechanical and diffusive equilibrium,

$$\begin{aligned} p(\rho_g) &= p(\rho_l) \equiv p_{\text{coex}}; \\ \mu(\rho_g) &= \mu(\rho_l) \equiv \mu_{\text{coex}}, \end{aligned} \tag{15.1}$$

where  $p_{\text{coex}}$  and  $\mu_{\text{coex}}$  are the coexistence pressure and chemical potential, and where  $\mu = (\partial f / \partial \rho)$  and  $p = -f + \rho(\partial f / \partial \rho) = -f + \mu\rho$ .

Here, we consider a fluid of volume  $V$  with overall density  $\rho \in [\rho_g, \rho_l]$  at  $T < T_c$ , such that it has phase separated into a gas phase (at high altitudes  $z$ ) and a liquid phase (at lower altitudes), separated by a planar interface of area  $A$ . We are interested in the density profile  $\rho(z)$  and the surface tension  $\gamma$ . The

boundary conditions are such that

$$\rho(z) = \begin{cases} \rho_g & z \rightarrow \infty \\ \rho_l & z \rightarrow -\infty \end{cases}. \quad (15.2)$$

Given that the chemical potential is a constant,  $\mu_{\text{coex}}$ , throughout the system, it is natural to work in the grand canonical ensemble and to consider the grand potential  $\Omega$  of this system. For a homogeneous system, we have seen that  $\Omega_{\text{hom}} = -pV$ , where  $p = p_{\text{coex}}$  in this case. We can therefore write, for a fixed value of  $\mu$

$$\frac{\Omega_{\text{hom}}}{V} = f(\rho) - \mu\rho, \quad (15.3)$$

which has a double-well structure as a function of  $\rho$ , with minimal values at  $\rho = \rho_g, \rho_l$ . The two minimum values are both  $-p_{\text{coex}}$ . We approximate this structure for  $\Omega_{\text{hom}}$  by the simple quartic expression

$$\frac{\Omega_{\text{hom}}}{V} \simeq -W(\rho) = -p + \frac{C}{2}(\rho - \rho_g)^2(\rho_l - \rho)^2, \quad (15.4)$$

where we dropped the subscript “coex” in  $p_{\text{coex}}$  for notational convenience, and where  $C > 0$  is a phenomenological positive constant. One easily checks that Eq. (15.4) is minimal at  $\rho = \rho_g, \rho_l$  and that the minimum values equal  $-p$ , as required.

In the case of a planar interface, the grand potential can be expanded in the gradients and higher-order derivatives of the density profile  $\rho(z)$ . By symmetry there is *no* contribution from terms linear in  $\rho'(z) \equiv \partial\rho(z)/\partial z$ , and the lowest-order nontrivial expansion is the square-gradient expression, where the grand potential of a system with a density profile  $\rho(z)$  is approximated by

$$\Omega = A \int_{-\infty}^{\infty} dz \left( -W(\rho(z)) + \frac{m}{2}(\rho'(z))^2 \right), \quad (15.5)$$

where  $m$  is a phenomenological prefactor that characterizes the stiffness of the interface — if  $m$  is large than there is large free-energy penalty for density gradients. Our task is now to find that profile  $\rho(z)$  that minimizes Eq. (15.5) for a given bulk gas-liquid coexistence characterized by  $\mu, p, \rho_g$ , and  $\rho_l$ .

If one is familiar with functional differentiation one directly sees that the minimization condition implies that  $\rho(z)$  must satisfy the condition

$$m \frac{\partial^2 \rho(z)}{\partial z^2} = -\frac{\partial W(\rho(z))}{\partial \rho(z)}. \quad (15.6)$$

This equation is analogous to the equation of motion of a particle at position  $x(t)$  at time  $t$  in a potential  $V(x)$ , for which the equation of motion (Newton’s law) reads  $\ddot{x}(t) = -V'(x)$ .

Those who are not so familiar with functional differentiation can arrive at Eq. (15.6) by discretizing the  $z$ -interval into equidistant points  $z_k$  separated from each other by  $\Delta z$ , such that

$$\Omega \simeq A \sum_k \Delta z \left[ -W(\rho_k) + \frac{m}{2} \left( \frac{\rho_{k+1} - \rho_{k-1}}{2\Delta z} \right)^2 \right], \quad (15.7)$$

where  $\rho_k = \rho(z_k)$ . Expression (15.7) is a function of a large discrete set of variables  $\{\rho_k\}$ , and we wish to find the minimum of this expression. This requires that the derivative w.r.t. to any of the  $\rho_k$ ’s must vanish, *i.e.*  $\partial\Omega/\partial\rho_i = 0$  for all  $i$ . This leads to

$$\begin{aligned} 0 &= -\frac{\partial W(\rho_i)}{\partial \rho_i} + \frac{m}{2} \left( \frac{1}{2\Delta z} \right)^2 \left( (\rho_i - \rho_{i-2}) - (\rho_{i+2} - \rho_i) \right); \\ &= -\frac{\partial W(\rho_i)}{\partial \rho_i} - m \frac{\rho_{i+2} + \rho_{i-2} - 2\rho_i}{(2\Delta z)^2}, \end{aligned} \quad (15.8)$$

which is indeed the discrete version of Eq. (15.6).

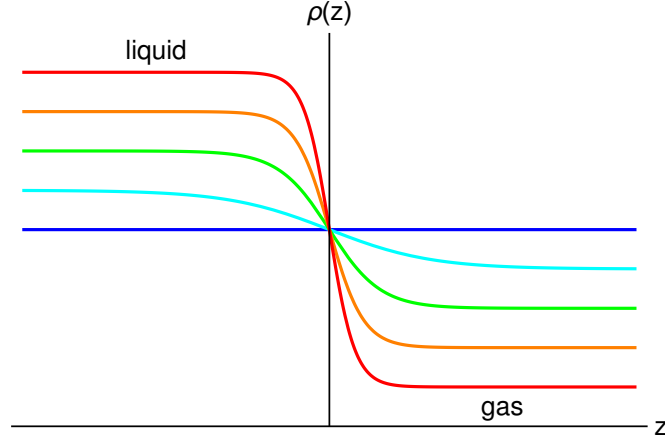


Figure 15.1: Sketch of Eq. (15.14) for a set of density differences with the density profile  $\rho$  given as a function of  $z$ , both in arbitrary units.

Multiplying both sides of Eq. (15.6) with  $\partial\rho(z)/\partial z$  yields

$$\begin{aligned} m \frac{\partial^2 \rho(z)}{\partial z^2} \frac{\partial \rho(z)}{\partial z} &= - \frac{\partial W(\rho(z))}{\partial \rho(z)} \frac{\partial \rho(z)}{\partial z} \Rightarrow \\ \frac{m}{2} \frac{\partial}{\partial z} \left( \frac{\partial \rho(z)}{\partial z} \right)^2 &= - \frac{\partial W(\rho(z))}{\partial z}, \end{aligned} \quad (15.9)$$

which can be integrated to yield

$$W(\rho(z)) + \frac{m}{2} (\rho'(z))^2 = \text{constant} = p, \quad (15.10)$$

where the constant value equals  $p$  because of the boundary conditions at  $z \rightarrow \pm\infty$ , where the gradients vanish. The mechanical analogue of this expression is conservation of the sum of potential and kinetic energy. It can be rewritten as

$$\frac{\partial \rho(z)}{\partial z} = -\sqrt{\frac{2}{m}} (p - W(\rho(z)))^{1/2} = -\sqrt{\frac{C}{m}} (\rho - \rho_g)(\rho_l - \rho), \quad (15.11)$$

where the minus sign is chosen because  $\rho'(z) < 0$ . Straightforward algebra yields

$$\begin{aligned} dz &= -\sqrt{\frac{m}{C}} \frac{d\rho}{(\rho - \rho_g)(\rho_l - \rho)} = -\underbrace{\sqrt{\frac{m}{C}} \frac{1}{\rho_l - \rho_g}}_{\equiv \xi} \left( \frac{d\rho}{\rho - \rho_g} - \frac{d\rho}{\rho_l - \rho} \right); \\ &= -\xi \left( d \log(\rho - \rho_g) - d \log(\rho_l - \rho) \right) = -\xi d \log \frac{\rho - \rho_g}{\rho_l - \rho}, \end{aligned} \quad (15.12)$$

where we defined the length scale

$$\xi = \sqrt{\frac{m}{C}} \frac{1}{\rho_l - \rho_g}. \quad (15.13)$$

Integration of Eq. (15.12) yields

$$z = -\xi \log \frac{\rho - \rho_g}{\rho_l - \rho} \Leftrightarrow \rho(z) = \frac{\rho_l + \rho_g}{2} - \frac{\rho_l - \rho_g}{2} \tanh \frac{z}{2\xi} \quad (15.14)$$

This analysis shows that  $\xi$  is the typical thickness of the meniscus, the length scale on which the crossover takes place from the bulk gas phase to the bulk liquid phase. Since  $(\rho_l - \rho_g) \rightarrow 0$  upon approaching the critical point, one sees that the interface thickness then diverges; a sketch is provided in Fig. 15.1.

The surface tension, the free energy cost of creating the interface per unit surface area, can be calculated by evaluation of the minimal grand potential, which yields

$$\begin{aligned}\Omega &= A \int dz \left( -W(\rho(z)) + \frac{m}{2} (\rho'(z))^2 \right) = A \int dz \left( -p + m(\rho'(z))^2 \right); \\ &= -pV + Am \int dz (\rho'(z))^2 \equiv -pV + \gamma A,\end{aligned}\tag{15.15}$$

where the surface tension  $\gamma$  can be calculated explicitly as

$$\begin{aligned}\gamma &= m \int_{-\infty}^{\infty} dz (\rho'(z))^2 = m \int_{-\infty}^{\infty} dz \frac{\partial \rho(z)}{\partial z} \rho'(z) \\ &= m \int_{\rho_l}^{\rho_g} d\rho \left( -\sqrt{\frac{C}{m}} \right) (\rho - \rho_g)(\rho_l - \rho) = \frac{\sqrt{Cm}}{6} (\rho_l - \rho_g)^3\end{aligned}\tag{15.16}$$

Note that the surface tension is positive per definition. Negative surface tensions are not permitted *in equilibrium*, because the system would be able to lower its free energy arbitrarily by creating increasing amounts of surface area. This is, to an extent, what happens within the spinodal region of the phase diagram, where the system is unconditionally unstable. In this context, note that Eq. (15.16) implies that  $\gamma \rightarrow 0$  upon approaching the critical point. This makes sense, as the system at the critical point is characterized by scale invariance with patches of either phase being present, and thus ‘interfaces’ on all length scales. In this context, phase-field models (relying on a free-energy density that has perturbative gradient contributions) can be used to study the behavior of such systems. One of the more well-known examples of this is the Cahn-Hilliard model.

Lastly, we note that you may have previously encountered the surface tension in a mechanical context, in the Young-Laplace equation, which describes the curvature of interfaces. The above result, derived from a statistical mechanics perspective, is exactly the surface tension that enters the Young-Laplace equation. For very small curvatures, corrections to the planar value of  $\gamma$  will need to be made, which requires the introduction of the Tolman length.

## 15.2 Classical Nucleation Theory

Now that we have defined the surface tension  $\gamma$ , we can examine what happens in the region between the binodal and spinodal of the phase diagram. Note that the system is unstable with respect to phase separation in this region of the phase diagram, but that it is conditionally unstable. An example of a such metastable state is a *supersaturated vapor*, *i.e.*, a gas phase that is metastable with respect to a state wherein gas and liquid coexist. Within the vapor, small clusters of liquid form and (provided they are small enough) shrink again throughout space and time. Only when a cluster becomes large enough, will it start to grow out to a bulk liquid phase. Depending on the degree of supersaturation, this may take a very, very long time to occur, as we will see in one of the exercises. Other instances of this kind of behavior, are found in *superheated liquids*, *supercooled liquids*, and *superheated crystals*, where the naming convention is unimagatively self-explanatory.

Classical nucleation theory (CNT) concerns itself with the description of these small nuclei — also sometimes referred to as condensates — of a daughter phase in the parent phase. Within the framework

of CNT it is also possible to predict the rate at which *critical nuclei* are formed, these are the nuclei that are of exactly the size required to cross the *nucleation threshold* or *nucleation barrier* and grow out to a bulk daughter phase. Before we proceed, we should remark on one additional concept. CNT in its simplest form concerns itself with *homogeneous* nucleation. That is, nucleation that occurs in the bulk of the parent phase. This is generally not the most prevalent or favorable form of nucleation, as *heterogeneous* nucleation has a lower nucleation barrier: ice tends to form on the edges of a container being cooled, rather than somewhere in the middle of the fluid. Or recall the example of Chapter 6 inducing crystallization in an undercooled liquid by inserting a needle.

### 15.2.1 Homogeneous Nucleation

The general starting point of CNT is to assume that all clusters that form are *spherical* with radius  $R$ . This is a rather strong assumption for the nucleation of crystals in a supercooled liquid, but it turns out to hold well for liquid nucleation in vapour and in many other cases of interest. Let the system have volume  $V$ , the nucleus (or daughter phase) volume  $V_n = (4/3)\pi R^3$ , and the pure (or mother) phase volume  $V_p = V - V_n$ . Then the total grand potential is given by

$$\Omega_{\text{tot}}(\mu, V, T; V_n) = \Omega_n(\mu, V_n, T) + \Omega_p(\mu, V_p, T) + \Omega_s(\mu, A, T), \quad (15.17)$$

where there are two terms  $\Omega_n$  and  $\Omega_p$  representing the volumetric contribution of the nucleus and pure phase, respectively, and the final term  $\Omega_s$  accounts for the contribution of the surface;  $A = 4\pi R^2$  is the area. Note that the total grand potential is conditioned on the presence of the nucleus. We can now determine the work required to form a nucleus using Eq. (15.17) as

$$\Delta\Omega = \Omega_{\text{tot}}(\mu, V, T; V_n) - \Omega_p(\mu, V, T) = \gamma A - (P_n - P_p)V_n \equiv \gamma A - \Delta P V_n. \quad (15.18)$$

Where in the penultimate step, we made use of thermodynamic identities from Chapter 1 and the definition of the surface tension  $\gamma$ , which we just obtained in the previous section. We will cover the derivation and features of Eq. (15.18) in Exercise Q89.

Note that the pressure in the pure and nucleating phase are not the same, in fact the pressure in the nucleus is higher. This might seem counterintuitive, as in bulk coexistence, there is mechanical equilibrium, which implies equal pressure between the coexisting phases. However, if you have studied the Young-Laplace equation, you may recall that the presence of interfacial tension induces a Laplace pressure (pressure difference) across any interface that is curved. Many textbooks make the connection between nucleation and the Gibbs free energy, which requires a Legendre transform of the grand potential in Eq. (15.18). However, you should exercise caution in reading such sources, as there are underlying assumptions that are not necessarily transparently presented. We refer the interested reader to W.W. Mullins [J. Chem. Phys. **81**, 1436 (1984)] for a more detailed and correct derivation of CNT, which is slightly involved, but that also covers crystal nucleation.

Examining the shape of Eq. (15.18) reveals that for small radii the surface term dominates the volume term, meaning that the formation of the daughter phase is not favored;  $\Delta\Omega > 0$ . For large radii the bulk (volume) term dominates, meaning that the nucleus can grow out, because  $\Delta\Omega < 0$ . These two behaviors are separated by an effective barrier to growth, the location of which can be computed by taking the derivative with respect to  $R$ , that is

$$\left. \frac{\partial \Delta\Omega}{\partial R} \right|_{R=R_c} = 0, \quad (15.19)$$

where  $R_c$  is the critical radius. However, be careful,  $\gamma$  is also dependent on  $R$  in this case. If one ignores this dependence, one readily finds  $R_c = 2\gamma/\Delta P$ . This should be familiar, as it is simply

an expression for the Laplace pressure. Plugging  $R_c$  into Eq. (15.18), gives the nucleation barrier  $\Delta\Omega_c \equiv \Delta\Omega(R_c) = 16\pi\gamma^3/(3\Delta P^2)$ . Clearly, the probability to form a nucleus of this size in the parent phase is given by  $p_c \propto \exp(-\beta\Delta\Omega_c)$ . Simulation studies have shown that this functional form indeed describes the probability of cluster sizes well. It is possible to determine the rate of nucleation under the assumption of single-particle attachment to a growing cluster in the parent phase. This makes use of both reaction rates and aspects of chemical equilibria as described in Chapter 5, but goes beyond the scope of these notes.

## 15.2.2 Heterogeneous Nucleation

We will finish this short excursion into CNT by considering why heterogeneous nucleation occurs more readily. Assume we have a flat wall with surface area  $A$ , which is in contact with our metastable phase, wherein nuclei are forming. We assume that the shape of the nucleus is a spherical cap<sup>1</sup>, such that its volume is given by

$$V_d = \frac{\pi h^2}{3} (3r - h), \quad (15.20)$$

with  $r$  the sphere radius and  $h$  the height of the top of the sphere cap above the plane. It will prove useful to express  $h = r(1 - \cos\theta)$ , with  $\theta$  the contact angle, as shown in Fig. 15.2.

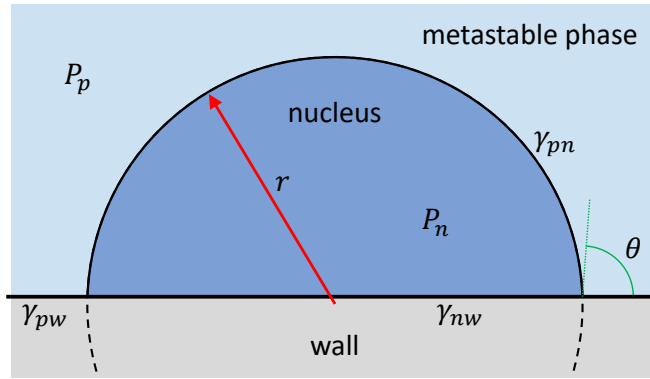


Figure 15.2: Cross-sectional sketch of a heterogeneous nucleation process taking place at a flat wall (grey). The nucleus (dark blue) is a spherical cap with radius  $r$  (red arrow) and contact angle  $\theta$ , as indicated by the angle in green. The pressures  $P_p$  and  $P_n$  of the metastable parent phase (light blue) and the nucleus-forming daughter phase are indicated, as well as the various surface tensions  $\gamma$ .

The area of between the parent and daughter phase is now given by  $A_{pn} = 2\pi rh$  and the area in of the nucleus in contact with the wall is given by  $A_{nw} = \pi(2rh - h^2)$ . Assume that the total volume of the system is given by  $V$  and that the parent phase has pressure  $P_p$ , the daughter phase has a pressure  $P_n$ , the surface tension between the wall and parent phase is  $\gamma_{pw}$ , and similarly  $\gamma_{nw}$  and  $\gamma_{pn}$  denote the respective daughter-wall and parent-daughter surface tensions. Then the total grand potential of the system is now given by

$$\Omega_{\text{tot}} = (P_n - P_p)V_n + (A - A_{nw})\gamma_{nw} + A_{nw}\gamma_{nw} + A_{pn}\gamma_{pn}, \quad (15.21)$$

<sup>1</sup>This assumption is justified as a spherical cap minimizes the surface area between the parent and daughter phase as well as the surface contact area and the three-phase contact line length.

such that the grand-potential difference with respect to the pure parent phase in contact with the wall is given by

$$\begin{aligned}\Delta\Omega &= \Delta PV_n + A_{\text{nw}}(\gamma_{\text{nw}} - \gamma_{\text{nw}}) + A_{\text{pn}}\gamma_{\text{pn}}; \\ &= \frac{\pi h^2}{3} (3r - h) \Delta P + \pi (2rh - h^2) (\gamma_{\text{nw}} - \gamma_{\text{pw}}) + 2\pi r h \gamma_{\text{pn}}.\end{aligned}\quad (15.22)$$

We now have an equation for  $\Delta\Omega$  in two (constrained) unknowns:  $r$  and  $0 \leq h \leq 2r$ , or equivalently  $r$  and  $0 \leq \theta \leq \pi$ . We now wish to eliminate one of the variables in order to proceed with our argument. Note that we could naively minimize  $\Delta\Omega$  with respect to both variables (under the assumption of constant  $\gamma$ s). However, it is advantageous to eliminate  $h$  at a given constant droplet volume, *i.e.*, as we vary  $h$  or  $\theta$  we must also vary  $r$  to ensure a constant volume. It is convenient to perform this minimization using  $\theta$  and we write

$$\Delta\Omega = \frac{4\pi r^3}{3} \Delta P (2 - 3 \cos \theta + \cos^3 \theta) + \pi r^2 (\gamma_{\text{nw}} - \gamma_{\text{pw}}) (1 - \cos^2 \theta) + 2\pi r \gamma_{\text{pn}} (1 - \cos \theta).\quad (15.23)$$

Here, the last two terms on the right-hand side constitute the surface contribution. We can now write this contribution in terms of  $dr$  and  $d\theta$ . Similarly, we can write  $dV_d = 0$ , since we impose a constraint on the volume. The differential for the constraint can be solved for  $dr$  and substituted back into the surface term. After some straightforward, but involved algebraic manipulation, we recover the relation

$$\cos \theta = \frac{\gamma_{\text{pw}} - \gamma_{\text{nw}}}{\gamma_{\text{pn}}}.\quad (15.24)$$

Note that this is simply the Young equation, which specifies the force balance on the contact line due to the difference in surface tensions between three phases that meet there. In this context,  $\theta$  is the contact angle and is a three-phase material property. In other words, at a constant droplet volume, the shape of the droplet is prescribed by energetic considerations involving the surface, for a given  $\theta$  and  $\gamma_{\text{pn}}$ .

Substituting the Young equation into Eq. (15.23), we finally obtain for fixed-volume clusters (the free parameter is  $r$ ) that the grand-potential difference for heterogeneous nucleation is given by

$$\Delta\Omega_{\text{het}} = \frac{\pi r^2}{3} (2 - 3 \cos \theta + \cos^3 \theta) (\Delta P r - 3\gamma_{\text{pn}}).\quad (15.25)$$

We can now compare this to the difference incurred in homogeneous nucleation, which is simply given by evaluating  $\Delta\Omega_{\text{het}}$  for  $\theta = \pi$ :

$$\Delta\Omega_{\text{hom}} = \frac{4\pi r^2}{3} (\Delta P r - 3\gamma_{\text{pn}}).\quad (15.26)$$

The normalized difference — recall that  $\Delta\Omega_{\text{hom}} > 0$  up to and (to an extent) beyond the critical radius — is thus

$$\frac{\Delta\Omega_{\text{het}} - \Delta\Omega_{\text{hom}}}{\Delta\Omega_{\text{hom}}} = -\frac{1}{4} (2 - \cos \theta) (1 + \cos \theta)^2 \leq 0,\quad (15.27)$$

where the last inequality obviously holds for all  $\theta$ . We conclude that heterogeneous nucleation is a favored pathway to nucleation, except in the limit of  $\theta = \pi$ . This limit corresponds to a fully hydrophobic surface in the case of water. Therefore, nucleation of water droplets occurs readily on hydrophilic surfaces.

### 15.3 Exercises

#### Q89. Classical Nucleation Theory

In this exercise, we examine the derivation of Eq. (15.18). Our starting point is Eq. (15.17).

- Explain using only a *few* words why it is possible to split the grand potential into three components.
- Use properties of the grand potential to introduce the pressure terms  $P_n$  and  $P_p$  into  $\Omega_{\text{tot}}$ . You will need to remove a constant term to obtain the result in Eq. (15.18), why is this permitted? Explain using a *few* words.
- Use the definition of the surface tension to rewrite the term  $\Omega_s(\mu, A, T)$ . Here, we assume that this term is only dependent on  $A$ , while in the derivation of  $\gamma$  we found that the interface has a finite width. What is assumed about the interface? Explain using a *few* words.
- Use a Legendre transform to convert the grand-potential difference to a Gibbs free-energy difference. What do you realize from this?
- The difference in pressures  $\Delta P$  is often converted into a difference in chemical potential  $V_n \Delta P = N_n [\mu_p(P_p) - \mu_n(P_p)]$ . This expression can be obtained by assuming the equation of state in the nucleus is approximately linear between the coexistence pressure and current pressure. Show this.

Be careful with your result from (e), it assumes that the nucleating vapor is incompressible, which may not be an accurate description.

#### Q90. Classical Nucleation in 2D

Here we use a simple 2D system to examine why nuclei are typically round.

- Assuming a surface tension given by  $\gamma$ , which is independent of size, and pressure difference  $\Delta P$ , calculate the free-energy barrier for nucleation in a two-dimensional system assuming that the nucleus that forms in the system is circular. What is the critical radius and the maximum barrier height?
- Calculate the barrier properties for nucleation in a 2D system assuming instead that the nucleus which forms is a square. What is the critical side length of the square? What is the maximum barrier height?
- Assuming that the kinetic prefactor  $\kappa$  is the same for both the square and spherical nuclei, which nuclei have a faster nucleation rate? Use this to explain why the nuclei in most systems are circular (or spherical in 3D).

#### Q91. Cylindrical Nucleation

A crystalline nucleus might form in a sample of needles at sufficient density. Provide the general expression for the Gibbs free energy difference and explain what the parameters represent that you need to specify in order to obtain a nucleation barrier. Derive an expression for the size of the critical nucleus and nucleation barrier, under the assumption that the nucleus is a cylinder with radius  $r/2$  and height  $r$ .

#### Q92. Classical Nucleation Theory with a Seed

Here we will rewrite classical nucleation theory with a “seed” crystal and see the effect this has on the nucleation barriers. For a seed, assume that we have a single crystal plane of diameter  $R_S$  as shown in Figure 15.3. Note that the seed is in exactly the same phase as the solid so we will not consider interactions between the seed and the nucleating crystal. However, the seed does change

the geometry of the nucleation. How does the volume of the nucleus depend on  $R_S$ ? The area? What is the resulting free energy barrier? Plot the free energy for different values of the surface tension and the chemical potential difference between the crystal and fluid. How does the seed change the free energy barriers? Note: Approximate all shapes as parts of spheres, not ellipses.

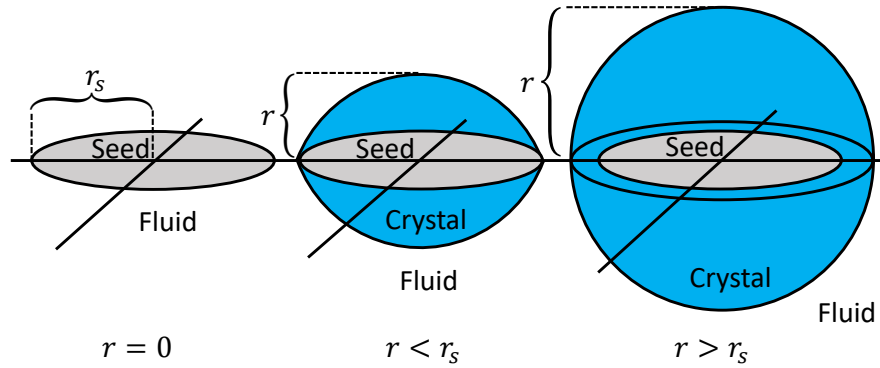


Figure 15.3: Illustration of nucleation with a seed, inspired by a similar figure from [Hermes *et al.*, *Soft Matter* **7**, 4517 (2011)].



## Chapter 16

# Multi-Component Fluids and Colloidal Suspensions

Important classes of systems in physical chemistry and biology are solutions and suspensions. They usually consist of *solvent* (*e.g.*, water, alcohol, cyclohexane) and *solute* (*e.g.*, ions in ionic solutions, polymers in polymeric solutions, and colloidal particles in colloidal suspensions). In many cases these systems are essentially classical — quantum mechanical effects can be ignored — and their thermodynamic properties can be studied from modifications and extensions of the statistical mechanics of one-component fluids discussed thus far. Such modifications and extensions are the topic of this chapter.

We distinguish two approaches. The first one is a direct generalization of the single-component theory discussed in the previous chapter; it treats all chemical components in the system on the same footing. For that reason it is most applicable to mixtures of fairly “similar” species, *e.g.*, Argon-Neon mixtures or salty water (*e.g.*, a mixture of  $\text{Na}^+$  and  $\text{Cl}^-$  in water). The second approach we discuss is more readily applicable to very asymmetric mixtures, *e.g.*, mesoscopic colloidal particles or macromolecules in a microscopic solvent. In this approach, we determine an effective Hamiltonian of the mesoscopic particles by integrating out the microscopic degrees of freedom in a suitably-defined partition function. This formalism will be worked out explicitly for a noninteracting (ideal) “solvent”. This example has direct relevance for understanding some colloid-polymer mixtures, since polymers can be modeled as objects that can interpenetrate, *i.e.*, an ideal gas.

### 16.1 Generalization of 1-Component Description to Mixtures

Consider a system of fixed volume  $V$  and temperature  $T$  with  $N_i$  particles of species  $i = 1, 2, \dots, s$ . The canonical partition sum of this multi-component mixture is given by

$$Z(\{N\}, V, T) = \int \left( \prod_{i=1}^s \frac{d\mathbf{r}_{(i)}^{N_i}}{N_i! \Lambda_i^{3N_i}} \right) \exp \left[ -\beta \Phi(\mathbf{r}_{(1)}^{N_1}, \dots, \mathbf{r}_{(s)}^{N_s}) \right], \quad (16.1)$$

where the coordinates of species  $i$  are denoted by  $\mathbf{r}_{(i)}^{N_i}$ . The Helmholtz free energy is given by

$$F(\{N\}, V, T) = -k_B T \log Z(\{N\}, V, T). \quad (16.2)$$

It is possible to extend the low-density virial expansion for the pressure and the Helmholtz free energy, as developed for one-component systems, to mixtures. In terms of the densities  $\rho_i = N_i/V$  and the De Broglie wavelength  $\Lambda_i$  of species  $i$ , as defined in Eq. (3.16), one obtains

$$\frac{F}{Vk_{\text{B}}T} = \sum_{i=1}^s \rho_i (\log \rho_i \Lambda_i^3 - 1) + \sum_{i,j=1}^s B_2^{(ij)}(T) \rho_i \rho_j + \frac{1}{2} \sum_{i,j,k=1}^s B_3^{(ijk)}(T) \rho_i \rho_j \rho_k + \cdots, \quad (16.3)$$

where the second virial coefficients are given in terms of the pair interactions  $\phi^{(ij)}(\mathbf{r})$  between species  $i$  and  $j$  by

$$B_2^{(ij)}(T) = -\frac{1}{2} \int d\mathbf{r} \left( \exp \left[ -\beta \phi^{(ij)}(\mathbf{r}) \right] - 1 \right). \quad (16.4)$$

This is a straightforward generalization of Eqs. (13.10) and (13.29) for one-component fluids. Higher-order virial coefficients can also be generated accordingly. The first term of Eq. (16.3) is the ideal gas contribution, the higher order terms are due to interactions.

One can also introduce pair correlation functions  $g^{(ij)}(r)$  analogously to the one-component case, and obtain the Helmholtz free energy  $F$  from a coupling constant integration after splitting  $\Phi = \Phi_0 + \Phi_1$  into a reference part  $\Phi_0$  and an excess part  $\Phi_1$ ,

$$F = F_0 + \frac{1}{2} V \sum_{i,j=1}^s \rho_i \rho_j \int_0^1 d\lambda \int d\mathbf{r} \phi_1^{(ij)}(r) g_\lambda^{(ij)}(r), \quad (16.5)$$

where  $F_0$  is the free energy of the  $s$ -component reference system, and where  $\phi_1^{(ij)}(r)$  is the perturbation of the pair-interaction between particles of species  $i$  and  $j$  with respect to the reference interaction.

The two above one-component expressions are useful provided the mixed chemical species are not too asymmetric, *e.g.*, for a mixture of Argon and Neon, or for a (dilute) mixture of colloidal particles with similar diameters.

## 16.2 Effective Interactions and the Osmotic Ensemble

In principle the formalism developed in the previous sections to deal with mixtures could also be used for, *e.g.*, a polymer solution or a colloidal suspension, where the species labeled say  $i = 1, \dots, s-1$  are the polymeric or colloidal particles, and species  $s$  the solvent. In the latter case, however, the density of the solvent is so high — even for very dilute solutions or suspensions — that a prohibitive number of virial coefficients or a very accurate theory for  $g^{(ss)}(r)$  is needed to describe the system realistically. In this approach most attention would thus be focused on the (often) least interesting part of the system: the solvent. This problem can be circumvented by changing the ensemble from canonical in all species  $i = 1, \dots, s$  to grand canonical in species  $s$  and still canonical in species  $i = 1, \dots, s-1$ . The corresponding partition sum  $\exp[-\beta\Omega]$ , with  $\Omega$  the “semi-grand” potential, is a function of the chemical potential of the solvent,  $\mu_s$ , the temperature  $T$ , the volume  $V$ , and the set of particle numbers  $N_1, \dots, N_{s-1}$ .

To ease the notation, from here on we will consider instead of an  $s$ -component system, a 2-component system of solutes (species 1, *e.g.*, colloids or macromolecules) and a solvent (species  $s$ ). It is straightforward to add more colloidal and solvent components later on, if desired. The role of the solvent can also be played by any other chemical component that we wish to integrate out, *e.g.*, ions in the case of charged colloids or depleting polymers in colloid-polymer mixtures.

The idea is to consider  $N_1 = N$  colloids in a volume  $V$  at temperature  $T$ , in a solvent at a chemical potential  $\mu_s$ . That is, we treat the colloids as a *canonical* ensemble, and the solvent as a *grand canonical* ensemble. Experimentally, one may envisage such a situation by a membrane equilibrium between a pure solvent at one side of a fixed membrane and a colloid-solvent mixture (of volume  $V$ ) at the other side, such that solvent molecules can permeate the membrane while the colloids cannot. The thermodynamic potential of this ensemble is  $F - \mu_s \langle N_s \rangle \equiv \Omega(N, V, T, \mu_s)$ , which satisfies

$$d\Omega = -pdV + \mu dN - SdT - \langle N_s \rangle d\mu_s, \quad (16.6)$$

with  $p$  the total pressure,  $\mu$  the chemical potential of the colloids,  $S$  the entropy, and  $\langle N_s \rangle$  the (average) number of solvent molecules in the volume  $V$ . Note that in the thermodynamic limit we may write  $N_s$  for  $\langle N_s \rangle$ , which we will do henceforth. Denoting the coordinates of the colloids by  $\{\mathbf{R}\}$ , and those of the solvent molecules by  $\{\mathbf{r}\}$ , the partition sum of this semi-grand or osmotic ensemble can be written as

$$\begin{aligned} \exp[-\beta\Omega] &= \sum_{N_s=0}^{\infty} \exp[\beta\mu_s N_s] Z(N, N_s, V, T); \\ (16.1) \quad &= \frac{1}{N! \Lambda_1^{3N}} \int d\mathbf{R}^N \underbrace{\sum_{N_s=0}^{\infty} \frac{\exp[\beta\mu_s N_s]}{N_s! \Lambda_s^{3N_s}} \int d\mathbf{r}^{N_s} \exp[-\beta\Phi(\{\mathbf{R}\}, \{\mathbf{r}\})]}_{\equiv \exp[-\beta\Phi^{\text{eff}}(\{\mathbf{R}\}; \mu_s, T)]}; \\ &= \frac{1}{N! \Lambda_1^{3N}} \int d\mathbf{R}^N \exp[-\beta\Phi^{\text{eff}}(\{\mathbf{R}\}; \mu_s, T)], \end{aligned} \quad (16.7)$$

where we defined the *effective interaction*  $\Phi^{\text{eff}}$  between the colloids. The effective interactions consist of direct interactions, *i.e.*, interactions that would be present between the colloid particles in vacuum, and of solvent-mediated interactions (that depend parametrically on  $\mu_s$  and  $T$ ). This can be made explicit by writing the interaction Hamiltonian as

$$\Phi(\{\mathbf{R}\}, \{\mathbf{r}\}) = \Phi_{11}(\{\mathbf{R}\}) + \Phi_{1s}(\{\mathbf{R}\}, \{\mathbf{r}\}) + \Phi_{ss}(\{\mathbf{r}\}), \quad (16.8)$$

where  $\Phi_{11}$  denotes the bare colloid-colloid interactions,  $\Phi_{1s}$  the colloid-solvent interactions, and  $\Phi_{ss}$  the solvent-solvent interactions. With this splitting of terms, which is completely general, we can write

$$\begin{aligned} \exp[-\beta\Phi^{\text{eff}}(\{\mathbf{R}\}; \mu_s, T)] &= \exp[-\beta\Phi_{11}(\{\mathbf{R}\})] \times \\ &\times \underbrace{\sum_{N_s=0}^{\infty} \frac{\exp[\beta\mu_s N_s]}{N_s! \Lambda_s^{3N_s}} \int d\mathbf{r}^{N_s} \exp[-\beta\Phi_{1s}(\{\mathbf{R}\}, \{\mathbf{r}\}) - \beta\Phi_{ss}(\{\mathbf{r}\})]}_{\equiv \exp[-\beta W(\{\mathbf{R}\}; \mu_s, T, V)]}; \\ &= \exp[-\beta\Phi_{11}(\{\mathbf{R}\}) - \beta W(\{\mathbf{R}\}; \mu_s, T, V)]. \end{aligned} \quad (16.9)$$

In words, the effective colloidal interactions consist of bare interactions  $\Phi_{11}$  and solvent-induced or solvent-mediated interactions  $W$ . In fact, one sees from its definition that  $W$  is the grand potential of the inhomogeneous solvent in the external field of the configuration  $\{\mathbf{R}\}$  of the colloids, and  $\exp[-\beta W]$  is the grand partition function of that system.

It is, of course, a gigantic problem to actually calculate  $W$  and hence  $\Phi^{\text{eff}} = \Phi_{11} + W$ , but the structure of Eq. (16.9) suggests the following scheme to calculate  $W$ . First, consider the case that *no* colloidal particles are present,  $N = 0$ . In that case the system is a one-component system consisting of solvent (at chemical potential  $\mu_s$ ) only, and  $W \equiv -p_0(\mu_s, T)V$  with  $p_0$  the pressure of that system. Note that  $p_0$  is

the pressure of the pure solvent reservoir at one side of the membrane. Next, consider the case that only 1 colloidal particle is present, at position  $\mathbf{R}_1$ . Then  $W = -p_0V + w_1(\mu_s, T)$ , where  $w_1$  is, by definition, the grand-potential excess of the solvent due to that solute particle. It incorporates entropic effects due to the restructuring of the solvent close to the colloidal surface, and energetic effects due to attractions and/or repulsions of the solvent molecules close to the colloidal surface. If  $w_1 \gg k_B T$  the solvent is a poor solvent for the colloids, and most likely the colloids will prefer to reside at the solvent meniscus or at the walls of the containers. If  $w_1 \ll -k_B T$  the solvent quality is good. Regardless the sign and magnitude, due to translational invariance  $w_1$  is independent of  $\mathbf{R}_1$  (for large enough  $V$ ). Finally consider the case of two colloidal particles, at positions  $\mathbf{R}_1$  and  $\mathbf{R}_2$ . Then  $W = -p_0V + 2w_1 + w_2(|\mathbf{R}_1 - \mathbf{R}_2|; \mu_s, T)$ , which defines the solvent-induced pair interaction between the colloids. Note that  $\lim_{r \rightarrow \infty} w_2(r) = 0$  by construction. Extending this reasoning to the  $N$ -colloid system yields

$$W(\{\mathbf{R}\}; \mu_s, T) = -p_0(\mu_s, T)V + Nw_1(\mu_s, T) + \sum_{i < j}^N w_2(R_{ij}; \mu_s, T) + \sum_{i < j < k}^N w_3(R_{ijk}; \mu_s, T) + \dots, \quad (16.10)$$

where  $R_{ijk}$  is short for the triangle-coordinates of the three colloids  $i, j, k$ , and where the dots represent solvent-induced four-and-higher-body interactions. Note that we have not explicitly *calculated*  $p_0, w_1, w_2$  etc. in terms of  $\Phi_{1s}$  and  $\Phi_{ss}$ , we have just split up the grand potential of the inhomogeneous solvent in terms of zero-, one-, two-body contributions, etc. But once they have been calculated, preferably by someone else, one can write the effective interactions as

$$\begin{aligned} \Phi^{\text{eff}}(\{\mathbf{R}\}) &= \Phi_{11}(\{\mathbf{R}\}) + W(\{\mathbf{R}\}; \mu_s, T); \\ &= -p_0(\mu_s, T)V + Nw_1(\mu_s, T) + \underbrace{\Phi_{11}(\{\mathbf{R}\}) + \sum_{i,j}^N w_2(R_{ij}; \mu_s, T) + \dots}_{\equiv H(\{\mathbf{R}\}; \mu_s, T)}, \end{aligned} \quad (16.11)$$

where we split of the coordinate-independent terms  $-p_0V + Nw_1$  from the coordinate-dependent terms that we collectively call  $H(\{\mathbf{R}\})$ . Before we carry on, we should note that main advantage of the series in Eq. (16.10) over a virial expansion is that the series is convergent and the approximation becomes better with the addition of higher-order terms.

We are now ready to evaluate the thermodynamic potential of interest,  $\Omega(N, \mu_s, V, T)$ . Insertion of Eq. (16.11) into Eq. (16.7) yields

$$\Omega(N, \mu_s, V, T) = -p_0(\mu_s, T)V + Nw_1(\mu_s, T) + A(N, V, T; \mu_s), \quad (16.12)$$

where  $A$  is defined by

$$\exp[-\beta A] = \frac{1}{N! \Lambda^{3N}} \int d\mathbf{R}_1 \cdots d\mathbf{R}_N \exp[-\beta H(\{\mathbf{R}\})]. \quad (16.13)$$

In other words,  $A$  is the *Helmholtz free energy* of the *canonical* system of  $N$  “dressed colloids” in a volume  $V$  at temperature  $T$  interacting with the Hamiltonian  $H(\{\mathbf{R}\}; \mu_s, T)$ . Note that Eqs. (16.12) and (16.13) are exact, *i.e.*, it is *not* an approximation to view the colloid-solvent mixture as a one-component system of colloids. Of course it will generally be difficult to calculate  $H$  exactly, and approximations will need to be made. Typically, one often ignores the induced triplet terms  $w_3$  and higher-body interactions, and often even the calculation of  $w_2$  involves drastic approximations. For colloid-polymer mixtures, with ideal polymers, an exact calculation is possible, as we will see in one of the problems.

The pressure  $p = -(\partial\Omega/\partial V)_{N,T,\mu_s}$  of the suspension, and the chemical potential  $\mu = (\partial\Omega/\partial N)_{V,T,\mu_s}$  of the colloids can be written from Eq. (16.13) as

$$p = p_0(\mu_s, T) + \Pi(\rho, \mu_s, T); \quad (16.14)$$

$$\mu = w_1(\mu_s, T) + \mu'(\rho, \mu_s, T), \quad (16.15)$$

where the *osmotic pressure*  $\Pi$  is the excess pressure (over that of the solvent reservoir) due to the presence of colloids,

$$\Pi = - \left( \frac{\partial A}{\partial V} \right)_{N,\mu_s,T}. \quad (16.16)$$

Here,  $\rho = N/V$  is the colloid density. Note that the osmotic pressure is the pressure of the effective colloids-only system, with interaction Hamiltonian  $H$ , *i.e.*, the pressure one would calculate if one had ignored the solvent from the start. The corresponding excess chemical potential is defined by

$$\mu' = \left( \frac{\partial A}{\partial N} \right)_{V,\mu_s,T}. \quad (16.17)$$

Note that the total chemical potential  $\mu$  is shifted by an amount  $w_1$  with respect to  $\mu'$ , due to the interactions with the solvent. As one is often interested in the effect of increasing colloid density for a given solvent at a given temperature, *i.e.*, at fixed  $T$  and  $\mu_s$ , one can view  $w_1$  as an arbitrary offset that need not be calculated or determined. The pressure of the solvent reservoir,  $p_0$ , can be treated similarly.

Of course it is still a big challenge to actually calculate  $w_1$ ,  $w_2(R_{ij})$ , *etc.* for given  $\mu_s$  and  $T$ , but the formalism shows that, once they have been determined, a solution or suspension can be treated as an interacting molecular “gas”, in which the dense solvent is solely present through  $\mu_s$  and  $T$ . Often  $w_3$  and higher body terms are ignored (just as in simple fluids), and one thus assumes pairwise additivity of the effective interactions. A well-known example of this is the Coulomb interaction  $q_1 q_2 / (\epsilon r)$  between charges  $q_1$  and  $q_2$  in a dielectric medium with dielectric constant  $\epsilon$ , where the *only* effect of the medium is to modify the bare interaction  $q_1 q_2 / r$  (the interaction in vacuum) by a factor  $\epsilon$ . Note that  $\epsilon = \epsilon(\mu_s, T)$ . In a solvent with mobile charges (e.g. salt ions), the bare Coulomb interaction are often approximated by  $q_1 q_2 \exp(-\kappa r) / (\epsilon r)$ , where  $\kappa(\{\mu_s\}, T)$  is the inverse Debye length of the reservoir, *i.e.*, it depends on the chemical potentials  $\{\mu_s\}$  of both the solvent and the ionic species.

The famous Van ‘t Hoff’s law  $\Pi = k_B T \rho$  follows if the solute interactions can be ignored,  $H \equiv 0$ , as *e.g.* in the low-density limit. At higher densities a virial expansion can be performed, and the second virial coefficient  $B_2(T, \mu_s)$  are given by integrals over Mayer functions of the effective pair interactions, *etc.* The free energy  $A$  and the osmotic pressure  $\Pi$  of dense suspensions can be studied by thermodynamic integration, exploiting radial distribution functions and their different routes to thermodynamics, the Ornstein-Zernike equation *etc.* for the effective colloids-only system. That is, the whole machinery of liquid state theory discussed in Chapters 13 - 15 can be applied.

### 16.3 Effective Interaction induced by Ideal Component

Let us discuss an example of the formalism of the effective Hamiltonian and the integrating out of component  $s$ . For simplicity we consider the case of an ideal “solvent”, *i.e.*, component  $s$  is assumed to be ideal. That is, the interaction part of the Hamiltonian of this two-component system is, for  $N_i$  particles of species  $i = 1, 2$ , given by

$$\Phi(\mathbf{R}^{N_1}, \mathbf{r}^{N_2}) = \Phi_{11}(\mathbf{R}^{N_1}) + \Phi_{12}(\mathbf{R}^{N_1}, \mathbf{r}^{N_2}) + \underbrace{\Phi_{22}(\mathbf{r}^{N_2})}_{\equiv 0 \text{ (ideal)}}, \quad (16.18)$$

where  $\mathbf{R}^{N_1}$  is the set of spatial coordinates of particles of species 1, and  $\mathbf{r}^{N_2}$  for species 2. Moreover, we focus attention to the pairwise additive case

$$\Phi_{12}(\mathbf{R}^{N_1}, \mathbf{r}^{N_2}) = \sum_{i=1}^{N_1} \sum_{j=1}^{N_2} \phi_{12}(\mathbf{R}_i - \mathbf{r}_j), \quad (16.19)$$

with  $\phi_{12}(r)$  the pair-interaction between particles of species 1 and 2 at separation  $r$ . This structure of  $\Phi_{12}$  leads straightforwardly to

$$\exp \left[ -\beta \Phi_{12}(\mathbf{R}^{N_1}, \mathbf{r}^{N_2}) \right] = \exp \left[ -\beta \sum_{i=1}^{N_1} \sum_{j=1}^{N_2} \phi_{12}(\mathbf{R}_i - \mathbf{r}_j) \right] = \prod_{j=1}^{N_2} \exp \left[ -\beta \sum_{i=1}^{N_1} \phi_{12}(\mathbf{R}_i - \mathbf{r}_j) \right]. \quad (16.20)$$

That is, dependence of the Boltzmann factor on  $\Phi_{12}$  is factorized according to  $\mathbf{r}_j$ . Consequently, we can write, using the thermal-volume-weighted fugacity  $\tilde{z}_2 = \exp[\beta\mu_2]/\Lambda_2^3$  of species 2 from Eq. (3.24),

$$\begin{aligned} \exp \left[ -\beta \Phi^{\text{eff}}(\mathbf{R}_1^N, \mu_2, T) \right] &= \\ &\stackrel{(16.7)}{=} \sum_{N_2=0}^{\infty} \frac{\exp[\beta\mu_2 N_2]}{N_2! \Lambda_2^{3N_2}} \int d\mathbf{r}_1 \dots d\mathbf{r}_{N_2} \exp \left[ -\beta \Phi(\mathbf{R}^{N_1}, \mathbf{r}^{N_2}) \right]; \\ &\stackrel{(16.20)}{=} \exp \left[ -\beta \Phi_{11}(\mathbf{R}^{N_1}) \right] \sum_{N_2=0}^{\infty} \frac{\tilde{z}_2^{N_2}}{N_2!} \left( \underbrace{\int d\mathbf{r} \exp \left[ -\beta \sum_{i=1}^{N_1} \phi_{12}(\mathbf{R}_i - \mathbf{r}) \right]}_{\equiv V_f(\mathbf{R}^{N_1})} \right)^{N_2}; \\ &= \exp \left[ -\beta \Phi_{11}(\mathbf{R}^{N_1}) \right] \sum_{N_2=0}^{\infty} \frac{\left( \tilde{z}_2 V_f(\mathbf{R}^{N_1}) \right)^{N_2}}{N_2!}; \\ &= \exp \left[ -\beta \Phi_{11}(\mathbf{R}^{N_1}) + \tilde{z}_2 V_f(\mathbf{R}^{N_1}) \right], \end{aligned} \quad (16.21)$$

where we defined the *free volume*  $V_f(\mathbf{R}^{N_1})$ . A comparison with Eq. (16.9) shows that  $W = -\tilde{z}_2 V_f$  now. Note that the dimension of  $V_f$  is indeed that of a volume. The reason of this nomenclature will be clarified later on. It follows from Eq. (16.21) that the effective interactions are given by

$$\Phi^{\text{eff}}(\mathbf{R}_1^N, \mu_2, T) = \Phi_{11}(\mathbf{R}^{N_1}) - \tilde{z}_2 k_B T V_f(\mathbf{R}^{N_1}), \quad (16.22)$$

where the first contribution is the “bare” and the second one the “induced” interaction, tunable by the fugacity (or chemical potential) of species 2. Since  $\tilde{z}_2 k_B T = p_0(\mu_2, T)$ , which is the pressure of the one-component ideal-gas system of species 1 in the reservoir, one can strengthen the effect of the induced interactions by increasing the pressure (or the density) of species 2.

## 16.4 Colloid-Polymer Mixtures

The explicit calculation of  $\Phi^{\text{eff}}(\mathbf{R}_1^N, \mu_2, T)$  for the case of an ideal component 2 is not only of academic interest, but actually finds a direct application in the description of mixtures of colloids and polymers. The reason is that polymers, under favorable circumstances, do behave like ideal particles as regards

their mutual interactions. Although they are statistically spherically symmetric, say with a diameter  $\sigma_p$ , their flexibility allows for center-to-center distances less than  $\sigma_p$  without a high energetic cost. This mutual interpenetration can, to a first approximation, be described by a vanishing polymer-polymer interaction,  $\Phi_{22} \equiv 0$ . We now regard the colloidal particles as hard spheres of diameter  $\sigma_c$ , *i.e.*, two colloids cannot approach each other more closely than a center-to-center distance  $\sigma_c$ . Moreover, although a polymeric particle can overlap with another polymer, it cannot overlap with a solid colloidal particle. This can be described by a colloid-polymer interaction,  $\phi_{12}(r)$ , that is hard-sphere like, with a distance of closest approach given by

$$\sigma_{cp} = \frac{\sigma_c + \sigma_p}{2}. \quad (16.23)$$

Recalling now the definition of the free volume,

$$V_f(\mathbf{R}^{N_1}) = \int d\mathbf{r} \exp \left[ -\beta \sum_{i=1}^{N_1} \phi_{12}(\mathbf{R}_i - \mathbf{r}) \right], \quad (16.24)$$

one sees that the only contribution to the integral over  $\mathbf{r}$  stems from those regions of space that are sufficiently far away from the center of *any* colloidal particle  $\mathbf{R}_i$ , *i.e.*, from those positions  $\mathbf{r}$  with  $|\mathbf{r} - \mathbf{R}_i| > \sigma_{cp}$  for all  $i = 1, \dots, N_1$ . This is indeed the “free” volume that is available to the polymers. The volume excluded to the polymers consists of  $N_1$  spheres of radius  $\sigma_{cp}$ , centered about the colloidal particles at positions  $\mathbf{R}_i$ . However, this does *not* imply that  $V_f = V - N_1(4\pi/3)\sigma_{cp}^3$ , since the exclusion-spheres (of radius  $\sigma_{cp}$ ) overlap with each other as soon as colloidal spheres are separated by a distance smaller than  $2\sigma_{cp}$ .

We will now restrict our attention, for simplicity, to pairwise exclusion overlaps only. It follows from basic geometry (see one of the problems) that the (lens-shaped) overlap volume of a pair of spheres of radius  $\sigma_{cp}$  at center-to-center distance  $R_{ij}$  is given by

$$v(R_{ij}) = \begin{cases} \frac{4\pi\sigma_{cp}^3}{3} \left[ 1 - \frac{3R_{ij}}{4\sigma_{cp}} + \frac{1}{16} \left( \frac{R_{ij}}{\sigma_{cp}} \right)^3 \right] & R_{ij} \leq 2\sigma_{cp} \\ 0 & R_{ij} > 2\sigma_{cp} \end{cases}. \quad (16.25)$$

Note that  $v(R_{ij})$  is non-negative, and varies smoothly from  $4\pi\sigma_{cp}^3/3$  at  $R_{ij} = 0$  to 0 at  $R_{ij} = 2\sigma_{cp}$ . Of course, the regime  $R_{ij} < \sigma_c$  is unphysical because of the colloidal hard-core, so the physically relevant interval of definition of  $v(R_{ij})$  is  $R_{ij} \geq \sigma_c$ . Ignoring triplet and higher-order overlaps, the free volume can now be written as

$$V_f(\mathbf{R}^{N_1}) = V - N_1(4\pi/3)\sigma_{cp}^3 + \sum_{i<j}^{N_1} v(R_{ij}). \quad (16.26)$$

Assuming now a pairwise additive bare interaction  $\Phi_{11}(\mathbf{R}^{N_1})$ , with a bare pair potential  $\phi_{11}(R_{ij})$ , one arrives with Eq. (16.22) at the effective colloid-colloid interaction Hamiltonian of the form

$$\Phi^{\text{eff}}(\mathbf{R}^{N_1}, \mu_2, T) = \Phi_0(N_1, V, \tilde{z}_2, T) + \sum_{i<j}^{N_1} \phi^{\text{eff}}(R_{ij}; \tilde{z}_2, T). \quad (16.27)$$

Here,  $\Phi_0(N_1, V, \tilde{z}_2, T) = -\tilde{z}_2 k_B T [V - N_1(4\pi/3)\sigma_{cp}^3]$  is independent of the colloidal coordinates  $\mathbf{R}^{N_1}$ . Due to the linear dependence of  $\Phi_0$  on  $N_1$  and  $V$  this term is irrelevant for the phase behavior; it can be seen as a mere shift of the pressure and the chemical potential as discussed in detail before. The

effective pair interaction  $\phi^{\text{eff}}$  is defined by

$$\beta\phi^{\text{eff}}(R_{ij}; \tilde{z}_2) = \beta\phi_{11}(R_{ij}) - \tilde{z}_2 v(R_{ij});$$

$$\stackrel{(16.25)}{=} \begin{cases} \infty & R_{ij} < \sigma_c \\ -\tilde{z}_2 \frac{4\pi\sigma_{cp}^3}{3} \left[ 1 - \frac{3R_{ij}}{4\sigma_{cp}} + \frac{1}{16} \left( \frac{R_{ij}}{\sigma_{cp}} \right)^3 \right] & \sigma_c \leq R_{ij} \leq \sigma_c + \sigma_p \\ 0 & R_{ij} > \sigma_c + \sigma_p \end{cases} \quad (16.28)$$

This effective pair potential, which is often referred to as the Asakura-Oosawa potential, describes an *attractive* interaction between a pair of colloids at separation  $R_{ij}$  in the range  $\sigma_c \leq R_{ij} \leq \sigma_c + \sigma_p$ . The strength of this attraction is proportional to the polymer volume-weighted fugacity  $\tilde{z}_2$  (or its dimensionless form  $\tilde{z}_2^* = (\pi/6)\sigma_p^3\tilde{z}_2$ ), whereas its range is determined by  $\sigma_p$  (or the dimensionless diameter ratio  $q \equiv \sigma_p/\sigma_c$ ). As an illustration we plot  $\beta\phi^{\text{eff}}$  for  $q = 0.4$  and two values of  $\tilde{z}_2^* = (\pi/6)\sigma_p^3\tilde{z}_2$  in Fig. 16.1. Note that the potential minimum occurs at contact,  $R_{ij} = \sigma_c$ .

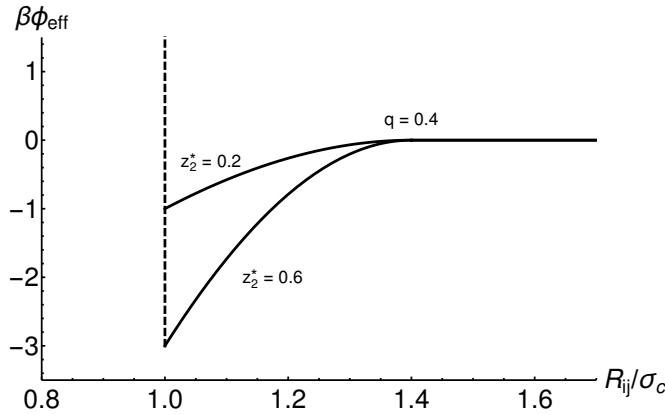


Figure 16.1: The effective pair interaction of two colloidal hard spheres (diameter  $\sigma_c$ ) in a sea of ideal polymers (diameter  $\sigma_p$ ) at the indicated dimensionless fugacity  $\tilde{z}_2^* = (\pi/6)\sigma_p^3\tilde{z}_2$ , for size ratio  $q = \sigma_p/\sigma_c = 0.4$ . The polymers induce an attraction for colloidal separations  $R_{ij} \in (\sigma_c, \sigma_c + \sigma_p)$ . The vertical dashed line indicates the hard-sphere divergence.

Now that the effective colloid-colloid interaction has been obtained, we can explicitly describe the colloid-polymer *mixture* as an effective one-component system with a pair interaction given by Eq. (16.28). It is now possible to apply all the techniques devised for one-component systems to calculate, *e.g.*, the (osmotic) pressure and the Helmholtz free energy, and from the latter the phase diagram. A convenient representation of such phase diagram is the  $\tilde{z}_2^*-\eta_c$  plane for a fixed diameter ratio  $q$ , with  $\eta_c = (\pi/6)\sigma_c^3 N_1/V$  the colloidal packing fraction, *i.e.*, the dimensionless density of colloids. This representation is very similar to the temperature-density representation of a truly one-component system such as Ar, for instance the tie-lines that connect two coexisting phases are horizontal. Note, however, that  $\tilde{z}_2$  plays the role of the *inverse* temperature: increasing  $\tilde{z}_2$  gives rise to a potential well that is deeper in units of  $k_B T$ , which corresponds to a lower temperature.

Figure 16.2 shows  $\tilde{z}_2^*-\eta_c$  phase diagrams for diameter ratios  $q = 0.1, 0.4, 0.6$ , and  $0.8$ , *i.e.*, for polymers smaller than colloids. These phase diagrams are obtained with a Monte Carlo technique to calculate  $F(N_1, V, T, \tilde{z}_2)$  at fixed  $\tilde{z}_2$  and  $T$  for many densities  $N_1/V$ , involving a coupling constant integration to gradually switch on the attractions starting from the hard-sphere fluid. The first observation is that all phase diagrams of Fig. 16.2 reduce, at  $\tilde{z}_2 = 0$ , to the hard-sphere phase diagram with a fluid phase

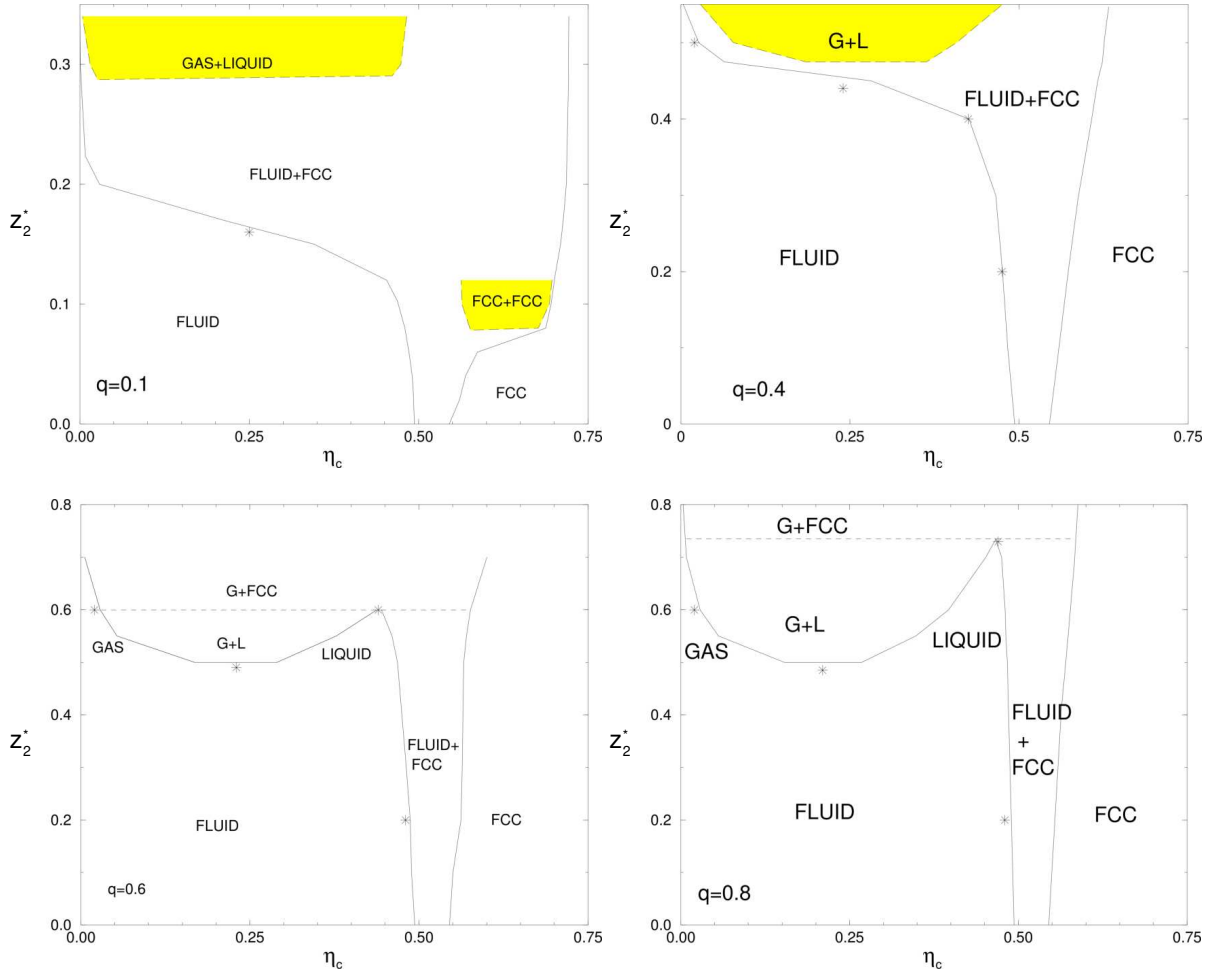


Figure 16.2: Phase diagrams of colloid-polymer mixtures for several size ratios  $q = \sigma_p/\sigma_c$  in the  $\eta_c$ - $\tilde{z}_2^*$  representation, with  $\eta_c = (\pi/6)\sigma_c^3 N_1/V$  the dimensionless colloid density and  $\tilde{z}_2^* = (\pi/6)\sigma_p^3 \tilde{z}_2$  the dimensionless polymer fugacity. We distinguish a face centered cubic (fcc) crystalline phase at sufficiently high  $\eta_c$ , and a fluid phase at lower  $\eta_c$ . For  $q = 0.1$  the system shows (metastable) fcc-fcc coexistence, where the two coexisting phase have a density (or lattice spacing). For  $q < q^* \simeq 0.5$ , the gas-liquid coexistence is metastable with respect to the fluid-fcc transition, *i.e.*, there is *no* liquid phase. At sufficiently high  $q$  and  $\tilde{z}_2^*$ , the fluid phase splits into a dilute colloidal gas and a dense colloidal liquid phase. Note that  $\tilde{z}_2^*$  is equal to the polymer packing fraction in a pure polymer system of fugacity  $\tilde{z}_2$ , since the polymers are ideal. Data kindly provided by M. Dijkstra.

at  $\eta_c < 0.494$ , an fcc solid phase at  $\eta_c > 0.545$ , and fluid-fcc coexistence in between. For nonzero  $\tilde{z}_2$  the phase diagrams are seen to strongly depend on the size ratio. For sufficiently large polymers, *e.g.*, at  $q = 0.8$  and  $0.6$ , the phase diagram features a gas-liquid coexistence regime, where a liquid phase exists between the critical and the triple point (dashed horizontal line). This is very similar to the phase diagram of Ar. This was to be expected, since the range of the attraction for these values of  $q$  is of the order of the colloidal diameter, just like the range of the Ar-Ar attractions is of the order of the Ar diameter (see the Lennard-Jones potential).

Upon decreasing  $q$ , *i.e.*, making the attractions relatively shorter ranged by using shorter polymers, it is found that the critical  $\tilde{z}_2$  and the triple point  $\tilde{z}_2$  approach each other, thereby decreasing the liquid regime, and finally annihilating it at  $q < q^* \simeq 0.5$ . That is, *there is no (stable) liquid phase when the range of the attractions is substantially shorter than the hard-core diameter*. Instead, for  $q < q^*$  there is a single fluid-fcc coexistence regime that broadens with increasing  $\tilde{z}_2$ . This coexistence regime does contain a gas-liquid binodal, as indicated by the grey areas, but this is metastable with respect to the fluid-fcc coexistence. Moreover, for  $q = 0.1$  another metastable transition appears that is very similar to the gas-liquid transition, except that it does not involve two fluid phases of different density but two fcc phases. This (metastable) fcc-fcc transition, which ends in a critical point just like the fluid-fluid (gas-liquid) transition, becomes stable at  $q = 0.05$  (not shown here).

## 16.5 Exercises

### Q93. Interactions in a Classical Two-Component Mixture

The interactions in a classical two-component mixture of  $N_1$  particles of type 1 (with coordinates  $\mathbf{R}^{N_1}$ ) and  $N_2$  particles of type 2 (with coordinates  $\mathbf{r}^{N_2}$ ) can always be written in the form

$$\Phi(\mathbf{R}^{N_1}, \mathbf{r}^{N_2}) = \Phi_{11}(\mathbf{R}^{N_1}) + \Phi_{22}(\mathbf{r}^{N_2}) + \Phi_{12}(\mathbf{R}^{N_1}, \mathbf{r}^{N_2}). \quad (16.29)$$

- (a) Give the canonical partition function  $Z(N_1, N_2, V, T)$  of this system, and the “semi-grand” partition function  $\Xi(N_1, \mu_2, V, T)$  with  $\mu_2$  the chemical potential of component 2. The “corresponding” thermodynamic potentials are the Helmholtz free energy  $F(N_1, N_2, V, T)$  and the semi-grand potential  $\Omega(N_1, \mu_2, V, T)$ , respectively. What is the relation between  $F$  and  $\Omega$ ?
- (b) It follows from (a) that  $\Omega$  can be written as

$$\exp[-\beta\Omega] = \frac{1}{N_1! \Lambda_1^{3N_1}} \int d\mathbf{R}^{N_1} \exp[-\beta\Phi^{\text{eff}}(\mathbf{R}^{N_1})], \quad (16.30)$$

with the “effective” 1-1 interaction  $\Phi^{\text{eff}} \equiv \Phi_{11}(\mathbf{R}^{N_1}) + W(\mathbf{R}^{N_1}; \mu_2, T)$ , with  $W$  the grand potential of the inhomogeneous fluid of species 2 in the static external potential due to particles of species 1 at positions  $\mathbf{R}_i$ . Show this and give a formal expression for the “induced” interactions  $W(\mathbf{R}^{N_1}; \mu_2, T)$ . Why is the nomenclature “effective” and “induced” useful?

- (c) If  $\Phi_{22} \equiv 0$  and  $\Phi_{12} = \sum_{i=1}^{N_1} \sum_{j=1}^{N_2} \phi_{12}(\mathbf{R}_i - \mathbf{r}_j)$ , *i.e.*, component 2 is an ideal gas and the 1-2 interaction is pairwise additive, then

$$W(\mathbf{R}^{N_1}; \mu_2, T) = -\tilde{z}_2 k_B T \underbrace{\int d\mathbf{r} \exp[-\beta \sum_{i=1}^{N_1} \phi_{12}(\mathbf{r} - \mathbf{R}_i)]}_{\equiv V_f(\mathbf{R}^{N_1})}, \quad (16.31)$$

with  $\tilde{z}_2 = \exp[\beta\mu_2]/\Lambda_2^3$  the thermal-volume-weighted fugacity of component 2. Prove this.

- (d) Give an interpretation of  $V_f(\mathbf{R}^{N_1})$  for the case that  $\phi_{12}$  is a hard-sphere potential with diameter  $\sigma_{12}$ . Calculate  $V_f(\mathbf{R}_1, \mathbf{R}_2) = V(R_{12})$  for  $N_1 = 2$  hard spheres (diameter  $\sigma_{11}$ ) at a distance  $R_{12} > \sigma_{11}$ . Does the ideal component induce an attraction or a repulsion between the two hard spheres? Is this effect stronger or weaker at increasing density of species 2?
- (e) The effective interaction between the spheres can also be interpreted as a larger available volume, and hence a larger entropy, for component 2 upon a decreasing  $R_{12}$ . Explain this.

### Q94. Demixing Revisited

Recall that a thermodynamic system at fixed particle numbers, volume, and temperature strives for a minimum of its Helmholtz free energy. Consider now the Helmholtz free energy  $F(N_1, N_2, V, T)$  of a binary mixture of  $N_1$  particles of species 1 and  $N_2$  particles of species 2 in a volume  $V$  at temperature  $T$ .

- (a) Show by considering 2 of these systems in diffusive contact, that for the system to be stable against demixing into coexisting phases, one requires that

$$2F(N_1, N_2, V, T) < F(N_1 + \Delta N_1, N_2 + \Delta N_2, V, T) + F(N_1 - \Delta N_1, N_2 - \Delta N_2, V, T), \quad (16.32)$$

for *any* (physically possible, positive or negative) change of particle numbers  $\Delta N_1$  and  $\Delta N_2$ . One could also consider a volume change  $\pm\Delta V$ , but because of extensivity reasons this does not lead to an additional stability condition.

- (b) Consider now the stability with respect to *infinitesimal* changes  $\delta N_1$  and  $\delta N_2$ , and show that the mixtures is stable with respect to these fluctuations provided

$$(\delta N_1, \delta N_2) \cdot \begin{pmatrix} \frac{\partial^2 F}{\partial N_1^2} & \frac{\partial^2 F}{\partial N_1 \partial N_2} \\ \frac{\partial^2 F}{\partial N_2 \partial N_1} & \frac{\partial^2 F}{\partial N_2^2} \end{pmatrix} \cdot \begin{pmatrix} \delta N_1 \\ \delta N_2 \end{pmatrix} > 0, \quad (16.33)$$

where the dots denote a matrix-vector (inner) product.

- (c) Argue that this implies that both the trace and the determinant of the  $2 \times 2$  matrix above must be positive for the mixture to be stable with respect to these infinitesimal fluctuations. State points where either the trace or the determinant is exactly zero are called *spinodal points*.

Within the second virial approximation  $F(N_1, N_2, V, T)$  is given by

$$\frac{F(N_1, N_2, V, T)}{k_B T} = N_1 \left( \log \frac{N_1 \Lambda_1^3}{V} - 1 \right) + N_2 \left( \log \frac{N_2 \Lambda_2^3}{V} - 1 \right) + \frac{B_{11} N_1^2 + 2B_{12} N_1 N_2 + B_{22} N_2^2}{V}, \quad (16.34)$$

where  $\Lambda_i$  de notes the thermal De Broglie wavelength of species  $i = 1, 2$ , and where  $B_{ij}$  denote the second virial coefficients, which we assume to be all positive here. We denote the densities by  $\rho_i = N_i/V$ .

- (d) Calculate the pressure  $p(\rho_1, \rho_2)$  and the chemical potentials  $\mu_i(\rho_1, \rho_2)$  for species  $i = 1, 2$ , and check that your expressions reduce to known one-component results for  $\rho_1 = 0$  and  $\rho_2 = 0$ .
- (e) Calculate the trace and the determinant of the  $2 \times 2$  matrix defined above. Can the trace be negative?
- (f) Define  $\rho_1 = x\rho$  and  $\rho_2 = (1-x)\rho$ , with  $x \in [0, 1]$  the composition variable and  $\rho = \rho_1 + \rho_2$  the total density, and show that the determinant vanishes if  $4x(1-x)\chi\rho^2 + 2(B_{11}x + B_{22}(1-x))\rho + 1 = 0$ , where  $\chi \equiv B_{11}B_{22} - B_{12}^2$ .
- (g) Show that the spinodal demixing condition of (f) has a physical (positive) solution  $\rho = \rho_{\text{spin}}(x)$  provided  $\chi < 0$ . Note that this physically means that the 1-2 repulsions are in some sense — the second virial sense — “stronger” than the 1-1 and 2-2 repulsions; it should agree with your intuition that mixtures demix if unlike species strongly repel.
- (h) Calculate  $\rho_{\text{spin}}(x)$  for the symmetric case that  $B_{11} = B_{22} \equiv B$  and  $\chi = -B^2\Delta$  for  $\Delta > 0$ , consider its limits at  $x = 0, 1, 1/2$  and sketch  $B\rho_{\text{spin}}(x)$  for  $x \in [0, 1]$ .
- (i) Why would the mixture as described in (h) only phase separate at a sufficiently high density  $\rho > \rho_{\text{spin}}(x)$ , *i.e.*, what stabilizes the mixture at lower densities?
- (j) Calculate  $\chi$  for hard spheres with diameters  $\sigma_1$  and  $\sigma_2$ . Could a mixture of these spheres possibly demix?

## Chapter 17

# Anisotropic Particles

Thus far, we have mostly considered fluids with spherically symmetric pair interactions  $\phi(|\mathbf{r}_1 - \mathbf{r}_2|)$ , *i.e.*, the interaction only depends on the positions of the center of mass  $\mathbf{r}_i$  of the particles. The only possible phases that these system can exhibit is gas, liquid, and solid<sup>1</sup>. However, many systems in nature cannot be described realistically by spherically symmetric interactions, and other phases apart from gas liquid and solid exist. Such phases are referred to as *mesophases* or *mesomorphic phases* to emphasize the in-between-ness of their structure: disordered in certain directions (liquid like) and ordered in others (solid like). We briefly touched upon mesophases for the example of ellipsoidal particles in the context of Landau theory in Chapter 9, but we return to this topic in more detail in this chapter.

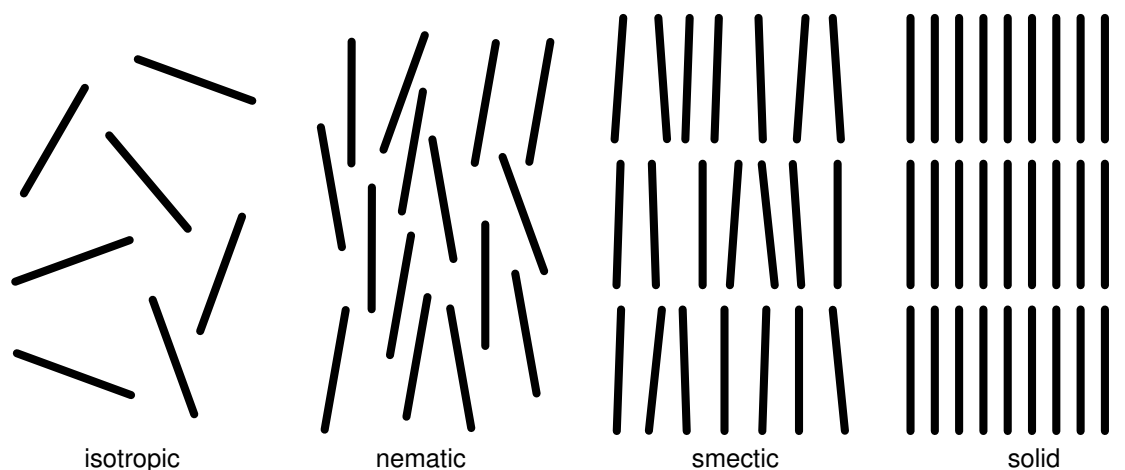


Figure 17.1: Two-dimensional impressions of typical three-dimensional configurations of rodlike particles in the isotropic, nematic, smectic, and crystalline (solid) phase, see Chapter 9 for the definitions.

To make the above more concrete, let us examine the phase behavior of needle-like objects. In general, “elongated” molecules like cholesterol or “rod-like” colloidal particles such as Tobacco Mosaic Virus

---

<sup>1</sup>Also the plasma phase, *i.e.*, a mixture of positive ions and electrons, can be described by the spherically symmetric Coulomb potential.

can show mesophases upon cooling or compressing<sup>2</sup>, see Fig. 17.1. For such molecules the phases are historically referred to as *liquid crystal phases* or simply *liquid crystals*, though the term is a bit of an oxymoron. Generally speaking, liquid crystals have a degree of ordering in between that of liquids (disordered, homogeneous, isotropic) and crystals (ordered, inhomogeneous, anisotropic). We refer back to Chapter 9 for the definitions of these terms.

Many other combinations of translational and rotational symmetries can be broken, and the number of liquid crystalline phases is vast (nematic, smectic, columnar, hexatic, blue phases, cholesteric, *etc.*). For this reason there is considerable fundamental interest in the structure of liquid crystals and phase transitions between different mesophases. Liquid crystals are also found in a wide range of industrial applications (*e.g.*, LCD's, sunroofs), thus the research into their properties has commercial and economic benefits. The importance of liquid crystals is essentially due to their character being in between that of liquids and crystals, *e.g.*, possessing the flow properties of a liquid and the light-scattering properties of a crystal. Lastly, liquid crystalline order has a strong connection with biophysics, *e.g.*, the behavior of suspension of viruses, the organization and colony development found in bacteria, and the structuring and dynamics of epithelia.

The properties of liquid crystals, their phases, and phase transitions can be (and are being) described using the principles of statistical mechanics. In this chapter, we will use the techniques of Chapter 13 to obtain a theory for the isotropic-nematic phase transition, focusing on interactions between rod-like particles. Perhaps surprisingly a direct generalization of the second virial approximation yields a realistic description of the nematic phase for rod-like particles. However, it should also be noted that colloid synthesis has advanced to the point that there is an entire zoo of shape-anisotropic particles, many of which are amenable to such a description, hence the title of the chapter “Anisotropic Particles”. Here, we will focus on rod-like systems here, but it is important to keep the generality in mind.

## 17.1 Partition Functions

A key ingredient of liquid crystallinity is the presence of *orientation* degrees of freedom. Referring back to Chapter 3, the microscopic state of a system with orientational degrees of freedom is fully characterized by the  $3N$  position coordinates  $\mathbf{r}^N \equiv \{\mathbf{r}_1, \dots, \mathbf{r}_N\}$  and  $3N$  orientation coordinates  $\mathbf{q}^N \equiv \{\mathbf{q}_1, \dots, \mathbf{q}_N\}$ , and the  $3N$  conjugate linear momenta  $\mathbf{p}^N \equiv \{\mathbf{p}_1, \dots, \mathbf{p}_N\}$  and  $3N$  conjugate angular momenta  $\mathbf{L}^N \equiv \{\mathbf{L}_1, \dots, \mathbf{L}_N\}$ , respectively. Note that we use  $\mathbf{q}_i$  for the orientations, as generally anisotropic interactions and particles require quaternions or Euler angles to describe the particle's orientation. The Hamiltonian of the system is appropriately extended to account for this in the following way:

$$\mathcal{H}(\mathbf{r}^N, \mathbf{p}^N, \mathbf{q}^N, \mathbf{L}^N) = \sum_{i=1}^N \frac{\mathbf{p}_i^2}{2m} + \sum_{i=1}^N \frac{\mathbf{L}_i^T \mathbf{I}^{-1} \mathbf{L}_i}{2} + \Phi(\mathbf{r}^N, \mathbf{q}^N), \quad (17.1)$$

where interaction potential  $\Phi$  is now dependent on the positions and orientations of all the particles. Here,  $\mathbf{I}$  is the moment of inertia tensor of particle  $i$  and the superscript  $T$  denotes transposition of the angular momentum. We work in a reference frame where the tensor is diagonal and it may contain three potentially different diagonal entries, say  $I_x$ ,  $I_y$ , and  $I_z$ , depending on the symmetry properties of the particles. The inverse of  $\mathbf{I}$  appears in Eq. (17.1) as a consequence of angular velocity  $\boldsymbol{\Omega}$  and angular momentum being linearly related *via* the inertia tensor:  $\mathbf{L} = \mathbf{I}\boldsymbol{\Omega}$ , which implies that the whole has units of energy.

---

<sup>2</sup>As we have seen in the Chapter 16 both molecular fluids and colloidal suspensions of systems may be described using similar theoretical means, with the difference lying in an “effective” interaction for the latter.

Despite the addition of angular-momentum and orientation terms to the Hamiltonian (17.1), much of the discussion in Chapter 3 can be readily extended to cover the new degrees of freedom. This should be clear from the rather general result of the equipartition theorem derived therein. Of particular relevance is the existence of a generalized partition function, which in the canonical ensemble is given by

$$Z(N, V, T) = \frac{1}{N!h^{6N}} \int d\mathbf{\Gamma} \exp[-\beta\mathcal{H}(\mathbf{\Gamma})] \quad (17.2)$$

where  $\mathbf{\Gamma} \equiv (\mathbf{r}^N, \mathbf{p}^N; \mathbf{q}^N, \mathbf{L}^N)$  here and we have  $h^{6N}$  instead of  $h^{3N}$  to also account for the contributions of the angular momenta. The canonical average of observables independent of linear and angular momentum, *i.e.*, observables described by phase functions  $\mathcal{A}(\mathbf{\Gamma}) = \mathcal{A}(\mathbf{r}^N, \mathbf{q}^N)$ , can be written as

$$\begin{aligned} \langle \mathcal{A} \rangle &= \frac{1}{N!h^{6N}Z(N, V, T)} \int d\mathbf{\Gamma} \exp[-\beta\mathcal{H}(\mathbf{\Gamma})] \mathcal{A}(\mathbf{r}^N, \mathbf{q}^N); \\ &= \frac{1}{Q(N, V, T)} \int d\mathbf{r}^N \int d\mathbf{q}^N \exp[-\beta\Phi(\mathbf{r}^N, \mathbf{q}^N)] \mathcal{A}(\mathbf{r}^N, \mathbf{q}^N), \end{aligned} \quad (17.3)$$

where the *configurational integral* is defined as over both positional and angular degrees of freedom

$$Q(N, V, T) = \int d\mathbf{r}^N \int d\mathbf{q}^N \exp[-\beta\Phi(\mathbf{r}^N, \mathbf{q}^N)]. \quad (17.4)$$

Note that

$$Z(N, V, T) = \frac{Q(N, V, T)}{N!\Lambda^{3N}\lambda_1^N\lambda_2^N\lambda_3^N}, \quad (17.5)$$

where the De Broglie wavelength  $\Lambda$  is as before. The  $\lambda_i$  ( $i = x, y, z$ ) are the dimensionless wavenumbers for the degrees of freedom associated with angular momentum and are given by

$$\lambda_i = \frac{h}{\sqrt{2\pi I_i k_B T}}. \quad (17.6)$$

This implies that the classical, canonical partition function for  $N$  noninteracting particles in a volume  $V$  at temperature  $T$  reduces to

$$Z(N, V, T) = \frac{1}{N!\Lambda^{3N}\lambda_1^N\lambda_2^N\lambda_3^N} \left( \frac{8\pi^2 V}{\sigma} \right)^N, \quad (17.7)$$

with the factor  $8\pi^2/\sigma$  stemming from the orientational integration. The factor  $\sigma$  is called the *symmetry number*. How does one arrive at this factor? Suppose that a particle has no symmetry properties, then one can choose an axis, usually one of the axes imposed by making  $\mathbf{I}$  diagonal. Complete rotation about this axis contributes a factor of  $2\pi$  to the orientational integral. Integration over all possible orientations of this axis, which is constrained to the unit sphere, contributes another factor of  $4\pi$ . However, this overcounts identical configurations whenever the particle has symmetries. It can be that the particle only possesses discrete symmetries, *e.g.*, the Platonic solids. In this case, the symmetry number is equal to the number of elements in its rotational symmetry group. Note that this leaves something to be desired for, when approximating continuous symmetries with discrete symmetries, such as a disk with a regular  $n$ -gon. Clearly the  $n$ -gon should have  $n \uparrow \infty$  symmetries to become a disk. The resolution to this problem comes from the freedom to ‘choose’ an orientational vector for the disk, which the  $n$ -gon does not possess. In general, one must be quite careful with symmetry, especially when mixing discrete and continuous symmetries. However, this is only an issue when examining the free energy or partition function, as for thermodynamic quantities (derivatives of the free energy) the prefactor drops out when considering single-component system. Situations where these considerations do play a role involve mixtures and/or chemical equilibria.

## 17.2 Onsager Theory

Let us now turn to the idealized case of uniaxial rod-like particles, *i.e.*, particles with the symmetry of a (circular) cylinder. The degrees of freedom are the center of mass position  $\mathbf{r} = (x, y, z)$  and the orientation  $\hat{\omega} = (\sin \theta \sin \varphi, \sin \theta \cos \varphi, \cos \theta)$ , where  $\theta$  and  $\varphi$  are the polar and azimuthal angle of the long axis of a rod with respect to some (arbitrary) frame. Note that we have ignored any rotations about the symmetry axis, as these do not lead to new configurations. In view of this, we have dropped the quaternion notation.

In the 1940's. Onsager described a system of identical rods as a multi-component system by (i) regarding particles with different orientations as chemically different species, (ii) applying the multi-component virial expansion of the free energy, Eq. (16.3), and (iii) minimizing the free energy with respect to the densities of particles pointing in each direction. With this scheme he could explain the (experimentally observed) phase transition from a disordered isotropic fluid phase at low densities to an orientationally ordered nematic phase at high densities. Moreover, he showed that the second virial approximation is *exact* in the limit of large length-to-diameter ratio of the rods (for the isotropic phase), a situation that we will consider in one of the exercises. Below we discuss the essential parts of Onsager's theory briefly.

Onsager's first step was to discretize the surface of the unit sphere into  $s$  domains ( $s \gg 1$ ) of area  $d\hat{\omega}_i$  centered around unit vectors  $\hat{\omega}_i$ , with  $i = 1, \dots, s$  and the normalization  $\sum_{i=1}^s d\hat{\omega}_i = 4\pi$ . He regarded a rod with orientation  $\hat{\omega}$  as a particle of species  $i$ , whenever  $\hat{\omega}$  is in the  $i$ -th domain of the unit sphere. Denoting the density of particles with orientation  $i$  by  $\rho_i$ , Onsager wrote the second-virial approximation to the Helmholtz free energy of the  $s$ -component system — using Eq. (16.3) — as

$$\begin{aligned} \frac{F}{Vk_{\text{B}}T} &= f = \sum_{i=1}^s \rho_i (\log(\rho_i \mathcal{V}) - 1) + \sum_{i,j=1}^s B_2^{(ij)}(T) \rho_i \rho_j; \\ &\stackrel{s \rightarrow \infty}{\equiv} \int d\hat{\omega} \rho(\hat{\omega}) (\log \rho(\hat{\omega}) \mathcal{V} - 1) + \int d\hat{\omega} d\hat{\omega}' B_2(\hat{\omega}, \hat{\omega}'; T) \rho(\hat{\omega}) \rho(\hat{\omega}'), \end{aligned} \quad (17.8)$$

where the continuum limit  $s \rightarrow \infty$  results in integrals over the unit sphere. Here, the “thermal volume”  $\mathcal{V}$  is the analogue for rods of the factor  $\Lambda^3$  for spheres; its precise form is immaterial as it has no bearing on physically measurable quantities. Recall that the second virial coefficient is given by

$$\begin{aligned} B_2^{(ij)}(T) &= -\frac{1}{2} \int d\mathbf{r} \left( \exp[-\beta \phi^{(ij)}(r)] - 1 \right); \\ &\stackrel{s \rightarrow \infty}{\equiv} -\frac{1}{2} \int d\mathbf{r} \left( \exp[-\beta \phi(r, \hat{\omega}, \hat{\omega}')] - 1 \right) \equiv B_2(\hat{\omega}, \hat{\omega}'; T), \end{aligned} \quad (17.9)$$

where the pair potential  $\phi(r, \hat{\omega}, \hat{\omega}')$  between two rods at separation  $r$  depends on the two orientations,  $\hat{\omega}$  and  $\hat{\omega}'$ , of the two rods under consideration. Before specifying the precise form of this pair potential, we discuss Onsager's next step: minimize the free-energy density  $f$  with respect to  $\rho_i$  (or  $\rho(\hat{\omega})$ ). Naively one would solve the  $s$  coupled equations  $\partial f / \partial \rho_i = 0$  for the  $s$  unknown quantities  $\rho_i$  at fixed  $T$  and total density of the rods  $\rho$ . The problem, however, is that the  $\rho_i$ s must satisfy the normalization constraint  $\sum_{i=1}^s \rho_i = \rho$ , (or in the continuum limit  $\int d\hat{\omega} \rho(\hat{\omega}) = \rho$ ). This constraint is most easily taken into account by introducing the Lagrange multiplier  $\lambda$  (see Chapter 2), and solving the resulting set of coupled nonlinear equations

$$\begin{aligned} 0 &= \frac{\partial}{\partial \rho_i} \left( f - \lambda \sum_{i=1}^s \rho_i \right) \\ &= \log \rho_i \mathcal{V} + 2 \sum_{j=1}^s B_2^{(ij)} \rho_j - \lambda. \end{aligned} \quad (17.10)$$

The value of  $\lambda$  will be fixed, at a later stage of the calculation, by the normalization constraint. The (implicit) solution of Eq. (17.10) reads

$$\rho_i = \frac{\exp(\lambda)}{\mathcal{V}} \exp \left[ -2 \sum_{j=1}^s B_2^{(ij)} \rho_j \right], \quad (17.11)$$

which can be interpreted as a self-consistent Boltzmann distribution, in the sense that the density  $\rho_i$  is proportional to a Boltzmann factor that depends on all  $\rho_j$ s (including the terms  $i = j$ ). That is, the term  $2 \sum_{j=1}^s B_2^{(ij)} \rho_j$  is like a potential (divided by  $k_B T$ ) that acts on species  $i$ . This potential is, of course, due to the interaction with all the other species (and its own species). The normalization follows from Eq. (17.11) as

$$\sum_{k=1}^s \rho_k = \frac{\exp(\lambda)}{\Lambda^3} \sum_{k=1}^s \exp \left[ -2 \sum_{j=1}^s B_2^{(kj)} \rho_j \right] = \rho. \quad (17.12)$$

The Lagrange multiplier  $\lambda$  must therefore satisfy

$$\frac{\exp(\lambda)}{\mathcal{V}} = \frac{\rho}{\sum_{k=1}^s \exp \left[ -2 \sum_{j=1}^s B_2^{(kj)} \rho_j \right]}, \quad (17.13)$$

and hence we obtain, from Eq. (17.11), the implicit equations for the minimizing densities

$$\rho_i = \frac{\rho \exp \left[ -2 \sum_{j=1}^s B_2^{(ij)} \rho_j \right]}{\sum_{k=1}^s \exp \left[ -2 \sum_{j=1}^s B_2^{(kj)} \rho_j \right]}. \quad (17.14)$$

The continuum version of this equation, which we will analyze from now on, is given by

$$\rho(\hat{\omega}) = \frac{\rho \exp \left[ -2 \int d\hat{\omega}' B_2(\hat{\omega}, \hat{\omega}') \rho(\hat{\omega}') \right]}{\int d\hat{\omega}'' \exp \left[ -2 \int d\hat{\omega}' B_2(\hat{\omega}'', \hat{\omega}') \rho(\hat{\omega}') \right]}. \quad (17.15)$$

This equation is a nonlinear integral equation for  $\rho(\hat{\omega})$ , that must be solved for given and fixed total density  $\rho$ .

It is possible to construct the trivial,  $\hat{\omega}$ -independent solution to Eq. (17.15)

$$\rho(\hat{\omega}) = \frac{\rho}{4\pi}, \quad (17.16)$$

for any  $\rho$  and  $T$ . That this a solution of Eq. (17.15) follows from the rotational invariance of the pair interactions, which leads to  $B_2(\hat{\omega}, \hat{\omega}') = B_2(\mathbf{R}\hat{\omega}, \mathbf{R}\hat{\omega}')$  for any SO(3) (rotation) matrix  $\mathbf{R}$ . This implies that  $\int d\hat{\omega}' B_2(\hat{\omega}, \hat{\omega}')$  is independent of  $\hat{\omega}$ . The distribution of Eq. (17.16) describes the *isotropic phase* of the rod system, *i.e.*, the phase with *no* preferred direction of the long axes of the rods. Inserting the isotropic solution Eq. (17.16) back into the expression for  $f$ , Eq. (17.8), yields the free-energy density of the isotropic phase (in the second virial approximation)

$$f_{\text{iso}}(\rho, T) = \rho \left( \log \frac{\rho \mathcal{V}}{4\pi} - 1 \right) + b(T) \rho^2, \quad (17.17)$$

with the orientation-averaged second virial coefficient

$$b(T) = \frac{1}{(4\pi)^2} \int d\hat{\omega} d\hat{\omega}' B_2(\hat{\omega}, \hat{\omega}'; T). \quad (17.18)$$

It turns out that the isotropic distribution is the *only* solution of Eq. (17.15) at sufficiently low densities  $\rho$  or sufficiently high temperatures  $T$ . That is, the second virial theory predicts that the isotropic phase is the only possible phase for a fluid of rods in these regimes — this is consistent with experimental observations. For typical rod interactions, which are such that  $B_2(\hat{\omega}, \hat{\omega}')$  is smaller for smaller angles between  $\hat{\omega}$  and  $\hat{\omega}'$ , there is also an *anisotropic* solution to Eq. (17.15) provided  $\rho$  is sufficiently high or  $T$  sufficiently low. This anisotropic solution describes the nematic phase. Unfortunately, it is not possible to calculate this nematic distribution analytically, but it is numerically straightforward to solve the equation by means of, *e.g.*, iteration. The idea is to guess, for fixed  $\rho$  and  $T$ , an explicit form for  $\rho(\hat{\omega})$ , from which a second guess follows by evaluating the right-hand side of Eq. (17.15), *etc.*, until a *self-consistent* solution for  $\rho(\hat{\omega})$  is found. This solution can then be inserted into Eq. (17.8) to obtain the free-energy density  $f_{\text{nem}}(\rho, T)$  of the nematic phase. Note that this quantity only exists at high  $\rho$  and/or low  $T$ . Of course, it should be clear that an explicit form for  $B_2(\hat{\omega}, \hat{\omega}')$  is needed for such numerical calculations.

The fact that  $f$  in Eq. (17.8) can be minimized by either an isotropic or a nematic distribution is due to the fact that the first (ideal-gas) term of Eq. (17.8) is minimized by the isotropic distribution (with a maximum entropy), while its second term is minimized by nematic distributions, since typical  $B_2(\hat{\omega}, \hat{\omega}')$  for rods is such that small angles between  $\hat{\omega}$  and  $\hat{\omega}'$  have a lower  $B_2$  than large angles. At a sufficiently low total density  $\rho$ , the second  $\mathcal{O}(\rho^2)$  term is dominated by the first  $\mathcal{O}(\rho \log \rho)$  term, and hence the minimum of the sum of these terms is realized by the minimum of the first term. At higher densities, the second term becomes relevant and its minimization requires orientational ordering.

### 17.3 The Hard-Rod Fluid

In order to be specific we apply Onsager's theory, as he did himself, to the case of a fluid of hard *spherocylinders*, which are model rod-like particles that consist of a cylinder of length  $L$  and diameter  $D$  with spherical end caps of diameter  $D$ . The volume  $v_0$  of such a particle consists of the volume of the cylinder,  $(\pi/4)LD^2$ , and that of the two hemispheres,  $(\pi/6)D^3$ , *i.e.*,  $v_0 = (\pi/6)D^3 + (\pi/4)LD^2$ . The aspect ratio  $L/D$  can vary between 0 (spheres) and  $\infty$  (needle). The fluid is characterized by the hard-rod pair potential

$$\phi_{\text{HR}}(\mathbf{r}_{12}, \hat{\omega}_1, \hat{\omega}_2) = \begin{cases} \infty & \text{in the case of overlap} \\ 0 & \text{otherwise} \end{cases}, \quad (17.19)$$

which is the direct analogue for “cigar” shaped particles of the hard-sphere potential for spheres. The Mayer function that corresponds with this potential is therefore -1 in the case of overlap and 0 otherwise. It then follows from the geometry of the problem that

$$B_2(\hat{\omega}, \hat{\omega}') = 4v_0 + L^2D|\sin \gamma(\hat{\omega}, \hat{\omega}')| \stackrel{L \gg D}{\approx} L^2D|\sin \gamma(\hat{\omega}, \hat{\omega}')|, \quad (17.20)$$

where  $\gamma$  is the angle between  $\hat{\omega}$  and  $\hat{\omega}'$ , *i.e.*,  $\cos \gamma \simeq \hat{\omega} \cdot \hat{\omega}'$ . In the long-rod limit  $L \gg D$ , the  $v_0$  term is  $\mathcal{O}(LD^2)$ , and is thus vanishingly small compared to the  $\mathcal{O}(L^2D)$  term<sup>3</sup>. From now on we will work, implicitly, in this thin-needle (long-rod) limit.

The isotropic distribution in Eq. (17.16) holds for any  $B_2(\hat{\omega}, \hat{\omega}')$ , and hence also for the hard-needle case of interest here. Its orientation average, defined in Eq. (17.18), is given by  $b = 4v_0 + (\pi/4)L^2D \rightarrow (\pi/4)L^2D$ , as will be worked out in one of the problems. It is independent of  $T$  in this hard-rod case. With this  $b$ , the free energy of the isotropic phase is thus completely specified by Eq. (17.17) within the

<sup>3</sup>This argument does not hold if the two rods are exactly parallel,  $\gamma = 0$ . This case is, however, of measure zero and thus statistically irrelevant.

second-virial approximation. One expects nematic solutions that minimize Eq. (17.8) at high enough  $\rho$ . The reason is that the last term of Eq. (17.8) is small, with the  $B_2$  of Eq. (17.20), if small angles  $\gamma$  occur frequently, *i.e.*, if  $\rho(\hat{\omega})$  is peaked about a specific director, say  $\hat{\mathbf{n}}$ . The direction of  $\hat{\mathbf{n}}$  is irrelevant for the resulting free energy of a bulk fluid by symmetry, since the free energy will not be affected by a global rotation. The symmetry is also such that a rotation about the symmetry axis  $\hat{\mathbf{n}}$  does not affect the free energy, and the resulting minimizing distribution can only depend on the polar angle  $\theta$  of the orientation  $\hat{\omega}$  with respect to  $\hat{\mathbf{n}}$ , *i.e.*,  $\rho(\hat{\omega}) = \rho(\theta)$  with  $\cos \theta = \hat{\omega} \cdot \hat{\mathbf{n}}$ . The nematic distribution of hard needles must therefore satisfy, from Eqs. (17.15) and (17.20), the nonlinear integral equation

$$\rho(\theta) = \frac{\rho \exp \left[ -2L^2 D \int_0^\pi d\theta' \sin \theta' K(\theta, \theta') \rho(\theta') \right]}{\int_0^\pi d\theta'' \sin \theta'' \exp \left[ -2L^2 D \int_0^\pi d\theta' \sin \theta' K(\theta'', \theta') \rho(\theta') \right]}, \quad (17.21)$$

with the azimuthally integrated kernel

$$K(\theta, \theta') = \int_0^{2\pi} d\varphi' |\sin \gamma| = \int_0^{2\pi} d\varphi' \sqrt{1 - (\cos \theta \cos \theta' + \sin \theta \sin \theta' \cos(\varphi' - \varphi))^2}. \quad (17.22)$$

Here, we use that we parameterized  $\hat{\omega}$  as  $(\sin \theta \sin \varphi, \sin \theta \cos \varphi, \cos \theta)$  (choosing  $\hat{\mathbf{n}} = (0, 0, 1)$ ). Note that  $K$  is independent of  $\varphi$ . Numerical solutions to Eq. (17.21) can be obtained for given dimensionless densities  $\rho L^2 D$ , and some resulting distributions are plotted in the left-hand panel to Fig. 17.2. Insertion of the orientation distributions into the free-energy expression (17.8) gives the isotropic and nematic free-energy densities  $f_{\text{iso}}(\rho)$  and  $f_{\text{nem}}(\rho)$ . These are plotted in the right-hand panel to Fig. 17.2.

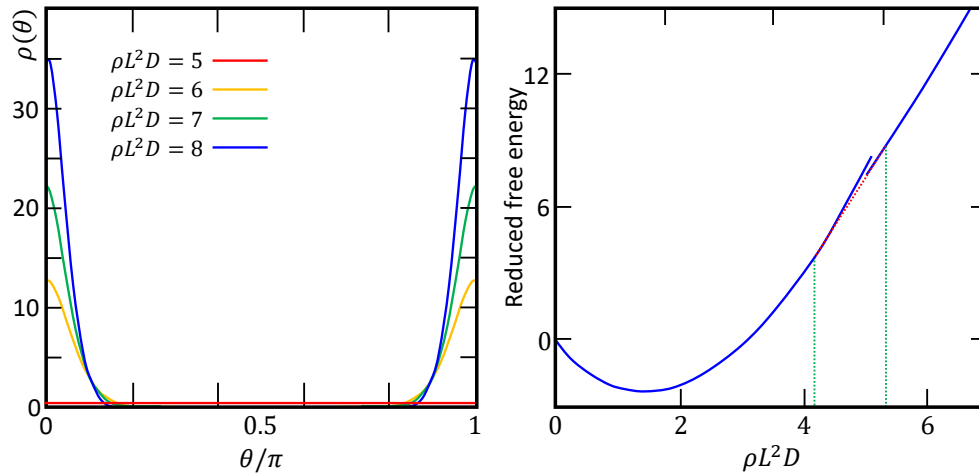


Figure 17.2: Properties of the Onsager theory for hard rods. (left) Angular distribution function of hard rods at several dimensionless densities  $\rho L^2 D$ . The distribution of  $\rho L^2 D = 5$  (red) is isotropic, *i.e.*, independent of  $\theta$ . The distributions for  $\rho L^2 D = 6$  (orange), 7 (green), and 8 (blue) are peaked about  $\theta = 0$  and  $\theta = \pi$  and represent nematic distributions. Note the up-down symmetry and the increasing orientational ordering with  $\rho$ . (right) The reduced Helmholtz free-energy density (blue curves) of the isotropic and nematic phase of infinitely elongated hard spherocylinders. The common-tangent construction (red, dashed line) yields coexistence of an isotropic phase at density  $\rho_I$  and a nematic phase at density  $\rho_N$ , with  $\rho_I L^2 D = 4.189$  and  $\rho_N L^2 D = 5.336$ , as indicated using the green, dashed lines. At densities  $\rho < \rho_I$  the system is isotropic, at densities  $\rho > \rho_N$  the system is nematic, with increasing orientational ordering as  $\rho$  increases.

## 17.4 Exercises

### Q95. The Orientation-Averaged Second Virial Coefficient

The orientation-averaged second virial coefficient of two hard spherocylinders is given by

$$B_2^{\text{iso}} = 4v_0 + L^2 D / (4\pi)^2 \int d\hat{\omega} d\hat{\omega}' |\sin \gamma|, \quad (17.23)$$

with  $\gamma$  the angle between  $\hat{\omega}$  and  $\hat{\omega}'$ . Check this expression, calculate  $B_2^{\text{iso}}$ , and discuss the importance of the first term  $4v_0$  as a function of  $L/D$ .

### Q96. Simple Model System for Rod-Like Particles

In a simple model of a system of rodlike particles one views the particles as rectangular blocks of length  $L$  and thickness  $D$ , *i.e.* of the form  $L \times D \times D$ . A further simplification is to restrict the number of possible orientations of each rod to three, such that the main axes of the rods can only point in the direction of a laboratory frame  $\hat{x}_\alpha$ ,  $\alpha = 1, 2, 3$ . A particle with orientation  $\alpha$  has its long axis along  $\hat{x}_\alpha$ . The interaction between the particles is *hard*, *i.e.*, overlap is not allowed. The Helmholtz free energy  $F$  of  $N = \rho V$  of such rods in a volume  $V$  at temperature  $T$  is given, within the second virial approximation, by

$$\frac{F}{V k_B T} = \sum_{\alpha=1}^3 \rho_\alpha (\log \rho_\alpha \mathcal{V} - 1) + \sum_{\alpha=1}^3 \sum_{\alpha'=1}^3 B_{\alpha\alpha'} \rho_\alpha \rho_{\alpha'}, \quad (17.24)$$

with  $\rho_\alpha$  the density of particles with orientation  $\alpha$ , and  $\mathcal{V}$  the (irrelevant) thermal volume.

- Argue that  $B_{\alpha\alpha'}$  is a symmetric  $3 \times 3$  matrix. Calculate the second virial coefficients  $B_{11} = B_{22} = B_{33} \equiv B_{\parallel}$  and  $B_{12} = B_{13} = B_{23} \equiv B_{\perp}$  for pairs of parallel and perpendicular rods, respectively.
- Consider from now on the “needle” limit  $L/D \rightarrow \infty$ . First calculate  $B_{\parallel}/L^2 D$  and  $B_{\perp}/L^2 D$  in this limit, and then show that the dimensionless free energy  $\psi = FL^2 D / V k_B T$  takes the form

$$\psi = \sum_{\alpha} c_{\alpha} (\log c_{\alpha} - 1 + \log \frac{\mathcal{V}}{L^2 D}) + 2(c_1 c_2 + c_1 c_3 + c_2 c_3), \quad (17.25)$$

with dimensionless densities  $c_{\alpha} = L^2 D \rho_{\alpha}$ . The constant term  $\log \mathcal{V} / L^2 D$  can be ignored, it is an irrelevant offset of the free energy or chemical potential as we will see.

- Define the *nematic order parameter*  $S$  by  $c_3 = c(1 + 2S)/3$  and  $c_1 = c_2 = c(1 - S)/3$ , with  $c = c_1 + c_2 + c_3 = \rho L^2 D$  the total dimensionless density. Explain this nomenclature. Give the range of the parameter  $S$ , keeping in mind that densities are non-negative.
- Calculate  $\psi(c, S)$ . For a given  $c$  one needs to determine  $S$  such that it minimizes  $\psi$  (at the fixed  $c$ ). Show that  $S = 0$  is a solution of  $(\partial\psi/\partial S)_{S=0}$  for any  $c$ . Which phase is associated with  $S = 0$ ?
- The result of (d) does *not* guarantee that  $S = 0$  yields a minimum of  $\psi$ . Argue on the basis of  $(\partial^2\psi/\partial S^2)_{S=0}$  that  $\psi$  is minimized by  $S \neq 0$  at  $c > c^*$ . Calculate  $c^*$ . Which phase do you associate with  $S \neq 0$ ?
- Phase coexistence of a low-density isotropic phase, with density  $c_I$  and order parameter  $S_I = 0$ , and a high-density nematic phase, with density  $c_N$  and order parameter  $S_N$ , requires *three* conditions to fix the three unknowns  $c_I$ ,  $c_N$ , and  $S_N$ . Give these conditions.

- (g) The coexistence conditions involve nonlinear algebraic equations that can easily be determined numerically, *e.g.*, with Mathematica root-finding procedures. Write such a code, and confirm that  $c_I = 1.258$ ,  $c_N = 1.915$ , and  $S_N = 0.915$ . Compare these numbers also to  $c^*$ .
- (h) Estimate, for hard rods with  $L/D = 100$ , the packing fractions beyond which orientational ordering is to be expected on the basis of the results of (g).

**Q97. Landau Theory for the Isotropic-Nematic Transition**

Here, we examine the phase behavior of anisotropic particles (long rods) using Landau theory for the isotropic-nematic (IN) phase transition.

- (a) What are the isotropic and nematic phase for a (colloidal) liquid crystal? Illustrate using sketches.

The nematic director is the average orientation of the rods in the liquid crystal. Let  $\theta$  measure the angle between a rod-like colloid and this director. It is sensible to create an order parameter that depends on a series in terms of  $\cos \theta$ , which takes values in the range  $[-1, 1]$ .

- (b) Explain why  $S = \langle (1/2)(3 \cos^2 \theta - 1) \rangle$  is a suitable order parameter for this transition, referencing the properties of the rods and Landau theory.

A general Landau theory can be written as  $F(p, T, S) = F_0(p, T) - hS + AS^2 + BS^3 + CS^4 + \dots$ , where the prefactors  $A$ ,  $B$ , and  $C$  may depend on pressure  $p$  and temperature  $T$ ;  $h$  is another prefactor.

- (c) The existence of an equilibrium state is guaranteed, if the highest order is even and the associated prefactor is positive. Explain.
- (d) What does the linear term  $hS$  represent and why may we set  $h = 0$ ?

The typical assumption is that  $A = a(T - T_c)$  with  $a$  a prefactor (dependent on  $p$ ) and  $T_c$  is the critical temperature.  $B$  and  $C$  are assumed to be nonzero and to not depend on the temperature, we write  $B = -b$  and  $C = c$  to indicate this and arrive at the following form for the IN Landau theory, after truncating the series to 4th order:  $F_{\text{IN}} = F_0 + a(T - T_c)S^2 - bS^3 + cS^4$ .

- (e) Show that  $F_{\text{IN}} - F_0 = [a(T - T_c) - b^2/(4c)]S^2 + cS^2[S - b/(2c)]^2$ .
- (f) For which two values of  $S$  does the right-hand side vanish? One solution requires an additional condition on the temperature, call it  $T^*$ . What is the physical meaning of  $T^*$ ?
- (g) What is the order of the isotropic-nematic phase transition? Use arguments supported by the above Landau theory.

## Chapter 18

# Moving away from Equilibrium

In this chapter, we will consider the dynamics of colloidal particles suspended in a fluid medium. We have previously examined the interplay between the fluid medium and suspended colloids in Chapter 16, focusing on the latter's effective interactions. Here, we will study the random motion exhibited by the colloids, *i.e.*, *Brownian motion*. We saw in Chapter 3 that a time average of a quantity, when taken over a sufficiently long interval and provided the system is ergodic, is equal to the ensemble average. That is, the dynamics of the particles generate, over time, the configurations that are the basis of the state-counting arguments that underlie statistical mechanics. Thus, the fluid medium may be said to fluctuate in time around a well-defined average, which coincides with that of the ensemble average.

Consider a larger particle is suspended in this fluctuating medium and examine a small fluid subvolume in contact with a small part of the particle's surface. Then we would expect that a difference in density, due to a fluctuation in particle number, would lead to a slightly different force experienced by that part of the particle's surface. Clearly, on average, the effect of fluctuations should wash out. However, there will be small positional excursions of the suspended particle, due to instantaneous heterogeneous distribution of forces acting on it. That is, the particle will diffuse around its average position. The effect is more pronounced, when the particle is closer to the size of the molecules of the fluid. This insight can be made mathematically rigorous, as was done by Einstein in one of his three seminal 1905 papers (the most cited one). It turns out that there is actually something more interesting going on, which was later generalized and formalized in the *fluctuation-dissipation theorem*. This theorem was proven by Herbert Callen and Theodore Welton in 1951 and expanded upon by Ryogo Kubo.

Briefly outlining the content, we will first set the historical background for the fluctuation-dissipation theorem, before deriving the static result. Next, we discuss the Langevin equation, by which the dynamics of a Brownian particle may be described macroscopically. Then we turn to the dynamic variant of the fluctuation-dissipation theorem. After that, we build upon the Langevin formalism to provide insight into a continuum description of the problem of diffusion, *i.e.*, using the continuity equation and density-based Fickian diffusion. This sets the stage for recovering the Stokes-Einstein relation, which is what triggered much of the discussion on the fluctuation-dissipation theorem to begin with. We close the chapter and these notes by giving a flavor of a truly non-equilibrium system that has received much attention in modern physics. We will extend the Langevin equation to a system of particles that are self-propelled, *e.g.*, bacteria and camphor boats. These systems show many interesting behaviors, for which a full description using the methods of statistical physics is thus far remains elusive.

## 18.1 Background to the Theory

The Brownian motion of colloidal particles (particles with a size of approximately  $1 \mu\text{m}$ ) is visible under a light microscope, which is what Brown had at his disposal, see his 1828 paper for details. We will return to the feasibility of his measurements at the end of the section. While the concept of Brownian motion is ascribed to Robert Brown (1828), the first reported observations predate him and were performed by Jan Ingenhousz (1785) a Dutch physicist working in Vienna, who observed random motion of coal dust on a fluid interface. Ingenhousz is more familiar for his work on gaseous exchange in plants. The Roman philosopher Lucretius ( $\sim 60 \text{ B.C.}$ ) also has a stake on the claim of discerning the core concept of Brownian motion. However, Lucretius' observations on the jittering of dust particles in air, which he connected to a molecular bombardment, are in fact caused by turbulence.

Nowadays, we do not find it strange to think that Brown's observations on the random motion of the "small particles inside the pollen of plants", is caused by the bombardment of those particles by solvent molecules. However, in the context of Brown's time, this interpretation was far from trivial. The existence of atoms and molecules was still widely disbelieved, with the continuum picture of matter being favored. In addition, Antonie van Leeuwenhoek had used a microscope to observe the motion of "tiny animals". Brown's work was on plants, so who was to say that the tiny particles in the pollen of plants were not such creatures, or that they moved under the influence of some kind of 'life force'? Brown (presumably) realized this and therefore demonstrated the robustness of his finding by creating powders of various minerals and even going as far as grinding up a piece of the nose of the Sphinx. In hindsight, the thinking was likely that the Sphinx was the oldest man-made object known at the time. Hence, powdering a piece of it would convince everyone that the effect was not life-based, as clearly Sphinx' material must be quite dead. These careful studies substantiated Brown's hypothesis that the motion was caused by the existence of molecules.

However, it took much longer before this picture was accepted, in part due to the efforts of Rutherford on demonstrating the existence of the nucleus, and in part due to careful measurements of Brownian motion and a theoretical description thereof in terms of molecular theory. It was Einstein who theoretically related the observable effect of Brownian displacements to the thermal motion of individual atoms or molecules, which are unobservable themselves — X-ray microscopes did not yet exist<sup>1</sup>. Einstein's 1905 analysis led to the following relation

$$D = \frac{k_B T}{6\pi\eta a} \quad (18.1)$$

where  $D$  is the diffusion coefficient of a spherical particle of radius  $a$  in a fluid medium with dynamic viscosity  $\eta$ . The viscosity is essentially the frictional damping coefficient of the medium, or more precisely the momentum diffusion coefficient. Convince yourself of this by examining the dimensions of the combination  $\eta/\rho$ , with  $\rho$  the density of the medium. The particle's diffusion coefficient in Eq. (18.1) is defined in terms of the variance of the particle displacements  $6Dt = \langle |\mathbf{R}(t) - \mathbf{R}(0)|^2 \rangle$ .

Equation (18.1) is remarkable. The diffusion coefficient and the viscosity are both (nontrivial) functions of the temperature and the pressure, but in such a way that their product  $D\eta \propto T$  for a given colloidal particle size  $a$ . We can make this a bit more explicit. The factor in the denominator is exactly the resistance experienced by a spherical particle under the application of an external force. That is, in the low Reynold's number regime of fluid dynamics — governed by the Stokes equation — we have that  $\mathbf{F} = 6\pi\eta a \mathbf{u}$  with  $\mathbf{F}$  the applied force and  $\mathbf{u}$  the sphere's velocity. The equation is therefore referred to as the Stokes-Einstein relation. Dimensionally, the results makes sense:  $D$  has units of  $\text{m}^2/\text{s}$  and  $\mathbf{u}$  of  $\text{m}/\text{s}$ , while  $k_B T$  has units of  $\text{J}$  and  $\mathbf{F}$  of  $\text{N} = \text{J}/\text{m}$ . However, the implication of Eq. (18.1) is very profound: thermodynamic fluctuations in a physical variable predict the response quantified by the susceptibility

<sup>1</sup>Visualizing the dynamics of single atoms in solids using X-ray microscopy is considered state of the art.

of the same physical variable. This sloppy definition of the *fluctuation-dissipation theorem* is a rather abstract, but we have encountered this concept at several points throughout the notes, without explicitly commenting on it. We will start to build towards a general theorem in Section 18.2.

Before turning to the fluctuation-dissipation theorem, we wish to make a few closing remarks with regards to Eq. (18.1) and its historical significance.

- The Stokes-Einstein relation can be used to estimate the time it takes a particle to diffuse over a distance of its radius. Denoting this *diffusion time* by  $t_D$ , it follows from Eq. (18.1) that  $t_D = a^2/6D = \pi a^3 \eta / k_B T$ . Inserting typical numbers for colloids,  $a = 1.0 \mu\text{m}$ ,  $\eta = 10^{-3} \text{kg/ms}$  (water), and  $k_B T \simeq 10^{-21} \text{J}$  (room temperature), one finds  $t_D \simeq 1 \text{ s}$ , *i.e.*, the motion is time-resolvable under a microscope. It is sometimes erroneously reported that Brown studied the random motion of pollen, a claim that is not substantiated by even a cursory examination of the title of his paper. Brown studied the particles *inside Clarkia pulchella* pollen, which are colloidal in size. The pollen themselves have a radius of  $\approx 25 \mu\text{m}$ , which implies that he would have had to wait at least 3 hours to have seen diffusive motion of pollen! Perhaps the mistake lies in disbelief over the level of optical resolution Brown would have needed to observe these particles. Indeed the colloidal matter that Brown studied was close to the edge of what could be resolved using the microscopes at his disposal. These were able to resolve structures as fine as  $0.7 \mu\text{m}$  [B.J. Ford, Notes Rec. R. Soc. Lond. **55**, 29–49 (2001)]; clearly, his observations are pretty impressive.
- Einstein pointed out that *all* quantities in Eq. (18.1) can be measured directly:  $D$  from the mean squared displacement of the colloids observed under the microscope;  $\eta$ , *e.g.*, from macroscopic mechanical experiments with the medium;  $a$  with the microscope;  $T$  with a thermometer. Consequently, the experiments on Brownian motion should yield the numerical value for the Boltzmann constant  $k_B$ . From this Avogadro's number follows, since  $N_A = R/k_B$  with  $R$  the gas constant, which is also known from macroscopic experiments of dilute gases.

Einstein's derivation motivated Jean Perrin to quantitatively study Brownian motion under the microscope, and he could verify the validity of the predictions quantitatively, as well as obtain a value of  $N_A$ . This provided conclusive evidence that atoms and molecules actually *exist* and deservedly resulted in Perrin's 1923 Nobel prize.

## 18.2 Static Fluctuation-Dissipation Theorem

Let us now delve into the fluctuation-dissipation theorem, where we shall focus on the static variant first to gain some familiarity with the concepts before moving on to the dynamic variant. Recall from Chapter 3 that the variance of the energy in a subvolume is proportional to the specific heat and that similarly the variance of the particle number is proportional to the compressibility. This indicates that in general, that there a relation between fluctuations of a macroscopic observable and the response of this observable to its *conjugate* force. Let us clarify that statement in the context of a more familiar statistical mechanics setting and considering the Ising model under an external field. The magnetic susceptibility  $\chi$  of the system is given by

$$\chi = \frac{\beta}{N} (\langle M^2 \rangle - \langle M \rangle^2). \quad (18.2)$$

That is, the susceptibility can be written in terms of the fluctuations of the magnetization  $M$ . However, this property also determines the magnetization of a system in response to an external magnetic field

$H$ . That is,  $M = \chi H$ , where  $H$  aligns the spins and competes with their internal, alignment-based interactions. Writing  $M = \sum_i S_i$  for the magnetization, we can rewrite the susceptibility as

$$\chi = \frac{\beta}{N} \sum_{i,j} (\langle S_i S_j \rangle - \langle S_i \rangle \langle S_j \rangle), \quad (18.3)$$

but the summand is obviously related to the spin-spin correlation function  $G(i, j)$ , see Chapter 11. Thus, the ability to align spins using external means is directly related to correlations in their thermal alignment. Similarly, for the other two examples — compressibility and heat capacity — the conjugate forces are the temperature and pressure, respectively. With this and the dynamic example of Brownian motion, where fluctuations in the position relate to the mobility of the particle, it should now be abundantly clear that there is something very generic about correlations in the system and the system's response to external driving. We shall formalize this next.

For the static case, consider an equilibrium system at temperature  $T$ , then the time-independent canonical distribution function is

$$f_c(\Gamma) = \frac{\exp[-\beta\mathcal{H}(\Gamma)]}{N!h^{3N}Z_{\mathcal{H}}(N, V, T)}; \quad (18.4)$$

$$Z_{\mathcal{H}}(N, V, T) = \frac{1}{N!h^{3N}} \int d\Gamma \exp[-\beta\mathcal{H}(\Gamma)], \quad (18.5)$$

with  $\mathcal{H}$  the Hamiltonian of the system. The equilibrium average of a macroscopic observable  $A(\Gamma)$  is given by

$$\langle A \rangle_{\mathcal{H}} = \int d\Gamma A(\Gamma) f_c(\Gamma). \quad (18.6)$$

The subscript  $\mathcal{H}$  is used to indicate against which Hamiltonian the distribution, partition function, and average are taken. Let us now perturb the system with a time-independent potential  $V = -\lambda A$ , which is linear in our observable of interest. The perturbed Hamiltonian may now be written as  $\mathcal{H}' = \mathcal{H} + V$ , the factor  $\lambda$  is a constant that determines the strength of the perturbation, we will assume  $\lambda \ll 1$ . Writing the Hamiltonian this way,  $\lambda$  can be easily seen to be the conjugate variable to  $A$ . That is, if we use the perturbed Hamiltonian to construct a free energy  $F$  then,  $\lambda = -\partial F/\partial A$ , which explains the naming convention. Referring back to our examples, think pressure for  $\lambda$  and volume for  $A$ .

We should stress that we consider the static case here, such that under the perturbation, expressions similar to those in Eqs. (18.4) and (18.5) are applicable, but then with  $\mathcal{H}'$  as the appropriate Hamiltonian. We start by Taylor expanding these to linear order in  $\lambda$  to obtain the following expression for the perturbed partition function

$$Z_{\mathcal{H}'}(N, V, T) = \frac{1}{N!h^{3N}} \int d\Gamma \exp[-\beta\mathcal{H}'(\Gamma)]; \quad (18.7)$$

$$\approx \frac{1}{N!h^{3N}} \int d\Gamma \exp[-\beta\mathcal{H}(\Gamma)] (1 - \beta V) = Z_{\mathcal{H}}(N, V, T) (1 - \beta \langle V \rangle_{\mathcal{H}}). \quad (18.8)$$

Suppose that we have another macroscopic observable  $B(\Gamma)$ , then the perturbed average of  $B$  to first order is given by

$$\begin{aligned} \langle B \rangle_{\mathcal{H}'} &= \frac{1}{N!h^{3N}Z_{\mathcal{H}'}(N, V, T)} \int d\Gamma B(\Gamma) \exp[-\beta\mathcal{H}'(\Gamma)]; \\ &\approx \frac{1}{N!h^{3N}Z_{\mathcal{H}}(N, V, T) (1 - \beta \langle V \rangle_{\mathcal{H}})} \int d\Gamma B(\Gamma) \exp[-\beta\mathcal{H}(\Gamma)] (1 - \beta V); \\ &\approx (1 + \beta \langle V \rangle_{\mathcal{H}}) (\langle B \rangle_{\mathcal{H}} - \beta \langle BV \rangle_{\mathcal{H}}); \\ &\approx \langle B \rangle_{\mathcal{H}} + \beta (\langle B \rangle_{\mathcal{H}} \langle V \rangle_{\mathcal{H}} - \langle BV \rangle_{\mathcal{H}}). \end{aligned} \quad (18.9)$$

This result ignores any terms that are quadratic in  $\lambda$ , as we linearize in the perturbation. Let now examine the change of  $B$  with respect to the unperturbed system

$$\begin{aligned}\langle B \rangle_{\mathcal{H}'} - \langle B \rangle_{\mathcal{H}} &= \beta (\langle B \rangle_{\mathcal{H}} \langle V \rangle_{\mathcal{H}} - \langle BV \rangle_{\mathcal{H}}); \\ &= \beta (\langle B \rangle_{\mathcal{H}} \langle \lambda A \rangle_{\mathcal{H}} - \langle B \lambda A \rangle_{\mathcal{H}}); \\ &= \beta \lambda (\langle B \rangle_{\mathcal{H}} \langle A \rangle_{\mathcal{H}} - \langle BA \rangle_{\mathcal{H}}) \equiv \beta \lambda C_{\mathcal{H}}(BA).\end{aligned}\quad (18.10)$$

In the last line, we have introduced the part of the observable  $B$  that is connected to the perturbation caused by observable  $A$ . That is, in a statistical sense, the part of  $B$  that is correlated with  $A$ . We can also rewrite this as the derivative of  $\langle B \rangle_{\mathcal{H}'}$  with respect to  $\lambda$ , *i.e.*, we have Taylor expanded so that the

$$\beta \lambda C_{\mathcal{H}}(BA) = \left. \frac{\partial \langle B \rangle_{\mathcal{H}'}}{\partial \lambda} \right|_{\lambda=0}.\quad (18.11)$$

However, the obvious physical interpretation of Eq. (18.11) is that this is the change of  $B$  with respect to an applied  $A$ , for small departures from the unperturbed system. Or in other words, this is the susceptibility of  $B$  to  $A$ , so that we may finally write

$$\chi_{BA} = \beta C_{\mathcal{H}}(BA).\quad (18.12)$$

This is the general static variant of the fluctuation-dissipation theorem. Summarizing, this theorem states that the *linear* response of the system to a perturbation is given by the connected part of the correlation function with respect to the *unperturbed* system. Clearly, the above examples assume  $A = B$ , but this is not necessary in general, as we have now seen. Before we can cover the dynamic variant of the fluctuation-dissipation theorem, we shall need to gain some feeling for dynamic correlation functions, which we will do next.

## 18.3 The Langevin Equation

Consider a small particle suspended in a molecular solvent, of which the solvent molecules are (substantially) smaller than the particle. Let the particle's mass be  $m$ , its position at time  $t$  is  $\mathbf{r}(t)$ , and its velocity  $\mathbf{v}(t)$ . By being suspended, the particle experiences a frictional drag force  $-m\xi\mathbf{v}$ , with  $m\xi$  the friction coefficient. We have introduced  $m$  in front of the friction for convenience here. Note that  $m\xi = 6\pi\eta a$  in the case of a small sphere, but that  $\xi$  should generally be a tensor that accounts for the particle's shape anisotropy. Even if the particle is at rest ( $\mathbf{v} = \mathbf{0}$ ), it will experience collisions with solvent molecules that move about. This random force is denoted  $\mathbf{f}$  here and has the property that  $\langle \mathbf{f} \rangle = \mathbf{0}$ , following our argument that the net effect of the fluctuations must be statistically vanishing. Using Newton's second law, we find the equation of motion of the particle

$$m \frac{d\mathbf{v}(t)}{dt} = -m\xi\mathbf{v}(t) + \mathbf{f}(t).\quad (18.13)$$

This equation is called the *Langevin equation*.

Let us ignore, for the moment, the effect of the random force; this situation is often referred to as *quiescent* to indicate that the suspending fluid is non-fluctuating. The Langevin equation is then

$$\frac{d\mathbf{v}(t)}{dt} = -\xi\mathbf{v}(t) \quad \Rightarrow \quad \mathbf{v}(t) = \mathbf{v}_0 \exp(-\xi t),\quad (18.14)$$

where the initial velocity  $\mathbf{v}_0$  is an integration constant. We have now found a physical interpretation of the parameter  $\xi$ : on a timescale  $\mathcal{O}(\xi^{-1})$  the drag force reduces the initial velocity considerably, such that

after a period of a few  $\xi^{-1}$  the particle has essentially come to rest. The situation is more interesting when  $\mathbf{f}$  is *not* ignored. In that case one checks that the solution of the Langevin equation (18.13) reads

$$\mathbf{v}(t) = \mathbf{v}_0 \exp(-\xi t) + \frac{1}{m} \int_0^t ds \mathbf{f}(s) \exp(\xi(s-t)). \quad (18.15)$$

That is, the equation depends on the details of  $\mathbf{f}$  in the time interval  $[0, t]$ . Figure 18.1 shows an illustration of the effect of the noise on the velocity decay.

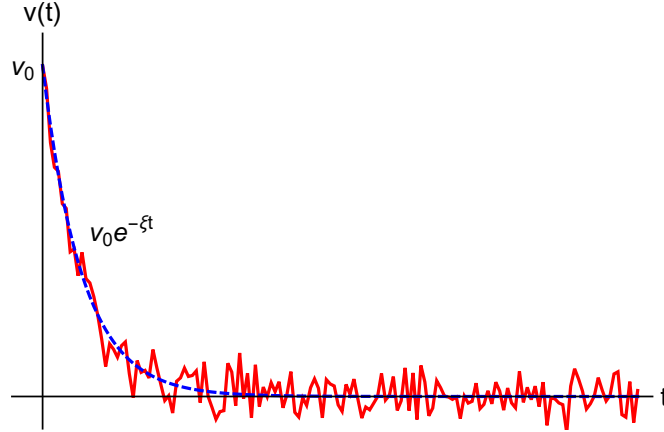


Figure 18.1: Illustration of the velocity decay from the Langevin equation without thermal noise (blue, dashed) and with thermal noise (red, solid) curves, respectively.

Even though we have now found the exact solution, we cannot say too much about the dynamics of the particle as long as we do not know the details of  $\mathbf{f}(t)$ . However, it seems physically reasonable to assume that the time average  $\langle \mathbf{v}_0 \cdot \mathbf{f}(t) \rangle = 0$  for all  $t$ , since one expects that the random force and the initial velocity are uncorrelated for all elapsed times. As a consequence, we can write for the correlation between the initial velocity and the velocity at time  $t$  that

$$\langle \mathbf{v}(t) \cdot \mathbf{v}_0 \rangle = \langle |\mathbf{v}_0|^2 \rangle \exp(-\xi t) = \frac{3k_B T}{m} \exp(-\xi t), \quad (18.16)$$

where the second equality follows from the equipartition theorem,  $(m/2)\langle \mathbf{v}_0 \cdot \mathbf{v}_0 \rangle = 3kT/2$ , and we have implicitly assumed that  $t > 0$ , which is rather important in order to properly account for causality! In equilibrium any time correlation function only depends on the time-difference that elapsed between the initial and final time, and therefore we can rewrite Eq. (18.16) slightly more generally as

$$\langle \mathbf{v}(t) \cdot \mathbf{v}(t') \rangle = \frac{3k_B T}{m} \exp(-\xi|t - t'|). \quad (18.17)$$

Note that a comparison of Eq. (18.17) with Eq. (18.15) shows that  $\langle \mathbf{f}(s) \otimes \mathbf{f}(s') \rangle \neq \mathbf{0}$ , *i.e.*, the random forces are correlated (but only for very short time intervals  $s - s'$ , or even for  $s = s'$  only). We now use Eq. (18.17) to calculate the typical distance that the particle has moved away from its initial position after a time  $t$ . Denoting the particle's center-of-mass position at time  $t$  by  $\mathbf{R}(t)$ , it is trivial to write

$$\mathbf{R}(t) = \mathbf{R}(0) + \int_0^t ds \mathbf{v}(s). \quad (18.18)$$

Since  $\langle \mathbf{v}(t) \rangle = \mathbf{0}$  in the absence of any macroscopic flow, we have  $\langle \mathbf{R}(t) - \mathbf{R}(0) \rangle = \mathbf{0}$ , *i.e.*, the random motion of the particle does not have a preferred direction. The mean *squared* distance, however, does

not vanish; with Eq. (18.18) it is given by

$$\begin{aligned}
\langle |\mathbf{R}(t) - \mathbf{R}(0)|^2 \rangle &= \int_0^t ds \int_0^t ds' \langle \mathbf{v}(s) \cdot \mathbf{v}(s') \rangle \\
&= \frac{3k_B T}{m} \int_0^t ds \int_0^t ds' \exp(-\xi|s - s'|) \\
&= \frac{6k_B T}{m\xi} \left( t + \frac{\exp(-\xi t) - 1}{\xi} \right) \\
&\simeq \begin{cases} \frac{3k_B T}{m} t^2, & t \ll \xi^{-1}; \\ \frac{6k_B T}{m\xi} t, & t \gg \xi^{-1}. \end{cases} \tag{18.19}
\end{aligned}$$

The short-time dynamics, where the displacement  $\sqrt{\langle |\mathbf{R}(t) - \mathbf{R}(0)|^2 \rangle}$  increases linear with  $t$ , is called *ballistic*. The long-time dynamics, where the displacement increases as  $t^{1/2}$ , is called *diffusive*. The crossover between these two regimes takes place at times  $t \simeq \xi^{-1}$ , *i.e.*, the time scale at which the particle loses memory of its earlier velocity according to Eq. (18.17). Expressed differently, the scaling with  $t$  in Eq. (18.19) is a consequence of the randomness of the motion, while the  $t^2$  scaling is indicative of coherent (or predictable, time-reversible) motion, which a ballistic trajectory clearly is. In relation to the fluctuation-dissipation theorem, note that Eq. (18.19) makes the connection between the diffusion coefficient (and by extension the mobility) and the dynamic velocity-velocity correlation function. However, the above does not constitute a proof, which is what we will consider in the next section.

Before we come to the dynamic fluctuation-dissipation theorem, we will first examine the physical consequences of the above formalism. We can calculate the typical time scale  $t_B \equiv \xi^{-1}$ , the *Brownian time*, at which the crossover from ballistic to Brownian motion takes place. Using Stokes law,  $m\xi = 6\pi\eta a$  as discussed above, we find that the Brownian time  $t_B = 1/\xi$ , is given by

$$t_B = \frac{m}{6\pi\eta a}. \tag{18.20}$$

We can now insert a few typical numbers for, *e.g.*, a colloidal particle in water at room temperature: radius  $a = 1 \mu\text{m}$ , mass density  $1\text{g/cm}^3$ , and solvent viscosity  $\eta = 10^{-3}\text{kg/ms}$ . This yields  $t_B \approx 10^{-7}$  s. The corresponding distance that is traveled during this time is  $\ell_B = t_B \sqrt{\langle v_0^2 \rangle} \approx 10^{-10}$  m, where we used the equipartition result and that  $k_B T \simeq 10^{-21}\text{J}$  at room temperature. From this we can conclude that  $\ell_B \ll a$ , *i.e.*, the ballistic dynamics only lasts for an extremely short period of time, and during this period the particle only travels a tiny distance compared to its own size. For this reason, we can ignore the ballistic short-time behavior for all practical purposes, and instead focus on the long-time diffusive dynamics for colloidal particles. This means that on the intermediate colloidal scale, the Langevin equation may be replaced by the Brownian dynamics equation  $m\xi\mathbf{v}(t) = \mathbf{f}(t)$ , which represents the overdamped dynamics only. We will see that for active particles, which are the focus of the last section, another ballistic regime will appear.

## 18.4 Dynamic Fluctuation-Dissipation Theorem

Having gained a bit more insight into the relation between a driving force and the velocity of a suspended particle, and time-dependent equilibrium correlations of the velocity, we are ready to examine the dynamic fluctuation-dissipation theorem and generalize the above. This is slightly more involved than the static case, but not considerably harder. Assume that the perturbation acts from  $t = -\infty$  to  $t < 0$  and

that the Hamiltonian remains unperturbed from  $t = 0$  onward. That is  $\mathcal{H}'(\Gamma, t) = \mathcal{H}(\Gamma) + \lambda\Theta(-t)A(\Gamma)$ , with  $A(\Gamma)$  an observable and  $\mathcal{H}$  and  $\mathcal{H}'$  the original and perturbed Hamiltonian, respectively. Lastly,  $\Theta$  denotes the Heaviside function, 1 for  $t > 0$  and 0 for  $t < 0$ . What we want to know is how the system relaxes back toward equilibrium, once the perturbing force is switched off. This will give us the same insights for the situation where we switch the disturbance on, but it is conceptually simpler.

The initial state of the system is well described by the static formalism of Eqs. (18.4) and (18.5), with  $\mathcal{H}'$  as the appropriate Hamiltonian. After the perturbation is switched off, however, the system will evolve according to  $\mathcal{H}$ . To first order in  $\lambda$ , using the same line of argument as for the static case, the time evolution of  $B$  for  $t > 0$  with respect to the unperturbed system is given by

$$\langle B(t) \rangle_{\mathcal{H}'} - \langle B(t) \rangle_{\mathcal{H}} = \beta\lambda C_{\mathcal{H}}(B(t)A(0)), \quad (18.21)$$

with  $C_{\mathcal{H}}(B(t)A(0))$  the equilibrium (unperturbed) time-correlation function, defined as

$$C_{\mathcal{H}}(B(t)A(0)) = (\langle B(t)A(0) \rangle_{\mathcal{H}} - \langle B(t) \rangle_{\mathcal{H}} \langle A(0) \rangle_{\mathcal{H}}). \quad (18.22)$$

The interpretation of Eq. (18.21) is that of a difference in averages between (i) a system that up to time  $t = 0$  has come into equilibrium with the perturbed Hamiltonian  $\mathcal{H}'$  — this is why it was necessary to let time run in the domain  $(-\infty, 0]$  — and (ii) a system which has remained in equilibrium with respect to  $\mathcal{H}$ . Thus, the average  $\langle \cdot \rangle_{\mathcal{H}'}$  is not truly an ensemble average over the entire time line. It is far more appropriate to write  $\Delta B(t) \equiv \langle B(t) \rangle_{\mathcal{H}'} - \langle B(t) \rangle_{\mathcal{H}}$  and work in terms of  $\Delta B(t)$  only. However, the above argument is how the derivation is presented in all textbooks the author of this chapter is familiar with. The interpretation of  $C_{\mathcal{H}}$  is that of the relaxation of an out-of-equilibrium  $B$  (in equilibrium with  $\mathcal{H}'$ ) relaxing toward equilibrium with  $\mathcal{H}$ .

We still need to introduce the dynamic susceptibility to make progress toward the fluctuation dissipation relation we seek. Briefly assume that we have an arbitrarily time-dependent  $\lambda(t)$ . The change in a parameter  $B$  is simply the dynamic susceptibility  $\chi_{AB}(t, s)$ , with  $t$  the time at which we probe a response to a perturbation applied at time  $s$ , integrated over time with respect to the applied field:

$$\Delta B(t) = \int_{-\infty}^t ds \chi_{BA}(t, s) \lambda(s). \quad (18.23)$$

Note that the susceptibility is defined with respect to a system in equilibrium, hence  $\chi_{AB}(t, s) = \chi_{AB}(t - s)$ , *i.e.*, it must be a function of differences in time. In addition, the susceptibility cannot look into the future (causality), so that  $\chi_{AB}(t - s)$  exists if  $t > s$ , and is zero otherwise. Now we return to our system with  $\lambda(t) = \lambda\Theta(-t)$ . Here we apply the force only for  $t < 0$ , so that

$$\Delta B(t) = \int_{-\infty}^0 ds \chi_{BA}(t - s) \lambda. \quad (18.24)$$

Using a change of variables allows us to write

$$\Delta B(t) = \lambda \int_t^{\infty} ds \chi_{BA}(s), \quad (18.25)$$

which only applies for  $t > 0$ . Taking the time derivative of the two forms of  $\Delta B$ , we arrive at

$$\frac{\partial \Delta B}{\partial t} = \beta\lambda \frac{\partial}{\partial t} C_{\mathcal{H}}(B(t)A(0)) = -\lambda \chi_{BA}(t) \quad \Rightarrow \quad (18.26)$$

$$\chi_{BA}(t) = -\beta \frac{\partial}{\partial t} C_{\mathcal{H}}(B(t)A(0)), \quad (18.27)$$

for  $t > 0$  and  $\chi_{BA}(t) = 0$  otherwise. For  $B = A$  we find  $\chi(t) \equiv \chi_{AA}(t) = -\beta(\partial/\partial t)\langle\delta A(t)\delta A(0)\rangle_{\mathcal{H}}$ . This expresses that the way a system responds in time to a perturbing potential is related the temporal nature of thermal excursions about its equilibrium. Returning to Fig. 18.1, the decay time of the velocity is exactly the time over which the particle decorrelates with respect to its original position. The above derivation is not quite as elegant as it could be, but a more general derivation requires more sophisticated mathematical techniques. In such a derivation, a Fourier transform is taken and the resulting frequency-based dynamic fluctuation-dissipation theorem is related to the spectral density of the system *via* the Wiener-Khinchin theorem. This makes the connection between fluctuations and dissipation explicit.

### 18.4.1 Applying Fluctuation-Dissipation to Brownian Motion

We shall close this section by applying the above real-space expression to Brownian motion, showing that the formalism indeed recovers our intuited Langevin-based result. However, the major difference is that we have formally shown that the mobility (or equivalently friction) that couples to an external force is related to the equilibrium velocity/position fluctuations. This allows us to relate this form to the known result from Stokesian fluid dynamics, as we will see. Consider an external perturbation given by a force  $f$  applied to a colloid immersed in a fluid medium. The response of the system is to develop a drift velocity  $v$ . The conjugate variable to the applied force is the displacement  $x$ , so that  $\mathcal{H}' = \mathcal{H} - fx$  and

$$\chi_{vx}(t) = -\beta \frac{\partial}{\partial t} C_{\mathcal{H}}(v(t)x(0)). \quad (18.28)$$

Clearly, the left-hand side of the equation will be related to the friction or mobility of the particle, but the right-hand side will need to be recast to make the connection more obvious. Using time invariance, it is relatively straightforward to show

$$\frac{\partial}{\partial t} C_{\mathcal{H}}(v(t)x(0)) = -\langle v(t)v(0) \rangle_{\mathcal{H}} \Rightarrow \chi_{vx}(t) = \langle v(t)v(0) \rangle_{\mathcal{H}} \quad (18.29)$$

The above expression already makes a clear connection between fluctuations in  $v$  and the mobility that relates  $v$  to an applied force  $f$ .

We can now ask ourselves what the expression for the susceptibility is. The change of the particle velocity due to the applied force can be related to the susceptibility according to

$$v(t) = f \int_t^{\infty} ds \chi_{vx}(s) \quad (18.30)$$

However, we also expect that  $m\xi v(0) = f$  from Eq. (18.13), so that

$$\frac{k_B T}{m\xi} = \int_0^{\infty} ds \chi_{vx}(s). \quad (18.31)$$

The Langevin equation (18.13) further tells us how the speed would decrease upon switching off the force  $f$  at  $t = 0$  in the absence of fluctuations, namely  $v(t) = v(0) \exp(-\xi t) = f \exp(-\xi t)/(m\xi)$ . Together with Eq. (18.30) this implies that  $\chi_{vx}(t) = \exp(-\xi t)/m$  and hence

$$\langle v(t)v(0) \rangle_{\mathcal{H}} = \frac{k_B T}{m} \exp(-\xi t), \quad (18.32)$$

which only holds for  $t > 0$  and is an expression of the memory of the noise. This is exactly and reassuringly the expression of Eq. (18.17). The system loses its memory with a characteristic time  $\xi^{-1}$ .

Lastly, we obtain the Stokes-Einstein relation (18.1) for a spherical particle. Note that we have used  $m\xi v(0) = f$  to arrive at Eq. (18.31). However, we know that the velocity must be that of a sphere that has been subjected to  $f$  from time  $t = -\infty$  onward, thus fully relaxed to its terminal velocity. For a small sphere in a fluid medium, the hydrodynamic Stokes equation states that  $6\pi\eta a v(0) = f$ , so that  $m\xi = 6\pi\eta a$  and we arrive at

$$\langle |x(t) - x(0)|^2 \rangle = 2 \frac{k_B T}{6\pi\eta a} t, \quad (18.33)$$

for  $t \gg m/(6\pi\eta a)$ . Here, we have used translational invariance on the correlation and double integration over time of Eq. (18.32) along the same lines as in the previous section. Since the above discussion was completely in terms of a 1-dimensional problem, we expect  $\langle |x(t) - x(0)|^2 \rangle = 2Dt$ , thus recovering the desired form of Eq. (18.1).

## 18.5 The Continuity Equation and Fickian Diffusion

Thus far, we have focused on the dynamics of a single colloidal particle, we now consider a system of many of these Brownian particles moving around in a background medium, *i.e.*, a drop of ink in water, colloidal particles in a solvent, or biomolecules in a cell. Instead of describing the whereabouts of these particles individually, we take here a more coarse-grained picture and view the particles as a continuum with a concentration (or density)  $\rho(\mathbf{r}, t)$  at position  $\mathbf{r}$  at time  $t$ .

Consider a hypothetical fixed volume  $V$  of arbitrary shape with linear dimensions small compared to the system size, but large compared to the particle's size; the system may be described by a continuum. The number of particles in this volume is given, at time  $t$ , by  $\int_V d\mathbf{r} \rho(\mathbf{r}, t)$ . Since particles cannot be destroyed or created, the only way that the number of particles in  $V$  can change is by a net flux of particles into or out of the surface of  $V$ . The flux of particles is called  $\mathbf{j}(\mathbf{r}, t)$  here, and is such that  $\mathbf{j} \cdot d\mathbf{s}$  is the number of particles that flows through a small surface element  $d\mathbf{s}$  per unit time, where the orientation of  $d\mathbf{s}$  is parallel to its normal. We can now write

$$\frac{\partial}{\partial t} \int_V d\mathbf{r} \rho(\mathbf{r}, t) = - \int_S d\mathbf{s} \cdot \mathbf{j}(\mathbf{r}, t) = - \int_V d\mathbf{r} \nabla \cdot \mathbf{j}(\mathbf{r}, t). \quad (18.34)$$

Here,  $S$  denotes the surface of  $V$ ,  $d\mathbf{s}$  is an outward pointing surface element, and  $\nabla$  denotes the gradient with respect to  $\mathbf{r}$ . We also employed Gauss' theorem to obtain the second equality. Note that the minus sign in Eq. (18.34) indicates that the number of particles in  $V$  increases if the flux is antiparallel with the outgoing surface normal, and decreases if it is parallel. Because the volume  $V$  is arbitrary, Eq. (18.34) should hold for any  $V$  and hence we have the *continuity equation*

$$\frac{\partial \rho(\mathbf{r}, t)}{\partial t} = -\nabla \cdot \mathbf{j}(\mathbf{r}, t), \quad (18.35)$$

which provides one relation between the two fields  $\rho(\mathbf{r}, t)$  and  $\mathbf{j}(\mathbf{r}, t)$ . Thus, a second equation is needed before a solution can be found.

Perhaps the simplest case emerges when the particle flux is *assumed* to be proportional to the (negative of the) concentration gradient,  $\mathbf{j} \propto -\nabla \rho$ , which describes that particles tend to flow from high to low concentrations. We call the proportionality factor  $D$  — we will see that  $D$  turns out to be the diffusion coefficient introduced before — and hence we have

$$\mathbf{j}(\mathbf{r}, t) = -D\nabla \rho(\mathbf{r}, t), \quad (18.36)$$

which is referred to as *Fick's law* and is the required second relation between  $\rho$  and  $\mathbf{j}$ . Combining it with the continuity equation leads to the partial differential equation known as the *diffusion equation*

$$\frac{\partial \rho(\mathbf{r}, t)}{\partial t} = D \nabla^2 \rho(\mathbf{r}, t), \quad (18.37)$$

which can be solved, in principle, if an initial density profile  $\rho(\mathbf{r}, t = 0)$  is given.

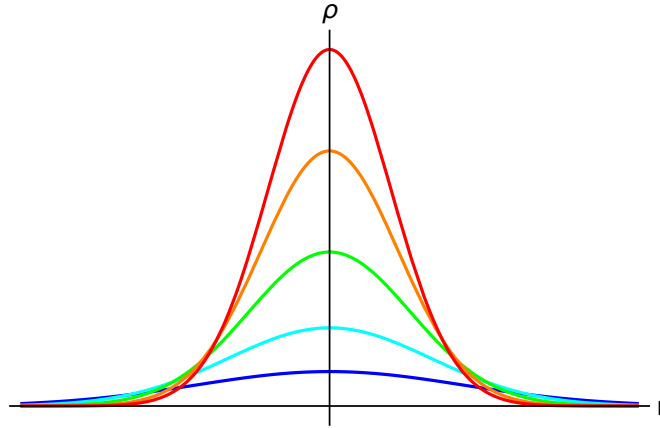


Figure 18.2: A cross section of the density profile for an initially  $\delta$ -localized particle density, which spreads out over time, from red to blue.

We consider the particular case  $\rho(\mathbf{r}, t = 0) = N\delta(\mathbf{r})$ , *i.e.*, all  $N$  particles are initially in the origin. The solution of the diffusion equation (18.37) can then be written as

$$\rho(\mathbf{r}, t) = \frac{N}{(4\pi Dt)^{3/2}} \exp(-\mathbf{r}^2/4Dt), \quad (18.38)$$

which is illustrated in Fig. 18.2. In three dimensions, we can decompose  $\mathbf{r}^2 = x^2 + y^2 + z^2$ , from which we see that  $\rho(\mathbf{r}, t) = f(x)f(y)f(z)$  with  $f(x) \propto \exp(-x^2/4Dt)$ . That is, we have a Gaussian with a time-dependent variance given by  $2Dt$ . From this we find the mean-square displacement of the particles  $\langle \mathbf{r}^2 \rangle = 6Dt$ , which upon comparison with Eqs. 18.19 and 18.1 shows that  $D$  as defined in Eq. (18.36) is indeed the diffusion coefficient.

## 18.6 Active Brownian Particles

In the previous sections, we have examined the response of a system to external perturbations in the linear-response regime to obtain the fluctuation-dissipation theorem. However, there are many systems where the objects are pushed so far out of equilibrium, that the linear response approximation does not hold. A specific class of these are particles which generate their own work by converting (internal) chemical energy. Think of bacteria, but also more macroscopic objects, such as ants, birds, and even humans; all of which eat to move, reproduce, *etc.* The individuals in the above examples display some level of collective self-organization: bacteria form colonies, ants perform their survival tasks communally, starlings (a type of bird) forms large flocks (murmurations) to deter predators, and humans come together to perform tasks or hinder each other (*e.g.*, traffic jams) in a wide range of situations. Statistical physicists have been very interested in the minimal requirements to capture the emergence of collective

effects. While a full description of these efforts goes beyond the scope of these notes, we will have a sneak peek at one of the most basic models for self-propulsion of bacteria.

Bacteria are mostly in the 1 to 10  $\mu\text{m}$  size range, though there are single-cell organisms called *Thiomargarita namibiensis* that can grow up to 0.3 mm. Clearly, overdamped dynamics is applicable to describe the dynamics of a single bacterium. In addition, it turns out that bacteria like to live near surfaces<sup>2</sup>, which implies that their motion is usually in plane. The problem of describing the bacterium's motion may thus be described by specifying the evolution of position of the center of mass  $\mathbf{r}(t)$  and the orientation  $\hat{\mathbf{n}}$ , which equivalently can be specified by an angle  $\theta$  for in-plane 2D motion.

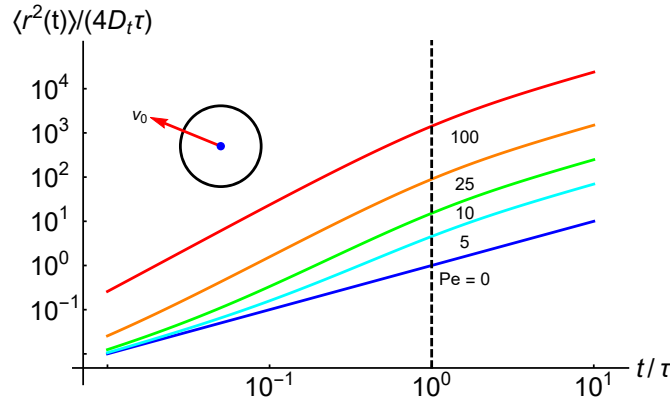


Figure 18.3: The reduced mean-squared displacement of an active particle, with several values of the activity parameter  $\text{Pe} = v_0/\sqrt{D_t D_r}$ . The blue straight line shows the result for a passive particle  $\text{Pe} = 0$ , which only has the linear increase with time expected for overdamped Brownian motion. The crossover between the ballistic short-time motion induced by self-propulsion ( $\propto t^2$ ) to enhanced diffusion ( $\propto t$ ) takes place at  $t = \tau$ , with  $\tau$  the reorientation time.

We start by specifying the Brownian dynamics equation for the bacterium's velocity  $\mathbf{v}(t) = \dot{\mathbf{r}}(t)$ :

$$\gamma_t [\mathbf{v}(t) - v_0 \hat{\mathbf{n}}(t)] = \mathbf{f}_t(t). \quad (18.39)$$

Here,  $\gamma_t$  is the hydrodynamic translational friction coefficient (generally a tensor for a shape-anisotropic particle) with associated diffusion coefficient  $D_t = k_B T / \gamma_t$ . The parameter  $v_0$  specifies the constant self-propulsion speed, which points in the direction  $\hat{\mathbf{n}}$  that co-moves with the swimmer, see the inset to Fig. 18.3 for an example. Lastly,  $\mathbf{f}_t$  is the thermal noise associated with translational motion as before:  $\langle \mathbf{f}_t(t) \rangle = \mathbf{0}$  and  $\langle \mathbf{f}_t(t) \cdot \mathbf{f}_t(t') \rangle = 4k_B T \gamma_t \delta(t - t')$ . The direction in which the bacterium points can be updated either randomly or according to some more biorealistic update rule, such as a run-and-tumble process<sup>3</sup>. For the sake of simplicity, reorientation on the basis of Brownian noise is typically used, which is also conveniently what we have studied thus far in the notes. Let  $\hat{\mathbf{n}}$  be specified by the angle  $\theta(t)$  (2D motion), then

$$\gamma_r \dot{\theta}(t) = f_r(t), \quad (18.40)$$

with  $\gamma_r$  the rotational friction coefficient and  $\langle f_r(t) \rangle = 0$  and  $\langle f_r(t) f_r(t') \rangle = 2k_B T \gamma_r \delta(t - t')$ . Note that the (inverse) rotational diffusion coefficient  $D_r^{-1} = \gamma_r / k_B T$  has a dimension of time and is often

<sup>2</sup>The discussion as to why this is the case exactly, is still ongoing, but very relevant to medical and commercial problems related to the formation of biofilms, *biofouling*.

<sup>3</sup>The bacterium has periods for which its direction remains unchanged, interspersed with moments of rapid reorientation. For example, in *Escherichia coli* straight swimming (running) can be accomplished by bundling all the self-propelling flagella into one helical 'braid', while tumbles are accomplished by the bacterium pulling one of the flagella out of the braid, reorienting, and re-braiding.

called the rotational diffusion time  $\tau$ . The evolution of the orientation with time then may be written as  $\langle \hat{\mathbf{n}}(t) \cdot \hat{\mathbf{n}}(t') \rangle = \exp(-|t - t'|/\tau)$ . These two equations specify what is known in the literature as the (2D) Active Brownian Model; variants exclude translational diffusion or use run-and-tumble statistics.

From the Active Brownian Model, it is straightforward to compute the translational mean-squared displacement. Working out the math, as you will do in one of the exercises, we find

$$\langle |\mathbf{r}(t) - \mathbf{r}(0)|^2 \rangle = \begin{cases} 4D_t t + v_0^2(t/\tau) & t \gg \tau \\ 4D_t t + 2v_0^2 t^2 & t \ll \tau \end{cases} \quad (18.41)$$

This implies that there is another ballistic regime of motion, associated with the self-propulsion of the particle. At times longer than the reorientation time, there is a fully diffusive regime with an enhanced diffusion coefficient  $D_{\text{eff}} = D_t + v_0^2/(2\tau)$ . The reorientation time is thus a control parameter for the transition between active ballistic and (enhanced) diffusive motion, see Fig. 18.3 for example full mean-squared displacement curves. Note that we can rewrite the result of Eq. (18.41) by introducing a Péclet number. Péclet number are dimensionless combinations that indicate the relative contribution of persistent to diffusive motion (typically) and a possible combinations here are: (i)  $\text{Pe} = v_0 a / D_t$  with  $a$  the size of the bacterium and (ii)  $\text{Pe} = v_0 / \sqrt{D_t \tau}$ . The former Pe number compares the time it takes to self-propel one particle radius, with the time it takes the particle to diffuse the same distance, while the latter does not make explicit reference to the size of the particle, *i.e.*, it may be used in a point-particle description. Clearly, whenever  $\text{Pe} \ll 1$  it is justified to reduce the above dynamics further and only have the rotational noise term, ignoring contributions from translational diffusion. This is also becomes clear by examining the evolution of the mean-squared-displacement curves in Fig. 18.3 with increasing Pe.

The above simple result of substantial enhancement of the diffusion coefficient has a number of implications. Microfluidic mixing turns out to be exceptionally time consuming due to laminarity of fluid flows, meaning that mixing only takes place through diffusion, rather than *via* turbulence, as is the case on our length scale. Bacteria and artificial variants thereof are proposed to enhance the diffusion in the fluid medium, thereby leading to faster mixing. There are many more interesting aspects of active matter, including how the Active Brownian Model together with simple interaction rules can give rise to clustering, but this unfortunately goes beyond the scope of these lecture notes.

## 18.7 Exercises

### Q98. The Diffusion Equation

The expression  $\partial\rho/\partial t = D\nabla^2\rho$  describes the evolution of the particle density  $\rho(\mathbf{r}, t)$ . In this exercise, we will use Fourier transforms to obtain the solution to this equation, given that  $\rho_0(\mathbf{r}) = \rho(\mathbf{r}, t = 0)$ . The Fourier transform of a function  $f(\mathbf{r})$  is defined as  $\hat{f}(\mathbf{k}) = \int d\mathbf{r} \exp(i\mathbf{k} \cdot \mathbf{r})f(\mathbf{r})$ .

- (a) Show that  $\partial\hat{\rho}(\mathbf{k}, t)/\partial t = -Dk^2\hat{\rho}(\mathbf{k}, t)$ .  
 (b) Use the result from (a) to write  $\hat{\rho}(\mathbf{k}, t) = \hat{\rho}_0(\mathbf{k}) \exp(-Dk^2t)$  and use this expression to obtain

$$\rho(\mathbf{r}, t) = \frac{1}{(2\pi)^3} \int d\mathbf{k} \exp(-i\mathbf{k} \cdot \mathbf{r}) \hat{\rho}_0(\mathbf{k}) \exp(-Dk^2t), \quad (18.42)$$

with  $k^2 = \mathbf{k} \cdot \mathbf{k}$ .

- (c) Compute  $\hat{\rho}_0(\mathbf{k})$  for  $\rho_0(\mathbf{r}) = N\delta(\mathbf{r})$ .  
 (d) Compute  $\rho(\mathbf{r}, t)$  from the answer to (c) and from this the mean-squared displacement

$$\langle r^2(t) \rangle = \frac{1}{N} \int d\mathbf{r} r^2 \rho(\mathbf{r}, t). \quad (18.43)$$

### Q99. From Fick and Boltzmann to Stokes-Einstein

In the main text we have considered single particle diffusion and continuum Fickian diffusion, here we will utilize this to obtain the Stokes-Einstein relation. Assume there is an external potential energy  $U(\mathbf{r})$  acting on a suspension of particles. Then an individual particle would move according to the velocity-force relation with a velocity  $\gamma\mathbf{v}(\mathbf{r}) = -\nabla U(\mathbf{r})$ . However, this leads to a spatially heterogeneous distribution of the particles, which is countered by Fickian diffusion. The flux of particles due to the external potential balances the diffusive flux. Write down the two flux contributions and use this to argue that

$$D = -\frac{1}{\gamma} \left( \frac{\partial\rho}{\partial U} \right)^{-1} \rho(\mathbf{r}) \quad (18.44)$$

Use the equilibrium distribution to rewrite the  $\rho$ - and  $U$ -dependent terms and obtain the Stokes-Einstein relation.

### Q100. Random Walks as a Microscopic Diffusion Model

A diffusing particle changes direction frequently and randomly. We will model this process in one dimension as a “random walk”, wherein the particle can move forward or backward by a step of length  $x_0$ ; it starts in the origin. The probability on either step is  $1/2$ . The goal is to determine the probability  $W(k, n)$  of finding the particle  $k$  steps away from the origin after  $n$  moves.

- (a) The number of forward steps is  $n_f$  and the number of backward steps is  $n_b$ . Express  $n_f$  en  $n_b$  in  $n$  en  $k$ .  
 (b) How many possible ways can  $n_f$  en  $n_b$  be chosen from  $n$  steps?  
 (c) What is the probability of one of those combinations?  
 (d) Derive

$$W(k, n) = \frac{n!2^{-n}}{[(n+k)/2]![(n-k)/2]!}. \quad (18.45)$$

- (e) Assume  $n \gg 1$  en  $n \gg k$  (is this reasonable?). Use the Stirling approximation and make use of the second-order Taylor approximation for the logarithm  $\ln(1+x) \approx x - x^2/2$  to show that

$$W(k, n) \approx \sqrt{\frac{2}{\pi n}} \exp(-k^2/2n). \quad (18.46)$$

The probability of returning to the origin after a large number of steps  $n$  is thus  $W(0, n) \approx \sqrt{2/(\pi n)}$ .

- (f) Define the covered distance as  $x = kx_0$  and introduce the time it takes to take  $n$  steps  $t = nt_0$ . Show that the probability  $W(x, t)dx$  that the particle is between  $x$  and  $x + dx$  at a time  $t$  is given by

$$W(x, t) = \frac{1}{\sqrt{4\pi Dt}} \exp(-x^2/4Dt). \quad (18.47)$$

This is a diffusion equation with diffusion coefficient  $D = x_0^2/(2t_0)$ .

- (g) Qualitatively sketch the behavior of  $W(x, t)$  as a function of  $t$  for a fixed  $x$ , as well as a function of  $x$  for a fixed  $t$ .
- (h) Show that  $W(x, t)$  satisfies

$$\frac{\partial W}{\partial t} = D \frac{\partial^2 W}{\partial x^2}. \quad (18.48)$$

#### Q101. Active Brownian Model

Derive Eq. (18.41) using a variant of the approach that was employed to determine the mean-squared displacement of the Langevin equation in Chapter 18. The first step should be to show that  $\langle \hat{\mathbf{n}}(t) \cdot \hat{\mathbf{n}}(t') \rangle = \exp(-|t - t'|/\tau)$ . Next, use this result to work out  $\langle \mathbf{r}(t) \cdot \mathbf{r}(t') \rangle$ . Finally, Taylor expand the obtained expression for large and small times compared to the reorientation time  $\tau$ .